DOCTORAL THESIS

HYDROGELS AS PLATFORMS FOR VACCINE DELIVERY AND MUCOSAL RESTORING

Lorena García del Río

INTERNATIONAL DOCTORAL SCHOOL

DOCTORAL PROGRAM IN DRUG RESEARCH AND DEVELOPMENT

SANTIAGO DE COMPOSTELA

2021

USC
UNIVERSIDADE
DE SANTIAGO
DE COMPOSTELA

TESE DE DOUTORAMENTO

HIDROXEIS COMO PLATAFORMAS PARA A ADMINISTRACIÓN DE VACINAS E REPARACIÓN DA MUCOSA

Lorena García del Río

ESCOLA INTERNACIONAL DE DOUTORAMENTO

PROGRAMA DE DOUTORAMENTO EN INVESTIGACIÓN E DESENVOLVEMENTO DE MEDICAMENTOS

SANTIAGO DE COMPOSTELA

2021

USC
UNIVERSIDADE
DE SANTIAGO
DE COMPOSTELA

PhD CANDIDATE STATEMENT

Hydrogels as platforms for vaccine delivery and mucosal restoring

Miss Lorena García del Río

I submit my Doctoral Thesis, following the procedure according to the Regulation, stating that:

1) This thesis gathers the results corresponding to my work.
2) When applicable, explicit mention is given to the collaborations the work may have had.
3) The present document is the final version submitted for its defence and coincide with the document sent in electronic format.
4) I confirm that this thesis does not incur in any plagiarism of any other authors or documents submitted by me for obtaining other degrees.

At Santiago de Compostela, on 2021

Sgd. Lorena García del Río

USC
UNIVERSIDADE
DE SANTIAGO
DE COMPOSTELA

DECLARACIÓN DO AUTOR DA TESE

Hidroxeis como plataformas para a administración de vacinas e reparación da mucosa

Dna Lorena García del Río

Presento a miña tese, seguindo o procedemento axeitado ao Regulamento, e declaro que:

1) A tese abarca os resultados da elaboración do meu traballo.
2) De ser o caso, na tese faise referencia ás colaboracións que tivo este traballo.
3) Confirmo que a tese non incorre en ningún tipo de plaxio doutros autores nin de traballos presentados por min para a obtención doutros títulos.
4) A tese e a versión definitiva presentada para a súa defensa e coincide a versión impresa coa presentada en formato electrónico.

E comprométome a presentar o Compromiso Documental de Supervisión no caso de que o orixinal non estea na Escola.

En Santiago de Compostela, a 2021

Sgd. Lorena García del Río

USC
UNIVERSIDADE
DE SANTIAGO
DE COMPOSTELA

AUTHORIZATION OF THE THESIS SUPERVISOR

Hydrogels as platforms for vaccine delivery and mucosal restoring

Prof. Mariana Landín, as director and tutor

REPORT:

That the present thesis, corresponds to the work carried out by Miss **Lorena García del Río**, under my supervision, and that I authorize its presentation considering that it gathers the necessary requirements of the USC Doctoral Studies Regulation, and that as supervisor of this thesis, it does not incur in the abstention causes established by the Law 40/2015.

According to the Regulation of Doctorate Studies, I also declare that the present doctoral thesis is suitable to be defended on the basis of the Monographic modality with reproduction of publications, in which the participation of the doctoral student was decisive for its elaboration and that the publications correspond to the research plan.

At Santiago de Compostela, on 2021

Sgd. Mariana Landín Pérez

USC
UNIVERSIDADE
DE SANTIAGO
DE COMPOSTELA

AUTORIZACIÓN DO DIRECTOR/SUPERVISOR DA TESE

Hidroxeis como plataformas para a administración de vacinas e reparación da mucosa

Prof. Mariana Landín, como directora e supervisora

INFORMA:

Que a presente tese, correspóndese co traballo realizado por Dna. **Lorena García del Río**, baixo a miña dirección, e autorizo a súa presentación, considerando que reúne os requisitos esixidos no Regulamento de Estudos de Doutoramento da USC, e que como director desta non incorre nas causas de abstención establecidas na Lei 40/2015.

De acordo co indicado no Regulamento de Estudos de Doutoramento, declara tamén que a presente tese de doutoramento é idónea para ser defendida en base á modalidade de Monográfica con reproducción de publicacións, nos que a participación da doutoranda foi decisiva para a súa elaboración e as publicacións se axustan ao Plan de Investigación.

En Santiago de Compostela, a 2021

Asdo. Mariana Landín Pérez

USC
UNIVERSIDADE
DE SANTIAGO
DE COMPOSTELA

"The true laboratory is the mind, where behind illusions we uncover the laws of truth"

Jogadish Chandra Bose

USC
UNIVERSIDADE
DE SANTIAGO
DE COMPOSTELA

AGRADECEMENTOS/ ACKNOWLEGMENTS

USC
UNIVERSIDADE
DE SANTIAGO
DE COMPOSTELA

Chegado este momento e botando unha ollada atrás no tempo, podo dicir con total seguridade que a miña primeira incursión no mundo da investigación veu a raíz da miña curiosidade por querer saber sempre o porqué das cousas e, a un golpe de sorte. Estar no momento e lugar adecuado fixo posible que hoxe estea escribindo estas palabras de agradecemento.

Por iso, en primeiro lugar, creo que debo de comezar pola persoa que me abriu as portas do mundo da investigación de par en par, *Mariana Landín*. Sen a oportunidade e a confianza que me brindou fai xa oito anos, a realización deste traballo non tería sido posible. Grazas a ela, o que *a priori* ía ser unha pequena aventura científica, rematou sendo toda unha carreira de fondo na que sempre intentou apoiarme como unha directora próxima, liberal, comprensiva e sobre todo, moi paciente. Baixo as súas directrices puiden experimentar unha gran evolución, tanto a nivel persoal coma académica.

En segundo lugar, non podía faltar *Patricia Díaz Rodríguez*, unha persoa extraordinaria en tódolos aspectos. Traballar con ela é un auténtico pracer, sempre cunha enerxía desbordante, contaxiando a súa paixón pola ciencia e disposta a botar unha man sen esperar nada a cambio. Durante todo este tempo sempre estivo aí, incluso desde a distancia, para escoitarme, aconsellarme e guiarme nos momentos máis incertos. Moitas grazas por todo Patri!

A tódolos meus compañeiros de laboratorio por facer máis amena esta experiencia, así como a *Fani*, *Cris* e "*os de Fran*". Aínda que coincidimos case o final desta etapa, gustaríame agradecerlle a *Rebeca* as súas palabras de ánimo, simpatía e amizade desinteresada. Especial mención merecen *Helena*, *Leti*, *Jorge*, *Víctor*, *Mirian* e *Jesús* que acabaron converténdose en bos amigos. Abofé que esta andanza non sería a mesma sen o seu apoio, bo humor e esas grandes vivencias compartidas dentro e fóra do laboratorio; abofé que non.

Ós profesores *Carmen Álvarez Lorenzo*, *Ángel Concheiro Nine* e *Francisco Otero Espinar* pola súa boa disposición e, por sempre sacar un oco para intentar axudarme con certas dúbidas que foron xurdindo ó longo da tese, así como a Profesora María del Carmen Remuñán por deixarme o seu laboratorio a miña total disposición.

Ocupan un lugar destacado os doutores *Dennis Christensen* e *Gabriel Kristian Pedersen* do Statens Serum Institut, que apostaron por este proxecto e recibíronme cos brazos abertos sen coñecerme de nada. Grazas a eles puiden explorar outros métodos de traballo e mergullarme no mundo da inmunoloxía dunha maneira amena, atractiva e "relativamente" fácil. A *Rune* e *Julia* pola súa amabilidade. A *Gregers*, *Frank*, *Joshua*, *Jes* e *Álvaro*, por esas charlas tan interesantes e divertidas. Ós meus compañeiros do SSI, *Nida*, *Nina*, *Julie*, *Dennis*, *Katharina*, *Elisa* e *Safiya*, por integrarme no grupo desde o primeiro momento e permitirme coñecela sociedade danesa dunha maneira afable e próxima. Máis aló do laboratorio, tampouco poden faltar as persoas que contribuíron a que a miña estadía en Copenhague fose algo incrible e inesquecible. Grazas *Kike*, *Vanessa*, *Federica*, *Cris*, *Andrea Arias*, *Andrea Castaño*, *Guido*, *Paula* e *Flor*, por tódalas experiencias vividas e por ser a miña familia no frío norte.

Tamén me gustaría agradecer a esas persoas que estiveron ó meu lado todos estes anos, ben desde os inicios ou que se foron incorporando ó longo desta andanza, mostrándome a súa amizade e apoio moral nos momentos máis escuros. Grazas a *Sheila*, *Ana*, *Laura*, *Vero*, *Cris*, *Jessi* e *Gabriele* por estar sempre dispostos a buscar unha boa escusa para ir de troula e así axudarme a desconectar da mellor maneira posible. Non podo esquecerme de *Gabriela*, a cal é a miña mellor amiga e unha das mellores persoas coas que puiden coincidir na carreira. Grazas por esas cañas; esas esmorgas con final imprevisible e a veces rozando o surrealista; e por compartir comigo unha das miñas grandes afeccións, viaxar e descubrir mundos novos.

Por último, pero non menos importante, teño que darlle as GRAZAS a miña familia. Sobre todo a miña nai, *Lourdes*. Por ela puiden subirme a este tren, xa que sen o seu esforzo, cariño, comprensión, paciencia e ganas de que me converta na mellor versión de min mesma, nada disto sería posible. A meu irmán, *Jorge*, por ese humor irónico, a veces un tanto negro, que en moitas ocasións conseguiu sacarme un gran sorriso. E finalmente, a miña tía *Concha*, por estar sempre presente e ser coma unha segunda nai.

Grazas a todos, porque sen a vosa contribución esta experiencia non sería igual de enriquecedora!

TABLE OF CONTENT

USC UNIVERSIDADE DE SANTIAGO DE COMPOSTELA

USC
UNIVERSIDADE
DE SANTIAGO
DE COMPOSTELA

CONTENT

List of abbreviations ..... **I**

Resumo/Abstract ..... **IX**

Resumo *in extenso* ..... **XVII**

Expanded abstract ..... **XXXVII**

1. Introduction **1**

1.1. Mucosal surfaces 3

1.1.1. Anatomy and function (small overview) 3

1.1.2. Mucus and mucins 5

1.2. Inmunity from mouth to rectum 6

1.2.1. Oral cavity immune system 6

1.2.2. Gut-associated lymphoid tissues or GALT 7

1.3. Mucosal vaccination: pros and cons 10

1.3.1. Adjuvants 11

1.3.2. Mucosal tissues as vaccination sites 12

1.3.2.1. Ocular vaccination 13

1.3.2.2. Nasal and pulmonary vaccination 14

1.3.2.3. Sublingual and buccal vaccination 15

1.3.2.4. Oral vaccination 16

1.3.2.5. Vaginal and rectal vaccination 17

1.4. Gastrointestinal inflammatory mucosal pathologies 17

1.5. Hydrogels: types and properties 20

1.5.1. Stimuli-sensitive hydrogels 24

1.5.1.1. Physically responsive hydrogels 24

1.5.1.2. Chemically and biochemically responsive hydrogels 27

1.5.2. Hydrogels as drug delivery platforms on mucosal surfaces 30

1.5.2.1. Formulation of hydrogels with desirable characteristics 30

1.6. Artificial intelligence techniques applied to pharmaceutical systems design..... 32

References 36

2. Objectives 61

References 65

3. Chapter I: "Design of novel orotransumucosal vaccine delivery platforms using artificial intelligence" 67

3.1. Introduction 71

3.2. Materials and methods..... 73

3.2.1. Materials..... 73

3.2.2. Proliferation assays in human macrophages..... 74

3.2.3. Experimental design 74

3.2.4. Hydrogels preparation and characterization 75

3.2.4.1. Rheological analysis 76

3.2.4.2. Texturometric assessments 76

3.2.5. Antigen-like microspheres loading and in vitro release studies 77

3.2.6. Artificial Neural Networks modelization..... 77

3.2.7. Statistical analysis 78

3.3. Results 79

3.3.1. Immunostimulatory capacity of selected polymers 79

3.3.2. Hydrogels performance and AIT modelling..... 80

3.3.2.1. T_{gel} is mainly determined by PF127 and Gantrez® concentration 81

3.3.2.2. Mucoadhesion, adhesion work and gel strength are dependent on proportions of PF127 and Gantrez® 82

3.3.2.3. Cohesion is modulated by PF127 83

3.3.2.4. GFM released at 5 min was fundamentally modulated by PF127 while total release time is also dependent on type of Gantrez® 84

3.4. Discussion 86

3.5. Conclusions 89

References 90

4. Chapter II: "Sublingual boosting with a novel mucoadhesive thermogelling hydrogel following parenteral CAF01 priming as strategy against Chlamydia trachomatis" **97**

4.1. Introduction 101

4.2. Materials and Methods 103

4.2.1. Materials 103

4.2.2. Hydrogel development and preparation 104

4.2.3. Hydrogel characterization 105

4.2.3.1. Rheological properties 105

4.2.3.2. Texturometric properties 106

4.2.3.3. Protein release 106

4.2.3.4. Stability properties 107

4.2.4. CAF01 liposomes preparation 107

4.2.5. Antigen and formulations loading 107

4.2.6. In vivo assays 108

4.2.6.1. Ethics statement 108

4.2.6.2. Mouse immunization 108

4.2.6.3. Antibody titers in blood and vaginal samples 109

4.2.6.4. IFN-γ and IL-17A responses in spleen and cervical lymph nodes 110

4.2.7. Statistical analysis 111

4.3. Results 111

4.3.1. Hydrogel preparation, characterization and stability 111

4.3.2. Prime immunization using CAF01 followed by OGEL mucosal boosting improves mucosal antibody responses 112

4.3.3. Prime immunization using CAF01 followed by OGEL sublingual boosting elicits high-magnitude IFN-γ responses in cervical lymph nodes 114

4.4. Discussion 115

References 119

5. Chapter III: "New tools to design smart thermosensitive hydrogels for protein rectal delivery in IBD" 127

5.1. Introduction 131

5.2. Materials and methods 132

5.2.1. Experimental designs 132

5.2.2. Hydrogel preparation 134

5.2.3. Texturometric analysis 134

5.2.4. Rheological assessment 135

5.2.5. Protein loading and in vitro release studies 135

5.2.6. Data modelization using Artificial Neural Networks 136

5.3. Results 137

5.3.1. Knowledge space analysis 137

5.3.2. Design space analysis 140

5.3.2.1. PF127 determines syringeability 142

5.3.2.2. PF127 and MK4M rule bioadhesiveness 142

5.3.2.3. PF127 and MK4M determine viscosity 142

5.3.2.4. PF68 rules mainly the T_{gel} 144

5.3.2.5. *In vitro* protein release studies 144

5.4. Discussion 145

5.5. Conclusions 149

References 150

6. **Chapter IV: "Tailored hydrogels as delivery platforms for conditioned medium from mesenchymal stem cells in a mouse model of acute colitis"** **157**

6.1. Introduction 161

6.2. Materials and methods 162

6.2.1. Materials 162

6.2.2. Hydrogel development and preparation 163

6.2.3. Hydrogel Characterization 164

6.2.3.1. Texturometric analysis 164

6.2.3.2. Rheological analysis 164

6.2.3.3. Stability assessments 164

6.2.4. Cell Cultures and hUCESC-CM preparation 165

6.2.5. Hydrogel loading with hUCESC-CM 165

6.2.6. *In vivo* assay 165

6.2.6.1. Ethics statement 165

6.2.6.2. Mice 165

6.2.6.3. Colitis induction and experimental groups 166

6.2.6.4. Clinical symptoms evaluation and colon macroscopic examination 167

6.2.6.5. Histological evaluation 167

6.2.6.6. RNA Extraction and Quantitative Real Time PCR 167

6.2.7. Statistical analysis 168

6.3. Results 168

6.3.1. Hydrogel preparation and characterization 168

6.3.2. Inducement of DSS-associated colitis in C57BL/6 mice 170

6.3.3. Effect of H-hUCESC-CM on body weight and colon length 170

6.3.4. H-hUCESC-CM hydrogel reduced the extension and severity of intestinal lesions 172

6.3.5. H-hUCESC-CM pro-inflammatory cytokines in colon 176

6.4. Discussion 177

6.5. Conclusions 180

References 181

7. Conclusions **187**

Annex I **193**

Annex II **201**

Statements: conflicts of interests, image use, cell culture, in vivo assays and published content **205**

Checklists and permissions **211**

USC UNIVERSIDADE DE SANTIAGO DE COMPOSTELA

LIST OF ABBREVIATIONS

USC
UNIVERSIDADE
DE SANTIAGO
DE COMPOSTELA

5-ASA: 5-Aminosalicylic acids

AIT: Artificial intelligence tools/techniques

AMPs: Antimicrobial peptides

AN119: Gantrez® AN119

ANN(s): Artificial neural network(s)

APCs: Antigen-presenting cells

AUC: Area under the curve

BALT: Bronchus-associated lymphoid tissue

BIC: Bayesian Information Criterion

BSA: Bovine serum albumin

CAF01: Cationic adjuvant liposomes type 01

CAFs: Cancer-associated fibroblasts

CALT: Conjunctiva-associated lymphoid tissue

CD: Crohn's disease

CM: Conditioned medium

CMC: Critical micelle concentration

Coa-ASC16: Nanostructure formed by self-assembly of 6-O-ascorbyl palmitate ester

CpG: Cytosine-guanine oligodeoxynucleotide

CpG-ODN: Cytosine-guanine motifs

Ct: *Chlamydia trachomatis*

CV: Cross validation

D: Diffusion coefficient of entrapped molecules

DALT: Salivary duct-associated lymphoid tissue

DCs: Dendritic cells

DDA: Dimethyldioctadecylammonium bromide

ddH_2O: Double distilled water

DDS: Dextran sulfate sodium

DMEM-F12: Dulbecco's Modified Eagle Medium: Nutrient Mixture F-12

EEI: Enfermidade Inflamatoria Intestinal

FAE: Follicle-associated epithelium

FCS: Foetal calf serum

FDA: Food and drug administration

G: Shear modulus

G': Storage modulus

G'': Loss modulus

GA: Genetic algorithms

GALT: Gut-associated lymphoid tissue

GFM: Green fluorescent microparticles

GIT: Gastrointestinal tract

H&E: Hematoxylin and eosin

H: Healthy control group

H-DMEM-F12: Hydrogels prepared in DMEM-F12 cell culture media

H-hUCESC-CM: Rectal optimized hydrogel loaded with hUCESC-CM

HIV: Human immunodeficiency virus

HIV-1: Human immunodeficiency virus type 1

H-PBS: Hydrogels prepared with PBS

HPV: Human papillomavirus

HS1200: Hybrane® S1200

HSV: Herpes simplex virus

hUCESC-CM: Conditioned medium from human uterine cervical stem cells

hUCESCs: Human uterine cervical stem cells

AI: Artificial Intelligence

IBD: Inflammatory bowel disease

IEC: Intestinal epithelial cells

IgA: Immunoglobulin A

IgG: Immunoglobulin G

USC UNIVERSIDADE DE SANTIAGO DE COMPOSTELA

IL-2: Interleukin 2

IL-6: Interleukin 6

kDa: Kilo Dalton

LALT: Larynx-associated lymphoid tissue

LCs: Langerhans cells

LCST: Low critical solution temperature

LDALT: Lacrimal duct-associated lymphoid tissue

LOG: Blinded expert pathologist

LOOCV: Leave One Out Cross Validation

M cells: Microfold cells

MALT: Mucosal-associated lymphoid tissues

mJ: Millijoules

MK4M: Methocel® K4M

MLD: Minimum Description Length

MSCs: Mesenchymal stem cells

MZ: Mesalazine group

N: Newton

NALT: Nasopharynx associated lymphoid tissue

NLRs: Nucleotide binding oligomerization domain- (NOD-) like receptors

NT: No-treated group

OGEL: Sublingual optimized hydrogel

PBS: Phosphate-buffered saline

pcDNA3-CRT/E7 DNA vaccine: DNA vaccine encoding the early protein E7 from human papillomavirus type 16 linked to calreticulin

PEO: Polyethylene oxide

PF127: Pluronic® F127

PF68: Pluronic® F68

PLGA: Poly lactic-*co*- glycolic acid

PMA: 2-mercaptoethanol and phorbol 12-myristate 13-acetate

PPO: Polypropylene oxide

Q: Swelling ratio

QbD: Quality by design

ROS: Reactive oxygen species

RLRs: Retinoic acid-inducible gene-I- (RIG-I-) like receptors

rMOMP: recombinant major outer membrane protein

RPMI: Roswell Park Memorial Institute medium

S97: Gantrez® S97

SCoF: Simulated colonic fluid

SED: Subepithelial dome

SEM: Standard error of the mean

sIgA: Secretory IgA antibodies

SRM: Structural risk minimisation

SSF: Simulated salivary fluid

TDB: Glycolipid trehalose 6,6´-dihibenate

T_{gel}: Gelation temperature

TLRs: Toll-like receptors

TNF-α: Tumour necrosis factor alpha

UC: Ulcerative colitis

UCST: Upper critical solution temperature

WST-1: Water Soluble Tetrazolium Salt-1

ξ: Mesh size

ρ_x: Crosslinking density

RESUMO/ABSTRACT

USC
UNIVERSIDADE
DE SANTIAGO
DE COMPOSTELA

RESUMO

A administración de moléculas activas na mucosa, como as proteínas, é unha aproximación moi atractiva e de indubidables vantaxes para inducir unha resposta local e/ou sistémica de carácter terapéutico e/ou inmunoestimulante. Non obstante, aspectos críticos como a drenaxe rápida e a degradación mediada por encimas ou o pH, limitan o tempo de permanencia das moléculas terapéuticas sobre a superficie das mucosas e tamén condicionan o paso de substancias a través destes tecidos, e polo tanto, a súa utilidade.

Os hidroxeis son redes poliméricas en 3D cuxas características poden modularse para lograr formulacións altamente mucoadhesivas, capaces de interactuar coas mucosas e incrementalo tempo de permanencia das proteínas no lugar de acción, conseguindo a súa absorción e o efecto terapéutico desexado. Ademais, cando se combinan características como biocompatibilidade, mucoadhesión, termosensibilidade e a elevada capacidade de carga de fármaco dos hidroxeis, estes sistemas convértense en excelentes candidatos para superar as limitacións da administración transmucosal. Con todo, o deseño deste tipo de formas farmacéuticas implica a preparación de sistemas multicompoñente, o que supón unha tarefa desafiante no ámbito da tecnoloxía farmacéutica. Nos últimos anos as ferramentas de intelixencia artificial (AI) como as redes neuronais, a lóxica difusa ou os algoritmos xenéticos (GA) mostraron a súa utilidade para estudalos efectos das variables de composición e operación sobre as características de diferentes formas farmacéuticas.

Por iso, o obxectivo deste traballo experimental é abordala utilidade das ferramentas de AI no desenvolvemento de hidroxeis multicompoñente con prestacións avanzadas. Así mesmo, explórase o potencial de combinacións ternarias de polímeros seleccionados para xerar hidroxeis termosensibles e altamente bioadhesivos para a carga e cesión de proteínas con dúas aplicacións; a vacinación sublingual e o tratamento local de úlceras colorectais na enfermidade inflamatoria intestinal (EII).

Con este fin, en primeiro lugar, levouse a cabo unha selección inicial de compoñentes e, estableceuse en cada caso un deseño experimental reducido utilizando o método de densidade balanceado.

Iso permitiu estudar, cun número moi limitado de formulacións, tanto o espazo de coñecemento coma o de deseño dos hidroxeis ternarios.

Caracterizáronse as propiedades texturometricas, reolóxicas e os perfís de cesión dos hidroxeis e, analizouse o efecto de cada compoñente nas súas características mediante o emprego combinado de redes neuronais artificiais (ANN) e técnicas de lóxica difusa.

A continuación, empregáronse ANN e GA de forma combinada para modelar e seleccionar, en cada caso, unha formulación optimizada que xelifique a temperatura fisiolóxica e que presente as mellores características para a súa aplicación e mantemento sobre a mucosa correspondente, resistencia ó lavado ou á dilución e elevada mucoadhesión.

Por último, realizáronse estudos en ratos. Por unha banda, no caso do hidroxel optimizado para aplicación sublingual, avaliouse a súa utilidade como portador da vacina CTH522 contra *Chlamydia trachomatis*. Os resultados do estudo mostraron que a estratexia máis prometedora para obter inmunidade local no tracto xenital foi a administración combinada da vacina CTH522 por vía parenteral e sublingual, utilizando respectivamente CAF01 (un sistema liposomal) e o hidroxel optimizado como portadores. Os estudos *in vivo* tamén demostraron que esta estratexia foi máis eficaz inducindo respostas inmunitarias celulares (Th1/Th17) e incrementou de maneira significativa o IFN-γ producido polos ganglios linfáticos cervicais, comparada coa vacinación parenteral soa.

Por outra banda, avaliouse a capacidade rexenerativa e antiinflamatoria do hidroxel optimizado para administración rectal previamente cargado con medio condicionado de células nai uterinas humanas (H-hUCESC-CM) nun modelo experimental de colite aguda en rato. Os datos experimentais indican que o tratamento co hidroxel cargado diminuiu significativamente a perda de peso corporal e o acurtamento do colon, a dexeneración da mucosa colónica e os niveis de ARNm de TNF-α, IFN-γ e IL-6. Os nosos datos indican que o H-hUCESC-CM alivia eficazmente a colite inducida por DSS en ratos, o que suxire que o H-hUCESC-CM podería representar unha terapia sen células moi atractiva para o tratamento local da EII.

Como conclusión, cabe destacar que o emprego de ferramentas de IA facilita enormemente o desenvolvemento de sistemas complexos e multicompoñente, dado que o seu uso permite reducir considerablemente o número de experimentos, o que aforra custos e tempo. Ademais o seu uso permite adquirir un coñecemento profundo dos sistemas farmacéuticos e establecelo espazo de deseño axeitado para cada formulación.

USC UNIVERSIDADE DE SANTIAGO DE COMPOSTELA

USC
UNIVERSIDADE
DE SANTIAGO
DE COMPOSTELA

ABSTRACT

Mucosal administration of active molecules, such as proteins, is an attractive and advantageous approach to induce local or systemic therapeutic and/or immunostimulatory responses. Critical aspects, such as rapid protein drainage or enzyme- or pH-mediated degradation, limit the residence time of therapeutic molecules on mucosal surfaces and condition the passage of substances through the mucosa and, therefore, their effectiveness.

Hydrogels are 3D polymeric networks with characteristics that can be modulated to achieve highly mucoadhesive formulations, capable of interacting with mucous membranes and increasing the residence time of drugs at the target site, enhancing their absorption and the desired therapeutic effect. In this sense, thermosensitive and mucoadhesive hydrogels are of particular interest to improve the efficacy or bioavailability of proteins when administered on mucous membranes. In addition, these hydrogels are excellent candidates to overcome the limitations of transmucosal delivery due to their biocompatibility, mucoadhesion, thermosensitivity and drug loading capacity. However, the design of such dosage forms involves the preparation of multicomponent systems, which is a challenging task. In recent years, artificial intelligence (AI) tools such as neural networks, fuzzy logic or genetic algorithms (GA) have proven to be very useful in studying the effects of composition and operational variables on the characteristics of different pharmaceutical systems.

Therefore, this thesis work addresses the usefulness of AI tools in the development of multicomponent hydrogels with advanced performance. Thus, we explore the potential of ternary combinations of selected polymers to generate thermosensitive and highly bioadhesive hydrogels suitable for protein loading and delivery with two applications; sublingual vaccination and local treatment of colorectal ulcers in inflammatory bowel disease (IBD).

For hydrogels design, after the initial selection of components, a reduced experimental design was established using a balanced density method. This made possible to delimit both the knowledge space and the design space of ternary systems using a limited number of formulations. Texturometric and rheological properties and release

profile of hydrogels were carried out. After hydrogel characterization, artificial neural networks (ANN) combined with fuzzy logic techniques were used to model the hydrogel characteristics according to their composition and, to analyze the effect of each material on their properties.

Then, the combination of ANN and GA was used to model and select, in each case, an optimal formulation that gels at physiological temperature and shows the best characteristics for application and maintenance on the corresponding mucosa (resistance to washout or dilution and high mucoadhesion).

Finally, mice experiments were conducted. In one hand, the sublingual optimized hydrogel was loaded with CTH522 *Chlamydia trachomatis* vaccine and tested in terms of immunostimulatory capacity. *In vivo* studies demonstrated that the most promising strategy for eliciting local immunity in the genital tract was parenteral-sublingual boost immunization, using CAF01 and the optimized hydrogel as carriers of CTH522 vaccine. This approach was the most effective in inducing cell-mediated immune responses (Th1/Th17) and significantly increasing IFN-γ production by cervical lymph nodes when compared with parenteral vaccination alone.

Conversely, the regenerative and anti-inflammatory capacity of the rectal optimized hydrogel, loaded with human uterine cervical stem cells conditioned medium (H-hUCESC-CM), was evaluated in an experimental mouse model of acute colitis. Experimental data indicate that treatment with the loaded hydrogel significantly decreases body weight loss, colon shortening, colonic mucosal degeneration and TNF-α, IFN-γ and IL-6 mRNA levels. Our data indicate H-hUCESC-CM effectively alleviates DSS-induced colitis in mice, suggesting that H-hUCESC-CM may represent a very attractive cell-free therapy for the local treatment of IBD.

In general, we demonstrate that the development of complex multicomponent systems is greatly facilitated by AI approaches, since their use allows a significant reduction of experiments, saving costs and time. In addition, the deep knowledge of pharmaceutical systems that derives from their use allows the establishment of the adequate design space for achieving advanced dosage forms.

RESUMO IN EXTENSO

USC
UNIVERSIDADE
DE SANTIAGO
DE COMPOSTELA

1. INTRODUCIÓN

A administración de moléculas activas na mucosa, como as proteínas, é unha aproximación moi atractiva e de indubidables vantaxes para inducir unha resposta local e/ou sistémica de carácter terapéutico e/ou inmunoestimulante. Con todo, os procesos de absorción a través das mucosas presentan limitacións importantes asociadas á propia natureza destas, con estruturas especialmente deseñadas para constituír barreiras físicas entre o organismo e o medio exterior. Aspectos críticos como a drenaxe rápida e a degradación mediada por encimas ou o pH, limitan o tempo de permanencia das moléculas terapéuticas sobre a superficie das mucosas e tamén condicionan o paso de substancias a través destes tecidos, e polo tanto, a súa utilidade [1-5].

Os hidroxeis son redes poliméricas en 3D que resultan moi útiles como formas de dosificación sobre mucosas. As súas características, moi modificables en función da súa composición, poden modularse para lograr formulacións altamente mucoadhesivas, capaces de interactuar coas mucosas e incrementalo tempo de permanencia dos fármacos no lugar de acción, conseguindo a súa absorción e o efecto terapéutico desexado [6-8]. A posibilidade de producilos por métodos suaves fainos especialmente interesantes para a formulación de fármacos cunha reducida estabilidade como as proteínas [9-14]. Neste sentido, os hidroxeis termosensibles e mucoadhesivos, resultan de especial interese para mellorala eficacia ou biodispoñibilidade destes fármacos cando se administran sobre as mucosas. A súa natureza líquida no momento da aplicación, facilita a súa completa extensión e a súa interacción coas mucosas. Trala súa administración, a súa transición sol-xel a temperatura fisiolóxica reduce as perdas da formulación por drenaxe ou a súa dilución nos fluídos corporais, facilitando a cesión dos fármacos durante un tempo adecuado [15-17]. Ademais, cando se combinan características como biocompatibilidade, mucoadhesión, termosensibilidade e a elevada capacidade de carga de fármaco dos hidroxeis, estes sistemas convértense en excelentes candidatos para superar as limitacións da administración transmucosal [6, 18-21].

Con todo, o deseño deste tipo de formas farmacéuticas implica a preparación de sistemas multicompoñente, o que supón unha tarefa desafiante no ámbito da tecnoloxía farmacéutica. Segundo o concepto de calidade por deseño (QbD), é necesario comprender e controlar o efecto de cada materia prima, as interaccións entre as mesmas e, alcanzar unha solución de compromiso para que a formulación posúa as características desexadas, como base para o deseño racional de sistemas farmacéuticos [22]. Nos últimos anos, as ferramentas de intelixencia artificial (AI) como as redes neuronais, a lóxica difusa ou os algoritmos xenéticos mostraron a súa utilidade para estudar os efectos das variables de composición e operación sobre as características de diferentes formas farmacéuticas como comprimidos, hidroxeis, nanopartículas ou micropartículas [22-26].

2. OBXECTIVOS

Neste traballo experimental abórdase a utilidade das ferramentas de AI no desenvolvemento de hidroxeis multicompoñente con prestacións avanzadas. Así mesmo, explórase o potencial de combinacións ternarias de polímeros seleccionados para xerar hidroxeis termosensibles e altamente bioadhesivos para a carga e cesión de proteínas con dúas aplicacións; a vacinación sublingual e o tratamento local de úlceras colorectais na enfermidade inflamatoria intestinal (EII).

Obxectivo I: Deseño de hidroxeis ternarios, termosensibles e mucoadhesivos como portadores de proteínas para vacinación sublingual. Propoñerase unha selección de polímeros, dos que se estudará a súa adecuación para o devandito propósito e a súa relación coas propiedades texturométricas, reolóxicas e de cesión de fármaco a partir do hidroxel. Optimizarase a composición dun hidroxel mediante ferramentas de AI e, avaliarase a súa utilidade como portador da vacina CTH522 contra *Chlamydia trachomatis* para provocar respostas inmunitarias sistémicas e/ou da mucosa en ratos. Os resultados relacionados con este obxectivo móstranse nos capítulos I e II desta memoria.

Obxectivo II: Deseño e caracterización dun clister optimizado, termosensible e altamente bioadhesivo, útil como portador de medio condicionado de células nai uterinas humanas para o tratamento local

de úlceras colorectais na EII. Propoñerase unha selección de polímeros e establecerase o espazo de deseño de formulacións de hidroxel ternario con características adecuadas (termosensibilidade, bioadhesividade, xiringabilidade e retención no tracto rectal) mediante ferramentas de AI. Optimizarase a formulación e avaliarase a capacidade rexenerativa e antiinflamatoria *in vivo* do hidroxel optimizado, previamente cargado con medio condicionado de células nai uterinas humanas nun modelo experimental de colite aguda en rato. Os resultados relacionados con este obxectivo móstranse nos capítulos III e IV desta memoria.

2. MATERIAIS E MÉTODOS

2.1 DESEÑODOS HIDROXEIS

Seleccionáronse o Pluronic® F127 (PF127), o Hybrane® S1200 (HS1200) e as variedades de Gantrez® AN119 (AN119) e S97 (S97) para o deseño dos hidroxeis de aplicación sublingual, e os Pluronic® F127 (PF127) e F68 (PF68) e o derivado celulósico Methocel® K4M (MK4M) para o do clister rectal.

No caso dos compoñentes seleccionados para o desenvolvemento de hidroxeis para vacinación sublingual, adicionalmente realizáronse ensaios de proliferación en macrófagos humanos, obtidos mediante cultivo e estimulación de monocitos THP-1 (ATCC®, EEUU), na presenza dos polímeros a diferentes concentracións. O efecto sobre a proliferación celular avaliouse utilizando o kit comercial de WST-1.

Para o deseño dos hidroxeis, tras unha selección inicial de compoñentes, estableceuse en cada caso un deseño experimental reducido mediante o software DataForm® v.3.1 (Intelligensys Ltd., UK) utilizando o método de densidade balanceado. Iso permitiu estudar, cun número moi limitado de formulacións, tanto o espazo de coñecemento coma o de deseño dos hidroxeis ternarios. O procedemento de elaboración está descrito en detalle en cada caso na sección correspondente (seccións 3.2.3, 3.2.4, 5.2.2 e 5.2.3 dos capítulos I e III).

2.2 CARACTERIZACIÓN DOS HIDROXEIS

As análises texturométricas dos hidroxeis leváronse a cabo nun texturómetro TA XT Plus (Surrey, Reino Unido), seguindo protocolos

previamente descritos [26-30]. Estes ensaios permitiron determinala xiringabilidade, a resistencia do xel ou dureza, a adhesión, a mucoadhesión e a cohesión dos hidroxeis a 37 °C.

Ademais, utilizouse un reómetro de esforzo controlado AR1000-N (TA Instruments, Reino Unido) para determinala temperatura de xelificación dos sistemas en función dos rexistros dos módulos de almacenamento (G′) e perda (G″) a diferentes temperaturas. Adicionalmente, no caso dos clisteres mediuse a viscosidade complexa de cada hidroxel a 20 ºC.

Para a avaliación *in vitro* do perfil de cesión de fármacos a partir dos hidroxeis, utilizáronse como "fármacos" modelo microesferas fluorescentes de cor verde (GFM) similares a antíxenos no caso dos hidroxeis destinados á vacinación da mucosa ou, albumina sérica bovina no caso dos clisteres. Os hidroxeis cargados colocáronse en células de cesión cun tamaño de poro de 40 μm e determinouse a porcentaxe de microesferas ou de proteína cedida a diferentes tempos usando métodos adecuados.

2.3 MODELAXE DOS HIDROXEIS UTILIZANDO TÉCNICAS DE INTELIXENCIA ARTIFICIAL

Trala caracterización dos hidroxeis, utilizouse o software FormRules® v4.03 (Intelligensys Ltd., Reino Unido) que combina redes neuronais artificiais con técnicas de lóxica difusa para modelalos resultados obtidos en función da súa composición e, así analizar o efecto que cada compoñente ten nas propiedades dos hidroxeis mediante as regras "SE-ENTÓN" que xera.

Adicionalmente, empregouse o software INForm® v.5.01 (Intelligensys, Ltd. UK) que combina as redes neuronais artificiais con algoritmos xenéticos para modelar e seleccionar, en cada caso, unha formulación optimizada que xelifique a temperatura fisiolóxica e que presente as mellores características para a súa aplicación e mantemento sobre a mucosa correspondente, resistencia ó lavado ou a dilución e elevada mucoadhesión. A calidade dos modelos avaliouse en función dos coeficientes de determinación e o ANOVA que compara os valores preditos polo modelo cos valores experimentais. Ademais, os modelos obtidos validáronse mediante a produción e caracterización das formulacións optimizadas.

2.4 AVALIACIÓN DA ACTIVIDADE TERAPÉUTICA DOS SISTEMAS DESENVOLVIDOS

2.4.1 Ensaio de inmunización en ratos

Realizouse un estudo en ratos femia CBF61 de 9 semanas para avaliar a utilidade do xel optimizado como portador sublingual da vacina CTH522 contra *Chlamydia trachomatis*, seguindo diferentes estratexias de vacinación. Para iso, os animais dividíronse en catro grupos con 3-5 ratos cada un. O esquema de inmunización móstrase na **Figura 1**. Do Grupo 1 ó 3 recibiron unha dose inicial do antíxeno CTH522 formulado en liposomas CAF01 [31] por vía subcutánea na base do rabo (Grupos 1, 2 e 3) e o Grupo 4 foi inmunizado co hidroxel optimizado (OXEL) cargado co mesmo antíxeno por vía sublingual. A segunda e terceira dose administráronse ós 15 e 35 días tal e como se describe a continuación. O Grupo 2 recibiu unha segunda e terceira dose do antíxeno CTH522 por vía sublingual. Os Grupos 3 e 4 recibiron unha segunda e terceira dose do hidroxel cargado coa vacina CTH522. O Grupo 1 non recibiu ningunha dose adicional.

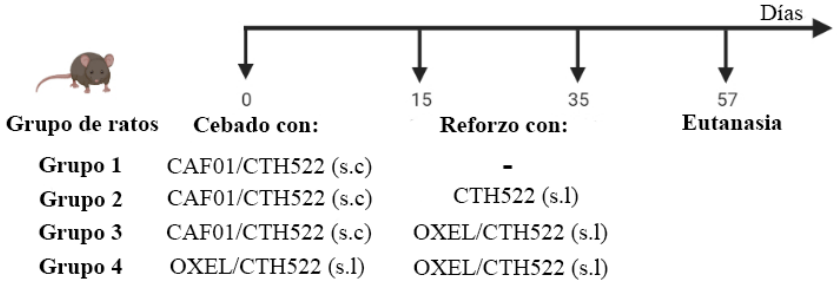

Figura 1. Esquema de inmunización e grupo de ratos testados. Os animais foron cebados por vía subcutánea (s.c) ou sublingual (s.l) usando CAF01 e OXEL como sistemas de cesión da vacina.

O día 57, os animais foron sacrificados. Ó final do estudo determináronse os anticorpos específicos IgG e IgA totais fronte a CTH522 en soro e lavado vaxinal. Adicionalmente, determináronse no bazo e nos ganglios linfáticos cervicais as concentracións de IFN-γ e IL-17A mediante ELISA. As diferenzas entre os grupos experimentais

establecéronse mediante os resultados dun ANOVA dunha vía e o test de Tukey para comparacións múltiples ($p<0.05$).

Os experimentos leváronse a cabo no Statens Serum Institut (SSI) de Dinamarca, de acordo coas regulacións establecidas polo Ministerio de Xustiza de Dinamarca e os comités de protección animal segundo o Permiso de Inspección de Experimentos con Animais Danés 2017-15-0201-01363 e de conformidade coa Directiva da Comunidade Europea 2010/63.

2.4.1 Ensaio nun modelo de rato con colite aguda

Realizouse un estudo nun modelo de colite aguda en ratos macho C57BL/6 para avaliar a utilidade do clister optimizado e cargado con medio condicionado de células nai cervicais humanas, para o tratamento local de úlceras colorectais en EII.

Para comprobar a utilidade dos hidroxeis cargados con medio condicionado na EII, utilizouse o protocolo descrito por Wirtz et al. (**Figura 2**) [32]. Induciuse unha colite aguda en ratos mediante a administración de dextrano sulfato de sodio (DSS) ó 3.5% na auga de bebida durante 9 días. Entre os días 10 e 15, administráronse dúas veces ao día 75 µl de cada tratamento por vía rectal utilizando unha agulla de punta redondeada de calibre 26. Os animais dividíronse en 5 grupos como segue: 1) Grupo de control san; 2) Grupo non tratado: ratos que non recibiron ningún tipo de tratamento tras a administración do DSS; 3) Grupo control H-DMEM-F12: ratos tratados soamente co hidroxel tras a indución da colite; 4) Grupo H-hUCESC-CM: ratos tratados co hidroxel cargado con medio condicionado tras a indución da colite; e 5) Grupo mesalazina (MZ): ratos tratados con escuma de mesalazina tras a indución da colite (tratamento habitual da EII). Ós animais practicóuselles a eutanasia no día 16 de ensaio.

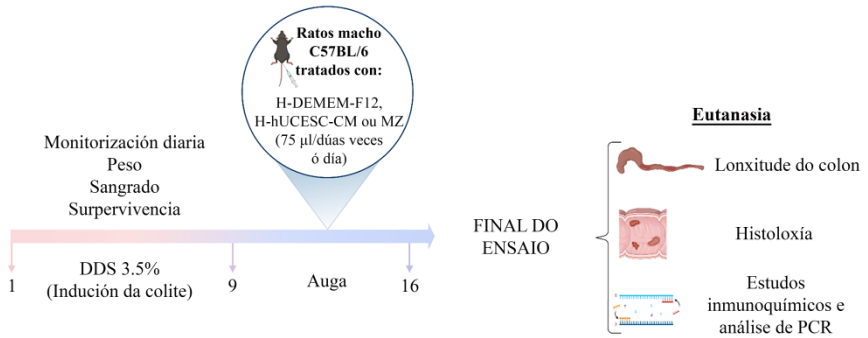

Figura 2. Diagrama do estudo. Indución da colite nos animais usando DSS e parámetros avaliados.

Avaliáronse os síntomas clínicos (supervivencia, cambios no peso corporal, consistencia das feces e severidade do sangrado) e, tras o sacrificio dos animais levouse a cabo un exame macroscópico do colon (lonxitude). Adicionalmente, tamén se levou a cabo unha avaliación histolóxica (grao de inflamación e infiltración celular, ulceracións microscópicas, arquitectura das criptas, atrofia e displasia epitelial) e a extracción de ARNm do colon para a realización de PCRs cuantitativas en tempo real para determinala expresión de TNF-α, IL-6 e IFN-γ.

Este estudo realizouse segundo o protocolo aprobado polo Comité de Ética de Experimentos con Animais da Universidade de Santiago de Compostela.

3. RESULTADOS E DISCUSIÓN

3.1 HIDROXEIS TERNARIOS, TERMOSENSIBLES E MUCOADHESIVOS COMO SISTEMAS PORTADORES DE PROTEÍNAS PARA VACINACIÓN SUBLINGUAL

En primeiro lugar, proponse a combinación do PF127, HS1200 e Gantrez® (AN119 ou S97) como materias primas para producir un hidroxel de aplicación sublingual, útil para a inmunización da mucosa. Os estudos realizados para lograr este obxectivo preséntanse no Capítulo I e aparecen resumidos na **Figura 3**.

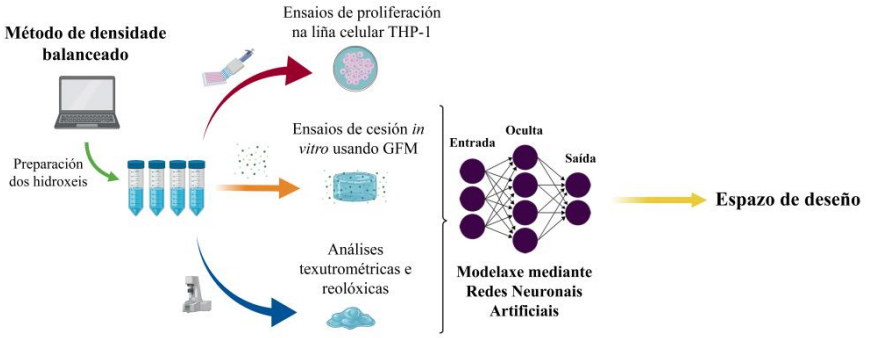

Figura 3. Diagrama xeral dos ensaios descritos no Capítulo I.

Os estudos realizados en macrófagos indicaron un potencial efecto inmunoestimulante do HS1200, promovendo a proliferación das devanditas células presentadoras de antíxeno. Por outra banda, ningún polímero presentou toxicidade algunha. As ferramentas de AI, en particular a combinación das redes neuronais artificiais coa lóxica difusa (neurofuzzy logic) permitiron establecer o papel de cada polímero no comportamento reolóxico e texturométrico do hidroxel, así como a súa capacidade para retelas microesferas (GFM) empregadas como antíxeno modelo. Así, a interacción entre o PF127 e o Gantrez® condiciona tanto a temperatura de xelificación como os traballos de mucoadhesión e adhesión, ou a resistencia do xel. Observáronse diferenzas entre as dúas variedades de Gantrez® avaliadas, sendo a variedade S97 a que permite unha cesión das micropartículas máis prolongada. A incorporación do HS1200 na formulación deu lugar a unha redución tanto na resistencia do xel como na súa capacidade de adhesión.

Utilizouse a combinación de redes neuronais artificiais con algoritmos xenéticos para modelala composición dos hidroxeis e optimizalo proceso, é dicir, seleccionar a composición ternaria que proporciona sistemas de máxima mucoadhesión, cohesión e resistencia e, que ademais xelifiquen a temperatura corporal. Os estudos realizados para lograr este obxectivo preséntanse no capítulo II e aparecen resumidos na **Figura 4**.

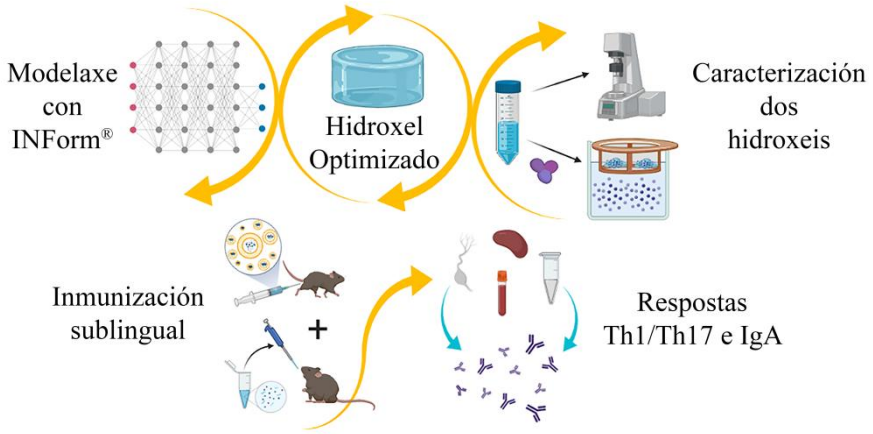

Figura 4. Diagrama xeral cos ensaios descritos no Capítulo II.

Elaborouse e caracterizouse o hidroxel coa composición óptima elixida polo modelo (21.1% de PF127, 5% de HS1200 e 0.08% de Gantrez® AN119). Adicionalmente, almacenouse en condicións controladas para avaliar a súa estabilidade. Tanto as características reolóxicas e texturométricas dos hidroxeis elaborados coma as preditas polo modelo concordaron completamente, o que permitiu a súa validación. Ademais, a formulación resultou ser estable.

A potencial utilidade do hidroxel optimizado como portador da vacina CTH522 fronte a *Chlamydia trachomatis* por vía sublingual avaliouse nun modelo de rato. Os resultados do estudo mostraron que a estratexia máis prometedora para obter inmunidade local no tracto xenital foi a administración combinada da vacina CTH522 por vía parenteral e sublingual, utilizando CAF01 (sistema liposomal) e o hidroxel optimizado como portadores, respectivamente. As propiedades termosensibles do hidroxel facilitan a súa aplicación debaixo da lingua e aumentan o seu contacto co tecido sublingual; polo que a súa xelificación a temperatura corporal xunto coa rápida cesión da proteína debe evitar a súa perda ó tragar e promover a súa absorción. Os estudos *in vivo* tamén demostraron que a inmunización combinada parenteral-sublingual foi máis eficaz inducindo IgA no tracto xenital e respostas inmunitarias celulares (Th1/Th17) que a vacinación da mucosa ou parenteral soa. Ademais, esta estratexia

provocou un incremento significativo do IFN-γ nos ganglios linfáticos cervicais comparada coa vacinación parenteral soa.

3.2 CLISTER TERMOSENSIBLE E ALTAMENTE MUCOADHESIVO COMO PORTADOR DE HUCESC-CM PARA O TRATAMENTO LOCAL DE ÚLCERAS COLORECTAIS EN EII

Proponse a combinación de PF127, PF68 e MK4M como materias primas para lograr un hidroxel útil para o tratamento de úlceras na mucosa colónica, características da enfermidade inflamatoria intestinal. Os estudos realizados para acadalo devandito obxectivo preséntanse no Capítulo III e aparecen resumidos na **Figura 5**.

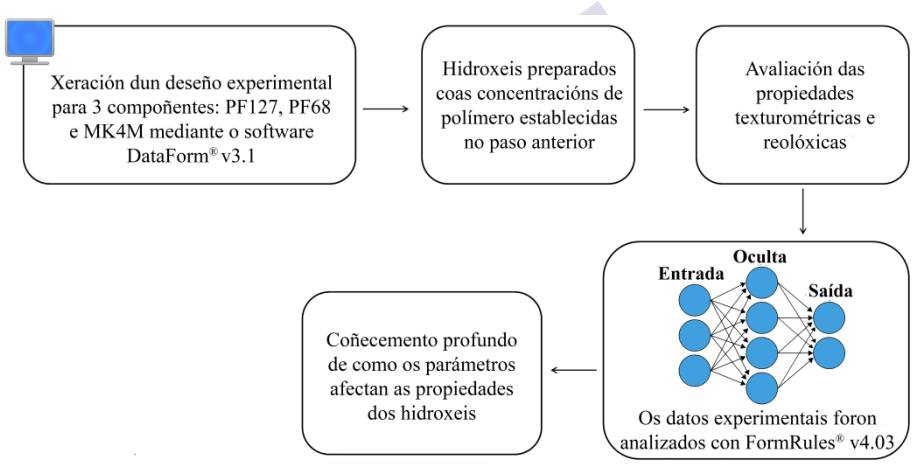

Figura 5. Diagrama xeral cos ensaios descritos no Capítulo III.

Coma no caso anterior, empregáronse as mesmas ferramentas de AI para estudar o efecto de cada ingrediente nas propiedades dos hidroxeis. Establecéronse os espazos de coñecemento e de deseño para producir sistemas termosensibles e altamente bioadhesivos, capaces de cargar e ceder material proteico. A xiringabilidade das mesturas ternarias está directamente relacionada coa proporción de PF127 no sistema. Ámbolos dous Pluronic® condicionan a temperatura de xelificación, a cal incrementase a medida que se incorpora PF68 no sistema. Por outra banda, o derivado celulósico contribúe á viscosidade e á bioadhesión do hidroxel.

De novo, a modelaxe con redes neuronais artificiais e algoritmos xenéticos permitiu seleccionar unha formulación que presentase unha xiringabilidade adecuada (<86 mJ para unha agulla de 24Gx1.5"), unha temperatura de xelificación entre 25-27 ºC e unha bioadhesion elevada. O sistema está composto por un 16.34% de PF127, un 2.55% de PF68 e un 0.26% de MK4M. As características fisicoquímicas obtidas para a formulación optimizada resultaron ser moi similares ás preditas polo modelo, o que permitiu a súa validación.

Este hidroxel empregouse como portador de medio condicionado derivado de células nai cervicais uterinas humanas (H-hUCESC-CM). Os resultados do estudo *in vivo* nun modelo experimental de rato con colite aguda preséntanse no capítulo IV e aparecen resumidos na **Figura 6.**

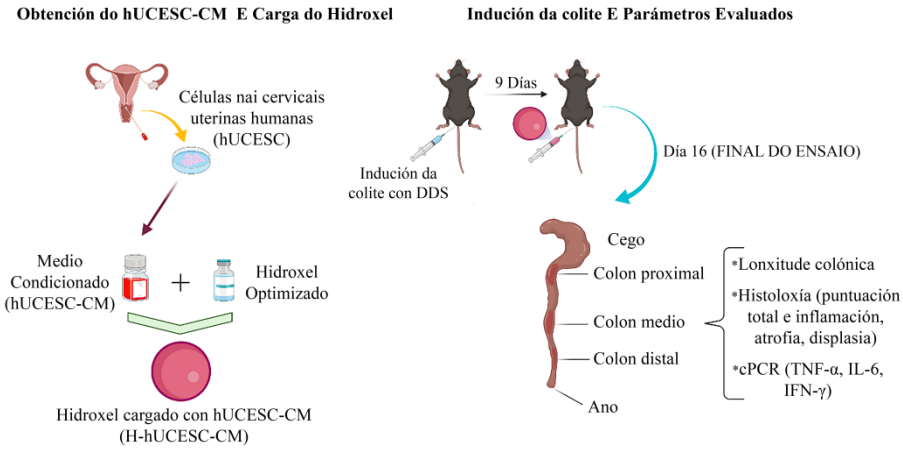

Figura 6. Diagrama xeral cos ensaios descritos no Capítulo IV.

Desta maneira, os datos experimentais indican que o tratamento co hidroxel cargado diminuiu significativamente a perda de peso corporal e o acurtamento do colon, a dexeneración da mucosa colónica e os niveis de ARNm de TNF-α, IFN-γ e IL-6. Os datos indican que o H-hUCESC-CM alivia eficazmente a colite inducida por DSS en ratos, suxerindo que o H-hUCESC-CM podería representar unha terapia sen células moi atractiva para o tratamento local da EII.

4. CONCLUSIÓNS

1. As ferramentas de IA permitiron estudar facilmente o espazo de coñecemento e establecer o espazo de deseño de formulacións ternarias para administración sublingual e rectal, incluso utilizando deseños experimentais moi reducidos. A modelaxe dos datos experimentais con estas tecnoloxías híbridas facilita extraordinariamente o deseño de hidroxeis con prestacións avanzadas. A técnica de "neurofuzzy logic" permitiu dilucidar os efectos de cada compoñente na formulación, así como as súas interaccións sobre o comportamento texturométrico, reolóxico e de liberación destes hidroxeis ternarios; adquirindo así un coñecemento profundo sobre o papel que desenrolan nos sistemas. Por outra banda, a combinación de redes neuronais artificiais e algoritmos xenéticos permitiu optimizar varias variables á vez, atopando a mellor formulación posible dentro do espazo de deseño.

2. Unha combinación adecuada de PF127, HS1200 e Gantrez® (AN119 ou S97) permitiu obter hidroxeis termosensibles e altamente mucoadhesivos con características adecuadas para a administración sublingual de moléculas proteicas (un xel cunha alta resistencia, mucoadhesión e cohesión e, rápida liberación de fármaco). Ademais, o HS1200 mostrou capacidade inmunoestimulante, potencialmente útil como adxuvante para o desenvolvemento de vacinas. O hidroxel optimizado acadado para a administración da vacina CTH522 foi capaz de estenderse sobre a mucosa sublingual, previr a fuga da proteína recombinante por inxestión ou dilución na saliva e, inducir a súa liberación de forma rápida para garantir unha absorción completa a través do tecido da mucosa oral.

   A formulación cargada coa vacina CTH522 probada en ratos CBF61 femia, mostrou unha efectividade dependente da estratexia de inmunización. Os resultados demostraron que a inmunización combinada de reforzo parenteral- sublingual foi capaz de provocar unha resposta de IgA local no tracto xenital

e mellorar de forma significativa a produción de IFN-γ polos ganglios linfáticos cervicais en comparación coa inmunización parenteral con liposomas CAF01.

3. Combinacións adecuadas de PF127, PF68 e MK4M son útiles para preparar clisteres que experimentan unha rápida transición de estado líquido a sólido cando alcanzan a temperatura corporal, minimizando a fuga e/ou a dilución das moléculas terapéuticas. Estas fórmulas intelixentes exhibiron unha boa bioadhesividade e unha rápida liberación do fármaco, e están deseñadas para promover un efecto inmediato sobre a mucosa intestinal danada. Desenvolveuse un hidroxel optmizado de caracterísiticas desexadas que mostrou unha xiringabilidade, bioadhesión e temperatura de xelificación adecuadas.

   Os resultados nun modelo de colite aguda en rato mostraron que esta formulación optimizada, cargada con medio condicionado de células nai uterinas cervicais humanas podería representar unha terapia atractiva sen necesidade de empregar células para o tratamento local das úlceras colorectais presentes na enfermidade inflamatoria intestinal.

REFERENCES

[1] J. Mayr, C. Saldias, D. Diaz Diaz, Release of small bioactive molecules from physical gels, Chem Soc Rev, 47 (2018) 1484-1515.
[2] A.A. Koffi, F. Agnely, G. Ponchel, J.L. Grossiord, Modulation of the rheological and mucoadhesive properties of thermosensitive poloxamer-based hydrogels intended for the rectal administration of quinine, Eur J Pharm Sci, 27 (2006) 328-335.
[3] A. Miquel-Clopes, E.G. Bentley, J.P. Stewart, S.R. Carding, Mucosal vaccines and technology, Clin Exp Immunol, 196 (2019) 205-214.
[4] M. Li, Y. Wang, Y. Sun, H. Cui, S.J. Zhu, H.J. Qiu, Mucosal vaccines: Strategies and challenges, Immunol Lett 217 (2020) 116-125.
[5] S. Longet, M.L.E Lundahl, E.C Lavelle, Targeted Strategies for Mucosal Vaccination, Bioconjug Chem 29 (2018) 613-23.
[6] F. Zahir-Jouzdani, J.D. Wolf, F. Atyabi, A. Bernkop-Schnürch, In situ gelling and mucoadhesive polymers: why do they need each other?, Expert Opinion on Drug Delivery, 15 (2018) 1007-1019.
[7] J. Chen, R. Zhou, L. Li, B. Li, X. Zhang, J. Su, Mechanical, rheological and release behaviors of a poloxamer 407/ poloxamer 188/carbopol 940 thermosensitive composite hydrogel, Molecules, 18 (2013) 12415-12425.
[8] J. Xu, M. Tam, S. Samaei, S. Lerouge, J. Barralet, M.M. Stevenson, M. Cerruti, Mucoadhesive chitosan hydrogels as rectal drug delivery vessels to treat ulcerative colitis, Acta Biomater, 48 (2017) 247-257.
[9] R. Waters, S. Pacelli, R. Maloney, I. Medhi, R.P. Ahmed, A. Paul, Stem cell secretome-rich nanoclay hydrogel: a dual action therapy for cardiovascular regeneration, Nanoscale, 8 (2016) 7371-7376.
[10] K.O. Allbright, J.M. Bliley, E. Havis, D.Y. Kim, G.A. Dibernardo, D. Grybowski, M. Waldner, I.B. James, W.N. Sivak, J.P. Rubin, K.G. Marra, Delivery of adipose-derived stem cells in poloxamer hydrogel improves peripheral nerve regeneration, Muscle Nerve, 58 (2018) 251-260.
[11] E.S. DeLyria, D. Zhou, J.S. Lee, S. Singh, W. Song, F. Li, Q. Sun, H. Lu, J. Wu, Q. Qiao, Y. Hu, G. Zhang, C. Li, K.J. Sastry, H.

Shen, Sublingual injection of microparticles containing glycolipid ligands for NKT cells and subunit vaccines induces antibody responses in oral cavity, Carbohydr Res, 405 (2015) 87-92.
[12] Y. Wu, W. Wei, M. Zhou, Y. Wang, J. Wu, G. Ma, Z. Su, Thermal-sensitive hydrogel as adjuvant-free vaccine delivery system for H5N1 intranasal immunization, Biomaterials, 33 (2012) 2351-2360.
[13] F. Raza, H. Zafar, Y. Zhu, Y. Ren, A. Ullah, A.U. Khan, X. He, H. Han, M. Aquib, K.O. Boakye-Yiadom, L. Ge, A Review on Recent Advances in Stabilizing Peptides/Proteins upon Fabrication in Hydrogels from Biodegradable Polymers, Pharmaceutics, 10 (2018).
[14] M.R. Matanovic, J. Kristl, P.A. Grabnar, Thermoresponsive polymers: insights into decisive hydrogel characteristics, mechanisms of gelation, and promising biomedical applications, Int J Pharm, 472 (2014) 262-275.
[15] L. Garcia-del Rio, P. Diaz-Rodriguez, M. Landin, Design of novel orotransmucosal vaccine-delivery platforms using artificial intelligence, European Journal of Pharmaceutics and Biopharmaceutics, 159 (2021) 36-43.
[16] M.L. Bruschi, O. de Freitas, Oral Bioadhesive Drug Delivery Systems. Drug Development and Industrial Pharmacy, 31 (2005) 293-310.
[17] A.I. Mendes, A.C Silva, J.A. Catita, F. Cerqueira, C. Gabriel, C.M. Lopes, Miconazole-loaded nanostructured lipid carriers (NLC) for local delivery to the oral mucosa: improving antifungal activity, Colloids Surf B Biointerfaces, 111 (2013) 755-763.
[18] L. Mude, B.K.R. Sanapalli, A.N. V, S.K. Singh, V. Karri, Overview of in situ gelling injectable hydrogels for diabetic wounds, Drug development research, (2021).
[19] M.R. Matanovic, J. Kristl, P.A. Grabnar, Thermoresponsive polymers: insights into decisive hydrogel characteristics, mechanisms of gelation, and promising biomedical applications, Int J Pharm, 472 (2014) 262-275.
[20] D.F. Argenta, B.D.C. Bernardo, A.F. Chamorro, P.R. Matos, T. Caon, Thermosensitive hydrogels for vaginal delivery of secnidazole

as an approach to overcome the systemic side-effects of oral preparations, Eur J Pharm Sci, 159 (2021) 105722.
[21] K. Bouchemal, A. Aka-Any-Grah, N. Dereuddre-Bosquet, L. Martin, V. Lievin-Le-Moal, R. Le Grand, V. Nicolas, D. Gibellini, D. Lembo, C. Pous, A. Koffi, G. Ponchel, Thermosensitive and mucoadhesive pluronic-hydroxypropylmethylcellulose hydrogel containing the mini-CD4 M48U1 is a promising efficient barrier against HIV diffusion through macaque cervicovaginal mucus, Antimicrob Agents Chemother, 59 (2015) 2215-2222.
[22] M. Landín, Introducción al uso de sistemas de inteligencia artificial para modelizar, comprender y optimizar formulaciones farmacéuticas, in: Biomateriais aplicados ao desenvolvimento de sistemas terapêuticos avançados, 2015, pp. 521-554.
[23] M.O. Jara, J. Catalan-Figueroa, M. Landin, J.O. Morales, Finding key nanoprecipitation variables for achieving uniform polymeric nanoparticles using neurofuzzy logic technology, Drug Deliv Transl Res, (2017).
[24] R. Rodriguez-Dorado, M. Landin, A. Altai, P. Russo, R.P. Aquino, P. Del Gaudio, A novel method for the production of core-shell microparticles by inverse gelation optimized with artificial intelligent tools, Int J Pharm, 538 (2018) 97-104.
[25] R. Lopez-Cebral, V. Romero-Caamano, B. Seijo, C. Alvarez-Lorenzo, M. Martin-Pastor, A. Concheiro, M. Landin, A. Sanchez, Spermidine cross-linked hydrogels as a controlled release biomimetic approach for cloxacillin, Mol Pharm, 11 (2014) 2358-2371.
[26] P. Diaz-Rodriguez, M. Landin, Smart design of intratumoral thermosensitive beta-lapachone hydrogels by Artificial Neural Networks, Int J Pharm, 433 (2012) 112-118.
[27] H. Blanco-Fuente, S. Anguiano-Igea, F.J. Otero-Espinar, J. Blanco-Méndez, In-vitro bioadhesion of carbopol hydrogels, International Journal of Pharmaceutics, 142 (1996) 169-174.
[28] R. Nigmatullin, V. Gabrielli J.C. Muñoz-García, A.E. Lewandowska, R. Harniman, Y.Z. Khimyak, et al. Thermosensitive supramolecular and colloidal hydrogels via self-assembly modulated by hydrophobized cellulose nanocrystals, Cellulose, 26 (2019) 529-542.

[29] C.A. Ramírez Barragán, E.R. Macías Balleza, L. García-Uriostegui, J.A. Andrade Ortega, G. Toríz, E. Delgado, Rheological characterization of new thermosensitive hydrogels formed by chitosan, glycerophosphate, and phosphorylated β-cyclodextrin. Carbohydrate polymers, 201 (2018) 471-481.
[30] M. Campana-Seoane, A. Peleteiro, R. Laguna, F.J. Otero-Espinar. Bioadhesive emulsions for control release of progesterone resistant to vaginal fluids clearance. Int J Pharm, 477 (2014) 495-505.
[31] C.B. Roces, S. Khadke, D. Christensen, Y. Perrie, Scale-Independent Microfluidic Production of Cationic Liposomal Adjuvants and Development of Enhanced Lymphatic Targeting Strategies, Mol Pharm, 16 (2019) 4372-4386.
[32] S. Wirtz, V. Popp, M. Kindermann, K. Gerlach, B. Weigmann, S. Fichtner-Feigl, M.F. Neurath, Chemically induced mouse models of acute and chronic intestinal inflammation, Nat Protoc, 12 (2017) 1295-1309.

USC UNIVERSIDADE DE SANTIAGO DE COMPOSTELA

USC
UNIVERSIDADE
DE SANTIAGO
DE COMPOSTELA

EXPANDED ABSTRACT

USC
UNIVERSIDADE
DE SANTIAGO
DE COMPOSTELA

1. INTRODUCTION

Mucosal administration of active molecules, such as proteins, is an attractive and advantageous approach to induce local or systemic therapeutic and/or immunostimulatory responses. However, absorption processes through mucous membranes present important limitations associated with their nature, whose structures are specially designed to constitute the physical barriers between the organism and the external environment. Critical aspects such as rapid protein drainage and enzyme- or pH-mediated degradation limit the residence time of therapeutic molecules on mucosal surfaces and condition the passage of substances through the mucosa and therefore, their usefulness [1-5].

Hydrogels are 3D polymeric networks very useful as mucosal dosage forms. Their characteristics, which are highly tunable depending on their composition, can be modulated to achieve highly mucoadhesive formulations, capable of interacting with mucous membranes and increasing the residence time of drugs at the target site, enhancing their absorption and the desired therapeutic effect [6-8]. The possibility of preparing hydrogels by gentle methods makes them particularly attractive for the formulation of drugs with low stability, such as proteins [9-14]. In this sense, thermosensitive and mucoadhesive hydrogels are of particular interest to improve the efficacy and bioavailability of these drugs when administered on mucous membranes. Their liquid nature when administered facilitates their complete spreading and interaction with mucous membranes. After administration, their sol-gel transition at physiological temperature reduces runoffs or dilution in body fluids, favouring drug absorption and guaranteeing the maintenance of the formulation in the area until all dose is absorbed [15-17]. In addition, these hydrogels are excellent candidates to overcome the limitations of transmucosal delivery due to their biocompatibility, mucoadhesion, thermosensitivity and drug loading capacity [6, 18-21]. However, the design of such dosage forms involves the preparation of multicomponent systems, which is a challenging task in the field of pharmaceutical technology. According to the concept of quality by design (QbD), for the rational design of these systems it is necessary

to understand and control the effect of each raw material, the interactions between them, and to reach a compromise solution to formulate hydrogels with desired characteristics [22].

In recent years, artificial intelligence (AI) tools such as neural networks, fuzzy logic or genetic algorithms have proven to be very useful in studying the effects of composition and operational variables on the characteristics of different dosage forms such as tablets, hydrogels, nanoparticles or microparticles [22-26].

2. OBJECTIVES

This thesis work addresses the usefulness of AI tools in the development of multicomponent hydrogels with advanced performance. Thus, we explore the potential of ternary combinations of selected polymers to generate thermosensitive and highly bioadhesive hydrogels for protein loading and delivery with two applications; sublingual vaccination and local treatment of colorectal ulcers in inflammatory bowel disease (IBD).

Objective I: Design of ternary, thermosensitive and mucoadhesive hydrogels as protein carriers for sublingual vaccination. A selection of polymers will be proposed, their suitability and influence on texturometric, rheological and drug release properties will be studied. In addition, the composition of the hydrogel will be optimized using AI tools and, the usefulness of the optimized hydrogel as a *Chlamydia trachomatis* vaccine carrier to elicit systemic and/or mucosal immune responses in mice will be evaluated. The results related to this objective are shown in chapters I and II of this report.

Objective II: Design and characterization of an optimized, thermosensitive and highly mucoadhesive enema useful as a human cervical stem cell conditioned medium carrier for the local treatment of colorectal ulcers in IBD. Polymer selection will be proposed and the design space of ternary hydrogel formulations with suitable characteristics (thermosensitivity, mucoadhesivity, extensibility and retention in the rectal tract) will be established using AI tools. Then, a formulation will be optimized and the *in vivo* regenerative and anti-inflammatory capacity of the optimized hydrogel, loaded with human cervical stem cell conditioned medium, will be evaluated in an

experimental model of acute colitis in mice. The results related to this objective are shown in chapters III and IV of this thesis.

2. MATERIALS AND METHODS

2.1 HYDROGELS DEVELOPMENT

Pluronic® F127 (PF127), Hybrane® S1200 (HS1200) and Gantrez® varieties AN119 (AN119) and S97 (S97) were selected for the design of sublingual hydrogels, whereas Pluronic® F127 (PF127) and F68 (PF68) and the cellulosic derivative Methocel® K4M (MK4M) for the rectal enema.

For the selected components to develop hydrogels for sublingual vaccination, proliferation assays were performed on human macrophages, obtained by culture and stimulation of THP-1 monocytes (ATCC®, USA), in the presence of the polymers at different concentrations. The effect on cell proliferation was assessed using the WST-1 assay kit.

For hydrogels design, after the initial selection of components, a reduced experimental design was established through DataForm® v.3.1 software (Intelligensys Ltd., UK) using a balanced density method. This made possible to delimit both the knowledge space and the design space of ternary systems using a limited number of formulations. The elaboration procedure is described in detail in each case, in the corresponding section (sections 3.2.3, 3.2.4, 5.2.2 and 5.2.3 of chapters I and III).

2.2 HYDROGELS CHARACTERIZATION

Texturometric analysis of hydrogels was carried out on a TA XT Plus Texture Analyzer (Surrey, UK), following previously described protocols [26-30]. This allowed the determination of syringeability parameters, gel strength, adhesion, mucoadhesion and cohesion work of hydrogels at 37 °C.

In addition, an AR1000-N controlled stress rheometer (TA Instruments, UK) was used to determine the gelation temperature of the hydrogels as a function of storage (G′) and loss (G″) moduli records at different temperatures. In addition, the complex viscosity of each hydrogel was measured at 20 °C.

For the evaluation of the *in vitro* drug release profile from hydrogels, green fluorescent antigen-like microspheres (GFM) in the case of hydrogels intended for mucosal vaccination or bovine serum albumin in the case of rectal enemas were used as "model drugs". Loaded hydrogels were placed in 40 μm pore size release strainers and the percentage of microspheres or protein released at pre-set times was determined by the appropriate method.

2.3 HYDROGEL MODELIZATION USING ARTIFICIAL INTELLIGENCE TECHNIQUES

The software FormRules® v4.03 (Intelligensys Ltd., UK), which combines artificial neural networks with fuzzy logic techniques, was used to model the hydrogel characteristics according to their composition and to analyze the effect of each material on the properties of the hydrogels using the "IF-THEN" rules it generates.

In addition, INForm® v.5.01 software (Intelligensys, Ltd. UK) was used to combine artificial neural networks with genetic algorithms to model and select, in each case, an optimal formulation that gels at physiological temperature and has the best characteristics for its application and maintenance on the corresponding mucosa (resistance to washout or dilution and high mucoadhesion). The quality of the models was assessed on the basis of the determination coefficients and ANOVAs, which compare the values predicted by the model with the experimental values. The models obtained were validated by the production and characterization of optimized formulations.

2.4 EVALUATION OF THE THERAPEUTIC ACTIVITY OF DEVELOPED SYSTEMS

2.4.1 Mouse immunization assay

A study was conducted in 9-week-old female CBF61 mice to evaluate the usefulness of the optimized hydrogel as a carrier for sublingual vaccines against *Chlamydia trachomatis* following different vaccination strategies. For this purpose, animals were divided into four groups of three to five mice. The immunization schedule is depicted in **Figure 1**. Groups 1 to 3 were subcutaneously

primed at the base of the tail with CTH522 chlamydia vaccine formulated in CAF01 liposomes [31]. Group 4 was sublingually primed with CTH522 vaccine dispersed in the optimized hydrogel (OGEL). Then, groups 2 to 4 were boosted twice sublingually (days 15 and 35) with CTH522 alone (Group 2) or included within the optimized system (Groups 3 and 4). Group 1 received no additional doses.

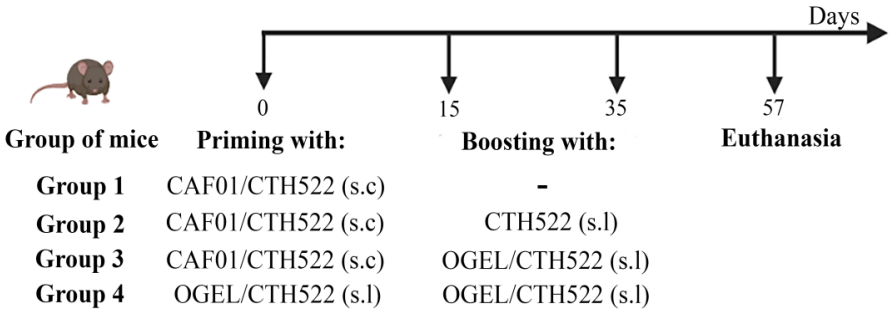

Figure 1. Immunization schedule and experimental groups tested. Animals were primed subcutaneously (s.c) or sublingually (s.l) using CAF01 and OGEL as vaccine delivery systems.

On day 57, mice were euthanized. Total IgG and IgA CTH522-specific antibodies were determined in serum and vaginal lavages at the end of the study. Additionally, IFN-γ and IL-17A concentrations were determined in spleen and cervical lymph nodes by ELISA. Differences between experimental groups were established by one-way ANOVA and Tukey's test for multiple comparisons ($p<0.05$).

Experiments were conducted at the Statens Serum Institut (SSI) in Denmark, in accordance with the regulations establish by the Danish Ministry of Justice and Animal Protection committees by the Danish Animal Experiments Inspection Permit 2017-15-0201-01363 and in accordance with the European Community Directive 2010/63.

2.4.1 Experimental mouse model of acute colitis

An acute colitis model study was performed in male C57BL/6 mice to evaluate the usefulness of an optimized enema loaded with conditioned medium from human cervical stem cells, for the local treatment of colorectal ulcers in IBD.

To this end, the protocol described by Wirtz et al [32] was used (**Figure 2**). Acute colitis was induced in mice by the administration of 3.5% dextran sulphate sodium (DSS) in the drinking water for 9 days. Between 10 and 15 days, 75 µl of each treatment was administered rectally twice daily using a 26-gauge probe needle. The animals were divided into 5 groups as follows: 1) Healthy control group; 2) Untreated group: mice that have not received any treatment after DSS administration; 3) H-DMEM-F12 control group: mice treated with the hydrogel after colitis induction; 4) H-hUCESC-CM group: mice treated with the gel loaded with conditioned medium after colitis induction; and 5) Mesalazine (MZ) group: mice treated with mesalazine foam after colitis induction (standard treatment in IBD). On day 16 animals were euthanized.

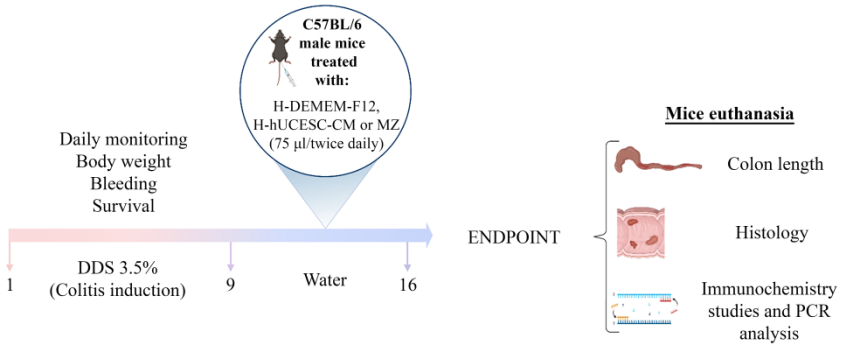

Figure 2. Diagram of the study design for DSS-induced colitis and parameters evaluated.

Clinical symptoms (survival, changes in body weight, stool consistency and bleeding severity) were assessed and, after euthanized animals, a macroscopic examination of the colon (length) was performed. In addition, histological evaluation (degree of inflammation and cellular infiltration, microscopic ulcerations, crypt architecture, epithelial atrophy and dysplasia) and mRNA extraction from colon samples for real-time quantitative PCR determining TNF-α, IL-6, and IFN-γ expression were performed.

The study was performed according to the protocol approved by the Ethics Committee for Animal Experiments of the University of Santiago de Compostela.

3. RESULTS AND DISCUSSION

3.1 THERMOSENSITIVE AND MUCOADHESIVE TERNARY HYDROGELS AS PROTEIN CARRIERS FOR SUBLINGUAL IMMUNIZATION

First, the combination of PF127, HS1200 and Gantrez® (AN119 or S97) is proposed to produce a hydrogel for sublingual application, useful for mucosal immunization. The studies carried out for this purpose are presented in chapter I and summarized in **Figure 3**.

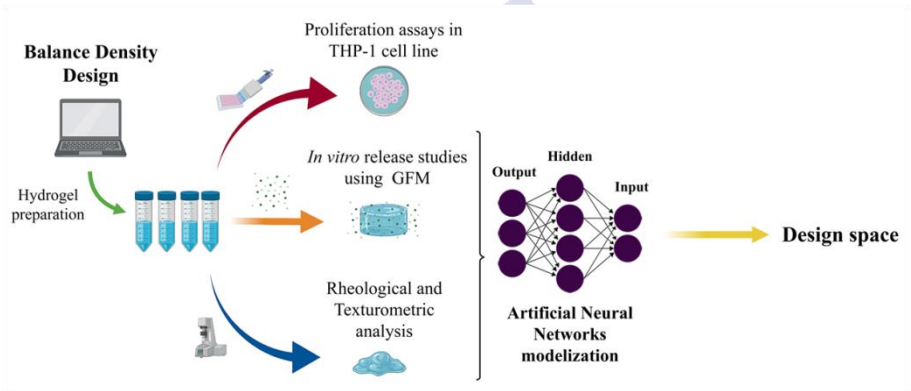

Figure 3. General diagram of assays performed on Chapter I.

Studies on macrophages indicated a potential immunostimulatory effect of HS1200 by promoting the proliferation of these antigen-presenting cells. On the other hand, no toxicity was observed for any of the polymers. AI tools, in particular the combination of artificial neural networks and fuzzy logic (neurofuzzy logic) allowed to establish the role of each polymer in the rheological and texturometric behaviour of hydrogels, as well as its capacity to retain microspheres used as model antigen (GFM). Thus, the interaction between PF127 and Gantrez® rules gelation temperature, mucoadhesion and adhesion work and, gel strength. Differences were observed between the two varieties of Gantrez® evaluated, with the S97 variety allowing a slower microspheres release. The incorporation of HS1200 in the

formulation resulted in a reduction in gel strength and adhesion capacity.

The combination of artificial neural networks and genetic algorithms was used to model the composition of hydrogels and to optimize the process and thus select the ternary composition that provides systems with maximum mucoadhesion, cohesion and gel strength, and which also gel at body temperature. The studies carried out for this purpose are presented in chapter II and summarized in **Figure 4**.

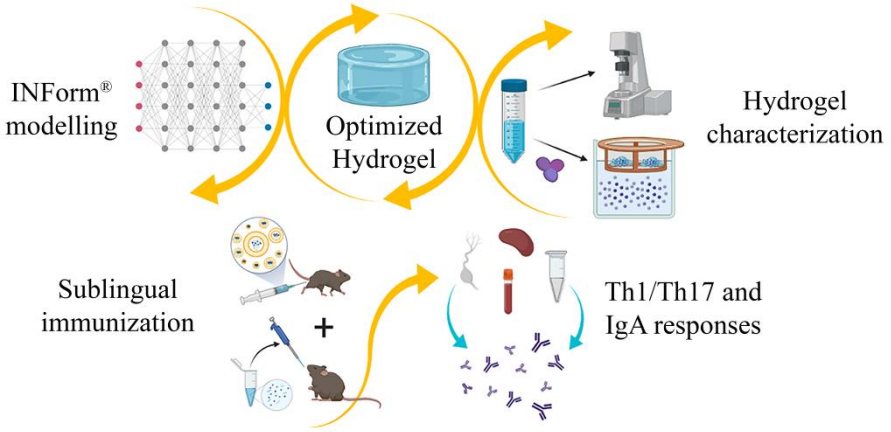

Figure 4. General diagram of assays performed on Chapter II.

The optimal composition selected by the model generated by the INForm® software (21.1% PF127, 5% HS1200 and 0.08% Gantrez® AN119) was elaborated and characterized. Additionally, it was stored under controlled conditions to evaluate its stability. The rheological and texturometric characteristics of the elaborated hydrogels are in complete agreement with those predicted by the model, which allowed its validation. Furthermore, the formulation was found to be stable.

The potential usefulness of this optimized hydrogel as sublingual carrier of CTH522 *Chlamydia trachomatis* vaccine was evaluated in a mouse model. The results of the study showed that the most promising strategy for obtaining local genital tract immunity was the combination of parenteral priming with CTH522 included in

liposomes, followed by sublingual boosting with the CTH522 vaccine-loaded optimized hydrogel, which achieved the best immune responses. The thermosensitive properties of the hydrogel facilitate its application under the tongue and increased contact with the sublingual tissue. The gelation at body temperature together with the fast release of antigen must prevent the loss of CTH522 vaccine by swallowing and promote its absorption. *In vivo* studies demonstrated that parenteral-sublingual boost immunization, using CAF01 and the optimized hydrogel as carriers of CTH522 vaccine, was more effective in inducing cell-mediated immune responses (Th1/Th17) than mucosal or parenteral vaccination alone. In addition, this strategy resulted in an increase in local production of IgA in the genital tract.

3.2 THERMOSENSITIVE AND HIGHLY BIOADHESIVE ENEMA AS CARRIER OF H-UCESC-CM FOR LOCAL TREATMENT OF COLORECTAL ULCERS IN IBD

A combination of PF127, PF68 and MK4M is proposed as raw materials to achieve a hydrogel useful in the treatment of rectal and colonic mucosal ulcers, which are characteristic of inflammatory bowel disease. The studies carried out towards this goal are presented in chapter III and summarized in **Figure 5**.

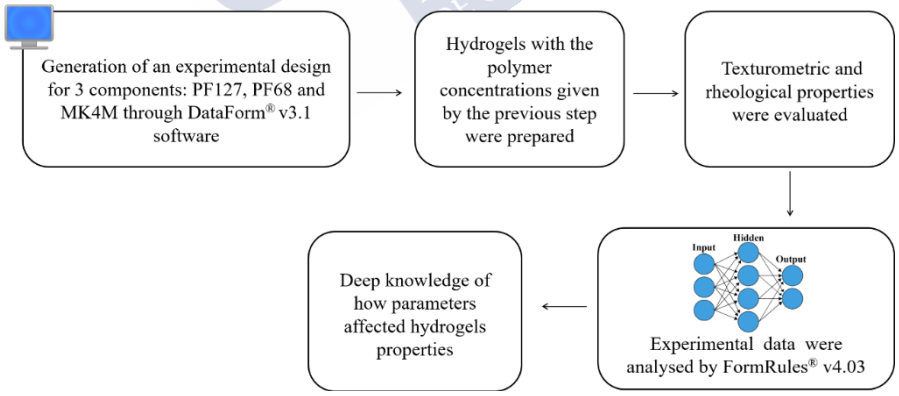

Figure 5. General scheme and assays performed on Chapter III.

As previously, identical AI tools were used to study the effect of each ingredient on hydrogels properties. Both, the knowledge space

and design space were established to produce thermosensitive and highly mucoadhesive systems capable of loading and releasing proteins. The syringeability of the ternary mixtures is directly related to the proportion of PF127 in the system. Both Pluronic® condition the gelation temperature, which increases as PF68 is incorporated into the system. The cellulose derivative contributes to the viscosity and bioadhesion of the hydrogel.

As in the previous case, modelling with artificial neural networks and genetic algorithms allowed the selection of a formulation with adequate syringeability (<86mJ for a 24Gx1.5" needle), gelation temperature between 25-27 ºC and high bioadhesion, whose composition was: 16.34% PF127, 2.55% PF68 and 0.26% MK4M. The physicochemical characteristics obtained for the optimized formulation were found to be very similar to those predicted by the model, which allowed its validation.

This hydrogel was used as carrier for conditioned medium derived from mesenchymal stem cells (H-hUCESC-CM). The results of the *in vivo* study in an experimental mouse model of acute colitis are presented in chapter IV and summarized in **Figure 6**.

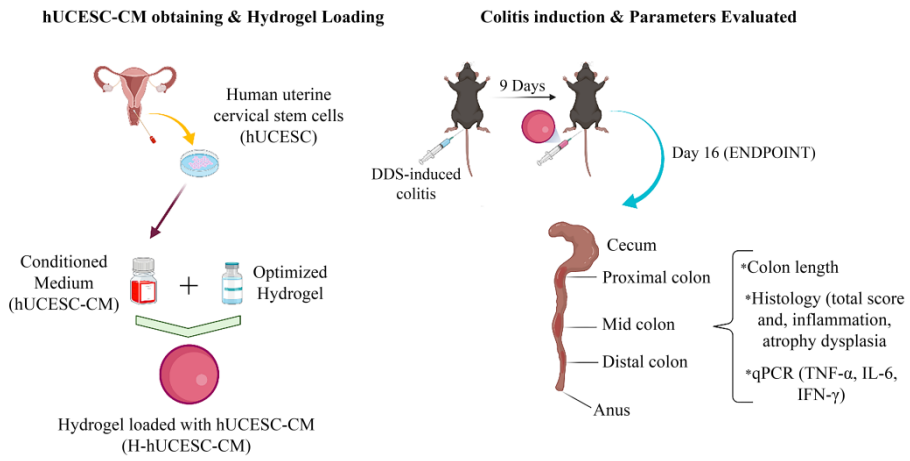

Figure 6. General diagram of assays performed on Chapter IV.

Thus, experimental data indicate the treatment with the loaded hydrogel significantly decreases body weight loss, colon shortening,

colonic mucosal degeneration and TNF-α, IFN-γ and IL-6 mRNA levels. These data indicate H-hUCESC-CM effectively alleviates DSS-induced colitis in mice, suggesting that H-hUCESC-CM may represent a very attractive cell-free therapy for the local treatment of IBD.

4. CONCLUSIONS

1. AI tools enable to easily study the knowledge space and establish the design space of rectal and sublingual ternary formulations, even using very small experimental designs. The experimental data modelling with these hybrid technologies facilitates the design of hydrogels with advanced performance. Neurofuzzy logic, allows establishing how the components of the formulation and their interactions affect the texturometric, rheological and release behavior of ternary hydrogels, thus acquiring in-depth knowledge about their role on systems performance. On the other hand, the combination of artificial neural networks and genetic algorithms allows the optimization of several variables simultaneously, finding the best possible formulation within the design space.

2. An adequate combination of PF127, HS1200 and Gantrez® (AN119 or S97) is useful for obtaining thermosensitive and mucoadhesive hydrogels of suitable characteristics for the mucosal administration of therapeutic molecules (high gel strength, bioadhesion and cohesion, and fast drug release). Moreover, HS1200 showed immune stimulatory capacity, rising as a potential polymer with suitable characteristics for the development of vaccines. The achieved optimal hydrogel for vaccine delivery was able to spread over the sublingual mucosa, prevent antigen leakage by swallowing or dilution on salivary fluid, and induce its rapid release to guarantee complete absorption through the oral mucosa tissue. Both, the optimal formulation and CAF01 liposomes including the Chlamydia CTH522 subunit vaccine, showed an immunization strategy-dependent efficacy in mice**.** The results demonstrated that

combined parenteral+sublingual immunization was able to elicit a local IgA response in the genital tract and enhance significantly the IFN-γ production by cervical lymph nodes compared to parenteral immunization alone.

3. Adequate combinations of PF127, PF68 and MK4M are useful to prepare enemas that undergo fast transition from liquid to solid state once at body temperature, minimizing the leakage and dilution of therapeutic molecules. These smart formulations exhibit good bioadhesiveness and a rapid drug release, designed to promote an immediate effect over the damaged intestinal mucosa. An optimal hydrogel was developed based on the desired formulation characteristics showing appropriate syringeability, bioadhesion and gelation temperature. Results in a mouse model of acute colitis showed that the optimized hydrogel, loaded with conditioned medium from human uterine cervical stem cells (H-hUCESC-CM), could represent an attractive cell-free therapy for the local treatment of colorectal ulcers in inflammatory bowel disease by significantly reducing colon shortening as well as the extension and severity of intestinal lesions by diminishing the grade of atrophy, inflammation, and dysplasia, compared to control group (untreated).

REFERENCES

[1] J. Mayr, C. Saldias, D. Diaz Diaz, Release of small bioactive molecules from physical gels, Chem Soc Rev, 47 (2018) 1484-1515.
[2] A.A. Koffi, F. Agnely, G. Ponchel, J.L. Grossiord, Modulation of the rheological and mucoadhesive properties of thermosensitive poloxamer-based hydrogels intended for the rectal administration of quinine, Eur J Pharm Sci, 27 (2006) 328-335.
[3] A. Miquel-Clopes, E.G. Bentley, J.P. Stewart, S.R. Carding, Mucosal vaccines and technology, Clin Exp Immunol, 196 (2019) 205-214.
[4] M. Li, Y. Wang, Y. Sun, H. Cui, S.J. Zhu, H.J. Qiu, Mucosal vaccines: Strategies and challenges, Immunol Lett 217 (2020) 116-125.
[5] S. Longet, M.L.E Lundahl, E.C Lavelle, Targeted Strategies for Mucosal Vaccination, Bioconjug Chem 29 (2018) 613-23.
[6] F. Zahir-Jouzdani, J.D. Wolf, F. Atyabi, A. Bernkop-Schnürch, In situ gelling and mucoadhesive polymers: why do they need each other?, Expert Opinion on Drug Delivery, 15 (2018) 1007-1019.
[7] J. Chen, R. Zhou, L. Li, B. Li, X. Zhang, J. Su, Mechanical, rheological and release behaviors of a poloxamer 407/ poloxamer 188/carbopol 940 thermosensitive composite hydrogel, Molecules, 18 (2013) 12415-12425.
[8] J. Xu, M. Tam, S. Samaei, S. Lerouge, J. Barralet, M.M. Stevenson, M. Cerruti, Mucoadhesive chitosan hydrogels as rectal drug delivery vessels to treat ulcerative colitis, Acta Biomater, 48 (2017) 247-257.
[9] R. Waters, S. Pacelli, R. Maloney, I. Medhi, R.P. Ahmed, A. Paul, Stem cell secretome-rich nanoclay hydrogel: a dual action therapy for cardiovascular regeneration, Nanoscale, 8 (2016) 7371-7376.
[10] K.O. Allbright, J.M. Bliley, E. Havis, D.Y. Kim, G.A. Dibernardo, D. Grybowski, M. Waldner, I.B. James, W.N. Sivak, J.P. Rubin, K.G. Marra, Delivery of adipose-derived stem cells in poloxamer hydrogel improves peripheral nerve regeneration, Muscle Nerve, 58 (2018) 251-260.
[11] E.S. DeLyria, D. Zhou, J.S. Lee, S. Singh, W. Song, F. Li, Q. Sun, H. Lu, J. Wu, Q. Qiao, Y. Hu, G. Zhang, C. Li, K.J. Sastry, H.

Shen, Sublingual injection of microparticles containing glycolipid ligands for NKT cells and subunit vaccines induces antibody responses in oral cavity, Carbohydr Res, 405 (2015) 87-92.
[12] Y. Wu, W. Wei, M. Zhou, Y. Wang, J. Wu, G. Ma, Z. Su, Thermal-sensitive hydrogel as adjuvant-free vaccine delivery system for H5N1 intranasal immunization, Biomaterials, 33 (2012) 2351-2360.
[13] F. Raza, H. Zafar, Y. Zhu, Y. Ren, A. Ullah, A.U. Khan, X. He, H. Han, M. Aquib, K.O. Boakye-Yiadom, L. Ge, A Review on Recent Advances in Stabilizing Peptides/Proteins upon Fabrication in Hydrogels from Biodegradable Polymers, Pharmaceutics, 10 (2018).
[14] M.R. Matanovic, J. Kristl, P.A. Grabnar, Thermoresponsive polymers: insights into decisive hydrogel characteristics, mechanisms of gelation, and promising biomedical applications, Int J Pharm, 472 (2014) 262-275.
[15] L. Garcia-del Rio, P. Diaz-Rodriguez, M. Landin, Design of novel orotransmucosal vaccine-delivery platforms using artificial intelligence, European Journal of Pharmaceutics and Biopharmaceutics, 159 (2021) 36-43.
[16] Bruschi ML, de Freitas O. Oral Bioadhesive Drug Delivery Systems. Drug Development and Industrial Pharmacy 2005;31:293-310.
[17] A.I. Mendes, A.C Silva, J.A. Catita, F. Cerqueira, C. Gabriel, C.M. Lopes, Miconazole-loaded nanostructured lipid carriers (NLC) for local delivery to the oral mucosa: improving antifungal activity, Colloids Surf B Biointerfaces, 111 (2013) 755-763.
[18] L. Mude, B.K.R. Sanapalli, A.N. V, S.K. Singh, V. Karri, Overview of in situ gelling injectable hydrogels for diabetic wounds, Drug development research, (2021).
[19] M.R. Matanovic, J. Kristl, P.A. Grabnar, Thermoresponsive polymers: insights into decisive hydrogel characteristics, mechanisms of gelation, and promising biomedical applications, Int J Pharm, 472 (2014) 262-275.
[20] D.F. Argenta, B.D.C. Bernardo, A.F. Chamorro, P.R. Matos, T. Caon, Thermosensitive hydrogels for vaginal delivery of secnidazole

as an approach to overcome the systemic side-effects of oral preparations, Eur J Pharm Sci, 159 (2021) 105722.
[21] K. Bouchemal, A. Aka-Any-Grah, N. Dereuddre-Bosquet, L. Martin, V. Lievin-Le-Moal, R. Le Grand, V. Nicolas, D. Gibellini, D. Lembo, C. Pous, A. Koffi, G. Ponchel, Thermosensitive and mucoadhesive pluronic-hydroxypropylmethylcellulose hydrogel containing the mini-CD4 M48U1 is a promising efficient barrier against HIV diffusion through macaque cervicovaginal mucus, Antimicrob Agents Chemother, 59 (2015) 2215-2222.
[22] M. Landín, Introducción al uso de sistemas de inteligencia artificial para modelizar, comprender y optimizar formulaciones farmacéuticas, in: Biomateriais aplicados ao desenvolvimento de sistemas terapêuticos avançados, 2015, pp. 521-554.
[23] M.O. Jara, J. Catalan-Figueroa, M. Landin, J.O. Morales, Finding key nanoprecipitation variables for achieving uniform polymeric nanoparticles using neurofuzzy logic technology, Drug Deliv Transl Res, (2017).
[24] R. Rodriguez-Dorado, M. Landin, A. Altai, P. Russo, R.P. Aquino, P. Del Gaudio, A novel method for the production of core-shell microparticles by inverse gelation optimized with artificial intelligent tools, Int J Pharm, 538 (2018) 97-104.
[25] R. Lopez-Cebral, V. Romero-Caamano, B. Seijo, C. Alvarez-Lorenzo, M. Martin-Pastor, A. Concheiro, M. Landin, A. Sanchez, Spermidine cross-linked hydrogels as a controlled release biomimetic approach for cloxacillin, Mol Pharm, 11 (2014) 2358-2371.
[26] P. Diaz-Rodriguez, M. Landin, Smart design of intratumoral thermosensitive beta-lapachone hydrogels by Artificial Neural Networks, Int J Pharm, 433 (2012) 112-118.
[27] H. Blanco-Fuente, S. Anguiano-Igea, F.J. Otero-Espinar, J. Blanco-Méndez, In-vitro bioadhesion of carbopol hydrogels, International Journal of Pharmaceutics, 142 (1996) 169-174.
[28] R. Nigmatullin, V. Gabrielli, J.C. Muñoz-García, A.E. Lewandowska, R. Harniman, Y.Z. Khimyak, et al. Thermosensitive supramolecular and colloidal hydrogels via self-assembly modulated by hydrophobized cellulose nanocrystals, Cellulose, 26 (2019) 529-542.

[29] C.A. Ramírez Barragán, E.R. Macías Balleza, L. García-Uriostegui, J.A. Andrade Ortega, G. Toríz, E. Delgado, Rheological characterization of new thermosensitive hydrogels formed by chitosan, glycerophosphate, and phosphorylated β-cyclodextrin, Carbohydrate polymers, 201 (2018) 471-481.
[30] M. Campana-Seoane, A. Peleteiro, R. Laguna, F.J. Otero-Espinar, Bioadhesive emulsions for control release of progesterone resistant to vaginal fluids clearance, Int J Pharm, 477 (2014) 495-505.
[31] C.B. Roces, S. Khadke, D. Christensen, Y. Perrie, Scale-Independent Microfluidic Production of Cationic Liposomal Adjuvants and Development of Enhanced Lymphatic Targeting Strategies, Mol Pharm, 16 (2019) 4372-4386.
[32] S. Wirtz, V. Popp, M. Kindermann, K. Gerlach, B. Weigmann, S. Fichtner-Feigl, M.F. Neurath, Chemically induced mouse models of acute and chronic intestinal inflammation, Nat Protoc, 12 (2017) 1295-1309.

USC UNIVERSIDADE DE SANTIAGO DE COMPOSTELA

1. INTRODUCTION

USC
UNIVERSIDADE
DE SANTIAGO
DE COMPOSTELA

1.1. MUCOSAL SURFACES

1.1.1. Anatomy and function (small overview)

A mucosal surface or mucous membrane is any tissue able to secrete mucus across a layer of epithelial cells [1, 2]. Mucosal surfaces are the interface between the external and internal environment [3, 4]. They cover an extensive part of the body (≈ 400 m^2), including the inner ear, eye conjunctiva, the ducts of all exocrine glands and the respiratory, gastrointestinal, and urogenital tracts [5, 6].

Mucous membranes are physical barriers for allergens, carcinogens, and infectious agents. Their selective permeability allows the nutrients and air uptake, as well as the flux of ions, solutes and water. Furthermore, they are also involved in other survival functions such as perception of signals and reproduction [3, 4, 7].

As mucosal surfaces are daily exposed to different environmental hazards, they are endowed with powerful chemical and mechanical defence mechanisms. Coating with a mucous network is one of the strategies of mucosal surfaces for protecting living cells from external agents [8]. The secretion of mucus is essential to shield epithelial cells against enzymatic, chemical, microbial and mechanical challenges [2, 9, 10]. Moreover, a large and highly specialized mucosal immune system ensures their protection developing innate and adaptive responses against potential threats [6, 11]. Higher mammals have evolved a sophisticated defence system associated to mucosal surfaces to: a) protect the body from invasion of viruses, bacteria, fungi and parasites; b) remove or isolate non-microbial environmental substances and; c) destroy potential cancer cells that emerge in the body, also known as immune surveillance [1, 12, 13]. Thereby, the mucosal immune system is a specific immune organization that protects mucosal compartments via articulating immune responses through the immune cells residing in them. In addition, the mucosal immune system has many unusual and unique features such as a distinctive anatomy, specialized mechanisms for antigen uptake, as well as, regulatory and effector responses to induce tolerance against food and innocuous antigens [11, 14].

In healthy human adults, the mucosal immune system comprises almost 80% of all lymphocytes, being the largest immune tissue of the body [15]. These lymphocytes can be accumulated in, or migrate between various mucosal-associated lymphoid tissues (MALT). MALT principal function is to produce and secrete immunoglobulins A (IgA) across mucosae via antigen specific, Th1, Th2 or cytotoxic T-cell mediated responses [16]. MALT functions independently of the systemic immune system and it is highly compartmentalized [6]. The best-known MALT representatives are: nasopharynx associated lymphoid tissue (NALT), bronchus-associated lymphoid tissue (BALT), gut-associated lymphoid tissue (GALT) and genital associated lymphoid tissue (**Figure 1**). However, the lacrimal duct-associated (LDALT), the conjunctiva-associated (CALT), the larynx-associated (LALT) and salivary duct-associated (DALT) lymphoid tissues have also been described [16, 17]. Although MALT compartments have similar histology and features, their immunobiology and histogenesis could differ depending on the location [17].

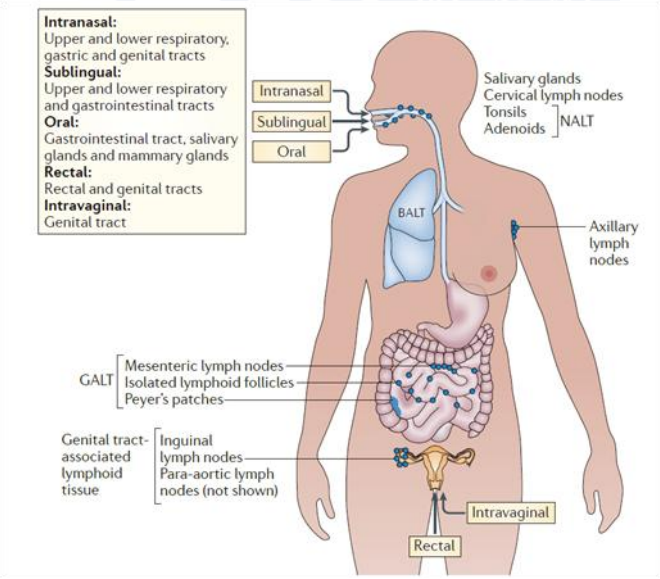

Figure 1. Overall scheme of mucosa-associated lymphoid tissue (MALT) and its most important subcompartments: nasopharynx associated lymphoid tissue

(NALT), bronchus-associated lymphoid tissue (BALT), gut-associated lymphoid tissue (GALT) and the genital lymphoid associated tissue. Reproduced from Nils Lycke (2012) with permission of Springer Nature.

1.1.2. Mucus and mucins

Mucus is an adhesive and viscoelastic complex hydrogel secreted by specialized Goblet and mucous cells located in the gastrointestinal and reproductive tracts, airways and the eyes. Mucus at the oral mucosa is secreted as part of saliva by the minor and major salivary glands [18-20]. It is continuously produced, discharged onto mucosal surfaces, and finally recycled, digested, or discarded, allowing surfaces removal of bacteria and debris [8, 18]. Mucus includes salts, nucleic acids, lipids, cells, cellular debris, antimicrobial molecules, secreted antibodies and a variety of proteins, being mucins the most representative. Mucins are glycoproteins with abundant serine, threonine and proline amino acid residues, which are characterized by threadlike core protein domains rich in O-linked oligosaccharides, giving rise to their characteristic "bottle brush" conformation. The high content of sialic acid and sulfate groups in their backbone confers a strong negative charge to mucins, which increases mucus stiffness through charge repulsion, giving gel-like properties [2, 10, 18, 21]. Mucus network has a high number of physical entanglements via covalent and non-covalent interactions, including electrostatic, hydrophobic, hydrogen bonds and also specific binding interactions. These interactions contribute to the viscoelasticity of the mucus, creating a mesh with a pore size that varies between 100 and 2000 nm depending on the mucosal tissue location [18, 21]. The properties of the mucosal barriers depend on the composition, the degree of glycosylation and conformation of the mucins. The tissue of origin and environmental factors (ionic strength, pH and the presence of other agents) determine the structure of the glycoproteins, and therefore, the thickness of the mucus and its functions [2, 22].

Mucus layer can difficult the holding of drug carriers on mucosal surfaces if prepared with non-mucoadhesive materials. These materials can interact with mucus glycoproteins through different chemical and physical mechanisms increasing the residence time of

delivery systems on mucosal surfaces and therefore, enhancing absorption, bioavailability and efficacy of the drugs [23-27].

1.2. INMUNITY FROM MOUTH TO RECTUM

1.2.1. Oral cavity immune system

The first compartment of the gastrointestinal tract is the oral cavity. Anatomically, the oral mucosa is located between the skin of the face and the mucosa lining of the gastrointestinal tract, sharing features with both tissues and the respiratory tract [14, 28, 29]. In the oral cavity there are keratinized (hard palate, gingiva and outer lips) and non-keratinized regions (ventral side of the tongue, the floor of the mouth and the inner surface of the lips and cheeks), the latter being more elastic and permeable for antigens or drug delivery [20, 29, 30].

Oral epithelium is stratified and made up of three layers: basal, intermediate and superficial, that act as a mechanical barrier protecting the subjacent tissues against environmental hazards or fluid loss. Beneath oral epithelium are the basement membrane, the lamina propria and the submucosa (**Figure 2**) [20, 29].

Oral tissue contains different immune cells such as lymphoid cells, macrophage-like cells, antigen-presenting cells (APCs) and some pro-inflammatory cells [31]. Langerhans cells (LCs), located in the suprabasal layer, are the most superficial APCs, meanwhile the myeloid and plasmacytoid dendritic cells subsets are in the lamina propria and submucosal tissue, respectively [29]. Little is known about the functioning of oral mucosa immune system. However, two theoretical models have been proposed:

1) The presence of different oral-pharyngeal domains comprising the MALT as: buccal mucosa (inner cheeks), salivary glands, Waldeyer's ring (consisted of palatine tonsils and adenoids) and pharyngeal lymphoid tissues [14, 32].

2) The presence of inductive and effector sites, resembling the gastrointestinal immune system: oral inductive sites as Waldeyer's ring, lymphoid follicles and proximal draining lymph nodes (submaxillary, internal jugular and superficial

cervical), and effector sites as the epithelium, the lamina propria and salivary glands [14, 28, 33].

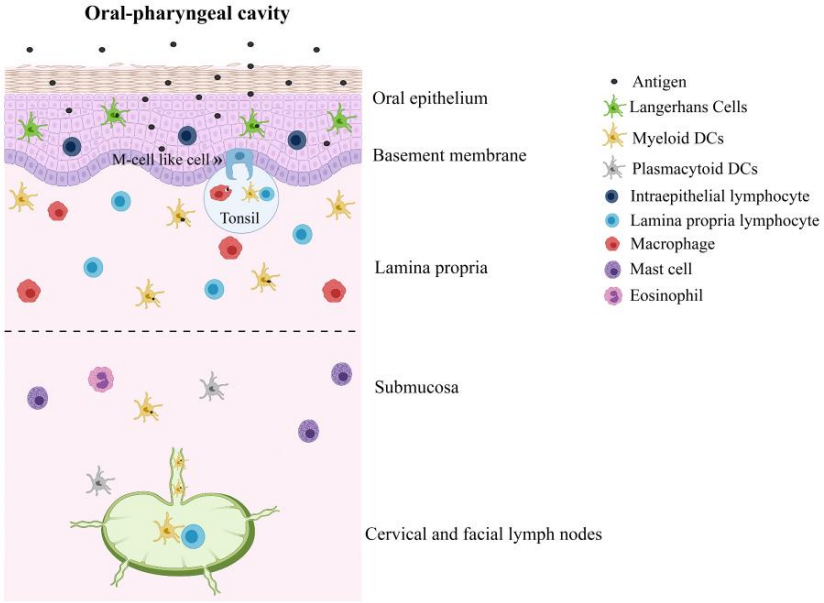

Figure 2. Structure of oral pharyngeal cavity and scheme of immunization process. Antigens delivered on the oral mucosa are taken up by Langerhans cells in the epithelial layer and also by myeloid dendritic cells and macrophages in the lamina propria. Antigen-bearing dendritic cells migrate to secondary lymphoid tissue and lymph nodes to induce adaptive immune responses. MALTs of the oral-pharyngeal cavity are located in the tonsils, where micro-fold cells transfer antigens to antigen-presenting cells.

Lastly, oral mucosa is moistened by salivary glands, that produce mucin and saliva. Saliva contains several antimicrobial peptides and proteins such as peroxidases, lysozymes, defensins, lactoferrin, and immunoglobulins (*e.g.* secretory IgA). Their functions are lubrication of tissues, swallowing, prevention of tooth demineralization and dental protection [20, 29, 34].

1.2.2. Gut-associated lymphoid tissues or GALT

The intestinal mucosa is the largest surface of the body, in close contact with commensal microbiota, food and pathogens [35]. In the defence of the intestinal mucosa participate the intestinal epithelial

barrier, the lamina propria, the GALT and the draining lymph nodes [36]. Specifically, the GALT and the duodenopancreatic, para-aortic and mesenteric lymph nodes are the main locations for priming adaptive immune cell responses in the gut [37].

The intestinal mucosa covers the small intestine, the caecum and the colon. The intestinal epithelial barrier is composed by a single layer of columnar epithelial cells arranged in crypts and villi, designed for nutrient absorption. Villi are not present in the caecum and colon [36, 37]. This epithelium is constantly renewed by immature cells arising from the base of the crypts. It is protected by substances such as mucins and antimicrobial peptides (AMPs), synthesized by Goblet and Paneth cells, respectively [4, 36]. Thus, the apical surface of intestinal epithelial cells (IEC) is covered by a protective mucus layer composed mainly by mucins [4]. Furthermore, in this mucous layer there is also IgA secreted by enterocytes [38].

The lamina propria is made up by loosely packed connective tissue. Different innate immune cells (*e.g.* macrophages, dendritic cells (DCs) and innate lymphoid cells) and adaptive lymphocytes (*e.g.* IgA-producing plasma cells and effector T cells) can be found diffusively in the lamina propria. This set of cells is called the immune effector site [38]. Furthermore, the lamina propria has other functions such as blood and nervous supply and lymph drainage [37].

The GALT is formed by organized subepithelial lymphoid follicles located in the intestinal mucosa and submucosa (**Figure 3**) [37] and characterized by an overlying follicle-associated epithelium (FAE) that contains microfold cells (M cells). M cells are a specialized subset of intestinal epithelial cells responsible for the uptake and transport of antigens from the lumen to the subepithelial dome (SED) region, which has plenty of dendritic cells (DCs) that deliver antigens to adaptive immune cells [37, 38].

When lymphoid follicles aggregate, they form macroscopic structures known as Peyer's, caecal and colonic patches. Specifically, Peyer's patches are oval-shaped aggregates of hundreds of B cells lymphoid follicles that are flanked by smaller T cell regions [37, 38]. Peyer's patches, predominant in the distal ileum, are considered the main inductive site for the mucosal immune response.

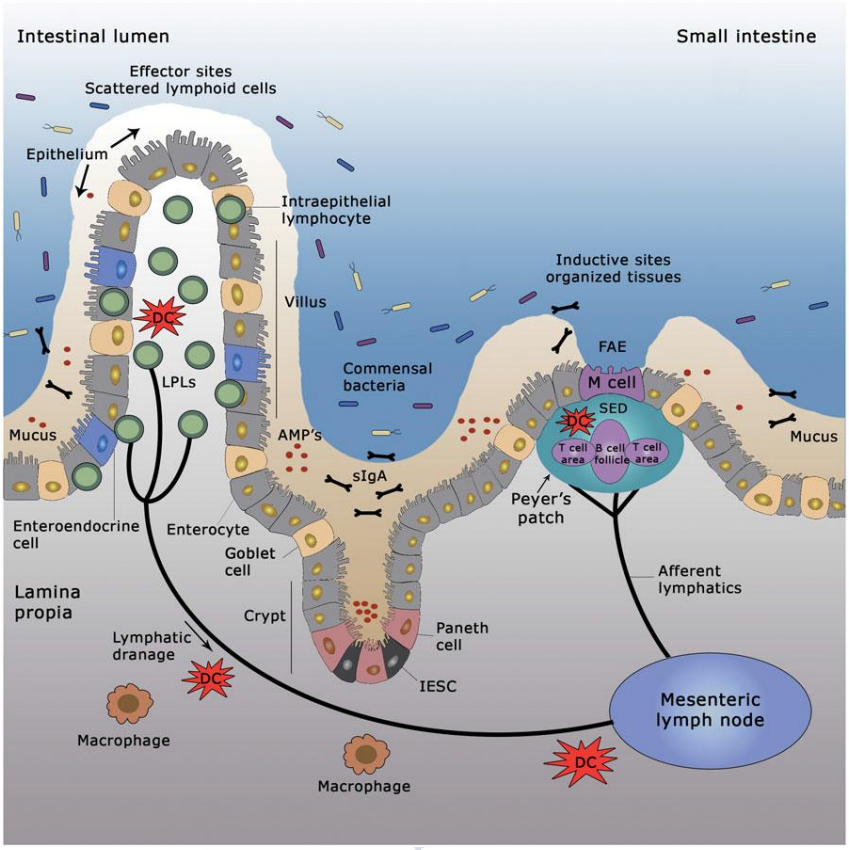

Figure 3. Scheme of intestinal mucosa and immune responses. Reproduced from Ahluwalia et al. (2017) with permission of Taylor & Francis.

Lymph nodes are also important immune organs that contain large numbers of lymphocytes housed in their paracortex, cortex and medulla. Unlike Peyer's patches, lymph nodes are encapsulated lymphoid tissue and have afferent lymphatics [36]. Mesenteric lymph nodes can filter the lymph coming from the gut and also initiate immune responses against free antigens or delivered by DCs from the lamina propria. The first line of defence to protect the host against harmful agents are the cells of the innate immune system, which include macrophages, DCs, neutrophils, natural killer cells, eosinophils, mast cells and basophils. When DCs and other phagocytic cells of intestinal mucosa interact with pathogenic microorganisms,

the immune system must respond appropriately and induce protective inflammatory responses [36, 39]. Microbes and parasites are detected and captured by "professional" APCs, including DCs, macrophages and B lymphocytes, through a range of innate immune sensors known as patter-recognition receptors, which are able to recognize the pathogen-associated molecular patterns. After antigen uptake, these activated APCs migrate to lymph nodes where they can interact with naïve T lymphocytes to promote their further activation and differentiation into T-helper 1, T-helper 2, T-helper 17 cells, T-follicular helper cells, regulatory T-cells and effector cytotoxic T lymphocytes. Recognition of germs lead to secretion of chemokines, AMPs and inflammatory cytokines, the recruitment of more innate immune cells as well as DCs and lymphocytes activation, favouring the development of stronger and broader immune responses.[6, 36].

1.3. MUCOSAL VACCINATION: PROS AND CONS

Vaccination is the most powerful and successful approach for preventing and eradicating infectious diseases. This process consists of stimulating individual's immune system to fight against potential future infections through the administration of inactivated or attenuated antigens, commonly via injections or oral routes [40, 41]. Mucosal surfaces are the main entry site of pathogens and where most infectious processes are initiated, therefore, the induction of local mucosal immune responses are essential for protection against disease [36, 40, 42]. Hence, the primary target of vaccines is to inhibit mucosal replication of bacterial and viral pathogens via production of secretory IgA antibodies (sIgA) or transcytosed IgG [43]. In general, parenteral vaccines are poor inducers of mucosal immunity. However, immunization through mucosal routes generates broader immune responses by priming systemic IgG responses, stimulating cell-mediated immune responses and efficiently inducing the production of local and loco-regional sIgA. Mucosal immunization has the potential to activate all the different arms of the immune system, which could help to protect the body against infection and reduce the transmission of mucosal pathogens. The simultaneous stimulation of the systemic and mucosal immune compartments is of particular interest for

pathogens that can infect the host via both systemic and mucosal routes [40, 42, 44, 45]. Mucosal vaccines have additional advantages. They are needle-free and non-invasive, therefore suitable for mass vaccination, limiting the transmission of blood-borne diseases and decreasing costs. Furthermore, mucosal vaccination could improve patient compliance by diminishing side effects and not require highly trained medical staff. However, despite its great benefits, mucosal vaccination is extremely challenging owing to the harsh mucosal environment [40, 41, 43].

Mucosal vaccines are diluted in mucosal fluids and captured by the mucus network. Bulk flow may limit their residence time onto mucosal surfaces. Furthermore, the antigen or other vaccine components could be inactivated by proteases and nucleases. Vaccine delivery vehicles must overcome these physiological barriers to efficiently target mucosal APCs. Consequently, relatively large doses of antigens are needed compared to traditional parenteral immunizations and, the impossibility of precisely knowing the amount of absorbed vaccine difficult establishing the accurate dose. Setting the dosage and boost time, when necessary to amplify primed immune responses to solidify immunological memory, is also a complex task [42, 43].

Furthermore, immunization through mucosal tissues is the natural way to induce tolerance, which is essential to avoid pathologic reactions against harmless environmental antigens and self-antigens. In some cases, such as allergen immunotherapy or autoimmune disease, tolerance induction is the goal of vaccination [41, 43, 46], but in others it may be an obstacle to reach protective immunity.

1.3.1. Adjuvants

The use of potent immune-potentiators, known as vaccine adjuvants, is imperative to enhance immunogenicity, but only a few show strong mucosal adjuvanticity without being toxic or reactogenic. Adjuvants are substances capable of eliciting a pro-inflammatory environment that recruits and promotes the infiltration of phagocytic cells to vaccine administration sites. In addition, they can increase and modulate the immunogenicity of vaccine antigens by enhancing antigen presentation, activating APCs or inducing cytokine expression

[43, 47]. Co-administration of antigens and adjuvants is required to overcome mucosal tolerance, particularly when soluble antigens are used [45]. Adjuvants can be classified in two groups; delivery systems and immunostimulators. The latter activate innate immune cells directly (*e.g*. cytokines) or through pattern-recognition receptors, such as Toll-like receptors (TLRs), retinoic acid-inducible gene-I- (RIG-I-) like receptors (RLRs) or nucleotide binding oligomerization domain- (NOD-) like receptors (NLRs) [47, 48].

Delivery systems act as vaccine carriers to ensure that an adequate number of antigens is presented to immune cells to induce immunity [47]. To this end, a multitude of vehicles have been proposed to deliver antigens to mucosal sites, preserving their structural integrity and increasing their bioavailability. Several inert systems have been evaluated as vaccine carriers such as hydrogels, DNA vaccines and particulate carriers, including emulsions, liposomes, proteoliposomes, archaeosomes, micro- and nanoparticles, nanocapsules, cochleates, immune stimulatory complexes (ISCOM® and ISCOMATRIX®), nonionic surfactant-based vesicles (niosomes and bilosomes), terrestrial plants and algae cells and chemically processed pollen grains [43, 45, 46, 49].

Live attenuated and inactivated microorganisms have also been used as adjuvants including pathogens (*e.g*. *Salmonella spp*, *Bordetella pertussis*, Bacille Calmette-Guérin, poxviruses and adenoviruses) or commensal bacteria (*e.g*. lactobacilli and certain staphylococci and streptococci). Safer alternatives to use viable microorganisms are bacterial ghosts' vectors, non-viable nanometer-sized lipid-containing microvesicles (bacterial outer membrane vesicles), virus-like particles, virosomes and recombinant bacterial and viral proteins [6, 43, 45, 46].

Most novel adjuvants include both, an immunostimulator and a delivery system, since their combination is more beneficial than using them separately [47].

1.3.2. Mucosal tissues as vaccination sites

Mucosal tissues are used for both priming and boosting immunity [50-54]. The circulation of lymphocytes within different mucosal tissues lead to the notion of a common mucosal immune system.

However, the entry and dissemination of activated lymphocytes into the mucosa is governed by chemokine receptors and tissue-specific adhesion molecules, leading to a significant degree of compartmentalization within the mucosal immune system. This fact limits the dissemination of activated immunocytes to those remote mucosal tissues that express and release the same ligands, explaining why some lymphocytes primed in the GALT can recirculate as effector cells to urogenital and respiratory tracts and lactating breast, and nasal immunization induces strong immune responses in the genital tract [6, 11]. Therefore, it is important to properly understand the cellular and molecular mechanisms that regulate the mucosal immune system to choose the immunization route and successfully induce protective mucosal responses [55]. Oral and nasal tissues are the most common routes for mucosal vaccine administration, but also, ocular, buccal, sublingual, pulmonary, vaginal and rectal mucosae in a lesser extent. Not all mucosal routes induce similar immune responses in terms of potency and longevity, which could be explained by the differences in the organization and cells forming the lymphoid structures of each mucosal tissue [29, 46, 56].

1.3.2.1. Ocular vaccination

Ocular immunization can induce serum IgG and antigen-specific antibodies in gut, ocular and nasal cavities [55, 57, 58]. Few formulations have been developed for ocular immunization and antigens are mainly administered by conjunctival instillation of eye drops [59, 60]. For example, the nanostructure Coa-ASC16 co-formulated with BLSOmp31 antigen and CpG-ODN adjuvant, and mannosylated poly(anhydride) nanoparticles loaded with a subcellular antigen of *Brucella ovis* have been proposed as ocular antibrucellosis vaccines. The incorporation of the bioadhesive polymer Gantrez® AN119 increased the residence time of the latter particulate carrier on the ocular surface. Furthermore, the fraction of nanoparticles that migrated to nasal and gastrointestinal mucosae was also retained longer in these areas, enabling a greater activation of the immune system and eliciting high levels of specific IgA in faecal samples [58, 59, 61]. Recombinant bacterial ghost technology has also been proposed to effectively stimulate the production of specific IgA

antibodies on the ocular surface against *Chlamydia trachomatis* to prevent trachoma in a guinea pig model [62]. Besides, local ocular vaccination using different antigens of herpes simplex virus provided better protection against ocular infection than systemic vaccination [63, 64]. The ocular mucosa has also been used to induce systemic and mucosal responses against respiratory infections such as influenza by incorporating avian influenza antigens into chitosan and mannan-coated PLGA nanoparticles or by administering three different strains of live attenuated influenza viruses at the same time [60, 65].

1.3.2.2. Nasal and pulmonary vaccination

Nasal route is also an attractive site for vaccination due to its accessibility and ability to stimulate both mucosal and systemic immune responses. Since the nose is a portal entry of pathogens to respiratory tract, nasal immunization has been proposed as a feasible approach to confer immunity against respiratory diseases such as influenza, tuberculosis and pneumonia [66-69]. Different technologies have been proposed to maximize antigen uptake through nasal mucosa such as particulate carriers, thermosensitive hydrogels and dry powder vaccines, among others [67, 68, 70, 71]. For example, several cationic formulations have been employed for intranasal delivery of antigens. Thus, formulating H5N1 avian influenza vaccine with the cationic polymers GenJet™ and in vivo-jetPEI® (polyethylenimine) have conferred protective immune responses against virus challenge [72]. Bacterial burden of *Mycobacterium bovis* has been reduced in mice after intranasal administration of a multi-epitope tuberculosis DNA vaccine incorporated into mannosylated chitosan nanoparticles. This strategy promoted a robust and an enhanced sIgA response in the bronchoalveolar lavage, as well as, induced the secretion of TNF-α, IFN-γ and IL-2 by potent antigen specific $CD4^+$ and $CD8^+$ effector T cells in the lung [66]. Furthermore, the incorporation of influenza and pneumococcal antigens into a thermosensitive chitosan-based hydrogel and a cationic cholesteryl-group-bearing pullulan nanogel, respectively, have allowed to effectively initiate the induction of systemic and mucosal antigen-specific immune responses by increasing the residence time of vaccines in the nasal cavity promoting their further uptake by nasal DCs [67, 68].

In addition, taking advantage of the ability of intranasal immunization to induce more efficiently protective immunity in the female genital tract than systemic immunization, different intranasal vaccines have been developed in an attempt to combat several of the most common sexually transmitted diseases such as genital herpes, chlamydia, human immunodeficiency virus and gonorrhea [51, 73-76].

Powder and liquid formulations have been designed for allowing immunization via pulmonary route, but it requires the employment of inhalation devices such as dry powder inhalers and nebulizers. Pulmonary mucosa has been proposed as vaccination site against respiratory pathogens such as *Mycobacterium tuberculosis*, *Streptococcus pneumonie* and measles and influenza viruses, but also against other diseases that do not affect lung mucosa such as hepatitis [77].

1.3.2.3. Sublingual and buccal vaccination

The mucosal linings of the oral cavity have gained a lot of attention as vaccination sites in recent years for their advantages over nasal and oral routes. Orotransmucosal vaccination allows needle-free administration of antigens, requires lower doses of antigen than oral route, avoids first pass effect as well as harsh stomach environment and, the risk of redirection of vaccine components to the brain is much lower than nasal vaccination [29, 55, 78, 79]. Sublingual immunization is able to elicit systemic immune responses and mucosal disseminated immunity through antibody-mediated and cytotoxic T-cell responses in the stomach, small intestine, upper and lower respiratory tract and reproductive tract [79]. This fact led to the use of sublingual tissue as vaccination site to induce protective immunity against several enteric, respiratory and genitourinary pathogens by administering whole inactivated and live attenuated microorganisms, and recombinant vaccines alone or included into delivery systems [44, 80-85]. For example, sublingual administration of Bacillus Calmette-Guérin provided long term protective immunity in mice against *Mycobacterium tuberculosis* after pulmonary challenge by mounting robust mycobacterial-specific T cell responses in the lung but failed to induce mycobaterial-specific serum IgG [84].

Thereby, several dosage forms for sublingual application including multi-layered nanofibrous mucoadhesive films, freeze drying formulations, nano- and microparticles, thermosensitive hydrogels and liposomes have been developed to protect and enhance antigen absorption and thus increase B and T cell immunogenicity [52, 81, 86-88]. In addition to confer immunity against harmful pathogens, sublingual delivery of antigens is also used in immunotherapy to induce tolerance against allergens such as pollen and food allergens [89].

On the other hand, despite buccal delivery of antigens has been less explored than sublingual one, some studies revealed that buccal route could also generate potent cell-mediated immune responses [90-92]. Very encouraging results have been obtained after buccal immunization with a vaccine based on bacteriophage MS2-L2 virus-like particles encoding epitopes of different human papillomavirus (HPV) adjuvanted with cholera toxin and monophosporyl lipid A. This approach effectively induced protective immunity in both genital and oral regions against eleven oncogenic HPV types associated with a 95% and a 99% of cervical and head and neck cancers, respectively [91]. In addition, the therapeutic potential of a HPV-16 synthetic long peptide has been evaluated in a buccal tumor model. Interestingly, intratumoral administration of this vaccine without any adjuvant increased systemic and local antigen-specific $CD8^+$ T cells, leading to a potent antitumor effect against HPV-associated lesions presented in buccal mucosa [92].

1.3.2.4. Oral vaccination

Oral administration of antigens is highly desirable because it is patient-friendly, cost-effective, and easy to use. However, the development of effective oral vaccine formulations is extremely challenging owing the intrinsic features of gastrointestinal tract [93]. Curiously, except FluMist™ (a nasal spray flu vaccine), the few licensed mucosal vaccines available are administrated by oral route and are inactivated or live attenuated vaccines against *Vibrio cholerae*, *Salmonella thyphimurium*, adenovirus (for military use only) and poliovirus [46]. Although a vast research has been made to find effective non-living oral vaccines against these and other enteric

pathogens, the efforts have not yet borne fruit. Lipid based delivery systems, including liposomes, ISCOM®s and emulsions; virus-like particles, micro- and nanoparticles, pH-responsive hydrogels, tablets and capsules have been proposed as vaccine delivery platforms to enhance enteric mucosal immune responses [94-98]. In addition to enteric infections, oral mucosa has been also evaluated to confer immunity against other diseases such as hepatitis, tuberculosis, chlamydia and HIV [96, 98-100].

1.3.2.5. Vaginal and rectal vaccination

Basically, intravaginal immunization is used generally to induce immunity against genital pathogens such as HIV, HSV and chlamydia. Although rectal mucosa has also been explored and evaluated for this purpose, vaginal antigen administration is a more common approach [101-106]. Intravaginal immunization is able to elicit specific-systemic and mucosal immune responses, promote local IgG and IgA secretion antibodies as well as IgG secretion. Vaginally-administered vaccine strategies include the use of live attenuated and DNA vaccines, as well as, delivery systems comprising liposome based gel formulations, lyophilized solid dosage formulations, viral vectors, peptide-based carriers or vaginal ring devices [106-112].

Intravaginal vaccination was also carried out as a successful method to treat HPV-associated cervical cancer and increased survival in mice. A therapeutic approach included submucosal vaginal immunization with the pcDNA3-CRT/E7 DNA vaccine encoding IL-2 following by electroporation. Other strategy was to administer carboplatin/paclitaxel chemotherapy prior to intravaginal vaccination using a HPV16-E7 synthetic long peptide adjuvanted with CpG (cytosine-guanine oligodeoxynucleotide) [113, 114].

1.4. GASTROINTESTINAL INFLAMMATORY MUCOSAL PATHOLOGIES

Inflammatory Bowel Disease (IBD) encloses a group of inflammatory disorders that affect the gastrointestinal tract [115, 116]. They are chronic, systemic, complex, and multifactorial pathologies in which patients suffer from relapsing and flares accompanied with stomach and abdominal pain, severe diarrhoea, weight loss, cramping and rectal bleeding [117, 118].

Ulcerative colitis (UC) and Crohn's Disease (CD) are the most representative gastrointestinal inflammatory disorders. Although CD and UC share clinical features such as mucosal injury, periods of relapsing and remitting mucosal inflammation, as well as a decrease in the mucus layer thickness and its spread depending on the severity of inflammation, their pathology is different [115, 119-121]. CD can discontinuously affect any region of the digestive tract, being the distal ileum and colon the most commonly damaged areas. It involves the entire intestine wall, from mucosa to serosa, implying a transmural inflammatory process which frequently lead to the development of perianal fistulas [115, 119, 122, 123].

On the other hand, UC is restricted to the large intestine where the mucosa and submucosa are uniformly affected. Starting in the rectum, the inflammation could spread to the whole colon. However, in some rare cases the ileum could also be harmed [115, 124-126]. Besides, their immunological basis are also well differentiated, whereas in CD predominate Th1 responses, in UC the overexpressed cytokines are Th2 type [123, 127].

Several theories have been proposed in order to elucidate the origin of IBD. Autoimmunity, the infection with microbes such as *Mycobacterium avium* subsp. *paratuberculosis* or *Escherichia coli* among others, dysbiosis in commensalism bacteria, together with genetic and environmental factors were attributed as potential causes for IBD development [127-132]. In addition, it is interesting to hallmark that IBD exists mainly in Western countries and, the incidence rate is continuously rising also in emerging countries [132, 133].

It seems that intestinal mucosal barrier dysfunction and immune dysregulation play a significant role in the development, progression and perpetuation of IBD [134-136]. IBD is related to augmented permeability in both non-ulcerated and ulcerated epithelia of the gastrointestinal tract, strongly suggesting that this defect in mucosal barrier function precedes gut inflammation [137, 138]. There are alterations in several components of the epithelium and its adhesion molecules. For example, some studies have shown decreased expression of tight junctions as well as changes in their function,

ultrastructure and protein composition during disease outbreaks. Multiple alterations in mucins expression and mucus composition together with a decreased number and depletion of Globet cells lead to a reduction in the thickness of the mucus layer, which can sometimes be disrupted. In addition, defects in defensin and AMPs production, as well as in pattern recognition receptors and low secretion of total IgA by B cells have also been linked with IBD. Finally, increased epithelial apoptosis in both UC and CD also contributes to barrier leakiness [2, 135, 136, 138].

Collectively, these alterations in mucosal epithelial barrier causes loss of fluid and solutes, leading to leak flux diarrhoea together with increased antigen translocation. Some studies suggested that inflammatory response is initiated due to an aberrant local immune response against commensal microbiota [2, 134, 135, 139]. Thus, the increased permeability of intestinal epithelium, owing to defects in N-cadherins synthesis, allows the entry of commensal flora into the lamina propria, triggering pro-inflammatory cytokine responses such as TNF-α, IL-6 and IL-1β that initiate and maintain gut inflammation [2, 134, 139]. It has also been suggested that DCs and macrophages could be related to the exacerbated immune response in IBD.

Macrophages contribute to CD pathogenesis owing to their capability to produce pro-inflammatory cytokines such as IL-12 and IL-23, and to activate T cells. In addition, disorders in phagocyte function of macrophages have frequently been associated to chronic colitis similar to CD. On the other hand, DCs populations in patients suffering from IBD are highly activated, producing high levels of pro-inflammatory cytokines. Besides, any dysregulation that affects one or more DCs subsets functions could result in a shift from regulatory to pathogenic T cells, exacerbating gut inflammation [2, 137].

However, despite many efforts, IBD aetiology remains unclear, but data obtained from different studies revealed that genetic, immune and environmental factors are mainly involved. Hence, meanwhile IBD origin is not completely elucidated, the main therapeutic goal is to regain epithelial barrier homeostasis and thus achieve mucosal healing and clinical remission. The process of intestinal mucosal healing is very complex and not fully understood. What is known,

however, is that restoring barrier integrity through rapid wound closure is crucial to limit antigen translocation and loss of fluids and electrolytes. Unfortunately, there are not therapies available that restore and regenerate epithelial barrier function, but some emerging and promising approaches such as immunotherapy, faecal microbiota transplantation, probiotics, antibiotics with immune-regulating properties like ciprofloxacin or metronidazole and cell therapies or its derivatives, among others, have been proposed [135, 138, 140, 141].

1.5. HYDROGELS: TYPES AND PROPERTIES

Hydrogels are translucent or transparent soft semisolid materials traditionally used in medicine, cosmetics, pharmacy or materials science. Recently, gels have attracted extraordinary attention for their advantageous properties in a wide variety of applications [142-145]. As delivery platforms they can protect the drug from extreme pH or enzyme degradation, improving its stability [142, 146]. The minimum hydrogel composition includes the liquid medium (or solvent), and a gelling agent (polymer). Small proportion of a crosslinker must be also necessary [147]. Gelling agents, form a three-dimensional (3D) colloidal network structure able of immobilizing and trapping solvent molecules, limiting fluid flow. The solvent can be found as free solvent, entrapped within the network or bound as a solvation layer. For hydrogels the solvent is always water [145].

Hydrogels are widely used in the pharmaceutical field due to their similarity to biological tissues and their biocompatibility. Their matrix, similar to extracellular matrices, have interstitial spaces capable of containing large amounts of water, while maintaining their structure and resistance to dilution due to physical or chemical crosslinking [148-150]. The aqueous medium gives them high permeability to oxygen and allows the diffusion of nutrients and small molecules. Therefore, hydrogels are extremely attractive platforms as superabsorbent materials, tissue engineering scaffolds, contact lenses, biosensors, and drug delivery systems [86, 151]. Despite their valuable advantages, hydrogels also present some limitations associated to high polymer crystallinity, low solubility, unfavourable thermal and mechanical properties, unreacted monomers, material-

dependent biodegradability and the employment of toxic crosslinkers [152].

Hydrogels are produced by the reaction of one or more polymer/monomer/cross-linker units. These small or large organic bridging molecules or particles generate two- and three-dimensional aggregates of various structured types, which through crosslinking and/or hierarchical self-assembly procedures give rise to a 3D hydrocolloidal network [144, 147, 153, 154]. The gelling process is determined by polymer-solvent and polymer-polymer interactions. An increase in the concentration of the polymer reduces the distance between bridging particles, which leads to crosslinking and entanglements. As a result, the immobilization of the components and an increase in the mechanical and viscoelastic properties of the system takes place [145].

The mechanical strength and the hydrogels diffusion properties are determined by the interactions between the aqueous solvent and the polymeric networks and by the nature of the bridging molecules, their shape, molecular size, ionic nature and degree of hydrophilicity [147, 153].

Hydrogels are capable of increasing more than 20% of their weight in contact with water or biological fluids, due to the presence of polar hydrophilic groups in their polymer chain, -COOH, -OH, -NH_2, -$CONH_2$ and -SO_3H [153, 155, 156]. The hydrogel structure does not collapse during swelling or dissolve in solution due to their reticulated meshwork [152, 157]. Thus, cross-linking provides the sufficient physical integrity and mechanical strength to maintain hydrogel 3D structure in the swollen state [153]. Cross-linking could take place during the preparation of the hydrogel or *in vivo*, once applied in the human body [152]. Hydrogel cross-linking can be achieved either chemically or physically. Chemical cross-linking involves the formation of new covalent bonds by reaction of functional groups between the different polymer chains with or without a cross-linking agent [152, 153, 158].

Physically cross-linked hydrogels or supramolecular hydrogels are also known as reversible hydrogels [142, 152]. Amphiphilic polymers are widely used to produce this type of systems. Physical

cross-linking does not require the use of cross-linking agents, being based on non-covalent interactions such as hydrogen bonding, dipole-dipole, van der Waals, π-π stacking or charge transfer that form non-permanent reticulation nodes between the short hydrophobic sequences present in the long hydrophilic polymer chains [142, 144]. Physical hydrogels frequently respond to changes in the environment, as pH, temperature or ionic strength, leading to reversible sol-gel transitions. The absence of external cross-linkers is beneficial to maintain low toxicity and biocompatibility and also to allow their post process bulk modification and reshaping [152, 158]. Thus, this type of hydrogels has received considerable attention during the last decade due to their tuneable properties and versatility [142].

Most of the hydrogel properties, such as the shear modulus (G), the swelling ratio (Q) or the diffusion coefficient of entrapped molecules (D), are controlled by the polymer concentration and the cross-linking density (ρ_x; number of physical or chemical cross-links by volume) (**Figure 4**) [159]. Cross-linking density, determines the pores or meshes of the network (ξ), and therefore, the maximum molecular size that can pass through the hydrogel matrix, controlling drug diffusivity [156, 159-161].

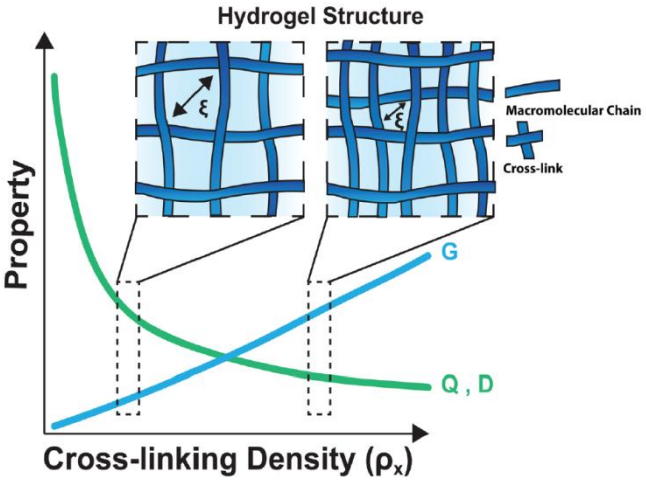

Figure 4. Two network structures presenting low and high cross-linking densities are shown to demonstrate the relationship between cross-linking

density and equilibrium swelling ratio (Q), diffusion coefficient (D) and shear modulus (G). As the cross-linking density increases, the space available between the polymer chains or mesh size (ξ) decreases, reducing the diffusion of solutes. Reprinted with permission from Kirschner and Anseth, 2013.

Generally, the mesh size reported range from 5 to 100 nm. Most hydrogels possess a broad distribution of mesh sizes due to polymer polydispersity and network heterogeneity. Other factors such as the selected polymer or external stimuli (pH and temperature) also can have an effect on hydrogel mesh size [156]. Mesh size is crucial when using hydrogels as drug delivery systems (**Figure 5**). If the drug is smaller than the mesh ($r_{mesh}/r_{drug} > 1$), the network will not limit the mobility of the bioactive compound and the drug release process will occur mainly by diffusion. If the mesh is similar in size to the drug ($r_{mesh}/r_{drug} \approx 1$), the steric hindrance effect becomes prominent. The polymer chains restrict drug diffusion, and an extended drug release profile can be obtained. Finally, when the mesh size is extremely small relative to the drug molecules ($r_{mesh}/r_{drug} < 1$), the strong steric hindrance prevents their mobility, resulting in their physically entrapment in the hydrogel matrix (reservoir), from which it can only be released by hydrogel degradation, mesh size enlargement by a swelling process or network deformation due to a mechanical force, a magnetic-field or ultrasounds [156, 162].

The release behaviour of hydrogels is also affected by other drug molecular configuration (*e.g.* charge, shape and deformability) [161]. Therefore, drug release kinetics from hydrogels is controlled by mechanisms of diffusion, swelling and/or degradation of the system as shown in **Figure 5** [161, 162]. Hydrogels are versatile and tunable platforms for drug delivery, whose release profiles can be tailored through a selection of suitable polymer or combination of polymers (variety, molecular weight, concentration), and crosslinking density [155, 160].

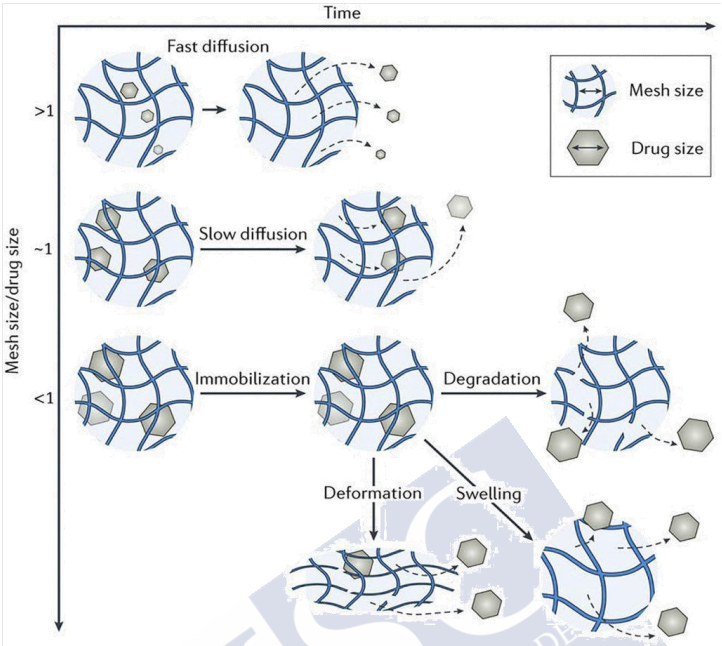

Figure 5. Drug diffusion is mediated by mesh size. Reprinted with permission from Li and Mooney, 2016.

1.5.1. Stimuli-sensitive hydrogels

Stimuli-sensitive hydrogels are smart hydrogels formed by polymers including stimuli-responsive moieties, enabling structural changes, triggered by an external stimulus such as pH, temperature, ionic strength, electrical and magnetic fields, light, ultrasound irradiation and redox processes. Stimuli-sensitive hydrogels can be classified as physically, chemically and biochemically responsive hydrogels [151, 152].

1.5.1.1. Physically responsive hydrogels

Thermosensitive hydrogels

Thermosensitive hydrogels are systems produced by polymers with hydrophobic and hydrophilic components in their structure. They are sensitive to temperature changes in the surrounding environment, which drastically affects their morphology

and can lead to a physical phase transition from solution to the gel state [163]. Their response to temperature can be negative or positive.

Positive responsive hydrogels as polyacrylamide and poly(acrylic acid)-based hydrogels, swell at temperatures over their upper critical solution temperature (UCST). Below the UCST, they shrink due to the formation of a complex structure through hydrogen bonding, which leads to network dehydration by releasing fluids or solvents from its matrix [155, 164].

Negative responsive hydrogels, as for example polyvinylpyrrolidon/poly(*N*-isopropylacrilamide), are characterized for swelling below their low critical solution temperature (LCST) due to hydrogen bonds formation between water and the hydrophilic part of the network. Whereas at a temperature above LCST, hydrophobic interactions predominate, weakening interchain hydrogen bonds and leading to the shrinkage of the hydrogel [165].

Another mechanism of temperature-dependent gel formation was observed for amphiphilic triblock copolymers composed of hydrophilic polyethylene oxide (PEO) and hydrophobic polypropylene oxide (PPO), commonly known as Pluronic® or Poloxamers. Above their critical micelle concentration (CMC), unassociated unimers of these copolymers equilibrate with micelles formed by PPO blocks in the inner part of micelles and a corona of PEO segments that interact with water. However, micelle formation strongly depends on temperature. The heating of the polymer solution to the LCST, usually designed as critical micelle temperature (CMT), promotes micelle formation as PPO chains become less soluble leading to micelle packing and gelation. Pluronic® are widely used for *in situ* gelling hydrogels characterized by their safety, bioadhesiveness, stability and ability to form gels at low concentrations at body temperature. Pluronic® gelation properties can be adjusted combining different Pluronic® or other excipients [166, 167].

In situ gelling hydrogels suffer a sol-gel transition under physiological conditions. As a consequence of this transition hydrogels are formed on the site of injection allowing easy drug loading, complete filling of the defect/wound and easy to handling, being suitable for intramuscular, subcutaneous, topical, transdermal

and mucosal drug delivery [166, 168, 169]. The sol-gel transition can be used to help in the drug formulation development as in liquid state can be easily mix with drugs and cells, and once administered at physiological temperature, undergo a sol-gel transition administration allowing to increase drug retention at the target tissues and the control release of the loaded drug [155, 164, 169, 170]. Thermoresponsive hydrogels have been used with good experimental outcomes for cell delivery and cancer, diabetes, thrombosis or pain therapy [171-174]. Moreover, thermoresponsive hydrogels with mucoadhesive properties are very attractive platforms for mucosal drug delivery. Their liquid nature when administered together with their gel transition at body temperature make them ideal for spreading and coating of mucosae [175].

Light responsive hydrogels

Light sensitive or photoresponsive hydrogels, are polymeric networks containing photosensitive moieties in the polymeric network. Several functional supramolecules, including stilbenes, ortho-nitrobenzyl groups, alkenes, azobenzene, spiropyranes and coumarins, have been incorporated into hydrogels to provide them with photo-responsive properties. The incorporation of photochromic chromophores into hydrogel networks allows the conversion of photoirradiation to photoreactions such as cleavage, dimerization or isomerization, some of which are reversible [176, 177].

Biomedical applications of light sensitive hydrogels are diverse, including scaffolds and advanced drug delivery systems [177, 178]. They have been proposed as carriers of antitumor drugs, immunotherapeutics or antimicrobial agents. Variations in the laser beam and wavelengths can be used to regulate the irradiated area and control drug release [178, 179].

Electro and magnetic responsive hydrogels

Electroresponsive hydrogels are characterized by changing their geometrical shape and size by swelling, shrinking or bending, when immersed in an electrolyte solution and exposed to an electric field [163, 180]. The electric responsiveness is explained by

the directional motion of ions in the hydrogel-electrolyte aqueous environment when electric voltage is applied, leading to their asymmetric distribution. As a result, osmotic pressure varies, triggering electroosmotic movement of water molecules and ultimately causing the deformation of the hydrogel [163, 181]. Several materials such as graphene, graphite, gold nanoparticles, silver nanowires or carbon nanotubes can be used to further provide conductive properties to hydrogels [182, 183]. These smart hydrogels can be used as biosensors, materials for 3D printing in tissue engineering or as drug delivery systems, the delivery of which can be precisely controlled by the correct amplitude, frequency and direction of the electrical stimulus [163, 184].

Magnetic responses are achieved by modifying hydrogels with inorganic magnetic responsive additives, such as Co and Fe_3O_4 nanoparticles, Fe microspheres, NdFeB microparticles and Cu beads. However, in the biomedical and pharmaceutical field, Fe_3O_4 nanoparticles are the most popular because of their super-paramagnetic characteristics, non-cytotoxicity and biocompatibility [163, 185]. Magnetic responsive hydrogels have been widely reported as drug delivery systems in cancer field, but also in tissue engineering, as smart drug delivery systems, drug targeting and theragnostic [186-192].

1.5.1.2. Chemically and biochemically responsive hydrogels

Stimuli-responsive hydrogels can also have the capability to change form and/or function when exposed to chemical and biochemical cues as the presence of specific molecules, redox reactions or antigens. These abilities make them useful as drug delivery systems, tissue engineering scaffolds, smart biodevices and biosensors [193]. Described below are the most commonly used chemically and biochemically responsive hydrogels categorized by the stimuli able to trigger the response.

pH responsive hydrogels

Their pH sensitivity is given by the functional pendant groups in the polymer backbone, which either can be basic or weak acid groups that become more ionized in lower or higher pH

environments, respectively [163, 194]. According to the nature of the pendant group, pH responsive hydrogels are classified into anionic and cationic hydrogels [155, 163]. Therefore, considering the pH variation within the human body, either at physiological and pathological conditions, cationic or anionic hydrogels will be selected as drug carriers depending on the pH of the target site [155, 195]. pH responsive hydrogels have been employed for oral, vaginal and intracellular (*e.g.* endosome/lysosome) drug delivery [196]. pH sensitive hydrogels are attractive platforms for intestine and colon targeting due to they can protect drugs from the harsh environment of stomach, prolong their residence time, increase bioavailability and reduce the dosing frequency [197, 198].

Glucose responsive hydrogels

Systems sensitive to changes in blood glucose concentration have been extensively studied for the diagnosis or the treatment of diabetes [143, 155]. According to their glucose-responsive mechanism can be classified as glucose oxidase (GOx), phenylboronic acid (PBA) or lectin [199].

Redox responsive hydrogels

Redox reactions can alter the optical, magnetic and electric properties of molecules by removing or adding electrons. Redox processes involve the formation of reactive oxygen species (ROS), which are single electron reduction products of oxygen that include, among others, non-radicals (hydrogen peroxide, H_2O_2) and free radicals (superoxide, $O_2^{\bullet-}$; hydroxyl radical, •OH; hypochlorite, OCl^-; peroxynitrite, $ONOO^-$...). At the cell level the endogenous formation of ROS is regulated by non-mitochondrial and mitochondrial producing enzymatic pathways. Thus, ROS play a key role in intercellular signalling and biological metabolism through stimulating the production of several hormones, modulating protein functions, mediating inflammatory processes and eliminating pathogens [200-202]. Thereby, ROS-responsive hydrogels have been employed as drug release platforms and as ROS-scavengers to eliminate or alleviate the cellular damages generated by ROS overproduction [200, 203, 204].

Antigen responsive hydrogels

The interactions between antigens and antibodies are highly specific and occur via multiple non-covalent bonds such as hydrogen bonds, hydrophobic, electrostatic and van der Waals interactions [205, 206]. Antigen responsive hydrogels can be prepared by physical trapping the antigen or antibody in the hydrogel matrix, by chemically conjugating the antigen or antibody to the hydrogel network or by grafting antigen-antibody pairs to the gel network to use them as reversible cross-linkers [205]. Explicit antigen-antibody binding has been exploited to develop immunosensors for the detection of various biological and environmental analytes [207].

Enzyme responsive hydrogels

Enzymatic-catalysed reactions are highly selective and specific towards their substrate and can also be carried out under quite mild conditions [208-210]. Other advantages of using enzymes as external stimuli are their biocompatibility and the possibility of being provided directly by the biological environment itself due to the great variety of enzymes presented in the human body. Therefore, research on enzyme responsive materials have been intensified over the last few years [210]. Enzyme-triggered transition processes or structural transformations in polymeric backbones are relevant for drug delivery and controlled release, diagnostics and imaging applications [208, 209]. Enzyme dysregulation associated to many pathological disorders and diseases, such as cardiovascular disease, cancer or osteoarthritis, has been exploited as a biological trigger for the controlled release of drugs at the target sites [208, 211].

Molecularly imprinted hydrogels

Hydrogels can be developed to specifically recognize molecules by a technique called molecular imprinting. This strategy is based on the creation of artificial receptors by the formation of a polymer network around a template molecule. In a first step the molecule is placed in the polymer mixture where the monomers arrange around it based on molecular interactions, such as hydrophobic interactions, hydrogen bonds, van der Waals forces and

electrostatic interactions. This spatial arrangement is then secured by the monomers polymerization [212]. Usually these hydrogels are highly crosslinked to achieve greater affinity, capacity, and selectivity [213].

1.5.2. Hydrogels as drug delivery platforms on mucosal surfaces

1.5.2.1. Formulation of hydrogels with desirable characteristics

An adequate therapeutic effect is achieved when a suitable concentration of drug reaches the target site and is maintained the required period of time [142]. When drug delivery platforms are designed for mucosal application, the anatomical characteristics of the mucosa play an important role to determine the permeability and the residence time of the therapeutic molecules. Therefore, hydrogels intended to be used for sublingual, buccal, vaginal, or rectal administration should present several characteristics to maximize mucosal contact, resist drainage or dilution, and accurately deliver the drug [166].

In this sense, the combination of thermosensitivity and bioadhesiveness in a hydrogel could result in more desirable therapeutic effects. This type of hydrogels can be administered in a liquid state at room temperature, achieving an easy distribution on the mucosal surface. Upon reaching physiological temperature, the gelling process increases its permanence in the area, avoiding runoffs and dilutions. Moreover, its bioadhesive character guarantees the maintenance of the formulation in the area and favours the local action of the drug [166].

The concept of including bioadhesive materials in pharmaceutical systems appeared in literature in the earlies 1980s [214]. There are two terms related to the interaction between mucosa and polymers; bioadhesion and mucoadhesion. Although they are often used synonymously, there is a clear difference between them. The phenomenon of molecular attraction between biological tissues and natural or synthetic polymers is known as bioadhesion. Mucoadhesion refers to the interaction between polymers and the mucus layer covering the biological substrate [214-216]. Interactions with the

mucus network can occur through non-covalent bonds, electrostatic interactions or even covalent crosslinking, allowing the polymers to adhere to mucosal surfaces for a prolonged period of time [215, 216]. The mucoadhesion process takes place in two sequential steps: wetting and consolidation. First, the system wets, swells and interacts with the mucous network. During the consolidation stage, the polymer chains interpenetrate the mucus layer, entangle and can form covalent bonds [217, 218].

Mucoadhesive strength is affected by several factors related to the polymer features such as molecular weight, charge, chain length, flexibility and diffusivity through the mucosal layer to facilitate entanglement and physicochemical interactions [216, 219-221]. In general, high molecular weight polymers (≥ 100 kDa) are considered better candidates for mucoadhesive systems [222]. Polymer chain length must be short enough to facilitate diffusion into mucous network but long enough to promote its interpenetration with the mucin chains. Moreover, highly flexible polymer chains allow a better entanglement and interpenetration of materials with the mucosal layer, favouring the interaction of the polymers [219].

The ability of polymers to form hydrogen bonds with the mucous layer is another characteristic that confers a mucoadhesive character. The presence of functional groups in the polymer chain such as amino, carboxyl or hydroxyl, is related to this property. In general, the adhesion is higher the more hydrogen bonds are formed [216, 221]. The charge and degree of ionization of the polymer chains are also of importance when considering mucoadhesive strength. Anionic polyelectrolytes exhibit a greater degree of adhesion compared to non-ionic polymers. In fact, the general trend for mucoadhesive strength of polymers is as follows: anion> cation> non-ionic [219]. Thus, the pH of the surrounding microenvironment can modify the ionization state of the polymer and therefore, its adhesion properties. In general, mucoadhesion is favoured at pHs above the pK of the polymer at which it will be mainly ionized [222].

Mucoadhesive properties of the formulations also are determined by the polymer concentration and the crosslinking degree. Every polymer has an optimal concentration at which it has the highest

mucoadhesiveness. At lower concentrations, the interaction between the polymer and the mucus is unstable due to the reduced number of penetrating polymer chains per volume of mucus. While at higher concentrations, the coiling of the polymer chains occurs, and the accessibility of the solvent and the interpenetration of polymer/mucin chains are reduced, worsening the mucoadhesive properties [220]. On the other hand, crosslinking degree affects mucoadhesive properties by controlling polymer chain mobility. Highly cross-linked materials are capable of swell in contact with biological fluids and retain water in their structure, resisting dissolution, but their mucoadhesiveness is reduced by decreasing the mobility of the polymer chains [222].

Polymer mucoadhesion is also affected by the magnitude of its hydration, which must be adequate to expand and create a macromolecular mesh that allows the polymer-mucin interactions to be established. When the polymer swells, its mucoadhesive areas are exposed, allowing its mechanical entanglement with the mucosal network. If excessive hydration occurs, mucoadhesion is reduced due to the formation of a slippery mucilage [219, 220, 222].

Since the properties of hydrogels are determined by the ingredients chosen for their preparation, an adequate selection of polymers together with a proper understanding of how selected materials interact with each other is crucial to obtain hydrogels of desired characteristics. Therefore, obtaining formulations that meet all the requirements for successful mucosal drug release can be feasible through proper hydrogel design, which should allow determining the optimal polymer concentration to achieve highly mucoadhesive formulations capable of overcoming intrinsic barriers present in mucosal tissues.

1.6. ARTIFICIAL INTELLIGENCE TECHNIQUES APPLIED TO PHARMACEUTICAL SYSTEMS DESIGN

The design and manufacture of multicomponent pharmaceutical systems is challenging as it involves a large number of variables whose single effects or in combination have a great impact on the final properties of the dosage forms [223-225]. The quality of pharmaceutical systems is directly related to the knowledge of the

effects of these variables on the characteristics of the formulations (knowledge space) and the production of the systems within the limits of the design space. Knowledge space and design space, make up the concept of Quality by Design (QbD), the systematic approach defined by the International Conference on Harmonization for pharmaceutical development (ICH Q8 guideline). The concept of QbD was first introduced into the pharmaceutical industry in 2004 as a consequence of the Food and Drug Administration (FDA) initiative named "cGMPs for the 21th century: A Risk-Based Approach". Then, European and Japanese regulatory authorities have also encouraged their use in Chemistry, Manufacturing and Controls review process. Thus, QbD has emerged as an approach to promote a better understanding of pharmaceutical products, from the early stages (design and development) to subsequent commercial production [226, 227].

Nevertheless, despite the advantages that QbD offers to pharmaceutical companies, it is not completely implemented on real product development or industrial applications [223, 227]. QbD points out the need to identify critical parameters that affect the quality, efficacy, stability and safety of pharmaceutical dosage forms which is extremely difficult in multivariate processes using traditional methodology. When the number of variables is large, the numerical solutions for a process optimization is time consuming and entered the realm of the complex statistics [228, 229].

In recent years, the growing development and introduction of Artificial Intelligence (AI) tools comes to help in the task of designing complex systems, including pharmaceutical formulations. AI is used to provide accurate analysis, interpretation and management of generated data throughout the development and production of a product, making easier to overcome potential setbacks as well as save time and money [223, 230]. Machine learning, a subset of AI, is the most widely used AI technology in pharmaceutical development. These computerized techniques include Artificial Neural Networks (ANNs), genetic algorithms and neurofuzzy logic [225, 231].

ANNs are the main tools for data mining. ANNs are mathematical models generated by computational systems, designed to mimic the biological processes of the human brain. Like biological neural

systems, ANNs are made up of unitary elements called *perceptrons*, or nodes, organized in layers and forming complex networks (**Figure 6**). Perceptrons receive one or more input from neighbouring neurons, process the information and produce an output to be transmitted to the next node. The strengths of connections between the artificial neurons are called "weights" [226].

ANNs is a supervised AI technique. During the training process, the network structure, weights, threshold, and transfer function must be established in order to find an algorithm that relates inputs and outputs of the training set. Thus, ANN learns and is able to answer "WHAT-IF" questions which can be used to predict results of unrealized experiences and identify complex and latent patterns between experimental data (input) and response values (output) (**Figure 6**). ANNs can detect intricate non-linear relationships within big datasets by creating nonlinear input-output mappings. For this reason, ANNs arouse as a powerful and robust technique for modelling, predicting, and optimizing pharmaceutical processes and formulations, underpinning the application of QbD in pharma industry [225, 227, 232-236].

The interpretation of ANNs is quite difficult due to the generation of black-box models. For that reason, ANNs can be combined with other techniques to facilitate their interpretation and/or utility. Its combination with fuzzy logic lead hybrid technologies named neurofuzzy logic systems. Fuzzy logic is a form of logic in which the truth value of a variable can be expressed with a word and a real number between 0 and 1, inclusive, called the degree of membership. Fuzzification and defuzzification processes allow encoding the structure of ANNs into a reasonably small number of logical rules. In addition to predictive models, neurofuzzy logic provides easy-to-follow rules generated in the explicit "IF-THEN" format (**Figure 6**), representing the output-input relationships within the database. This makes cause-and-effect relationships between inputs and outputs easier to understand and therefore, allow to define the knowledge space and the design space [223, 224, 234, 237].

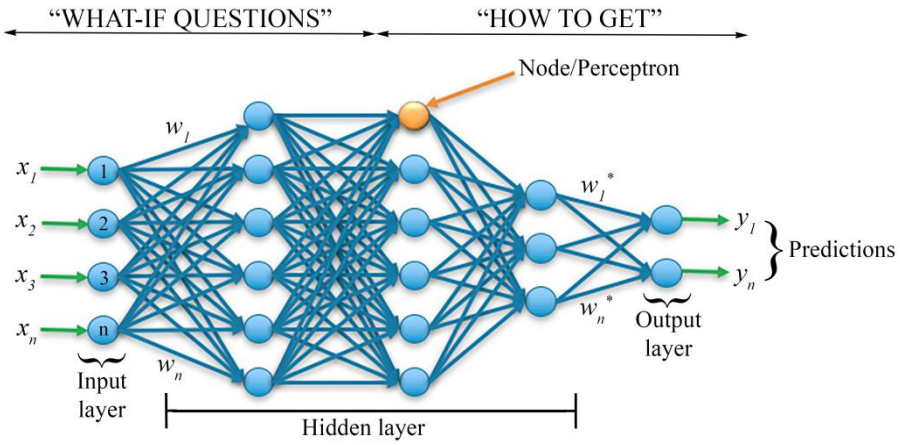

Figure 6. Typical diagram of an artificial neural network, which consists of unitary elements called perceptrons or nodes. The main structural components of an artificial neural network are input, hidden and output layers. The input layer transfer information to the hidden layer. This layer consists of several interconeccted nodes that link the input and output layers via weights (*w*). After the training process, the inputs and outputs are linked by an algorithm that allows answering the "WHAT-IF" questions and thus predicting the outcomes of the unrealized experiences.

ANNs can also be combined with genetic algorithms (GA). GA are also bioinspired AI tools. Based on the biological principles of genetic variation and natural selection, genetic algorithms are designed to select the best solution of a specific problem. When combined ANN and GA, a set of candidate solutions to the problem are generated and selected according to their fitness to previous established criteria. After several generations, GA are able to find a global optimal solution for different attributes simultaneously [238].

Overall, the combination of ANNs with neurofuzzy logic or genetic algorithms is a feasible and promising approach to design drug delivery systems. It allows to precisely control how procedural variables affect the final properties of pharmaceutical formulations as well as the further obtaining of optimized dosage forms with suitable characteristics.

REFERENCES

[1] A.E. Williams, Immunology: Mucosal and Body Surface Defences, Wiley, 2011.
[2] J. Mestecky, W. Strober, M.W. Russell, H. Cheroutre, N. Lambrecht, B.L. Kelsall, Mucosal Immunology, Elsevier Science, 2015.
[3] J.H. Rhee, Current and New Approaches for Mucosal Vaccine Delivery, in: Mucosal Vaccines, 2020, pp. 325-356.
[4] M.M. France, J.R. Turner, The mucosal barrier at a glance, J Cell Sci, 130 (2017) 307-314.
[5] S.H. Kim, Y.-S. Jang, The development of mucosal vaccines for both mucosal and systemic immune induction and the roles played by adjuvants, Clinical and Experimental Vaccine Research, 6 (2017).
[6] J. Holmgren, C. Czerkinsky, Mucosal immunity and vaccines, Nat Med, 11 (2005) S45-53.
[7] P. Brandtzaeg, Mucosal immunity: induction, dissemination, and effector functions, Scand J Immunol, 70 (2009) 505-515.
[8] G.C. Hansson, Mucus and mucins in diseases of the intestinal and respiratory tracts, J Intern Med, 285 (2019) 479-490.
[9] S.K. Linden, P. Sutton, N.G. Karlsson, V. Korolik, M.A. McGuckin, Mucins in the mucosal barrier to infection, Mucosal Immunol, 1 (2008) 183-197.
[10] J. Witten, T. Samad, K. Ribbeck, Selective permeability of mucus barriers, Curr Opin Biotechnol, 52 (2018) 124-133.
[11] K.M. Murphy, C. Weaver, Janeway's Immunobiology: Ninth International Student Edition, Taylor & Francis Group, 2016.
[12] J.R. McGhee, K. Fujihashi, Inside the mucosal immune system, PLoS Biol, 10 (2012) e1001397.
[13] E.P. Widmaier, H. Raff, K.T. Strang, Vander's Human Physiology: The Mechanisms of Body Function, McGraw-Hill Education, 2018.
[14] R.Q. Wu, D.F. Zhang, E. Tu, Q.M. Chen, W. Chen, The mucosal immune system in the oral cavity-an orchestra of T cell diversity, Int J Oral Sci, 6 (2014) 125-132.
[15] H. Tlaskalová-Hogenová, L. Tucková, R. Lodinová-Zádniková R. Stepánková, B. Cukrowska, D.P. Funda, I. Striz, H. Kozáková, I.

Trebichavský, D. Sokol, Z. Reháková, J. Sinkora, P. Fundová, D. Horáková, L. Jelínková, D. Sánchez, Mucosal immunity: its role in defense and allergy.
[16] M.F. Cesta, Normal structure, function, and histology of mucosa-associated lymphoid tissue, Toxicol Pathol, 34 (2006) 599-608.
[17] G.A. Parker, T.L. Papenfuss, Immune System, in: Atlas of Histology of the Juvenile Rat, 2016, pp. 293-347.
[18] J. Leal, H.D.C. Smyth, D. Ghosh, Physicochemical properties of mucus and their impact on transmucosal drug delivery, Int J Pharm, 532 (2017) 555-572.
[19] R. Bansil, B.S. Turner, The biology of mucus: Composition, synthesis and organization, Adv Drug Deliv Rev, 124 (2018) 3-15.
[20] V.F. Patel, F. Liu, M.B. Brown, Advances in oral transmucosal drug delivery, J Control Release, 153 (2011) 106-116.
[21] T. Pelaseyed, J.H. Bergström, J.K. Gustafsson, A. Ermund, G.M.H. Birchenough, A. Schütte, S. van der Post, F. Svensson, A.M. Rodríguez-Piñeiro, E.E.L. Nyström, C. Wising, M.E.V. Johansson, G.C. Hansson, The mucus and mucins of the goblet cells and enterocytes provide the first defense line of the gastrointestinal tract and interact with the immune system, Immunol Rev, 260 (2014) 8-20.
[22] H.H. Sigurdsson, J. Kirch, C.M. Lehr, Mucus as a barrier to lipophilic drugs, Int J Pharm, 453 (2013) 56-64.
[23] J.D. Smart, Theories of Mucoadhesion, (2014) 159-174.
[24] N.A. Peppas, J.B. Thomas, J. McGinty, Molecular aspects of mucoadhesive carrier development for drug delivery and improved absorption, J Biomater Sci Polym Ed, 20 (2009) 1-20.
[25] B.M. Boddupalli, Z.N. Mohammed, R.A. Nath, D. Banji, Mucoadhesive drug delivery system: An overview, J Adv Pharm Technol Res, 1 (2010) 381-387.
[26] J. Xu, S. Strandman, J.X. Zhu, J. Barralet, M. Cerruti, Genipin-crosslinked catechol-chitosan mucoadhesive hydrogels for buccal drug delivery, Biomaterials, 37 (2015) 395-404.
[27] J. Xu, M. Tam, S. Samaei, S. Lerouge, J. Barralet, M.M. Stevenson, M. Cerruti, Mucoadhesive chitosan hydrogels as rectal drug delivery vessels to treat ulcerative colitis, Acta Biomater, 48 (2017) 247-257.

[28] M. Ana Valentich, T. Analia Cafaro, H. Marcelo Serra, Oral Cavity-Associated Immune System: What is New?, Current Immunology Reviews, 7 (2011) 253-263.
[29] H. Kraan, H. Vrieling, C. Czerkinsky, W. Jiskoot, G. Kersten, J.P. Amorij, Buccal and sublingual vaccine delivery, J Control Release, 190 (2014) 580-592.
[30] N.M. Moutsopoulos, J.E. Konkel, Tissue-Specific Immunity at the Oral Mucosal Barrier, Trends Immunol, 39 (2018) 276-287.
[31] P. Moingeon, Update on immune mechanisms associated with sublingual immunotherapy: practical implications for the clinician, J Allergy Clin Immunol Pract, 1 (2013) 228-241.
[32] F.X. Lu, R.S. Jacobson, Oral mucosal immunity and HIV/SIV infection, J Dent Res, 86 (2007) 216-226.
[33] C.W. Cutler, R. Jotwani, Dendritic cells at the oral mucosal interface, J Dent Res, 85 (2006) 678-689.
[34] M. Naafs, Oral Mucosal Immune Suppression, Tolerance and Silencing: A Mini-Review, Modern Approaches in Dentistry and Oral Health Care, 1 (2018).
[35] M. Flach, A. Diefenbach, Development of Gut-Associated Lymphoid Tissues, in: Mucosal Immunology, 2015, pp. 31-42.
[36] B. Ahluwalia, M.K. Magnusson, L. Ohman, Mucosal immune system of the gastrointestinal tract: maintaining balance between the good and the bad, Scand J Gastroenterol, 52 (2017) 1185-1193.
[37] A.M. Mowat, W.W. Agace, Regional specialization within the intestinal immune system, Nat Rev Immunol, 14 (2014) 667-685.
[38] H. Ohno, Intestinal M cells, J Biochem, 159 (2016) 151-160.
[39] M.R. Neutra, N.J. Mantis, J.P. Kraehenbuhl, Collaboration of epithelial cells with organized mucosal lymphoid tissues, Nat Immunol, 2 (2001) 1004-1009.
[40] A. Srivastava, D.V. Gowda, S.V. Madhunapantula, C.G. Shinde, M. Iyer, Mucosal vaccines: a paradigm shift in the development of mucosal adjuvants and delivery vehicles, APMIS, 123 (2015) 275-288.
[41] M. Li, Y. Wang, Y. Sun, H. Cui, S.J. Zhu, H.J. Qiu, Mucosal vaccines: Strategies and challenges, Immunol Lett, 217 (2020) 116-125.

[42] M.R. Neutra, P.A. Kozlowski, Mucosal vaccines: the promise and the challenge, Nat Rev Immunol, 6 (2006) 148-158.
[43] K.A. Woodrow, K.M. Bennett, D.D. Lo, Mucosal vaccine design and delivery, Annu Rev Biomed Eng, 14 (2012) 17-46.
[44] C. Hervouet, C. Luci, N. Cuburu, M. Cremel, S. Bekri, L. Vimeux, C. Maranon, C. Czerkinsky, A. Hosmalin, F. Anjuere, Sublingual immunization with an HIV subunit vaccine induces antibodies and cytotoxic T cells in the mouse female genital tract, Vaccine, 28 (2010) 5582-5590.
[45] M.T. De Magistris, Mucosal delivery of vaccine antigens and its advantages in pediatrics, Adv Drug Deliv Rev, 58 (2006) 52-67.
[46] A. Miquel-Clopes, E.G. Bentley, J.P. Stewart, S.R. Carding, Mucosal vaccines and technology, Clin Exp Immunol, 196 (2019) 205-214.
[47] D. Christensen, Vaccine adjuvants: Why and how, Hum Vaccin Immunother, 12 (2016) 2709-2711.
[48] S. Apostolico Jde, V.A. Lunardelli, F.C. Coirada, S.B. Boscardin, D.S. Rosa, Adjuvants: Classification, Modus Operandi, and Licensing, J Immunol Res, 2016 (2016) 1459394.
[49] J.F. Mann, R. Acevedo Campo, J.D Campo, O. Pérez, V.A. Ferro, Delivery systems: a vaccine strategy for overcoming mucosal tolerance?, Expert Rev Vaccines, 8 (2009) 103-112.
[50] H.X. Tan, A.K. Wheatley, R. Esterbauer, S. Jegaskanda, J.J. Glass, D. Masopust, R. De Rose, S.J. Kent, Induction of vaginal-resident HIV-specific CD8 T cells with mucosal prime-boost immunization, Mucosal Immunol, 11 (2018) 994-1007.
[51] A. Sato, A. Suwanto, M. Okabe, S. Sato, T. Nochi, T. Imai, N. Koyanagi, J. Kunisawa, Y. Kawaguchi, H. Kiyono, Vaginal memory T cells induced by intranasal vaccination are critical for protective T cell recruitment and prevention of genital HSV-2 disease, J Virol, 88 (2014) 13699-13708.
[52] J.A. White, J.S. Blum, N.A. Hosken, J.O. Marshak, L. Duncan, C. Zhu, E.B. Norton, J.D. Clements, D.M. Koelle, D. Chen, W.C. Weldon, M.S. Oberste, M. Lal, Serum and mucosal antibody responses to inactivated polio vaccine after sublingual immunization

using a thermoresponsive gel delivery system, Hum Vaccin Immunother, 10 (2014) 3611-3621.
[53] J.S. Woodworth, D. Christensen, J.P. Cassidy, E.M. Agger, R. Mortensen, P. Andersen, Mucosal boosting of H56:CAF01 immunization promotes lung-localized T cells and an accelerated pulmonary response to Mycobacterium tuberculosis infection without enhancing vaccine protection, Mucosal Immunol, 12 (2019) 816-826.
[54] P. Ralli-Jain, D. Tifrea, C. Cheng, S. Pal, L.M. de la Maza, Enhancement of the protective efficacy of a Chlamydia trachomatis recombinant vaccine by combining systemic and mucosal routes for immunization, Vaccine, 28 (2010) 7659-7666.
[55] Y. Fujkuyama, D. Tokuhara, K. Kataoka, R.S. Gilbert, J.R. McGhee, Y. Yuki, H. Kiyono, K. Fujihashi, Novel vaccine development strategies for inducing mucosal immunity, Expert Rev Vaccines, 11 (2012) 367-379.
[56] N. Marasini, L.M. Kaminskas, Subunit-based mucosal vaccine delivery systems for pulmonary delivery - Are they feasible?, Drug Dev Ind Pharm, 45 (2019) 882-894.
[57] A.B. Nesburn, I. Bettahi, X. Zhang, X. Zhu, W. Chamberlain, R.E. Afifi, S.L. Wechsler, L. Benmohamed, Topical/Mucosal Delivery of Sub-Unit Vaccines That Stimulate the Ocular Mucosal Immune System, The Ocular Surface, 4 (2006) 178-187.
[58] R. Da Costa Martins, C. Gamazo, M. Sanchez-Martinez, M. Barberan, I. Penuelas, J.M. Irache, Conjunctival vaccination against Brucella ovis in mice with mannosylated nanoparticles, J Control Release, 162 (2012) 553-560.
[59] M. Sánchez-Martínez, R. da Costa Martins, G. Quincoces, C. Gamazo, C. Caicedo, J.M Irache, I. Peñuelas, Radiolabeling and biodistribution studies of polymeric nanoparticles as adjuvants for ocular vaccination against brucellosis, Rev Esp Med Nucl Imagen Mol, 32 (2013) 92-97.
[60] S. Yoon, E.D. Kim, M.S. Song, S.J. Han, T.K. Park, K.S. Choi, Y.K. Choi, K.Y. Seo, Eyedrop Vaccination Induced Systemic and Mucosal Immunity against Influenza Virus in Ferrets, PLoS One, 11 (2016) e0157634.

[61] M.C. Moran, A.R. Bence, M.F.S. Vallecillo, C.M. Lutzelschwab, M.G. Rodriguez, R. Pardo, F.A. Goldbaum, V. Zylberman, S.D. Palma, B.A. Maletto, S.M. Estein, Polymeric antigen BLSOmp31 formulated with class B CpG-ODN in a nanostructure (BLSOmp31/CpG-ODN/Coa-ASC16) administered by parenteral or mucosal routes confers protection against Brucella ovis in Balb/c mice, Res Vet Sci, 135 (2021) 217-227.
[62] A. Inic-Kanada, M. Stojanovic, S. Schlacher, E. Stein, S. Belij-Rammerstorfer, E. Marinkovic, I. Lukic, J. Montanaro, N. Schuerer, N. Bintner, V. Kovacevic-Jovanovic, O. Krnjaja, U.B. Mayr, W. Lubitz, T. Barisani-Asenbauer, Delivery of a Chlamydial Adhesin N-PmpC Subunit Vaccine to the Ocular Mucosa Using Particulate Carriers, PLoS One, 10 (2015) e0144380.
[63] A.B. Nesburn, S. Slanina, R.L.Burke, H. Ghiasi, S. Bahri, S.L. Wechsler, Local periocular vaccination protects against eye disease more effectively than systemic vaccination following primary ocular herpes simplex virus infection in rabbits, J Virol, 72 (1998) 7715-7721.
[64] A.B. Nesburn, T.V. Ramos, X. Zhu, H. Asgarzadeh, V. Nguyen, L. BenMohamed, Local and systemic B cell and Th1 responses induced following ocular mucosal delivery of multiple epitopes of herpes simplex virus type 1 glycoprotein D together with cytosine-phosphate-guanine adjuvant, Vaccine, 23 (2005) 873-883.
[65] T.N. Alkie, A. Yitbarek, K. Taha-Abdelaziz, J. Astill, S. Sharif, Characterization of immunogenicity of avian influenza antigens encapsulated in PLGA nanoparticles following mucosal and subcutaneous delivery in chickens, PLoS One, 13 (2018) e0206324.
[66] M. Wu, H. Zhao, M. Li, Y. Yue, S. Xiong, W. Xu, Intranasal Vaccination with Mannosylated Chitosan Formulated DNA Vaccine Enables Robust IgA and Cellular Response Induction in the Lungs of Mice and Improves Protection against Pulmonary Mycobacterial Challenge, Front Cell Infect Microbiol, 7 (2017) 445.
[67] R. Nakahashi-Ouchida, Y. Yuki, H. Kiyono, Cationic pullulan nanogel as a safe and effective nasal vaccine delivery system for respiratory infectious diseases, Hum Vaccin Immunother, 14 (2018) 2189-2193.

[68] Y. Wu, W. Wei, M. Zhou, Y. Wang, J. Wu, G. Ma, Z. Su, Thermal-sensitive hydrogel as adjuvant-free vaccine delivery system for H5N1 intranasal immunization, Biomaterials, 33 (2012) 2351-2360.
[69] H. Vinson, G. Singh, A. Pillatzki, B. Webb, E. Nelson, S. Ramamoorthy, Delivery of a thermo-enzymatically treated influenza vaccine using pulmonary surfactant in pigs, Vet Microbiol, 239 (2019) 108492.
[70] B. Bernocchi, R. Carpentier, D. Betbeder, Nasal nanovaccines, Int J Pharm, 530 (2017) 128-138.
[71] T.F. Bahamondez-Canas, Z. Cui, Intranasal immunization with dry powder vaccines, Eur J Pharm Biopharm, 122 (2018) 167-175.
[72] W. Cao, M. Mishina, S. Amoah, W.P. Mboko, C. Bohannon, J. McCoy, S.K. Mittal, S. Gangappa, S. Sambhara, Nasal delivery of H5N1 avian influenza vaccine formulated with GenJet or in vivo-jetPEI((R)) induces enhanced serological, cellular and protective immune responses, Drug Deliv, 25 (2018) 773-779.
[73] A.K. Murthy, J.P. Chambers, P.A. Meier, G. Zhong, B.P. Arulanandam, Intranasal vaccination with a secreted chlamydial protein enhances resolution of genital Chlamydia muridarum infection, protects against oviduct pathology, and is highly dependent upon endogenous gamma interferon production, Infect Immun, 75 (2007) 666-676.
[74] J. Hinkula, M. Hagbom, B. Wahren, U. Schroder, Safety and immunogenicity, after nasal application of HIV-1 DNA gagp37 plasmid vaccine in young mice, Vaccine, 26 (2008) 5101-5106.
[75] G.A. Price, M.W. Russell, C.N. Cornelissen, Intranasal administration of recombinant Neisseria gonorrhoeae transferrin binding proteins A and B conjugated to the cholera toxin B subunit induces systemic and vaginal antibodies in mice, Infect Immun, 73 (2005) 3945-3953.
[76] Y. Jiang, M. Li, Z. Zhang, T. Gong, X. Sun, Enhancement of nasal HIV vaccination with adenoviral vector-based nanocomplexes using mucoadhesive and DC-targeting adjuvants, Pharm Res, 31 (2014) 2748-2761.

[77] W.F. Tonnis, A.J. Lexmond, H.W. Frijlink, A.H. de Boer, W.L.J. Hinrichs, Devices and formulations for pulmonary vaccination, Expert Opin Drug Deliv, 10 (2013) 1383-1397.
[78] G. Pedersen, R. Cox, The mucosal vaccine quandary: intranasal vs. sublingual immunization against influenza, Hum Vaccin Immunother, 8 (2012) 689-693.
[79] A.L. Paris, E. Colomb, B. Verrier, F. Anjuere, C. Monge, Sublingual vaccination and delivery systems, J Control Release, 332 (2021) 553-562.
[80] C. Ramirez Sevilla, E. Gomez Lanza, J.L. Manzanera, J.A.R. Martin, M.A.B. Sanz, Active immunoprophyilaxis with uromune(R) decreases the recurrence of urinary tract infections at three and six months after treatment without relevant secondary effects, BMC Infect Dis, 19 (2019) 901.
[81] H.S. Oberoi, Y.M. Yorgensen, A. Morasse, J.T. Evans, D.J. Burkhart, PEG modified liposomes containing CRX-601 adjuvant in combination with methylglycol chitosan enhance the murine sublingual immune response to influenza vaccination, J Control Release, 223 (2016) 64-74.
[82] A. Khan, S. Singh, G. Galvan, C. Jagannath, K.J. Sastry, Prophylactic Sublingual Immunization with Mycobacterium tuberculosis Subunit Vaccine Incorporating the Natural Killer T Cell Agonist Alpha-Galactosylceramide Enhances Protective Immunity to Limit Pulmonary and Extra-Pulmonary Bacterial Burden in Mice, Vaccines (Basel), 5 (2017).
[83] S. Raghavan, A.K. Ostberg, C.F. Flach, A. Ekman, M. Blomquist, C. Czerkinsky, J. Holmgren, Sublingual immunization protects against Helicobacter pylori infection and induces T and B cell responses in the stomach, Infect Immun, 78 (2010) 4251-4260.
[84] C.S. Eickhoff, A. Blazevic, E.A. Killoran, M.S. Morris, D.F. Hoft, Induction of mycobacterial protective immunity by sublingual BCG vaccination, Vaccine, 37 (2019) 5364-5370.
[85] J. Liao, J.A. Gibson, B.S. Pickering, P.I. Watnick, Sublingual Adjuvant Delivery by a Live Attenuated Vibrio cholerae-Based Antigen Presentation Platform. mSphere, 3 (2018) e00245-18.

[86] J. Masek, D. Lubasova, R. Lukac, P. Turanek-Knotigova, P. Kulich, J. Plockova, E. Maskova, L. Prochazka, S. Koudelka, N. Sasithorn, J. Gombos, E. Bartheldyova, F. Hubatka, M. Raska, A.D. Miller, J. Turanek, Multi-layered nanofibrous mucoadhesive films for buccal and sublingual administration of drug-delivery and vaccination nanoparticles - important step towards effective mucosal vaccines, J Control Release, 249 (2017) 183-195.
[87] S.M. Hanson, S. Singh, A. Tabet, K.J. Sastry, M. Barry, C. Wang, Mucoadhesive wafers composed of binary polymer blends for sublingual delivery and preservation of protein vaccines, J Control Release, 330 (2021) 427-437.
[88] E.S. DeLyria, D. Zhou, J.S. Lee, S. Singh, W. Song, F. Li, Q. Sun, H. Lu, J. Wu, Q. Qiao, Y. Hu, G. Zhang, C. Li, K.J. Sastry, H. Shen, Sublingual injection of microparticles containing glycolipid ligands for NKT cells and subunit vaccines induces antibody responses in oral cavity, Carbohydr Res, 405 (2015) 87-92.
[89] P. Moingeon, V. Lombardi, V. Baron-Bodo, L. Mascarell, Enhancing Allergen-Presentation Platforms for Sublingual Immunotherapy, J Allergy Clin Immunol Pract, 5 (2017) 23-31.
[90] C. Hensley, P. Zhou, S. Schnur, H.M. Mahsoub, Y. Liang, M.X. Wang, C. Page, L. Yuan, V. Bronshtein, Thermostable, Dissolvable Buccal Film Rotavirus Vaccine Is Highly Effective in Neonatal Gnotobiotic Pig Challenge Model, Vaccines (Basel), 9 (2021).
[91] L. Zhai, R. Yadav, N.K. Kunda, D. Anderson, E. Bruckner, E.K. Miller, R. Basu, P. Muttil, E. Tumban, Oral immunization with bacteriophage MS2-L2 VLPs protects against oral and genital infection with multiple HPV types associated with head & neck cancers and cervical cancer, Antiviral Res, 166 (2019) 56-65.
[92] M.C. Yang, A. Yang, J. Qiu, B. Yang, L. He, Y.C. Tsai, J. Jeang, T.C. Wu, C.F. Hung, Buccal injection of synthetic HPV long peptide vaccine induces local and systemic antigen-specific CD8+ T-cell immune responses and antitumor effects without adjuvant, Cell Biosci, 6 (2016) 17.
[93] M. Uddin, A. Allon, M.A. Roni, S. Kouzi, S. Kouzi, Overview and Future Potential of Fast Dissolving Buccal Films as Drug

Delivery System for Vaccines, J Pharm Pharm Sci, 22 (2019) 388-406.
[94] C.J. Davitt, E.C. Lavelle, Delivery strategies to enhance oral vaccination against enteric infections, Adv Drug Deliv Rev, 91 (2015) 52-69.
[95] M. Duran-Lobato, B. Carrillo-Conde, Y. Khairandish, N.A. Peppas, Surface-modified P(HEMA-co-MAA) nanogel carriers for oral vaccine delivery: design, characterization, and in vitro targeting evaluation, Biomacromolecules, 15 (2014) 2725-2734.
[96] C.A. Hayden, M.E. Fischer, B.L. Andrews, H.C. Chilton, D.D. Turner, J.H. Walker, I.R. Tizard, J.A. Howard, Oral delivery of wafers made from HBsAg-expressing maize germ induces long-term immunological systemic and mucosal responses, Vaccine, 33 (2015) 2881-2886.
[97] M. Yoshida, N. Kamei, K. Muto, J. Kunisawa, K. Takayama, N.A. Peppas, M. Takeda-Morishita, Complexation hydrogels as potential carriers in oral vaccine delivery systems, Eur J Pharm Biopharm, 112 (2017) 138-142.
[98] Q. Zhu, J. Talton, G. Zhang, T. Cunningham, Z. Wang, R.C. Waters, J. Kirk, B. Eppler, D.M. Klinman, Y. Sui, S. Gagnon, I.M. Belyakov, R.J. Mumper, J.A. Berzofsky, Large intestine-targeted, nanoparticle-releasing oral vaccine to control genitorectal viral infection, Nat Med, 18 (2012) 1291-1296.
[99] C. Zhu, H. Lin, L. Tang, J. Chen, Y. Wu, G. Zhong, Oral Chlamydia vaccination induces transmucosal protection in the airway, Vaccine, 36 (2018) 2061-2068.
[100] Y. Yuki, H. Kiyono, Mucosal vaccines: novel advances in technology and delivery.
[101] R. Pais, Y. Omosun, Q. He, U. Blas-Machado, C. Black, J.U. Igietseme, K. Fujihashi, F.O. Eko, Rectal administration of a chlamydial subunit vaccine protects against genital infection and upper reproductive tract pathology in mice, PLoS One, 12 (2017) e0178537.
[102] M. Yu, M. Vajdy, Mucosal HIV transmission and vaccination strategies through oral compared with vaginal and rectal routes, Expert Opin Biol Ther, 10 (2010) 1181-1195.

[103] L.L. Grando, D.C. Machado, S. Spitzer, S. Nachman, F. Ferguson, B. Berentsen, L.S. Yurgel, Viral coinfection in the oral cavity of HIV-infected children: relation among HIV viral load, CD4+ T lymphocyte count and detection of EBV, CMV and HSV, Braz Oral Res, 19 (2005) 228-234.
[104] H. Kato, H. Bukawa, E. Hagiwara, K.Q. Xin, K. Hamajima, S. Kawamoto, M. Sugiyama, M. Sugiyama, E. Noda, M. Nishizaki, K. Okuda, Rectal and vaginal immunization with a macromolecular multicomponent peptide vaccine candidate for HIV-1 infection induces HIV-specific protective immune responses, Vaccine, 18 (2000) 1151-1160.
[105] J. das Neves, R. Nunes, A. Machado, B. Sarmento, Polymer-based nanocarriers for vaginal drug delivery, Adv Drug Deliv Rev, 92 (2015) 53-70.
[106] D.I. Bernstein, D.A. Pullum, R.D. Cardin, F.J. Bravo, D.A. Dixon, K.G. Kousoulas, The HSV-1 live attenuated VC2 vaccine provides protection against HSV-2 genital infection in the guinea pig model of genital herpes, Vaccine, 37 (2019) 61-68.
[107] P.N. Gupta, A. Pattani, R.M. Curran, V.L. Kett, G.P. Andrews, R.J. Morrow, A.D. Woolfson, R.K. Malcolm, Development of liposome gel based formulations for intravaginal delivery of the recombinant HIV-1 envelope protein CN54gp140, Eur J Pharm Sci, 46 (2012) 315-322.
[108] L. Donnelly, R.M. Curran, J.S. Tregoning, P.F. McKay, T. Cole, R.J. Morrow, V.L. Kett, G.P. Andrews, A.D. Woolfson, R.K. Malcolm, R.J. Shattock, Intravaginal immunization using the recombinant HIV-1 clade-C trimeric envelope glycoprotein CN54gp140 formulated within lyophilized solid dosage forms, Vaccine, 29 (2011) 4512-4520.
[109] Z. Xie, Z. Ji, Z. Zhang, T. Gong, X. Sun, Adenoviral vectors coated with cationic PEG derivatives for intravaginal vaccination against HIV-1, Biomaterials, 35 (2014) 7896-7908.
[110] T. Kanazawa, T. Tamura, M. Yamazaki, Y. Takashima, H. Okada, Needle-free intravaginal DNA vaccination using a stearoyl oligopeptide carrier promotes local gene expression and immune responses, Int J Pharm, 447 (2013) 70-74.

[111] K. Schautteet, E. Stuyven, D.S. Beeckman, S. Van Acker, M. Carlon, K. Chiers, E. Cox, D. Vanrompay, Protection of pigs against Chlamydia trachomatis challenge by administration of a MOMP-based DNA vaccine in the vaginal mucosa, Vaccine, 29 (2011) 1399-1407.
[112] P.F. McKay, J.F. Mann, A. Pattani, V. Kett, Y. Aldon, D. King, R.K. Malcolm, R.J. Shattock, Intravaginal immunisation using a novel antigen-releasing ring device elicits robust vaccine antigen-specific systemic and mucosal humoral immune responses, J Control Release, 249 (2017) 74-83.
[113] Y. Sun, S. Peng, A. Yang, E. Farmer, T.C. Wu, C.F. Hung, Coinjection of IL2 DNA enhances E7-specific antitumor immunity elicited by intravaginal therapeutic HPV DNA vaccination with electroporation, Gene Ther, 24 (2017) 408-415.
[114] S. Domingos-Pereira, G. Galliverti, D. Hanahan, D. Nardelli-Haefliger, Carboplatin/paclitaxel, E7-vaccination and intravaginal CpG as tri-therapy towards efficient regression of genital HPV16 tumors, J Immunother Cancer, 7 (2019) 122.
[115] S. Hua, E. Marks, J.J. Schneider, S. Keely, Advances in oral nano-delivery systems for colon targeted drug delivery in inflammatory bowel disease: selective targeting to diseased versus healthy tissue, Nanomedicine, 11 (2015) 1117-1132.
[116] Q. Zhang, H. Tao, Y. Lin, Y. Hu, H. An, D. Zhang, S. Feng, H. Hu, R. Wang, X. Li, J. Zhang, A superoxide dismutase/catalase mimetic nanomedicine for targeted therapy of inflammatory bowel disease, Biomaterials, 105 (2016) 206-221.
[117] R. Awasthi, M. Kumar, Development of Metronidazole-Loaded Colon-Targeted Microparticulate Drug Delivery System, Polymers in Medicine, 45 (2015) 57-65.
[118] C. Corbo, W.E. Cromer, R. Molinaro, N.E. Toledano Furman, K.A. Hartman, E. De Rosa, C. Boada, X. Wang, D.C. Zawieja, M. Agostini, F. Salvatore, B.P. Abraham, E. Tasciotti, Engineered biomimetic nanovesicles show intrinsic anti-inflammatory properties for the treatment of inflammatory bowel diseases, Nanoscale, 9 (2017) 14581-14591.

[119] N. Gobbato, M. Rachid, G. Perdigon, Anti-inflammatory effect of yoghurt in an experimental inflammatory bowel disease in mouse, J Dairy Res, 75 (2008) 497-504.
[120] X.Y. Bai, Y. Yan, L. Wang, L.G. Zhao, K. Wang, Novel pH-sensitive hydrogels for 5-aminosalicylic acid colon targeting delivery: in vivo study with ulcerative colitis targeting therapy in mice, Drug Deliv, 23 (2016) 1926-1932.
[121] J. Zhou, M. O'Keeffe, G. Liao, F. Zhao, C. Terhorst, B. Xu, Design and Synthesis of Nanofibers of Self-assembled de novo Glycoconjugates towards Mucosal Lining Restoration and Anti-Inflammatory Drug Delivery, Tetrahedron, 72 (2016) 6078-6083.
[122] P.L. Kozuch, S.B. Hanauer, Treatment of inflammatory bowel disease: a review of medical therapy, World J Gastroenterol, 14 (2008) 354-377.
[123] L. Steidler, Microbiological and immunological strategies for treatment of inflammatory bowel disease, Microbes Infect, 3 (2001) 1157-1166.
[124] A.K. Dash, Z. Gong, D.W. Miller, H. Huai-Yan, J. Laforet, Development of a rectal nicotine delivery system for the treatment of ulcerative colitis, Int J Pharm, 190 (1999) 21-34.
[125] J. Meier, A. Sturm, Current treatment of ulcerative colitis, World J Gastroenterol, 17 (2011) 3204-3212.
[126] T.J. Keane, J. Dziki, E. Sobieski, A. Smoulder, A. Castleton, N. Turner, L.J. White, S.F. Badylak, Restoring Mucosal Barrier Function and Modifying Macrophage Phenotype with an Extracellular Matrix Hydrogel: Potential Therapy for Ulcerative Colitis, J Crohns Colitis, 11 (2017) 360-368.
[127] C.N. Bernstein, J.D. Forbes, Gut Microbiome in Inflammatory Bowel Disease and Other Chronic Immune-Mediated Inflammatory Diseases, Inflamm Intest Dis, 2 (2017) 116-123.
[128] J.T. Kuenstner, S. Naser, W. Chamberlin, T. Borody, D.Y. Graham, A. McNees, J. Hermon-Taylor, A. Hermon-Taylor, C.T. Dow, W. Thayer, J. Biesecker, M.T. Collins, L.A. Sechi, S.V. Singh, P. Zhang, I. Shafran, S. Weg, G. Telega, R. Rothstein, H. Oken, S. Schimpff, H. Bach, T. Bull, I. Grant, J. Ellingson, H. Dahmen, J. Lipton, S. Gupta, K. Chaubey, M. Singh, P. Agarwal, A. Kumar, J.

Misri, J. Sohal, K. Dhama, Z. Hemati, W. Davis, M. Hier, J. Aitken, E. Pierce, N. Parrish, N. Goldberg, M. Kali, S. Bendre, G. Agrawal, R. Baldassano, P. Linn, R.W. Sweeney, M. Fecteau, C. Hofstaedter, R. Potula, O. Timofeeva, S. Geier, K. John, N. Zayanni, H.M. Malaty, C. Kahlenborn, A. Kravitz, A. Bulfon, G. Daskalopoulos, H. Mitchell, B. Neilan, V. Timms, D. Cossu, G. Mameli, P. Angermeier, T. Jelic, R. Goethe, R.A. Juste, L. Kuenstner, The Consensus from the Mycobacterium avium ssp. paratuberculosis (MAP) Conference 2017, Front Public Health, 5 (2017) 208.

[129] A. Watad, S. Azrielant, N.L. Bragazzi, K. Sharif, P. David, I. Katz, G. Aljadeff, M. Quaresma, G. Tanay, M. Adawi, H. Amital, Y. Shoenfeld, Seasonality and autoimmune diseases: The contribution of the four seasons to the mosaic of autoimmunity, J Autoimmun, 82 (2017) 13-30.

[130] T. Azimi, M.J. Nasiri, A.S. Chirani, R. Pouriran, H. Dabiri, The role of bacteria in the inflammatory bowel disease development: a narrative review, APMIS, 126 (2018) 275-283.

[131] H. Ebrahimiyan, S. Aslani, N. Rezaei, A. Jamshidi, M. Mahmoudi, Survivin and autoimmunity; the ins and outs, Immunol Lett, 193 (2018) 14-24.

[132] G. Rogler, L. Biedermann, M. Scharl, New insights into the pathophysiology of inflammatory bowel disease: microbiota, epigenetics and common signalling pathways, Swiss Med Wkly, 148 (2018) w14599.

[133] S.C. Ng, G.G. Kaplan, W. Tang, R. Banerjee, B. Adigopula, F.E. Underwood, D. Tanyingoh, S.C. Wei, W.C. Lin, H.H. Lin, J. Li, S. Bell, O. Niewiadomski, M.A. Kamm, Z. Zeng, M. Chen, P. Hu, D. Ong, C.J. Ooi, K.L. Ling, Y. Miao, J. Miao, H.J. de Silva, M. Niriella, S. Aniwan, J. Limsrivilai, P. Pisespongsa, K. Wu, H. Yang, K.K. Ng, H.H. Yu, Y. Wang, Q. Ouyang, M. Abdullah, M. Simadibrata, J. Gunawan, I. Hilmi, K.L. Goh, Q. Cao, H. Sheng, A. Ong-Go, V.H. Chong, J.Y.L. Ching, J.C.Y. Wu, F.K.L. Chan, J.J.Y. Sung, Population Density and Risk of Inflammatory Bowel Disease: A Prospective Population-Based Study in 13 Countries or Regions in Asia-Pacific, Am J Gastroenterol, (2018).

[134] M. Vasovic, N. Gajovic, D. Brajkovic, M. Jovanovic, N. Zdravkovaic, T. Kanjevac, The relationship between the immune system and oral manifestations of inflammatory bowel disease: a review, Cent Eur J Immunol, 41 (2016) 302-310.
[135] F.E.O. Holmberg, J. Pedersen, P. Jørgensen, C. Soendergaard, K.B. Jensen, O.H. Nielsen, Intestinal barrier integrity and inflammatory bowel disease: Stem cell-based approaches to regenerate the barrier, Journal of Tissue Engineering and Regenerative Medicine, 12 (2017) 923-935.
[136] E. Martini, S.M. Krug, B. Siegmund, M.F. Neurath, C. Becker, Mend Your Fences: The Epithelial Barrier and its Relationship With Mucosal Immunity in Inflammatory Bowel Disease, Cell Mol Gastroenterol Hepatol, 4 (2017) 33-46.
[137] F. Sanchez de Medina, I. Romero-Calvo, C. Mascaraque, O. Martinez-Augustin, Intestinal inflammation and mucosal barrier function, Inflamm Bowel Dis, 20 (2014) 2394-2404.
[138] M.A. Odenwald, J.R. Turner, The intestinal epithelial barrier: a therapeutic target?, Nature Reviews Gastroenterology & Hepatology, 14 (2016) 9-21.
[139] I. Koboziev, F. Karlsson, M.B. Grisham, Gut-associated lymphoid tissue, T cell trafficking, and chronic intestinal inflammation, Ann N Y Acad Sci, 1207 Suppl 1 (2010) E86-93.
[140] S. Danese, G. Roda, L. Peyrin-Biroulet, Evolving therapeutic goals in ulcerative colitis: towards disease clearance, Nat Rev Gastroenterol Hepatol, 17 (2020) 1-2.
[141] S. Pouya, M. Heidari, K. Baghaei, H. Asadzadeh Aghdaei, A. Moradi, S. Namaki, M.R. Zali, S.M. Hashemi, Study the effects of mesenchymal stem cell conditioned medium injection in mouse model of acute colitis, Int Immunopharmacol, 54 (2018) 86-94.
[142] J. Mayr, C. Saldias, D. Diaz Diaz, Release of small bioactive molecules from physical gels, Chem Soc Rev, 47 (2018) 1484-1515.
[143] C. Echeverria, S.N. Fernandes, M.H. Godinho, J.P. Borges, P.I.P. Soares, Functional Stimuli-Responsive Gels: Hydrogels and Microgels, Gels, 4 (2018).

[144] C.M. Papadakis, C. Tsitsilianis, Responsive Hydrogels from Associative Block Copolymers: Physical Gelling through Polyion Complexation, Gels, 3 (2017).
[145] M. Justin-Temu, F. Damian, R. Kinget, G.Van Den Mooter, Intravaginal gels as drug delivery systems, J Womens Health (Larchmt), 13 (2004) 834-844.
[146] L. Mao, Y. Lu, M. Cui, S. Miao, Y. Gao, Design of gel structures in water and oil phases for improved delivery of bioactive food ingredients, Crit Rev Food Sci Nutr, 60 (2020) 1651-1666.
[147] M.J. Taylor, P. Tomlins, T.S. Sahota, Thermoresponsive Gels, Gels, 3 (2017).
[148] J. Hurler, A. Engesland, B. Poorahmary Kermany, N. Škalko-Basnet, Improved texture analysis for hydrogel characterization: Gel cohesiveness, adhesiveness, and hardness, Journal of Applied Polymer Science, 125 (2012) 180-188.
[149] A. Sosnik, K.P. Seremeta, Polymeric Hydrogels as Technology Platform for Drug Delivery Applications, Gels, 3 (2017).
[150] S. Chatterjee, P.C. Hui, C.W. Kan, Thermoresponsive Hydrogels and Their Biomedical Applications: Special Insight into Their Applications in Textile Based Transdermal Therapy, Polymers (Basel), 10 (2018).
[151] M. Vazquez-Gonzalez, I. Willner, Stimuli-Responsive Biomolecule-Based Hydrogels and Their Applications, Angew Chem Int Ed Engl, (2019).
[152] F. Ullah, M.B. Othman, F. Javed, Z. Ahmad, H. Md Akil, Classification, processing and application of hydrogels: A review, Mater Sci Eng C Mater Biol Appl, 57 (2015) 414-433.
[153] K. Varaprasad, G.M. Raghavendra, T. Jayaramudu, M.M. Yallapu, R. Sadiku, A mini review on hydrogels classification and recent developments in miscellaneous applications, Mater Sci Eng C Mater Biol Appl, 79 (2017) 958-971.
[154] H. Li, N. Kong, B. Laver, J. Liu, Hydrogels Constructed from Engineered Proteins, Small, 12 (2016) 973-987.
[155] F. Raza, H. Zafar, Y. Zhu, Y. Ren, A. Ullah, A.U. Khan, X. He, H. Han, M. Aquib, K.O. Boakye-Yiadom, L. Ge, A Review on Recent

Advances in Stabilizing Peptides/Proteins upon Fabrication in Hydrogels from Biodegradable Polymers, Pharmaceutics, 10 (2018).
[156] J. Li, D.J. Mooney, Designing hydrogels for controlled drug delivery, Nat Rev Mater, 1 (2016).
[157] S. Bashir, M. Hina, J. Iqbal, A.H. Rajpar, M.A. Mujtaba, N.A. Alghamdi, S. Wageh, K. Ramesh, S. Ramesh, Fundamental Concepts of Hydrogels: Synthesis, Properties, and Their Applications, Polymers (Basel), 12 (2020).
[158] A. Ali, S. Ahmed, Recent Advances in Edible Polymer Based Hydrogels as a Sustainable Alternative to Conventional Polymers, J Agric Food Chem, 66 (2018) 6940-6967.
[159] C.M. Kirschner, K.S. Anseth, Hydrogels in Healthcare: From Static to Dynamic Material Microenvironments, Acta Mater, 61 (2013) 931-944.
[160] A. Chyzy, M. Tomczykowa, M.E. Plonska-Brzezinska, Hydrogels as Potential Nano-, Micro- and Macro-Scale Systems for Controlled Drug Delivery, Materials (Basel), 13 (2020).
[161] S. Kirchhof, M. Abrami, V. Messmann, N. Hammer, A.M. Goepferich, M. Grassi, F.P. Brandl, Diels-Alder Hydrogels for Controlled Antibody Release: Correlation between Mesh Size and Release Rate, Mol Pharm, 12 (2015) 3358-3368.
[162] D. Rocha-García, A. Guerra-Contreras, S. Rosales-Mendoza, G. Palestino, Role of porous silicon/hydrogel composites on drug delivery, Open Material Sciences, 3 (2016).
[163] Q. Shi, H. Liu, D. Tang, Y. Li, X. Li, F. Xu, Bioactuators based on stimulus-responsive hydrogels and their emerging biomedical applications, NPG Asia Materials, 11 (2019).
[164] S. Graham, P.F. Marina, A. Blencowe, Thermoresponsive polysaccharides and their thermoreversible physical hydrogel networks, Carbohydr Polym, 207 (2019) 143-159.
[165] C. Alvarez-Lorenzo, V.Y. Grinberg, T.V. Burova, A. Concheiro, Stimuli-sensitive cross-linked hydrogels as drug delivery systems: Impact of the drug on the responsiveness, Int J Pharm, 579 (2020) 119157.

[166] F. Zahir-Jouzdani, J.D. Wolf, F. Atyabi, A. Bernkop-Schnürch, In situ gelling and mucoadhesive polymers: why do they need each other?, Expert Opinion on Drug Delivery, 15 (2018) 1007-1019.
[167] B. Shriky, A. Kelly, M. Isreb, M. Babenko, N. Mahmoudi, S. Rogers, O. Shebanova, T. Snow, T. Gough, Pluronic F127 thermosensitive injectable smart hydrogels for controlled drug delivery system development, Journal of Colloid and Interface Science, 565 (2020) 119-130.
[168] L. Mude, B.K.R. Sanapalli, A.N. V, S.K. Singh, V. Karri, Overview of in situ gelling injectable hydrogels for diabetic wounds, Drug development research, (2021).
[169] M.R. Matanovic, J. Kristl, P.A. Grabnar, Thermoresponsive polymers: insights into decisive hydrogel characteristics, mechanisms of gelation, and promising biomedical applications, Int J Pharm, 472 (2014) 262-275.
[170] M. Norouzi, B. Nazari, D.W. Miller, Injectable hydrogel-based drug delivery systems for local cancer therapy, Drug Discov Today, 21 (2016) 1835-1849.
[171] S.M. Rossi, B.K. Ryan, H.M. Kelly, Evaluation of the activity of a chemo-ablative, thermoresponsive hydrogel in a murine xenograft model of lung cancer, Br J Cancer, 123 (2020) 369-377.
[172] W.K. Bae, M.S. Park, J.H. Lee, J.E. Hwang, H.J. Shim, S.H. Cho, D.E. Kim, H.M. Ko, C.S. Cho, I.K. Park, I.J. Chung, Docetaxel-loaded thermoresponsive conjugated linoleic acid-incorporated poloxamer hydrogel for the suppression of peritoneal metastasis of gastric cancer, Biomaterials, 34 (2013) 1433-1441.
[173] S.M. Rossi, T.E. Murray, J. Cassidy, M.J. Lee, H.M. Kelly, A Custom Radiopaque Thermoresponsive Chemotherapy-Loaded Hydrogel for Intratumoural Injection: An In Vitro and Ex Vivo Assessment of Imaging Characteristics and Material Properties, Cardiovasc Intervent Radiol, 42 (2019) 289-297.
[174] R. Li, Y. Li, Y. Wu, Y. Zhao, H. Chen, Y. Yuan, K. Xu, H. Zhang, Y. Lu, J. Wang, X. Li, X. Jia, J. Xiao, Heparin-Poloxamer Thermosensitive Hydrogel Loaded with bFGF and NGF Enhances Peripheral Nerve Regeneration in Diabetic Rats, Biomaterials, 168 (2018) 24-37.

[175] D.F. Argenta, B.D.C. Bernardo, A.F. Chamorro, P.R. Matos, T. Caon, Thermosensitive hydrogels for vaginal delivery of secnidazole as an approach to overcome the systemic side-effects of oral preparations, Eur J Pharm Sci, 159 (2021) 105722.
[176] L. Li, J.M. Scheiger, P.A. Levkin, Design and Applications of Photoresponsive Hydrogels, Adv Mater, 31 (2019) e1807333.
[177] I. Tomatsu, K. Peng, A. Kros, Photoresponsive hydrogels for biomedical applications, Adv Drug Deliv Rev, 63 (2011) 1257-1266.
[178] T.L. Rapp, C.A. DeForest, Targeting drug delivery with light: A highly focused approach, Adv Drug Deliv Rev, 171 (2021) 94-107.
[179] M.E. Roth-Konforti, M. Comune, M. Halperin-Sternfeld, I. Grigoriants, D. Shabat, L. Adler-Abramovich, UV Light-Responsive Peptide-Based Supramolecular Hydrogel for Controlled Drug Delivery, Macromol Rapid Commun, 39 (2018) e1800588.
[180] J. Shang, Z. Shao, X. Chen, Electrical behavior of a natural polyelectrolyte hydrogel: chitosan/carboxymethylcellulose hydrogel, Biomacromolecules, 9 (2008) 1208-1213.
[181] X. Ying, Y. Wang, J. Liang, J. Yue, C. Xu, L. Lu, Z. Xu, J. Gao, Y. Du, Z. Chen, Angiopep-conjugated electro-responsive hydrogel nanoparticles: therapeutic potential for epilepsy, Angew Chem Int Ed Engl, 53 (2014) 12436-12440.
[182] J.H. Ha, H.H. Shin, H.W. Choi, J.H. Lim, S.J. Mo, C.D. Ahrberg, J.M. Lee, B.G. Chung, Electro-responsive hydrogel-based microfluidic actuator platform for photothermal therapy, Lab Chip, 20 (2020) 3354-3364.
[183] N. Vigues, F. Pujol-Vila, A. Marquez-Maqueda, X. Munoz-Berbel, J. Mas, Electro-addressable conductive alginate hydrogel for bacterial trapping and general toxicity determination, Anal Chim Acta, 1036 (2018) 115-120.
[184] I. Carayon, A. Gaubert, Y. Mousli, B. Philippe, Electro-responsive hydrogels: macromolecular and supramolecular approaches in the biomedical field, Biomater Sci, 8 (2020) 5589-5600.
[185] I. Lee, C.W. Park, S.S. Yoon, H.M. Yang, Facile synthesis of copper ferrocyanide-embedded magnetic hydrogel beads for the enhanced removal of cesium from water, Chemosphere, 224 (2019) 776-785.

[186] Q. Liu, H. Li, K.Y. Lam, Optimization of Deformable Magnetic-Sensitive Hydrogel-Based Targeting System in Suspension Fluid for Site-Specific Drug Delivery, Mol Pharm, 15 (2018) 4632-4642.
[187] A. Najafipour, A. Gharieh, A. Fassihi, H. Sadeghi-Aliabadi, A.R. Mahdavian, MTX-Loaded Dual Thermoresponsive and pH-Responsive Magnetic Hydrogel Nanocomposite Particles for Combined Controlled Drug Delivery and Hyperthermia Therapy of Cancer, Mol Pharm, 18 (2021) 275-284.
[188] M. Noh, Y.H. Choi, Y.H. An, D. Tahk, S. Cho, J.W. Yoon, N.L. Jeon, T.H. Park, J. Kim, N.S. Hwang, Magnetic Nanoparticle-Embedded Hydrogel Sheet with a Groove Pattern for Wound Healing Application, ACS Biomater Sci Eng, 5 (2019) 3909-3921.
[189] X. Chen, M. Fan, H. Tan, B. Ren, G. Yuan, Y. Jia, J. Li, D. Xiong, X. Xing, X. Niu, X. Hu, Magnetic and self-healing chitosan-alginate hydrogel encapsulated gelatin microspheres via covalent cross-linking for drug delivery, Mater Sci Eng C Mater Biol Appl, 101 (2019) 619-629.
[190] W. Xue, X.L. Liu, H. Ma, W. Xie, S. Huang, H. Wen, G. Jing, L. Zhao, X.J. Liang, H.M. Fan, AMF responsive DOX-loaded magnetic microspheres: transmembrane drug release mechanism and multimodality postsurgical treatment of breast cancer, J Mater Chem B, 6 (2018) 2289-2303.
[191] S. Kondaveeti, A.T.S. Semeano, D.R. Cornejo, H. Ulrich, D.F.S. Petri, Magnetic hydrogels for levodopa release and cell stimulation triggered by external magnetic field, Colloids Surf B Biointerfaces, 167 (2018) 415-424.
[192] H. Wu, L. Song, L. Chen, Y. Huang, Y. Wu, F. Zang, Y. An, H. Lyu, M. Ma, J. Chen, N. Gu, Y. Zhang, Injectable thermosensitive magnetic nanoemulsion hydrogel for multimodal-imaging-guided accurate thermoablative cancer therapy, Nanoscale, 9 (2017) 16175-16182.
[193] R.V. Ulijn, N. Bibi, V. Jayawarna, P.D. Thornton, S.J. Todd, R.J. Mart, A.M. Smith, J.E. Gough, Bioresponsive hydrogels, Materials Today, 10 (2007) 40-48.

[194] A. Hendi, M. Umair Hassan, M. Elsherif, B. Alqattan, S. Park, A.K. Yetisen, H. Butt, Healthcare Applications of pH-Sensitive Hydrogel-Based Devices: A Review, Int J Nanomedicine, 15 (2020) 3887-3901.
[195] M. Rizwan, R. Yahya, A. Hassan, M. Yar, A.D. Azzahari, V. Selvanathan, F. Sonsudin, C.N. Abouloula, pH Sensitive Hydrogels in Drug Delivery: Brief History, Properties, Swelling, and Release Mechanism, Material Selection and Applications, Polymers (Basel), 9 (2017).
[196] S. Bazban-Shotorbani, M.M. Hasani-Sadrabadi, A. Karkhaneh, V. Serpooshan, K.I. Jacob, A. Moshaverinia, M. Mahmoudi, Revisiting structure-property relationship of pH-responsive polymers for drug delivery applications, J Control Release, 253 (2017) 46-63.
[197] S. Das, U. Subuddhi, pH-Responsive guar gum hydrogels for controlled delivery of dexamethasone to the intestine, Int J Biol Macromol, 79 (2015) 856-863.
[198] D.S. Seeli, M. Prabaharan, Guar gum oleate-graft-poly(methacrylic acid) hydrogel as a colon-specific controlled drug delivery carrier, Carbohydr Polym, 158 (2017) 51-57.
[199] Q. Wu, L. Wang, H. Yu, J. Wang, Z. Chen, Organization of glucose-responsive systems and their properties, Chem Rev, 111 (2011) 7855-7875.
[200] D. Eleftheriadou, D. Kesidou, F. Moura, E. Felli, W. Song, Redox-Responsive Nanobiomaterials-Based Therapeutics for Neurodegenerative Diseases, Small, 16 (2020) e1907308.
[201] H. Ye, Y. Zhou, X. Liu, Y. Chen, S. Duan, R. Zhu, Y. Liu, L. Yin, Recent Advances on Reactive Oxygen Species-Responsive Delivery and Diagnosis System, Biomacromolecules, 20 (2019) 2441-2463.
[202] G. Saravanakumar, J. Kim, W.J. Kim, Reactive-Oxygen-Species-Responsive Drug Delivery Systems: Promises and Challenges, Adv Sci (Weinh), 4 (2017) 1600124.
[203] Q. Xu, C. He, K. Ren, C. Xiao, X. Chen, Thermosensitive Polypeptide Hydrogels as a Platform for ROS-Triggered Cargo Release with Innate Cytoprotective Ability under Oxidative Stress, Adv Healthc Mater, 5 (2016) 1979-1990.

[204] H. Zhao, J. Huang, Y. Li, X. Lv, H. Zhou, H. Wang, Y. Xu, C. Wang, J. Wang, Z. Liu, ROS-scavenging hydrogel to promote healing of bacteria infected diabetic wounds, Biomaterials, 258 (2020) 120286.
[205] R. Zhang, A. Bowyer, R. Eisenthal, J. Hubble, A smart membrane based on an antigen-responsive hydrogel, Biotechnol Bioeng, 97 (2007) 976-984.
[206] T. Miyata, T. Uragami, K. Nakamae, Biomolecule-sensitive hydrogels, Adv Drug Deliv Rev, 54 (2002) 79-98.
[207] S.M. George, S. Tandon, B. Kandasubramanian, Advancements in Hydrogel-Functionalized Immunosensing Platforms, ACS Omega, 5 (2020) 2060-2068.
[208] R. Chandrawati, Enzyme-responsive polymer hydrogels for therapeutic delivery, Exp Biol Med (Maywood), 241 (2016) 972-979.
[209] J. Hu, G. Zhang, S. Liu, Enzyme-responsive polymeric assemblies, nanoparticles and hydrogels, Chem Soc Rev, 41 (2012) 5933-5949.
[210] M. Zelzer, S.J. Todd, A.R. Hirst, T.O. McDonald, R.V. Ulijn, Enzyme responsive materials: design strategies and future developments, Biomater Sci, 1 (2013) 11-39.
[211] M. Shahriari, M. Zahiri, K. Abnous, S.M. Taghdisi, M. Ramezani, M. Alibolandi, Enzyme responsive drug delivery systems in cancer treatment, J Control Release, 308 (2019) 172-189.
[212] E. Verheyen, J.P. Schillemans, M. van Wijk, M.-A. Demeniex, W.E. Hennink, C.F. van Nostrum, Challenges for the effective molecular imprinting of proteins, Biomaterials, 32 (2011) 3008-3020.
[213] M.E. Byrne, K. Park, N.A. Peppas, Molecular imprinting within hydrogels, Advanced Drug Delivery Reviews, 54 (2002) 149-161.
[214] K. Edsman, H. Hagerstrom, Pharmaceutical applications of mucoadhesion for the non-oral routes, J Pharm Pharmacol, 57 (2005) 3-22.
[215] A. Partenhauser, A. Bernkop-Schnürch, Mucoadhesive polymers in the treatment of dry X syndrome, Drug Discovery Today, 21 (2016) 1051-1062.

[216] S. Roy, K. Pal, A. Anis, K. Pramanik, B. Prabhakar, Polymers in Mucoadhesive Drug-Delivery Systems: A Brief Note, Designed Monomers and Polymers, 12 (2012) 483-495.
[217] J.D. Smart, The basics and underlying mechanisms of mucoadhesion, Adv Drug Deliv Rev, 57 (2005) 1556-1568.
[218] P. Schattling, E. Taipaleenmäki, Y. Zhang, B. Städler, A Polymer Chemistry Point of View on Mucoadhesion and Mucopenetration, Macromolecular Bioscience, 17 (2017).
[219] S. Mansuri, P. Kesharwani, K. Jain, R.K. Tekade, N.K. Jain, Mucoadhesion: A promising approach in drug delivery system, Reactive and Functional Polymers, 100 (2016) 151-172.
[220] N. Salamat-Miller, M. Chittchang, T.P. Johnston, The use of mucoadhesive polymers in buccal drug delivery, Adv Drug Deliv Rev, 57 (2005) 1666-1691.
[221] K. Kumar, N. Dhawan, H. Sharma, S. Vaidya, B. Vaidya, Bioadhesive polymers: novel tool for drug delivery, Artif Cells Nanomed Biotechnol, 42 (2014) 274-283.
[222] R. Shaikh, T.R. Raj Singh, M.J. Garland, A.D. Woolfson, R.F. Donnelly, Mucoadhesive drug delivery systems, J Pharm Bioallied Sci, 3 (2011) 89-100.
[223] B. Aksu, A. Paradkar, M. de Matas, O. Ozer, T. Guneri, P. York, Quality by design approach: application of artificial intelligence techniques of tablets manufactured by direct compression, AAPS PharmSciTech, 13 (2012) 1138-1146.
[224] M. Landin, R.C. Rowe, P. York, Advantages of neurofuzzy logic against conventional experimental design and statistical analysis in studying and developing direct compression formulations, Eur J Pharm Sci, 38 (2009) 325-331.
[225] S.A. Damiati, Digital Pharmaceutical Sciences, AAPS PharmSciTech, 21 (2020) 206.
[226] M. Landín, Introducción al uso de sistemas de inteligencia artificial para modelizar, comprender y optimizar formulaciones farmacéuticas, in: Biomateriais aplicados ao desenvolvimento de sistemas terapêuticos avançados, 2015, pp. 521-554.
[227] M.F. Simoes, G. Silva, A.C. Pinto, M. Fonseca, N.E. Silva, R.M.A. Pinto, S. Simoes, Artificial neural networks applied to quality-

by-design: From formulation development to clinical outcome, Eur J Pharm Biopharm, 152 (2020) 282-295.
[228] B. Singh, M. Dahiya V. Saharan, N. Ahuja, Optimizing drug delivery systems using systematic "design of experiments." Part II: retrospect and prospects, Crit Rev Ther Drug Carrier Syst, 22 (2005) 215-294.
[229] B. Singh, N. Kumar, N. Ahuja, Optimizing drug delivery systems using systematic "design of experiments." Part I: fundamental aspects, Crit Rev Ther Drug Carrier Syst, 22 (2005) 27-105.
[230] P. Hassanzadeh, F. Atyabi, R. Dinarvand, The significance of artificial intelligence in drug delivery system design, Adv Drug Deliv Rev, 151-152 (2019) 169-190.
[231] A. Lavecchia, Deep learning in drug discovery: opportunities, challenges and future prospects, Drug Discov Today, 24 (2019) 2017-2032.
[232] A.A. Metwally, R.M. Hathout, Computer-Assisted Drug Formulation Design: Novel Approach in Drug Delivery, Mol Pharm, 12 (2015) 2800-2810.
[233] S. Imai, Y. Takekuma, H. Kashiwagi, T. Miyai, M. Kobayashi, K. Iseki, M. Sugawara, Validation of the usefulness of artificial neural networks for risk prediction of adverse drug reactions used for individual patients in clinical practice, PLoS One, 15 (2020) e0236789.
[234] Q. Shao, R.C. Rowe, P. York, Comparison of neurofuzzy logic and neural networks in modelling experimental data of an immediate release tablet formulation, Eur J Pharm Sci, 28 (2006) 394-404.
[235] S. Agatonovic-Kustrin, R. Beresford, Basic concepts of artificial neural network (ANN) modeling and its application in pharmaceutical research.
[236] E. Vlamou, B. Papadopoulos, Fuzzy logic systems and medical applications, AIMS Neurosci, 6 (2019) 266-272.
[237] A. Mendyk, S. Gures, R. Jachowicz, J. Szlek, S. Polak, B. Wisniowska, P. Kleinebudde, From Heuristic to Mathematical Modeling of Drugs Dissolution Profiles: Application of Artificial Neural Networks and Genetic Programming, Comput Math Methods Med, 2015 (2015) 863874.

[238] E.A. Colbourn, R.C. Rowe, Novel approaches to neural and evolutionary computing in pharmaceutical formulation: challenges and new possibilities.

USC UNIVERSIDADE DE SANTIAGO DE COMPOSTELA

2. OBJECTIVES

USC
UNIVERSIDADE
DE SANTIAGO
DE COMPOSTELA

Mucosal membranes are very attractive and patient friendly sites for inducing both local and systemic therapeutic responses. However, (trans)mucosal drug delivery is extremely challenging due to the intrinsic physical and chemical barriers of mucosal tissues. Drug absorption is mainly limited by their fast drainage from the target mucosa as well as enzymatic and/or pH degradation. The development of highly mucoadhesive formulations, capable of increasing the drugs residence time on mucosal surfaces is essential to obtain the desirable therapeutic effects.

Hydrogels are extremely attractive platforms for drug delivery due to their resemblance to biological tissues, their biocompatibility, and tunability. Their ability to be manufactured and loaded by gentle methods allow the incorporation of labile drugs such as proteins. Especially *in situ* gelling mucoadhesive hydrogels have emerged as a promising strategy to improve the efficacy and bioavailability of drugs administered in mucosal tissues. Their liquid nature when administered, facilitates the formulation spreading on the mucous membranes while their rapid sol-gel transition after application reduces its leakage and dilution in body fluids. The combination of mucoadhesive and thermogelling properties in a hydrogel should make possible to overcome the drawbacks indicated for transmucosal administration, however, it implies the design of complex formulations with a significant number of polymers, leading to a challenging task. Their nature and particular combination will determine the properties and behaviour of the hydrogel as drug delivery system.

On this basis, the general objective of this work is to explore the potential of ternary combinations of selected polymers to produce customized thermosensitive and highly bioadhesive hydrogels with advanced performance for mucosal administration.

This general objective is divided into two partial objectives:

<u>Objective I</u>: Design of ternary, thermosensitive and mucoadhesive hydrogels as protein carriers for sublingual vaccination.

- Assess the suitability, performance, and accuracy of artificial intelligence tools such as neurofuzzy logic to select suitable polymers and to establish the influence of each ingredient on the texturometric, rheological, and drug-release properties of the hydrogels. Results related to this objective are displayed in Chapter I: "*Design of novel orotransmucosal vaccine-delivery platforms using artificial intelligence*" and have already been published [1].

- Evaluate the utility of a hybrid AI software to optimize a sublingual hydrogel formulation presenting the desired texturometric, rheological and release properties. Furthermore, assess the utility of the optimized system as a Chlamydia vaccine carrier to elicit systemic and mucosal immune responses in mice. Results related to this objective are displayed in Chapter II: "*Sublingual boosting with a novel mucoadhesive thermogelling hydrogel following parenteral CAF01 priming as a strategy against Chlamydia trachomatis*".

<u>Objective II</u>: Design of an optimized, thermosensitive and highly mucoadhesive enema useful as a carrier of human cervical stem cells conditioned medium for the treatment of inflammatory bowel disease (IBD).

- Demonstrate the utility of artificial intelligence tools to establish the design space of ternary hydrogel formulations with appropriate characteristics (thermosensitivity, mucoadhesivity, extensibility and retention in the rectal tract) for the treatment of IBD. Results related to this objective are displayed in Chapter III: "*New tools to design smart thermosensitive hydrogels for protein rectal delivery in IBD*" and have already been published [2].

- Evaluate the *in vivo* performance of the optimized hydrogel, loaded with conditioned medium from human uterine cervical stem cells in an experimental mouse model of acute colitis. Results related to this objective will be displayed in Chapter IV: "*Tailored hydrogels as delivery platforms for conditioned medium from mesenchymal stem cells in a mouse model of acute colitis*".

REFERENCES

[1] L. Garcia-del Rio, P. Diaz-Rodriguez, M. Landin, Design of novel orotransmucosal vaccine-delivery platforms using artificial intelligence, European Journal of Pharmaceutics and Biopharmaceutics, 159 (2021) 36-43.

[2] L. Garcia-Del Rio, P. Diaz-Rodriguez, M. Landin, New tools to design smart thermosensitive hydrogels for protein rectal delivery in IBD, Mater Sci Eng C Mater Biol Appl, 106 (2020) 110252.

USC UNIVERSIDADE DE SANTIAGO DE COMPOSTELA

USC
UNIVERSIDADE
DE SANTIAGO
DE COMPOSTELA

3. CHAPTER I: DESIGN OF NOVEL OTROTRANSMUCOSAL VACCINE DELIVERY PLATFORMS USING ARTIFICIAL INTELLIGENCE

*The results from this chapter and its corresponding annex, have already been published as L. Garcia-del Rio[1], P. Diaz-Rodriguez[2], M. Landin[1], Design of novel orotransmucosal vaccine-delivery platforms using artificial intelligence, European Journal of Pharmaceutics and Biopharmaceutics, 159 (2021) 36-43.
ISSN: 0939-6411; E-ISSN:1873-0191.

[1]R+D Pharma Group (GI-1645), Department of Pharmacology, Pharmacy and Pharmaceutical Technology, Facultad de Farmacia, Universidade de Santiago de Compostela-Campus Vida, 15782, Santiago de Compostela, Spain.
[2]Departament of Chemical Engineering and Pharmaceutical Technology, Facultad de Ciencias de la Salud, Universidad de La Laguna (ULL), Campus de Anchieta, 38200, La Laguna, Spain.

USC
UNIVERSIDADE
DE SANTIAGO
DE COMPOSTELA

ABSTRACT

The linings of the oral cavity are excellent needle-free vaccination sites, able to induce immune responses at distal sites and confer systemic protection. However, owing to the mucosal tissues' intrinsic characteristics, the design of effective antigen-delivery systems is not an easy task. In the present work, we propose to develop and characterize thermosensitive and mucoadhesive hydrogels for orotransmucosal vaccination taking advantage of artificial intelligence tools (AIT). Hydrogels of variable composition were obtained combining Pluronic® F127 (PF127), Hybrane® S1200 (HS1200) and Gantrez® AN119 (AN119) or S97 (S97). Systems were characterized in terms of physicochemical properties, adhesion capacity to mucosal tissues and antigen-like microspheres release. Additionally, polymers biocompatibility and their immune-stimulation capacity were assessed in human macrophages. Interestingly, cells treated with HS1200 exhibited a significant proliferation enhancement compared to control. The use of AIT allowed to determine the effect of each polymer on formulations properties. The used proportions of PF127 and Gantrez® are mainly the factors controlling gelation temperature, mucoadhesion, adhesion work and gel strength. Meanwhile, cohesion and short-term microsphere release are dependent on the PF127 concentration. However, long-term microsphere release varies depending on the Gantrez® variety and the PF127 concentration used. Hydrogels prepared with S97 showed slower microsphere release. The use of AIT allowed to establish the conditions able to produce ternary hydrogels with immunostimulatory properties together with adequate mucoadhesion capacity and antigen-like microspheres release.

USC
UNIVERSIDADE
DE SANTIAGO
DE COMPOSTELA

3.1. INTRODUCTION

The rise of biologics has intensified the interest on employing the mucosal surfaces as administration sites. As an example, peptides have been already successfully delivered through the nasal route. However, this administration approach presents more limitations than the oral cavity mucous membranes such as lower absorption surface and higher susceptibility to irreversible tissue damage or irritation [1, 2]. Therefore, the linings of the oral cavity have been suggested as excellent alternative sites for needleless administration of biomacromolecules [2-7]. Currently, sublingual and buccal routes are the most commonly used for non-invasive orotransmucosal delivery of biomacromolecules [8]. On these administration routes the drug absorption takes place through non-keratinized tissues characterized by low enzymatic activity, good vascularization that improves systemic bioavailability and relatively high permeability. Moreover, the nature of the oral cavity allows easy access for administration and removal in case of adverse events. Furthermore, both epithelia can induce immune responses at several distal sites, being suitable for vaccine administration [1, 2, 9-12]. Thus, different dosage forms such as sprays, films, droplets, tablets and hydrogels have been designed as vaccine carriers for orotransmucosal delivery [12-14].

Compared to parenteral vaccination, mucosal immunization is able to elicit stronger and more effective immune responses at mucosal sites together with systemic immunity. Moreover, it does not require specialized staff for administration and allows greater patient compliance [15, 16]. However, the development of suitable mucosal vaccines is extremely challenging, due to the mucosal tissues' intrinsic characteristics [16, 17]. Besides, the characteristics of the selected immunostimulatory molecules should be taken into account when designing new vaccine delivery platforms. For infectious diseases' vaccines these molecules can be specific antigens or the whole organism [18]. Whole inactivated or attenuated bacteria stimulate the immune system by promoting their phagocytosis and presentation by APCs (antigen-presenting cells). From the technological point of view, the bacteria suspensions used in vaccine formulations behave like a microparticulated system.

Among the suitable vaccine carriers for orotransmucosal delivery, hydrogels stand out by their capacity to allow homogenous particle dispersion. Moreover, hydrogels present several advantages as ability to be distributed over a wide area of the oral cavity minimizing the risk of drug low retention and delivery deficiency [11, 19]. More specifically, thermosensitive mucoadhesive hydrogels can form hydrogen bonds with mucins, dramatically increasing the residence time of the formulation in contact with the mucosa [20]. Furthermore, their thermogelling character ensure their easy administration while reducing their washing by saliva. These benefits make mucoadhesive and thermosensitive hydrogels good and feasible candidates for orotransmucosal antigen delivery.

Hydrogels can be obtained combining diverse polymers, which depending on their nature and concentration, will give to systems with variable characteristics. Pluronic® are amphiphilic copolymers capable of self-assembly, generating physical crosslinked hydrogels in aqueous media above their critical micellar concentration (CMC) when they reach a certain temperature [20]. PF127 variety has been widely used in the vaccine delivery field, especially for subcutaneous formulations due to its well-known sol-gel transition at body temperature, which allows an easy handling together with a depot effect at the injection site [21-23]. Thereby, PF127 would confer thermosensitive properties to hydrogels, obtaining liquid systems ease to apply in the oral cavity that become solid at body temperature. Furthermore, its immunomodulatory properties have been previous reported [24].

Hyperbranched polymers are characterized by their tree-like globular topology and large number of functional groups, which confers them high reactivity. The high crosslinking densities of these polymers constitutes its main advantage, leading to well integrated polymeric networks with low viscosity [25]. Hybrane® S1200 is a hyperbranched polyesteramide with various multifunctional end groups (*e.g.* hydroxyl groups) conferring potential mucoadhesive properties [26]. On the other hand, Gantrez® or poly(methyl vinyl ether-co-maleic) anhydride (AN) or acid (S) are well-known high bioadhesive anionic amphiphilic copolymers [27, 28]. These materials

are widely employed in the pharmaceutical field as suspending and thickening agents, denture adhesives and adjuvants for the preparation of transdermal patches. They have been previously used in the field of vaccine delivery [29-32].

In this work we propose to combine Pluronic® F127, Hybrane® S1200 and Gantrez® S97 or AN119 to obtain ternary thermosensitive mucoadhesive hydrogels. The design of complex multicomponent systems involves many difficulties associated with the number of variables implicated. Recently, Artificial Neural Networks (ANN) combined with other Artificial Intelligence Techniques (AIT) as genetic algorithms and fuzzy logic have been proposed as useful approaches to develop smart hydrogels with desired properties using extremely reduced experimental designs [33]. AIT modelling allow to understand how final pharmaceutical system properties are affected by the ingredients and operation conditions [34-36].

Thereby, the aim of the present work is to develop suitable thermosensitive and mucoadhesive hydrogels for orotransmucosal delivery of whole attenuated microbes. To achieve this goal, the workflow can be summarized as follows: a) test the potential *in vitro* immunostimulatory capacity of the polymers selected; b) evaluate the suitability of ternary compositions to achieve hydrogels with appropriate thermosensitive and mucoadhesive properties; c) compare the properties of the hydrogels elaborated with Gantrez® AN119 and S97; and d) select the hydrogel composition able to meet all the requirements for orotransmucosal vaccine-delivery. AIT were employed to model the properties of ternary systems, understand their behaviour and explore their design space.

3.2. MATERIALS AND METHODS

3.2.1. Materials

Pluronic® F127 (PF127) was obtained from Sigma-Aldrich (USA). Hybrane® S1200 (HS1200) was purchased from Polymer Factory (Sweden). Gantrez® AN119 (AN119) and Gantrez® S97 (S97) were kindly provided by Ashland (Spain). Fluoro-Max™ Green fluorescent microspheres (1 µm) were acquired from Thermo Scientific (USA). Cell Strainers presenting a pore size of 40 µm were

obtained from Corning® Incorporated (USA) and bovine buccal mucosa was provided by a local slaughterhouse. Roswell Park Memorial Institute (RPMI) 1640 medium, foetal bovine serum (FBS) and penicillin/streptomycin were purchased from Gibco (USA). 2-mercaptoethanol and phorbol 12-myristate 13-acetate (PMA) were purchased from Sigma-Aldrich (Germany). WST-1 (Water Soluble Tetrazolium Salt-1) kit (Cat. No. 11 644 807 001) was purchased from Roche (USA).

3.2.2. Proliferation assays in human macrophages

Human monocytes THP-1 (ATCC®, USA) were cultured with RPMI 1640 medium supplemented with 10% heat-inactivated FBS, 1% penicillin/streptomycin and 2-mercaptoethanol 0.05 mM at 37 °C and 5% CO_2. Five days before the assay, human monocytes at a density of 2×10^5 cells/mL were stimulated with PMA at 200 nM for three days to differentiate them to macrophages following well-established protocols [37]. Afterwards, the medium containing PMA was replaced by supplemented fresh medium and macrophages were cultured for two additional days. The day before the experiment, macrophages were seeded in 96-well plates, at a density of 2.5×10^4 cells/well. Cells were then treated with the four polymers at variable concentration and the effect on cell proliferation was assayed using the WST-1 assay kit following the manufacturer's protocol. After 24 hours of culture with the different polymer solutions, cell monolayers were washed and incubated with phenol red free media containing the WST-1 reagent for 2 hours. Then, absorbance was measured at 450 nm on a plate reader (Biorad, USA). Two different concentrations were tested in triplicate for each polymer 1% and 0.5% for PF127, from 0.25 to 5% for HS1200 or 0.25% and 0.125% for Gantrez® polymers. The lower concentrations used for Gantrez® polymers are justified by the high viscosity of these polymers.

3.2.3. Experimental design

DataForm® v.3.1 software (Intelligensys Ltd., UK) was able to generate a reduced experimental design for 4 components (PF127, HS1200 and AN119 or S97) using a balanced density method with a minimum pattern of 5, allowing to study the knowledge space of the

ternary systems. As result, 19 compositions were established, using different proportions of PF127, HS1200 and AN119 or S97 (**Table 1**).

Table 1. Composition of hydrogels. Percentages (w/w) of Pluronic® F127 (PF127), Hybrane® S1200 (HS1200) and Gantrez® AN119 (AN119) or S97 (S97) generated by DataForm® software using the Balance Density Method.

Sample	Concentration (%)			
	PF127	HS1200	AN119	S97
H1	22	2.5	3	0
H2	22	0	0	0
H3	19	0	3	0
H4	20.5	5	1.5	0
H5	20.5	5	0	0
H6	22	5	0	0
H7	19	2.5	3	0
H8	12	1.8	2.8	0
H9	14	0.5	0.5	0
H10	17	5	3	0
H11	20.5	2.5	0	1.5
H12	18	5	0	3
H13	22	2.5	0	0
H14	19	2.5	0	1.5
H15	22	0	0	3
H16	20.5	0	0	1.5
H17	12	1.8	0	2.8
H18	14	0.5	0	0.5
H19	17	5	0	3

3.2.4. Hydrogels preparation and characterization

Accurate amounts of AN119 or S97 polymers were dissolved in Milli-Q® water at 50 ºC to obtain the required concentration (**Table 1**). Then, solutions were cooled in an ice bath and the corresponding HS1200 quantity was added when required. Finally, PF127 (%w/w) was incorporated into the obtained solutions and dissolved overnight at 4 °C. Afterwards, pH was adjusted to 6.8 using stock solutions of

NaOH (5M) or HCl (1M). Hydrogels were stored at 4 °C until characterization.

3.2.4.1. Rheological analysis

Hydrogels gelation temperature (T_{gel}) was assessed using a rheometer AR1000-N (TA Instruments, UK). A cone-plate geometry of 6 cm Ø and 2.1 degrees was used to record storage (G') and loss moduli (G") from 15 to 40 °C at 0.4 °C/min at an angular frequency of 5 rad/s. The T_{gel} (ºC) was recognized by the crossover of both moduli. The angular frequency settings were selected considering the commonly used parameters to test thermosensitive hydrogels (between 2 rad/s and 6.34 rad/s) [38-40].

3.2.4.2. Texturometric assessments

Mucoadhesion and adhesion work, cohesion and gel strength were measured at 37 ºC employing a TA XT Plus Texture Analyser (Surrey, UK).

Mucoadhesion work was measured on bovine buccal tissue as previously described with slight modifications [41]. On this purpose, buccal tissue was excised to separate muscular tissue from the mucous membrane and used as substrate to perform the mucoadhesion experiments as reported elsewhere [42, 43]. Then, a piece of bovine buccal mucosa (1.5 x 1.5 cm) was glued to the punch of the texturometer and, a Petri dish containing 3 g of each sample was attached to the lower holder of the texturometer. Afterwards, the punch descended at 1 mm/s applying a force of 0.5 N for 60 s on the hydrogels placed on the Petri dish. The force exerted by the punch when rising at 1 mm/s was plotted against the distance, and the hydrogel mucoadhesion work (mJ) was calculated as the area under the curve (AUC). All measurements were made in quadruplicate.

Additionally, to estimate adhesion work, cohesion and gel strength, the probe descended at 1 mm/s on each hydrogel, which was compressed to 5 mm in depth, allowing a relaxation time of 30 s before a second compression cycle. Thus, two force-distance texturometric profiles were obtained. Gel strength (N) was calculated as the height of the first peak, while adhesion work (mJ) was estimated as the AUC of the first negative peak. Cohesion was

obtained dividing the AUC of the second positive peak by the AUC of the first positive peak of each graph. Cohesion is a dimensionless parameter with values ranging from 0 to 1 [44].

3.2.5. Antigen-like microspheres loading and in vitro release studies

Green fluorescent microspheres (GFM), 1 µm in diameter, were chosen as model of whole inactivated bacteria to study the microsphere release rate of the developed hydrogels. For hydrogels loading, 350 µL of a dispersion of green fluorescent microspheres at 1.64 x 10^9 particles/ml were centrifuged at 10,000 rpm for 10 minutes. The supernatant was removed and the microspheres pellet was dispersed in 1 ml of hydrogel.

GFM release studies were carried out at 37 ºC and 400 rpm in an orbital shaker Tritamax 1000 (Heidolph Instruments, Germany), using the simulated salivary fluid (SSF) described by Pindáková et al. as release media [45]. Loaded hydrogels (1 ml) were placed in a Corning® Cell Strainer of 40 µm pore size and placed in 6-well plates containing 8 ml of SSF. At pre-set times (5, 10, 15, 30, 60, 90 and 120 minutes), the strainer was removed and placed into another well containing 8 ml of fresh SSF. The fluorescent intensity of released microspheres was measured using a FLUOstar OPTIMA plate reader (BMG Labtech, Germany) with adequate controls. The percentage of GFM released at 5 minutes and the time to reach 100% GFM release were calculated.

3.2.6. Artificial Neural Networks modelization

FormRules® v4.03 (Intelligensys Ltd., UK), a neurofuzzy logic software, that combines Artificial Neural Networks with fuzzylogic techniques was used to model the results and analyse how the formulation components modulate its properties through the simple "IF…THEN" rules that generates [35].

The concentration of PF127, HS1200, AN119 or S97, as well as, the type of Gantrez® were introduced as inputs while the systems properties (gelation temperature, mucoadhesion and adhesion work, cohesion, gel strength, GFM released at 5 min (%) and total release time at 37 ºC) were selected as outputs.

Among the different statistical criteria of software fitting: Structural Risk Minimisation (SRM), Cross validation (CV), Leave One Out Cross Validation (LOOCV), Minimum Description Length (MDL) and Bayesian Information Criterion (BIC), CV was selected because it produced the most predictable models along with the simplest rule sets avoiding overtraining. The number of subsets for CV ranged from 3 to 5. For all models, a maximum of 2 inputs per submodel and 15 maximum nodes per input were selected.

The predictability of the generated models was evaluated through the coefficient of determination (R^2) calculated as follows [33]:

$$R^2 = \left[1 - \frac{\sum_{i=1}^{n}(y_i - y_i^*)^2}{\sum_{i=1}^{n}(y_i - y_i^{**})^2}\right] \times 100$$

Where, y_i represents the output's experimental value in the data set, y_i^* is the predicted value of the output computed by the model and finally, y_i^{**} is the mean value of the parameter that is being evaluated.

The coefficient of determination is commonly used to establish model predictability for the response variables [46, 47]. Good model predictabilities are considered when R^2 is higher than 70% [34]. Accuracy was verified by statistically comparing experimental results and those predicted by the model through a one-way ANOVA. Models which computed f-value in the ANOVA is greater than critical f-value for the corresponding degrees of freedom (α=0.05), show good accuracy [36].

3.2.7. Statistical analysis

Values from cell proliferation assays are expressed as mean ± standard deviation. SPSS software (IBM SPSS Statistics 26) was used to perform a one-way ANOVA test following HSD Tukey's post hoc to compare polymer groups and find statistical significant differences between them. $p < 0.05$ was considered as significant.

3.3. RESULTS

3.3.1. Immunostimulatory capacity of selected polymers

The proliferation of human macrophages when subjected to different polymer concentrations was tested to evaluate their biocompatibility, as well as, their intrinsic immunostimulatory capacity. All polymers showed good biocompatibility with viability values higher than 90% (**Figure 1**). In addition, proliferation rates above 100% were obtained for HS1200, reaching statistically significant higher values compared to control with 120% and 130% macrophage proliferation when treated with concentrations of 0.5% and 1% respectively. Further proliferation studies were performed for HS1200 at a wider concentration range (**Annex I, Figure A1**) to analyse a possible dose-response behaviour. However, no significant differences were observed between the different concentration tested.

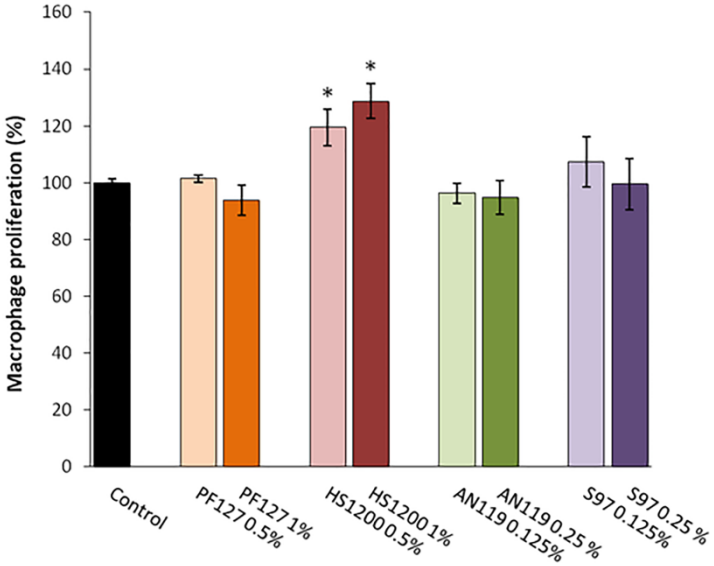

Figure 1. Effect of PF127, HS1200, AN119 and S97 treatments on cell proliferation of THP-1 derived macrophages after incubation for 24 h. Assays were performed in triplicate and results are expressed as mean ± SD. * denotes statistical significant differences (p<0.05) compared to control, human macrophages without treatment.

3.3.2. Hydrogels performance and AIT modelling

The physicochemical properties of hydrogels are summarized in **Table 2**. AIT succeeded in modelling mucoadhesion, adhesion work and the release parameters with high predictability ($R^2 \geq 70\%$) and accuracy (**Table 3**). However, the T_{gel} model ANOVA results did not confirm its accuracy, probably due to the model low degrees of freedom, nevertheless it presents excellent predictability. On the other hand, the variations in cohesion were not explained with good predictability by the variables studied. However, those models were statistically significant and the rules generated by FormRules® v4.03 agreed with the experimental data. The complete set of rules for the models is presented in **Tables A1.1 to A1.7** (**Annex I**).

Table 2. Experimental results (mean and standard deviation, the latter in brackets) for T_{gel} (ºC), mucoadhesion and adhesion work in millijoules (mJ), gel strength (N), amount of GFM released at 5 minutes (%) and Total release time in minutes (min) for the different formulations.

Sample	T_{gel} (ºC)	Mucoadhesion work (mJ)	Gel strength (N)	Adhesion work (mJ)	Cohesion	GFM released at 5 min (%)	Total release time (min)
H1	<15	1.07(0.26)	0.74(0.01)	1.93(0.04)	0.11(0.00)	42.36(8.45)	30(0.0)
H2	18.25(0.06)	0.80(0.18)	1.07(0.03)	2.04(0.10)	0.14(0.02)	51.58(7.30)	30(0.0)
H3	17.15(0.25)	1.14(0.40)	0.39(0.02)	1.06(0.12)	0.32(0.12)	50.54(9.84)	15(0.0)
H4	17.62(0.63)	1.04(0.30)	0.81(0.02)	1.98(0.07)	0.16(0.04)	46.48(6.75)	30(0.0)
H5	23.26(0.99)	1.16(0.20)	0.10(0.02)	0.12(0.03)	0.92(0.11)	68.56(7.91)	15(0.0)
H6	18.60(0.24)	0.81(0.24)	0.95(0.06)	2.51(0.36)	0.14(0.03)	34.76(0.77)	30(0.0)
H7	18.66(0.48)	0.75(0.12)	0.36(0.02)	0.92(0.14)	0.43(0.19)	86.20(11.86)	10(0.0)
H8	39.81(0.17)	0.14(0.04)	0.04(0.00)	0.03(0.00)	1.02(0.03)	42.36(8.44)	30(0.0)
H9	25.38(0.12)	0.09(0.04)	0.04(0.00)	0.03(0.00)	1.01(0.04)	96.10(1.82)	10(0.0)
H10	25.58(0.38)	0.12(0.05)	0.04(0.00)	0.05(0.01)	1.04(0.02)	94.20(2.70)	15(0.0)
H11	17.49(0.16)	1.01(0.18)	0.85(0.02)	2.10(0.07)	0.17(0.11)	36.14(9.71)	30(0.0)
H12	21.60(0.70)	0.76(0.23)	0.53(0.01)	1.34(0.21)	0.27(0.13)	54.43(10.41)	30(0.0)
H13	18.62(0.32)	0.91(0.19)	0.99(0.04)	2.30(0.17)	0.19(0.06)	28.80(4.22)	30(0.0)
H14	19.00(0.45)	1.09(0.22)	0.74(0.03)	1.85(0.11)	0.13(0.02)	42.40(8.44)	30(0.0)
H15	<15	0.87(0.05)	0.86(0.02)	2.22(0.06)	0.10(0.00)	25.78(4.04)	60(0.0)

H16	17.03(0.21)	1.14(0.41)	1.26(0.10)	2.94(0.26)	0.14(0.02)	40.01(12.92)	30(0.0)
H17	33.53(0.84)	0.08(0.05)	0.04(0.00)	0.05(0.02)	1.03(0.05)	93.10(6.25)	10(0.0)
H18	29.10(1.71)	0.16(0.06)	0.04(0.00)	0.04(0.00)	1.03(0.04)	96.00(3.39)	10(0.0)
H19	26.23(0.84)	0.22(0.06)	0.04(0.00)	0.08(0.02)	1.08(0.02)	93.80(10.0)	15(0.0)

Table 3. Inputs and submodels generated by FormRules® for the different outputs evaluated in this work, with their respective parameters to evaluate the quality of each submodel. The most relevant submodels are bolded.

Output	Submodel	Inputs from FormRules®	R^2	Computed f value	ANOVA freedom degrees	α
T_{gel}	**1** 2	**[PF127]x[Gantrez®]** [HS1200]	95.89	5.39	13 and 3	0.096
Mucoadhesion work	**1**	**[PF127]x[Gantrez®]**	94.73	22.47	8 and 10	<0.01
Adhesion work	**1** 2 3	**[PF127]x[Gantrez®]** Gantrez® type [HS1200]	96.09	15.64	11 and 7	<0.01
Gel strength	**1** 2 3	**[PF127]x[Gantrez®]** HS1200 Gantrez® type	95.14	5.59	14 and 4	<0.05
Cohesion	**1**	**[PF127]**	66.92	16.19	2 and 16	<0.01
GFM released at 5 min	**1** 2	**[PF127]** [Gantrez®]	70.11	6.10	5 and 13	<0.01
Total release time	**1** 2 3	**[PF127]xGantrez® type** [Gantrez®] HS1200	86.75	5.24	10 and 8	<0.05

3.3.2.1. T_{gel} is mainly determined by PF127 and Gantrez® concentration

Most of the PF127/HS1200/Gantrez® mixtures lead to thermosensitive hydrogels. To achieve efficient thermosensitive mucoadhesive formulations the desired T_{gel} range was set at 30-35 °C to ensure adequate administration and fast gelation. The model for T_{gel} indicates this property mainly depends on the complex interaction between the thermosensitive polymer (PF127) and Gantrez® concentrations. Although is also slightly affected by the concentration of HS1200 (**Table 3**). The set of rules for this parameter (**Annex I,**

Table A1.1) allows to deduce the lowest T_{gel} values can be obtained by mixing high proportions of PF127 (>19.5%) and Gantrez® (>1.5%). There is no difference between the Gantrez® varieties with regards to this parameter (**Figure 2**). Moreover, the addition of low proportions of HS1200 (<2.5%) promotes a further decrease in T_{gel}. As expected, the experimental results confirm these statements (**Table 2**), since the hydrogels with the lowest T_{gel} values, below 15 ºC, were H1 (22/2.5/3) and H15 (22/0/3). On the other hand, the highest gelation temperatures were those corresponding to hydrogels H8 (12/1.8/2.8) and H17 (12/1.8/2.8) with mean values of 39.81 ± 0.17 ºC and 33.53 ± 0.84 ºC, respectively.

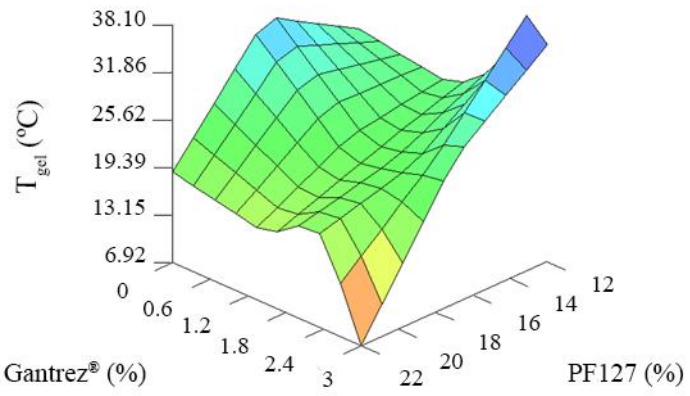

Figure 2. 3D plot generated by FormRules® for predicted T_{gel} as a function of PF127 and Gantrez® concentrations for formulations containing 5% of HS1200. High proportions of PF127 and Gantrez® would lead to lowest T_{gel} values (orange-yellow area), while the highest ones would be obtained when low percentages of PF127 were incorporated to the hydrogels (dark blue area).

3.3.2.2. Mucoadhesion, adhesion work and gel strength are dependent on proportions of PF127 and Gantrez®

Our goal is to obtain highly adhesive and mucoadhesive hydrogels to minimize foreign body sensation and hence saliva production, preventing swallowing before antigen release into the oral cavity. Regarding gel strength, a compromise must be achieved to generate soft hydrogels without jeopardizing mucoadhesive and adhesive properties.

Mucoadhesion, adhesion work and gel strength are interrelated properties, whose variations are mainly explained by the interaction of PF127 and Gantrez® (**Table 3**). The model predicts the highest mucoadhesive hydrogels can be obtained when using PF127 percentages between 18.5% and 21% together with Gantrez® concentrations below 1.5%, independently of the variety used (Darkest blue area of **Figure 3**).

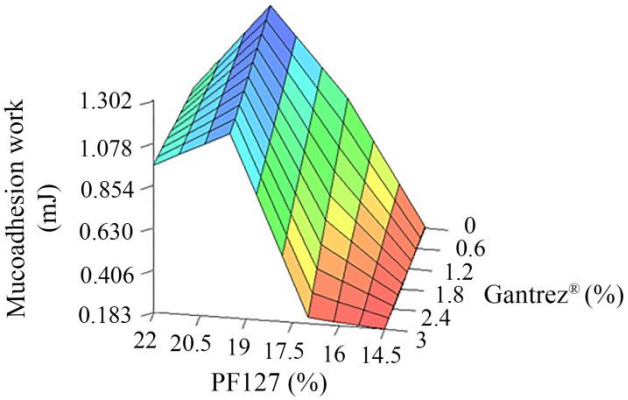

Figure 3. 3D plot generated by FormRules® displaying the effect of PF127 and Gantrez® concentrations on predicted mucoadhesion work. Dark blue area corresponds to the highest mucoadhesive hydrogels.

In addition, adhesion work and gel strength can also be modulated by varying the amount of HS1200 and the type of Gantrez® used (**Table 3**). Thus, as can be derived from the corresponding rules (**Annex I, Tables A1.3 and A1.5**), softness can be favoured when high concentrations of HS1200 (>2.5%) and Gantrez® AN119 are selected. Despite high amounts of HS1200 jeopardize adhesion properties when PF127 concentrations below 22% are used (*e.g.* formulation H5 (20.5/5/0) in **Table 2**), this problem could be overcome by adding either type of Gantrez®.

3.3.2.3. Cohesion is modulated by PF127

Just 66.92% of the cohesion variations are explained by the composition, in particular by the concentration of PF127 in the formulation. The rules indicate formulations with PF127 proportions

higher than 17% are more cohesive (cohesion ≈ 0). Values close to 0 indicate the inability of a hydrogel to recover its initial shape due to the high intermolecular forces that exist between the polymer chains. The rules agree with the experimental values in **Table 2**. The less cohesive formulations (≈ 1) were H8 (12/1.8/2.8), H9 (14/0.5/0.5), H10 (17/5/3), H17 (12/1.8/2.8), H18 (14/0.5/0.5) and H19 (17/5/3). The more cohesive samples were H15 (22/0/3), H1 (22/2.5/3) and H14 (19/2.5/1.5) with mean cohesion values of 0.103 ± 0.00, 0.115 ± 0.00 and 0.127 ± 0.02, respectively.

3.3.2.4. GFM released at 5 min was fundamentally modulated by PF127 while total release time is also dependent on type of Gantrez®

Within the limits of the study, all inputs affect GFM release from the hydrogels (**Table 3)**. At the beginning of the process, the release of GFM from hydrogels is governed by the proportion of PF127 and Gantrez® in the formulation. Thus, the percentage of GFM released at 5 min decreases as the concentrations of these polymers increase, being the lowest for percentages of PF127 and Gantrez® over 19.5% and 1.5 % respectively (**Figure 4A**). Gantrez® varieties behave similarly with respect to this parameter.

As it can be derived from the set of rules (**Annex I, Tables A1.6 and A1.7**), when the process is considered globally, and the total release time is analyzed, the influence of the HS1200 concentration and the type of Gantrez® used is observed. The inclusion of HS1200 in the formulation generates quantitatively small variations in this parameter, which presents a minimum when HS1200 is 2.5%. The effect of the type of Gantrez® is clear from **Figures 4B-C** indicating Gantrez® variety has an important impact on the time required to complete the release process, being S97 able to control GFM release for longer.

Experimental results completely agree with model predictions. Formulations H9 (14/0.5/0.5) and H18 (14/0.5/0.5) with low percentages of PF127, HS1200 and Gantrez® present high burst release (**Table 2**). However, H15 system (22/0/3) including high proportions of FP127 and Gantrez® shows 25.78% of GFM released at 5 min and the release extends over a period of 60 min (**Table 2**).

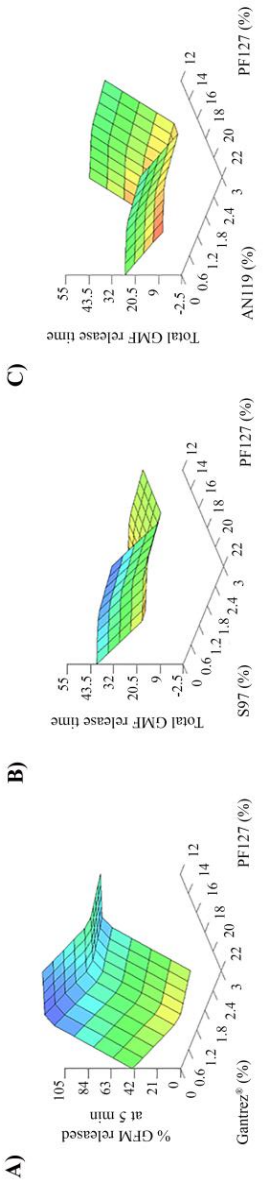

Figure 4. 3D plot generated by FormRules® displaying the effect of PF127 and Gantrez® concentrations on predicted GFM release parameters. A) Predicted percentage of GFM released at 5 min; B) Predicted total GFM release time for formulations containing Gantrez® S97 and 0% of HS1200; C) Predicted total GFM release time for formulations containing Gantrez® AN119 and 0 % of HS1200.

3.4. DISCUSSION

The development of thermosensitive and mucoadhesive hydrogels answers the need for patient-friendly routes of administration for new efficient vaccines capable of eliciting mucosal immunity by the delivery of antigens in the oral cavity. These hydrogels could be easily applied to the oral mucosa by a needle-free syringe equipped with a cannula. In order to design those hydrogels, three polymers, PF127, HS1200 and Gantrez® (two varieties, AN119 or S97) were selected.
Seeking for efficient and appropriate platforms for mucosal vaccine delivery, the first step was to evaluate the selected polymers' capacity to stimulate macrophage proliferation *in vitro* [48]. These phagocytic cells act as professional antigen-presenting cells, playing a crucial role in innate and acquired immunity [49].

Surprisingly, HS1200 showed the greater increase in macrophage proliferation, significantly higher than the control (**Figure 1**). Similar mean proliferation rates (≈ 140-150%) were obtained for macrophages exposed to polysaccharides of fungal origin and curdlan used as adjuvants [48, 50]. Although the proliferation of THP-1 derived macrophages was significantly increased after HS1200 treatment compared to control, this polymer did not show a dose dependent effect on macrophage proliferation. To our knowledge, the immunostimulatory capacity of this polymer has never been reported. Contrary to expected [30], Gantrez® polymers do not show any macrophage stimulatory response.

The combination of the three polymers at variable proportions gives rise to hydrogels with diverse characteristics. The design of formulations able to fulfil the requirements of orotransmucosal vaccine delivery requires to know the effect of each material and its interactions on the obtained hydrogels. To stimulate immunity through the oral mucosa, the developed hydrogels should ideally be thermosensitive and mucoadhesive, capable of increasing the residence time and the contact of antigens with the oral mucosa.

In the studied design space, hydrogels with a T_{gel} in the range <15 ºC-38.1 ºC are obtained (**Figure 2**). The gelation phenomenon of the thermosensitive polymer, PF127, is basically due to the dehydration of its polypropylene oxide blocks [33, 51]. Systems that contain enough

concentration of PF127 to generate a sufficient number of micelles to entangle efficiently, form rigid and adhesive networks. HS1200 addition, even at high percentage, has little effect on T_{gel}, gel strength and cohesion values. However, the addition of Gantrez® up to 1% to hydrogels containing low PF127 amount decreases T_{gel} values when compared to systems with the same PF127 but higher Gantrez®. Higher concentrations of Gantrez® disturb micelles formation, leading to weaker and less adhesive networks [51]. Hence, hydrogels T_{gel}, gel strength and adhesion could be modulated varying PF127 and Gantrez® concentrations in the polymeric mixture.

The interaction between PF127 and Gantrez® polymers also determines mucoadhesion (**Figure 3**). PF127 confers a bioadhesive character due to the presence of ethylene oxide blocks in its structure, meanwhile the mucoadhesive properties of Gantrez® are due to the carboxylic groups that can interact with mucins [33, 52-54]. The combination of both with HPMC K15 has been previously employed to develop bioadhesive gels for transbuccal delivery of 5-Fluouracil [52]. The authors found the best positive effect on bioadhesion with the highest amount of S97 [52]. Our results do not show this trend. FormRules® software predicts that maximum mucoadhesion is reached when Gantrez® percentages are less than 1.5%. The discrepancies found can be explained by the greater Gantrez® concentrations used in our work. Smaller concentrations can mask the effect of adding Gantrez®. Additionally, phenomena of chain coiling above the optimal concentration have been described for mucoadhesive polymers related to reductions in mucoadhesion [55]. The interaction between PF127 and Gantrez® can modify the optimal concentration, which would justify the variations observed in this parameter.

Furthermore, the combination of PF127, HS1200 and Gantrez® proposed in our work exhibited better mucoadhesive properties than the formulations described in the above-mentioned work, which could be attributed to an increase in interpenetration and entanglement of hydrogels with hydrated mucins [54]. Although HS1200 has a high ratio of hydroxyl groups per molecule (8/1), contrary to our initial

hypothesis, FormRules® was not able to detect any influence of this material on mucoadhesion.

The effect of PF127 on mucoadhesion could be more related to the increase in gel strength, as well as, to formulation adhesion and cohesion. Hydrogels should maintain a balance between cohesion and adhesion to prolong their retention at the application site [56]. As expected, formulations having the highest PF127 concentration showed higher adhesion. Moreover, the release of the antigen-like microspheres at short times is determined by the concentration of the two major polymers in the formulation, PF127 and Gantrez®. The effect of both on the microspheres release percentage reduction at 5 min is additive (**Figure 4A**). The slowdown in drug release as a consequence of the increase in the concentration of PF127 has been attributed to the boost in size and number of the micelles formed, which promotes cross-linking and tortuosity in the gel structure [52].

At longer release times, the effect of two additional inputs, HS1200 concentration and the type of Gantrez®, is observed. The microspheres release from Pluronic® hydrogels is through extramicellar aqueous channels, where microviscosity controls sphere diffusion. The addition of hydrophilic polymers to PF127 solutions could affect the polymer molecules orientation in the hydrogel matrix and reduce the amount of free water in the channels, decreasing the release rate [52]. While there is no effect of the Gantrez® type on gelation temperature, mucoadhesion, cohesion and microparticles burst release, the use of AN119 leads to hydrogels with lower adhesion work and gel strength and faster total microsphere release compared to hydrogels prepared with S97 (**Figures 4B-C**). This effect is probably related to the higher viscosity that Gantrez® S97 variety confers to aqueous dispersions.

The application of hydrogels for the administration of whole inactivated microbes, would require their release as fast as possible to facilitate uptake in a short period of time, minimizing the potential risk of swallowing part of the formulation before all the dose is absorbed. In this sense, the comparison favours the Gantrez® AN119 variety.

3.5. CONCLUSIONS

Hybrane® S1200 immunostimulatory capacities are described for the first time suggesting this polymer may be a good candidate as raw material for vaccine formulations. The combination of PF127, HS1200 and AN119 or S97 is useful for obtaining thermosensitive and mucoadhesive hydrogels. AIT enabled to elucidate the physicochemical, adhesion capacity to mucosal tissues and antigen-like microspheres release properties dependent on the interaction between PF127 and Gantrez® concentrations. Additionally, the increase in the concentration of HS1200 slightly reduces gel strength and adhesion, and improves release rate. The use of Gantrez® AN119 variety allows a faster release of the microspheres, which can favour their complete uptake through the oral mucosal tissue. Our results suggest that combinations of PF127 (18-21.5%), Gantrez® AN119 (<1.5%) and Hybrane® HS1200 (>2.5%) can meet all the requirements for orotransmucosal vaccine delivery.

USC UNIVERSIDADE DE SANTIAGO DE COMPOSTELA

REFERENCES

[1] S. Senel, M. Kremer, K. Nagy, C. Squier, Delivery of bioactive peptides and proteins across oral (buccal) mucosa, Current pharmaceutical biotechnology, 2 (2001) 175-86.
[2] A.C. Anselmo, Y. Gokarn, S. Mitragotri, Non-invasive delivery strategies for biologics, Nat Rev Drug Discov, 18 (2019) 19-40.
[3] M. Montenegro-Nicolini, J.O. Morales, Overview and Future Potential of Buccal Mucoadhesive Films as Drug Delivery Systems for Biologics, AAPS PharmSciTech, 18 (2017) 3-14.
[4] T. Caon, L. Jin, C.M. Simoes, R.S. Norton, J.A. Nicolazzo, Enhancing the buccal mucosal delivery of peptide and protein therapeutics, Pharm Res, 32 (2015) 1-21.
[5] S.I. Pather, M.J. Rathbone, S. Senel, Current status and the future of buccal drug delivery systems, 5 (2008) 531-542.
[6] J.K. Lam, Y. Xu, A. Worsley, I.C. Wong, Oral transmucosal drug delivery for pediatric use, Adv Drug Deliv Rev, 73 (2014) 50-62.
[7] J.O. Morales, D.J. Brayden, Buccal delivery of small molecules and biologics: of mucoadhesive polymers, films, and nanoparticles, Curr Opin Pharmacol, 36 (2017) 22-28.
[8] R.M. Gilhotra, M. Ikram, S. Srivastava, N. Gilhotra, A clinical perspective on mucoadhesive buccal drug delivery systems, J Biomed Res, 28 (2014) 81-97.
[9] V.F. Patel, F. Liu, M.B. Brown, Advances in oral transmucosal drug delivery, J Control Release, 153 (2011) 106-116.
[10] M.A. Attia, I. El-Gibaly, S.E. Shaltout, G.N. Fetih, Transbuccal permeation, anti-inflammatory activity and clinical efficacy of piroxicam formulated in different gels, Int J Pharm, 276 (2004) 11-28.
[11] M.L. Bruschi, O. de Freitas, Oral Bioadhesive Drug Delivery Systems, Drug Development and Industrial Pharmacy, 31 (2005) 293-310.
[12] H. Kraan, H. Vrieling, C. Czerkinsky, W. Jiskoot, G. Kersten, J.P. Amorij, Buccal and sublingual vaccine delivery, 190 (2014) 580-592.
[13] J.A. White, J.S. Blum, N.A. Hosken, J.O. Marshak, L. Duncan, C. Zhu, E.B. Norton, J.D. Clements, D.M. Koelle, D. Chen, W.C. Weldon, M.S. Oberste, M. Lal, Serum and mucosal antibody

responses to inactivated polio vaccine after sublingual immunization using a thermoresponsive gel delivery system, Hum Vaccin Immunother, 10 (2014) 3611-3621.
[14] S. Murugappan, H.P. Patil, H.W. Frijlink, A. Huckriede, W.L.J. Hinrichs, Simplifying Influenza Vaccination During Pandemics: Sublingual Priming and Intramuscular Boosting of Immune Responses with Heterologous Whole Inactivated Influenza Vaccine, The AAPS Journal, 16 (2014) 342-349.
[15] M. Li, Y. Wang, Y. Sun, H. Cui, S.J. Zhu, H.J. Qiu, Mucosal vaccines: Strategies and challenges, Immunol Lett, 217 (2020) 116-125.
[16] S. Longet, M.L.E. Lundahl, E.C. Lavelle, Targeted Strategies for Mucosal Vaccination, Bioconjug Chem, 29 (2018) 613-623.
[17] A. Miquel-Clopes, E.G. Bentley, J.P. Stewart, S.R. Carding, Mucosal vaccines and technology, Clin Exp Immunol, 196 (2019) 205-214.
[18] C.P. Karch, P. Burkhard, Vaccine technologies: From whole organisms to rationally designed protein assemblies, Biochem Pharmacol, 120 (2016) 1-14.
[19] A.I. Mendes, A.C. Silva, J.A. Catita, F. Cerqueira, C. Gabriel, C.M. Lopes, Miconazole-loaded nanostructured lipid carriers (NLC) for local delivery to the oral mucosa: improving antifungal activity, Colloids Surf B Biointerfaces, 111 (2013) 755-763.
[20] A. Sosnik, K.P. Seremeta, Polymeric Hydrogels as Technology Platform for Drug Delivery Applications, Gels, 3 (2017).
[21] C.M. Coeshott, S.L. Smithson, E. Verderber, A. Samaniego, J.M. Blonder, G.J. Rosenthal, M.A. Westerink, Pluronic F127-based systemic vaccine delivery systems, Vaccine, 22 (2004) 2396-2405.
[22] S. Bobbala, B. Gibson, A.B. Gamble, A. McDowell, S. Hook, Poloxamer 407-chitosan grafted thermoresponsive hydrogels achieve synchronous and sustained release of antigen and adjuvant from single-shot vaccines, Immunol Cell Biol, 96 (2018) 656-665.
[23] E. Moreno, J. Schwartz, E. Larraneta, P.A. Nguewa, C. Sanmartin, M. Agueros, J.M. Irache, S. Espuelas, Thermosensitive hydrogels of poly(methyl vinyl ether-co-maleic anhydride) -

Pluronic((R)) F127 copolymers for controlled protein release, Int J Pharm, 459 (2014) 1-9.
[24] G. Dumortier, J.L. Grossiord, F. Agnely, J.C. Chaumeil, A review of poloxamer 407 pharmaceutical and pharmacological characteristics, Pharm Res, 23 (2006) 2709-2728.
[25] S.S.S. Omara, Preparation, Characterization and Electrical Properties of Nanocomposites Based on Hyperbranched Polymers, Berlin, Technische Universität Berlin, 2018.
[26] M.I. Ugwoke, N. Verbeke , R. Kinget, The biopharmaceutical aspects of nasal mucoadhesive drug delivery, 53 (2001) 3-22.
[27] M.A. Tawfik, M.I. Tadros, M.I. Mohamed, Lipomers (Lipid-polymer Hybrid Particles) of Vardenafil Hydrochloride: a Promising Dual Platform for Modifying the Drug Release Rate and Enhancing Its Oral Bioavailability, AAPS PharmSciTech, 19 (2018) 3650-3660.
[28] B. Luppi, T. Cerchiara, F. Bigucci, A.M. Di Pietra, I. Orienti, V. Zecchi, Crosslinked poly(methyl vinyl ether-co-maleic anhydride) as topical vehicles for hydrophilic and lipophilic drugs, Drug Deliv, 10 (2003) 239-244.
[29] J. Ochoa, J.M. Irache, I. Tamayo, A. Walz, V.G. DelVecchio, C. Gamazo, Protective immunity of biodegradable nanoparticle-based vaccine against an experimental challenge with Salmonella Enteritidis in mice, Vaccine, 25 (2007) 4410-4419.
[30] K. Vandamme, V. Melkebeek, E. Cox, J.P. Remon, C. Vervaet, Adjuvant effect of Gantrez(R)AN nanoparticles during oral vaccination of piglets against F4+enterotoxigenic Escherichia coli, Vet Immunol Immunopathol, 139 (2011) 148-155.
[31] S. Gómez, C. Gamazo, B. San Roman, C. Vauthier, M. Ferrer, J.M. Irachel, Development of a novel vaccine delivery system based on Gantrez nanoparticles, J Nanosci Nanotechnol, 6 (2006) 3283-3289.
[32] A. Ripolin, J. Quinn, E. Larraneta, E.M. Vicente-Perez, J. Barry, R.F. Donnelly, Successful application of large microneedle patches by human volunteers, Int J Pharm, 521 (2017) 92-101.
[33] L. Garcia-Del Rio, P. Diaz-Rodriguez, M. Landin, New tools to design smart thermosensitive hydrogels for protein rectal delivery in IBD, Mater Sci Eng C Mater Biol Appl, 106 (2020)110252.

[34] P. Diaz-Rodriguez, M. Landin, Smart design of intratumoral thermosensitive beta-lapachone hydrogels by Artificial Neural Networks, Int J Pharm, 433 (2012) 112-118.
[35] R. Rodriguez-Dorado, M. Landin, A. Altai, P. Russo, R.P. Aquino, P. Del Gaudio, A novel method for the production of core-shell microparticles by inverse gelation optimized with artificial intelligent tools, Int J Pharm, 538 (2018) 97-104.
[36] H. Rouco, P. Diaz-Rodriguez, S. Rama-Molinos, C. Remunan-Lopez, M. Landin, Delimiting the knowledge space and the design space of nanostructured lipid carriers through Artificial Intelligence tools, Int J Pharm, 553 (2018) 522-530.
[37] M.E. Lund, J. To, B.A. O'Brien, S. Donnelly, The choice of phorbol 12-myristate 13-acetate differentiation protocol influences the response of THP-1 macrophages to a pro-inflammatory stimulus, Journal of immunological methods, 430 (2016) 64-70.
[38] P. Diaz-Rodriguez, M. Landin, Smart design of intratumoral thermosensitive beta-lapachone hydrogels by Artificial Neural Networks, Int J Pharm, 433 (2012) 112-118.
[39] R. Nigmatullin, V. Gabrielli, J.C. Muñoz-García, A.E. Lewandowska, R. Harniman, Y.Z. Khimyak, J. Angulo, S.J. Eichhorn, Thermosensitive supramolecular and colloidal hydrogels via self-assembly modulated by hydrophobized cellulose nanocrystals. Cellulose. 26 (2019) 529-542.
[40] C.A. Ramírez Barragán, E.R. Macías Balleza, L. García-Uriostegui, J.A. Andrade Ortega, G. Toríz, E. Delgado, Rheological characterization of new thermosensitive hydrogels formed by chitosan, glycerophosphate, and phosphorylated β-cyclodextrin, Carbohydrate polymers, 201 (2018) 471-481.
[41] M. Campana-Seoane, A. Peleteiro, R. Laguna, F.J. Otero-Espinar, Bioadhesive emulsions for control release of progesterone resistant to vaginal fluids clearance, Int J Pharm, 477 (2014) 495-505.
[42] P.K. Metia, A.K. Bandyopadhyay, In vitro evaluation of novel mucoadhesive buccal tablet of oxytocin prepared with Diospyros peregrina fruit mucilages, Yakugaku zasshi : Journal of the Pharmaceutical Society of Japan, 128 (2008) 603-609.

[43] J. Sahni, S. Raj, F.J. Ahmad, R.K. Khar, Design and in vitro characterization of buccoadhesive drug delivery system of insulin, Indian journal of pharmaceutical sciences, 70 (2008) 61-65.
[44] M.J. Hernández Lucas, M. Dolz Planas, J. Delegido Gómez, Introducción a la reología. Aplicación a sistemas farmacéuticos y alimentarios, Moliner-40, Spain, 2006.
[45] L. Pindakova, V. Kasparkova, K. Kejlova, M. Dvorakova, D. Krsek, D. Jirova, L. Kasparova, Behaviour of silver nanoparticles in simulated saliva and gastrointestinal fluids, Int J Pharm, 527 (2017) 12-20.
[46] D. Zhang, A Coefficient of Determination for Generalized Linear Models, The American Statistician, 71 (2017) 310-316.
[47] S. Nakagawa, P.C.D. Johnson, H, Schielzeth, The coefficient of determination R(2) and intra-class correlation coefficient from generalized linear mixed-effects models revisited and expanded, J R Soc Interface 14 (2017) 20170213.
[48] W.K. Chan, C.C. Cheung, H.K. Law, Y.L. Lau, G.C. Chan, Ganoderma lucidum polysaccharides can induce human monocytic leukemia cells into dendritic cells with immuno-stimulatory function, J Hematol Oncol, 1 (2008) 9.
[48] [49] Y. Huang, L. Nan, C. Xiao, Q. Ji, K. Li, Q. Wei, Y. Liu, G. Bao, Optimum Preparation Method for Self-Assembled PEGylation Nano-Adjuvant Based on Rehmannia glutinosa Polysaccharide and Its Immunological Effect on Macrophages, Int J Nanomedicine, 14 (2019) 9361-9375.
[50] S. Zhang, H. Jiang, S. Huang, P. Li, F. Wang, Curdlan sulfate/O-linked quaternized chitosan nanoparticles acting as potential adjuvants promote multiple arms of immune responses, Carbohydr Polym, 213 (2019) 100-111.
[51] X. Xu, Y. Shen, W. Wang, C. Sun, C. Li, Y. Xiong, J. Tu, Preparation and in vitro characterization of thermosensitive and mucoadhesive hydrogels for nasal delivery of phenylephrine hydrochloride, Eur J Pharm Biopharm, 88 (2014) 998-1004.
[52] M. Dhiman, P. Yedurkar, K.K. Sawant, Formulation, characterization, and in vitro evaluation of bioadhesive gels containing 5-Fluorouracil, Pharm Dev Technol, 13 (2008) 15-25.

[53] C. Bretti, R.M. Cigala, F. Crea, C. De Stefano, G. Gattuso, A. Irto, G. Lando, D. Milea, S. Sammartano, Thermodynamic Properties of O-Donor Polyelectrolytes: Determination of the Acid–Base and Complexing Parameters in Different Ionic Media at Different Temperatures, Journal of Chemical & Engineering Data, 62 (2017) 2676-2688.
[54] G.P. Andrews, L. Donnelly, D.S. Jones, R.M. Curran, R.J. Morrow, A.D. Woolfson, R.K. Malcolm, Characterization of the rheological, mucoadhesive, and drug release properties of highly structured gel platforms for intravaginal drug delivery, Biomacromolecules, 10 (2009) 2427-2435.
[55] N.S. Barakat, Evaluation of glycofurol-based gel as a new vehicle for topical application of naproxen, AAPS PharmSciTech, 11 (2010) 1138-1146.
[56] J. Hurler, A. Engesland, B. Poorahmary Kermany, N. Škalko-Basnet, Improved texture analysis for hydrogel characterization: Gel cohesiveness, adhesiveness, and hardness, Journal of Applied Polymer Science, 125 (2012) 180-188.

USC UNIVERSIDADE DE SANTIAGO DE COMPOSTELA

USC
UNIVERSIDADE
DE SANTIAGO
DE COMPOSTELA

4. CHAPTER II: SUBLINGUAL BOOSTING WITH A NOVEL MUCOADHESIVE THERMOGELLING HYDROGEL FOLLOWING PARENTERAL CAF01 PRIMING AS STRATEGY AGAINST *CHLAMYDIA TRACHOMATIS*

USC UNIVERSIDADE DE SANTIAGO DE COMPOSTELA

USC
UNIVERSIDADE
DE SANTIAGO
DE COMPOSTELA

ABSTRACT

Chlamydia trachomatis is the most prevalent sexually transmitted disease of bacterial origin. The high number of asymptomatic cases makes difficult to stop the transmission, requiring a vaccine development. Herein, we propose a strategy to obtain local genital tract immunity against *Chlamydia trachomatis* through parenteral prime and sublingual boost. Subcutaneous administration of Chlamydia CTH522 subunit vaccine loaded in the adjuvant CAF01 was combined with sublingual administration of CTH522 loaded in a novel thermosensitive and mucoadhesive hydrogel. Briefly, a ternary optimized hydrogel (OGEL) with desirable biological and physicochemical properties was obtained using artificial intelligence techniques. This formulation exhibited a high gel strength and a strong mucoadhesive, adhesive and cohesive nature. The thermosensitive properties of the hydrogel facilitate application under the tongue. Meanwhile the fast gelation at body temperature together with rapid antigen release should avoid CTH522 leakage by swallowing and increase the contact with sublingual tissue, thus promoting absorption. *In vivo* studies demonstrated that parenteral-sublingual prime-boost immunization, using CAF01 and OGEL as CTH522 vaccine carriers, was more effective at inducing cellular (Th1/Th17) immune responses than mucosal or parenteral vaccination alone. Furthermore, parenteral prime with CTH522 formulated in CAF01 followed by sublingual boosting with CTH522 formulated in OGEL elicited a local IgA response in the genital tract.

USC
UNIVERSIDADE
DE SANTIAGO
DE COMPOSTELA

4.1. INTRODUCTION

Sexual transmitted infections lead to significant morbidity and mortality worldwide. Their high incidence rate has a great impact on healthcare systems, causing high social and economic costs [1]. *Chlamydia trachomatis* (Ct) is an intracellular pathogen that infects around 131 million people annually and can affect vaginal, pulmonary and conjunctiva mucosae [2, 3].

Mucosal surfaces are the main entry site for most pathogens – including Ct– and are therefore, protected by a highly specialized immune system. The stimulation of the mucosal immune system by pathogen invasion or vaccination can induce both systemic and local mucosal immune responses [4, 5]. Furthermore, mucosal immunization can also elicit immune responses at remote mucosal surfaces due to the migration of activated B and T cells [4, 6, 7]. Therefore, sublingual and intranasal vaccination could confer protection against genital tract infections. Moreover, unlike vaginal immunization, sublingual and intranasal vaccination does not depend on the host hormonal status [8].

Nasal mucosa has been used as an effective immunization route against chlamydia and other sexually transmitted infections [3, 9, 10]. However, this strategy presents safety concerns since the administration of certain enterotoxins used as adjuvants by nasal route has been associated to Bell's palsy in some patients [6, 8, 11]. On the contrary, recent clinical trials have shown that sublingual vaccination allows to decrease the infectious episodes of the urinary tract with only rare side effects and no facial nerve disturbance after enterotoxin administration [12, 13]. Furthermore, the results of sublingual administration of the quadrivalent human papillomavirus vaccine Gardasil® show this route can be used for boosting and induces functional antibody responses [14]. Finally, studies in mice immunized against chlamydia have showed a stronger immune response when parenteral and mucosal vaccines were given in tandem [15, 16].

The sublingual route is accessible for drug administration and patient-friendly. Moreover, sublingual tissue contains plenty of antigen-presenting dendritic cells that can recirculate to distant lymph

nodes and spleen, and also induce IgA and IgG antibodies, and cytotoxic T cells in the genital tract [17, 18]. However, sublingual vaccine administration in both humans and non-human primates is challenging and may fail to elicit mucosal immunity [12, 14]. These discouraging results are most probably caused by poor antigen delivery due to swallowing of vaccine components. Jones et al. thus demonstrated in macaques that the administration of HIV-1 antigens directly in the oral underlying tissue using a needle-free injector, ensuring reduced loss due to swallowing, facilitates increased uptake by dendritic cells and the development of strong humoral and cellular responses in both systemic and mucosal compartments [19]. Thereby, the development of delivery systems able to protect the antigen(s) from salivary enzyme degradation and promote antigen permeation through sublingual mucosa might be the answer to achieve better mucosal immune responses.

A promising strategy could be the development of mucoadhesive thermogelling hydrogels. These formulations can be easily administered under the tongue due to their liquid nature and resist wash out by becoming semisolid at body temperature [20]. Thus, antigens can remain in contact with sublingual mucosa for longer, facilitating increased uptake by dendritic cells. In addition to act as carriers for antigens, hydrogels may have intrinsic immunostimulatory properties, and can also be loaded with other adjuvants, such as dmLT and CpG [21, 22].

As described above, the combination of systemic and mucosal routes is beneficial to induce more robust immune responses against chlamydia [15, 16, 23]. Herein, we propose a systemic priming followed by a sublingual boosting as vaccination strategy for Ct. For that purpose, chlamydia subunit vaccine CTH522, which is a recombinant Ct outer membrane protein comprising immunorepeats of the D, E, F and G Ct serovars, was used [24]. CAF01 (cationic adjuvant liposomes type 01) is an adjuvant composed by dimethyldioctadecylammonium bromide (DDA) and glycolipid trehalose 6,6´-dihibenate (TDB), successfully used in several clinical trials, including one trial with CTH522, demonstrating its safety and tolerability [24-27]. This adjuvant has furthermore been shown to

prime a parenteral immune response that supports the establishment of mucosal memory upon mucosal boosting [28, 29]. Parenteral administration of CAF01-adjuvanted CTH522 combined with intranasal boosting using the same formulation induced a synergistic protective effect against chlamydia in minipigs [23]. However, systemic priming using CAF01 followed by sublingual boosting has not been explored. In order to maintain the contact of CTH522 with the sublingual mucosa and favour its permeation and uptake by dendritic cells, a novel and optimized mucoadhesive hydrogel (OGEL) was proposed [20]. The optimal ternary composition was selected using artificial intelligence techniques giving rise to a hydrogel with desirable biological and physicochemical properties.

The aim of the present work was to explore the usefulness of sublingual boosting with vaccine loaded mucoadhesive thermosensitive hydrogels posterior to systemic priming as a strategy for immunization against chlamydia. For this purpose, chlamydia CTH522 vaccine antigen was administered in two sequential doses. First subcutaneously using CAF01 as adjuvant and then sublingually using either CHT522 alone or loaded into hydrogels. The capacity to induce immune responses of two sequential sublingual administrations with the CHT522-loaded hydrogel was also evaluated.

4.2. MATERIALS AND METHODS

4.2.1. Materials

Pluronic® F127 (PF127) and bovine serum albumin (BSA) were obtained from Sigma-Aldrich (USA). Hybrane® S1200 (HS1200) was acquired from Polymer Factory (Sweden). Gantrez® AN119 (AN119) was kindly provided by Ashland (Spain). Trehalose 6,6´dibehenate (TDB) and dimethyldioctadecylammonium bromide (DDAB) were purchased from Avanti Polar Lipids Inc. (USA). Cell Strainers presenting a pore size of 40 µm and 100 µm were purchased from Corning® Incorporated (USA). Purified rat anti-mouse IL-17A, biotin rat anti-mouse IL-17A, purified rat anti-mouse IFN-γ, biotin rat anti-mouse IFN-γ and streptavidin HRP were purchased from BD Pharmingen (USA). Rabbit anti-mouse IgG (H+L)-HRP was obtained from Invitrogen (USA). Goat anti-mouse IgA-HRP was purchased

from Southern Biotech (USA). Carbonate buffer pH 9.6 was supplied by SSI Diagnostics (Denmark). TMB PLUS2™ was obtained from Kem-En-Tec Diagnostics (Denmark). *Chlamydia trachomatis* vaccine CTH522 was supplied by Statens Serum Institut (SSI) (Denmark).

4.2.2. Hydrogel development and preparation

The database generated in our previous investigation (**Annex I, Tables A1.1 to A1.7**) [20] was used to create a model with the commercial software INForm® v.5.01 (Intelligensys, Ltd. UK) which combines Artificial Neural Networks (ANN) and genetic algorithms. The database includes 19 records of ternary hydrogel formulations of different composition. The independent variables were, Gantrez® variety (AN119 or S97), and the percentages of Gantrez®, Pluronic® F127 and Hybrane® S1200. Additionally, the dependent variables were the rheological (gelation temperature), texturometric (mucoadhesion and adhesion work, cohesion and gel strength at 37 ºC) and release properties of the produced hydrogels.

Data were split in two sets, 16 records for training and 3 for error testing. The parameters selected for INForm® modelling are shown in **Table 1**.

The accuracy of the ANN models was assessed using the determination coefficient (R^2) (**eq.1**), calculated for train and test data.

$$R^2 = \left[1 - \frac{\sum_{i=1}^{n}\left(y_i - y_i^{*}\right)^2}{\sum_{i=1}^{n}\left(y_i - y_i^{**}\right)^2}\right] \times 100 \qquad \textbf{(eq. 1)}$$

Where, y_i represents the output's experimental value in the data set, y_i^{*} is the predicted value of the output predicted by the ANN model and finally, y_i^{**} is the mean value of the parameter that is being evaluated.

Table 1. Training parameters used for INForm® modelling.

ANN Network Structure:	Test data:
Nº hidden layers = 1	Screen update set = 5
Nº nodes in hidden layer = 2	Smart stop enabled
Transfer functions:	Minimum interactions = 20
Hidden layer transfer function = Asymmetric sigmoid	Test error weighting = 0.2
Output transfer function type = Linear	Optimization:
Back propagation type = RPROP	Number of Populations = 1
ANN Targets:	Number of Iterations = 100
Targets epochs = 1000	Population Size = 100
Target MS error = 0.0001	Replacement % = 50
Random seed = 10,000	Mutation Standard Deviation = 0.1
	Random seed = 1

The optimal hydrogel formulation (OGEL) obtained following the INForm® model was produced following the protocol previously reported by Garcia-del Rio et al. [20]. Briefly, an accurate amount of Gantrez® (AN119) was dissolved in Milli-Q® water at 50 ºC. Then, Hybrane® S1200 (HS1200) was incorporated to this solution, previously cooled in an ice bath. Finally, Pluronic® F127 (PF127) was added and dissolved overnight at 4 °C, and pH was adjusted to 6.8. Afterwards, hydrogel sterilization was carried out by autoclaving (Trade Raypa® steam sterilizer AES-12, Barcelona, Spain). Sterile hydrogels were stored at 4 °C until use.

4.2.3. Hydrogel characterization

4.2.3.1 Rheological properties

A rheometer AR1000-N (TA Instruments, UK) was used to hydrogels estimate storage (G') and loss moduli (G"), using a cone-plate geometry of 6 cm Ø and 2.1 degrees. Both moduli were recorded

from 15 to 40 °C at 0.4 °C/min at an angular frequency of 5 rad/s. Gelation temperature (T_{gel}) was established by the crossover of both moduli.

4.2.3.2. Texturometric properties

A TA XT plus Texture Analyzer (Surrey, UK) was used to obtain the texturometric profile of the optimized hydrogels. All texturometric properties (mucoadhesion, gel strength, adhesion and cohesion) evaluated in this work were performed at 37 ºC following protocols previously described [20].

Briefly, bovine buccal tissue was used as model of oral mucosa to measure mucoadhesion work. Buccal mucosa was cut in pieces of 1.5 cm x 1.5 cm and glued to the punch of the texturometer, then a Petri dish containing 3 g of OGEL was attached to the lower support of the texturometer. The punch descended at 1 mm/s and applied a force of 0.5 N on the optimized hydrogel for 60 s. The mucoadhesion work (mJ) was calculated as the force exerted by the punch when rising at 1 mm/s.

To estimate gel strength, adhesion work and cohesion, two compression cycles were performed. As for mucoadhesion, the punch descended at 1 mm/s and compressed the hydrogel to 5 mm in depth. After a required relaxation time of 30 s, a second compression cycle was carried out. Gel strength (N) and adhesion work (mJ) were calculated using the force-distance plot generated during the first compression cycle. Meanwhile, for cohesion assessment both force-distance plots were required [20].

4.2.3.3. Protein release

Bovine serum albumin (BSA), having a similar molecular weight to CTH522 [30], was used as protein model to asses OGEL release properties following the protocol established by Garcia-del Rio et al. [31] with slight modifications. BSA was dissolved in OGEL reaching a final concentration of 0.75 mg/mL and stored at 4 °C overnight. Release studies were performed at 37 ºC and 400 rpm in an orbital shaker Tritamax 1000 (Heidolph Instruments, Germany) using simulated salivary fluid (SSF) as release media [32]. Then, 2 mL of the loaded hydrogel were placed in a Corning® Cell Strainer of 40 µm

pore size, previously located in 6-well plates containing 8 ml of SSF. The amount of BSA released was quantified employing the Pierce™ BCA Protein Assay according to manufacturer's protocol. Absorbance was measured using a FLUOstar OPTIMA plate reader (BMG Labtech, Germany) and the percentage of BSA released at 5 minutes was calculated using adequate controls and validated calibration curves.

4.2.3.4. Stability properties

The effect of storage on the properties of OGEL was evaluated after one year at 4 °C in closed containers. Texturometric, rheological and release properties were re-analyzed after storage.

4.2.4. CAF01 liposomes preparation

CAF01 liposomes were obtained through the hydration method, allowing the formation of large and heterogeneous multilamellar vesicles as it was previously reported [33]. Briefly, both lipids, TDB and DDA, were individually dissolved in a mixture of chloroform and methanol (9:1 v/v). Afterwards, accurate amounts of the lipid solutions were transferred to round-bottom flasks to get a final concentration of 1 mg/mL for TDB and 5 mg/mL for DDAB, and rota evaporated for 15 min at 200 rpm to remove the organic solvent. Finally, the desired volume of 10 mM Tris buffer (pH 7.4) was added and the lipid film was hydrated for 20-30 min at 60 °C.

4.2.5. Antigen and formulations loading

CAF01 and OGEL formulations were loaded under sterile conditions with the antigen selected, the recombinant CTH522 chlamydia protein [34].

CAF01 liposomes were loaded by dissolving CTH522 in Tris-buffer (10 mM, pH 7.4) supplemented with 9% trehalose and then mixed in a 1:1 ratio with CAF01. The final CTH522 concentration was 0.025 µg/µL.

An accurate amount of CTH522 stock solution was added to OGEL hydrogel to achieve an antigen concentration of 0.2 µg/µL, and gently mixed in a vortex. Loaded OGEL was stored overnight at 4 °C to ensure total bubbles removal.

4.2.6. In vivo assays

4.2.6.1. Ethics statement

Animal experiments were conducted at Statens Serum Institut (SSI) according the regulations established by the Danish Ministry of Justice and Animal Protection committees by Danish Animal Experiments Inspectorate Permit 2017-15-0201-01363 and in compliance with the European Community Directive 2010/63. All protocols have been subjected to ethical review and approved by SSI.

4.2.6.2. Mouse immunization

Seven to nine-week old CBF61 female mice were housed at SSI and handled by authorized staff. Animals were divided into four groups of three to five mice. The immunization schedule is depicted in **Figure 1**. Mice immunized sublingually were anesthetized with Zoletil® mixture.

Groups one to three were subcutaneously primed at the base of the tail with 200 µL of CAF01/CTH522, which contained 5 µg of CTH522, 250 µg of DDA and 50 µg of TDB. Group four was sublingually primed with 10 µL of OGEL (OGEL/CTH522), which contained 2 µg of CTH522 dispersed in the hydrogel. After mucosal vaccination, mice were placed in ante-flexion posture for 20 minutes. Then, groups two to four were boosted twice sublingually (days 15 and 35), with 2 µg of CTH522 alone (Group two) or included within 10 µL of OGEL system (Groups three and four). Group one, vaccinated only with CAF01/CTH522 was established as control. Mice were euthanized 3 weeks after the last mucosal boosting.

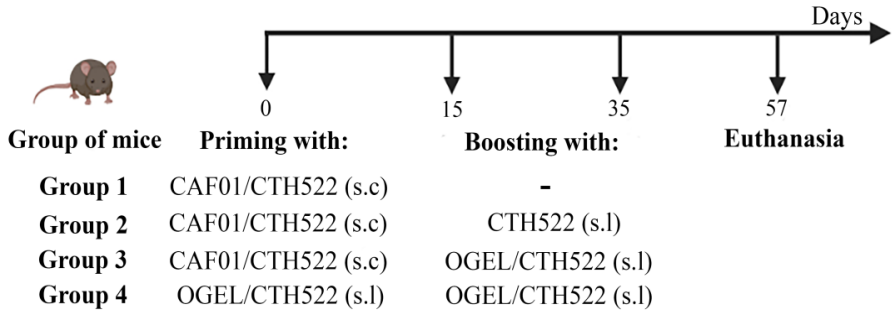

Figure 1. Immunization schedule and experimental groups tested. Animals were primed subcutaneously (s.c) or sublingually (s.l) using CAF01 and OGEL as vaccine delivery systems, respectively. Thus, mice from Groups 1, 2 and 3 were immunized with CAF01/CTH522 (s.c) meanwhile Group 4 was mucosally vaccinated with OGEL/CTH522 (s.l). On days 15 and 35, except animals from Group 1, mice were boosted twice through sublingual (s.l) route with CHT522 alone (Group 2) or loaded into OGEL formulation (Groups 3 and 4).

4.2.6.3. Antibody titers in blood and vaginal samples

At the end of the study, an enzyme-linked immunosorbent assay (ELISA) was employed for the quantification of IgA and total IgG in serum and vaginal lavage. Briefly, blood samples were collected from the tail vein in a heparinized tube (1% w/v heparin) and centrifuged at 10,000 *g* for 10 minutes to separate sera from cells. Serum samples were stored in a 96-well plate at -20 °C until use.

Vaginal wash samples were obtained washing out the vagina with 100 µl of phosphate-buffered saline (PBS) and stored at -80 °C until further use. Vaginal samples were treated with bromelaine (2.5%) and diluted 5 times with PBS containing 1% of BSA. Afterwards, samples were incubated during 1 hour at 37 °C to break vaginal mucous network. 96 well MaxiSorp flat bottom plates were coated overnight at 4 °C with 100 µL/well CTH522 (1 µg/mL) diluted in carbonate buffer (pH 9.6), and then blocked with 200 µL/well PBS (pH 7.2) containing 2% BSA during at least 1.5 h at room temperature. Then vaginal (37.5 µL) or serum (12.5 µL) samples were added in serial dilutions and incubated for 2 hours at room temperature. Finally, antigen-specific IgA and total IgG were detected employing HRP-conjugated goat anti-mouse IgA or rabbit anti-mouse IgG antibodies respectively, TMB substrate and sulfuric acid (0.2 M). Plates were

measured at 450 nm with wavelength correction (570/620 nm) in a spectrophotometer (Sunrise Tecan, Austria).

4.2.6.4. IFN-γ and IL-17A responses in spleen and cervical lymph nodes

IFN-γ and IL-17A produced by splenocytes and cervical lymph nodes were evaluated through a sandwich ELISA. Individually in 6-well cell culture plates, organs were disrupted with cell strainers of 100 µm pore size using sterile syringe pistons. Each strainer was washed with PBS (pH 7.2) and cell suspensions were transferred to 15 mL tubes and filled with PBS (pH 7.2) supplemented with 10% foetal calf serum (FCS) up to 12 mL. Then, tubes were spun down at 2,000 rpm for 5 minutes. Supernatants were discarded and cell-pellets suspended in 12 mL of RPMI media. Samples were spun down again, supernatants were withdrawn, and cell-pellets suspended in either 0.5 or 2 mL of RPMI media for lymph nodes or splenocytes respectively, subsequently the cell concentration of each sample was quantified using a Nucleo counter (Chemometec, Denmark). Afterwards, known amounts of cell suspensions were diluted in RPMI media supplemented with FCS (10%), HEPES buffer (1%), penicilin-streptomycin, L-Glutamine, sodium pyruvate and non-essential amino acids to get a concentration of 2 x 10^6 cells/mL. Then, 100 µL of each cell-suspension were transferred to 96-cell round bottom plates and re-stimulated with 100 µL of RPMI media, CTH522 (5 µg/mL) or Concanavalin A (3 µg/mL) for 72 h at 37 °C, 5% CO_2 and 95% humidity. Cells re-stimulated with media alone and Concanavalin A were used as negative and positive controls, respectively. Lastly, supernatants were collected and stored at -20 °C until use.

Secreted IFN-γ and IL-17A cytokines in splenic and lymph nodes supernatants were quantified using ELISA kits following protocols reported elsewhere [33]. Briefly, specific amounts of purified rat anti-mouse IL-17A or IFN-γ were diluted in carbonate buffer (pH 9.6), added (100 µL/well) to MaxiSorp plates and incubated overnight at 4 °C. Then, plates were blocked with PBS containing skimmed milk powder (2%) for 1.5-2 h at room temperature and, subsequently plates were incubated for 2 h with 2% BSA in PBS. Finally, IL-17A or IFN-γ concentration was determined using standard curves and the

corresponding biotin anti-mouse antibody, streptavidin, TMB substrate and sulfuric acid (0.2 M). Plates were read at 450 nm with wavelength correction (570/620 nm).

4.2.7. Statistical analysis

Results from hydrogel characterization and *in vivo* experiments are expressed as mean ± standard deviation and mean ± error of the mean (SEM), respectively. SPSS software (IBM SPSS Statistics 26) was employed to perform a one-way ANOVA and HSD Tukey's post hoc tests ($p < 0.05$).

4.3. RESULTS

4.3.1. Hydrogel preparation, characterization and stability

Combinations of PF127, HS1200 and AN119 polymers have been demonstrated to be useful for obtaining thermosensitive and mucoadhesive hydrogels [20]. INForm® succeeded in modelling the composition variables as inputs and the rheological, texturometric and release properties as outputs. Models for all the parameters had Train R^2 higher than 95% and test R^2 over 82%, indicating excellent predictabilities. The generated INForm® model was asked about how to get hydrogels with gelation temperature between 28 and 32 ºC together with maximum mucoadhesion, adhesion work, cohesion and gel strength at 37 ºC and fast release. The model predicted optimal hydrogels can be obtained with the following composition: 21.10% of PF127, 5.00% of HS1200 and 0.08% of Gantrez® AN119 (Total desirability =77.5%).

The properties of the optimal hydrogel composition (OGEL) selected by INForm® following **Table 1** conditions, were close to those predicted, validating the obtained ANN model. As shown in **Table 2**, OGEL is a thermosensitive system that gels at 19.7 °C and thus immediately after application within the mouth. It has a gel strength of 0.7 N, a mucoadhesion and adhesion work of 1.24 and 1.74 mJ respectively and a cohesion of 0.2. Finally, it releases up to 41.11% of the protein at 5 minutes, quick enough to ensure vaccine absorption in few minutes [35-37] and avoid formulation leakage by swallowing. OGEL has long-term stability at 4 ºC (**Table 2**) and

statistically significant differences could not be found between OGEL freshly prepared and after 1-year storage at 4 ºC (p<0.05).

Table 2. Values predicted by the ANN model and experimental values for the parameters (mean ± standard deviation) characterized for OGEL freshly prepared and after 1 year of storage at 4 ºC in closed containers.

Parameter	Predicted by ANN	OGEL (t=0)	OGEL (t=1 year)
T_{gel} (˚C)	20.6	19.7 ± 0.14	19.5 ± 0.23
Gel Strength (N)	0.6	0.70 ± 0.01	0.67 ± 0.01
Mucoadhesion work (mJ)	1	1.24 ± 0.18	1.26 ± 0.15
Adhesion work (mJ)	1.5	1.74 ± 0.12	1.75 ± 0.05
Cohesion	0.3	0.20 ± 0.07	1.16 ± 0.00
%BSA released at 5 min	43.5	41.11 ± 1.88	44.2 ± 4.7

4.3.2. Prime immunization using CAF01 followed by OGEL mucosal boosting improves mucosal antibody responses

An *"in vivo*" study was conducted to evaluate the usefulness of OGEL as sublingual vaccine carrier against chlamydia. Thus, mice were treated with CTH522 in CAF01 alone or followed by a sublingual boost with OGEL. In addition, sublingual vaccination alone was also evaluated.

Figure 2 shows total IgG and IgA CTH522 specific antibodies determined in serum (**A, B**) and vaginal lavage (**C, D**) at the end of the study. Serum results showed that mice receiving mucosal boosting with antigen alone or loaded in OGEL after subcutaneous antigen stimulation, produced lower CTH522-specific IgG antibody levels than their counterparts only immunized parenterally. Nevertheless, parenterally primed and sublingually boosted animals exhibited higher IgA responses both in serum and vaginal washes, particularly when loaded on the hydrogel (OGEL/CTH522). These results are consistent with previous studies that describe the boosting effect of the sublingual route [14, 38, 39]. Animals vaccinated parenterally with CAF01/CTH522 had significantly higher serum IgG responses than mice immunized exclusively by the sublingual route (p<0.05) (**Figure**

2A-D). Although the group boosted with OGEL/CTH522 produced the highest IgA and IgG mean titers in vaginal secretions, which is one of the vaccination targets against sexual diseases, this enhancement was not statistically significant compared to animals only vaccinated with CAF01/CTH522.

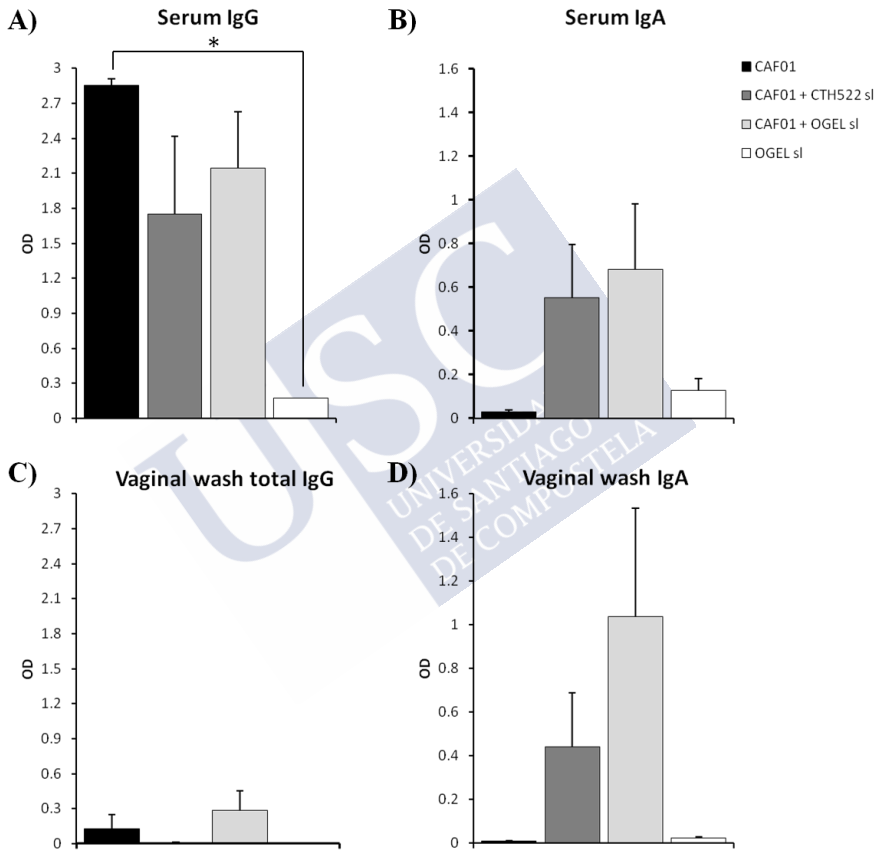

Figure 2. Total IgG and IgA determined by ELISA in serum (A, B) and vaginal lavage (C, D). The y-axis shows the optical density (OD). Results are expressed as mean ± SEM. * denotes statistically significant differences between depicted groups (p<0.05).

4.3.3. Prime immunization using CAF01 followed by OGEL sublingual boosting elicits high-magnitude IFN-γ responses in cervical lymph nodes

Optimal vaccination against *Chlamydia trachomatis* requires stimulating Th1 cell-mediated immunity in addition to elicit neutralizing antibodies. Th17 cells have a crucial role as accelerators of mucosal immunity. Besides, these cells can also acquire functional features of follicular helper T cells, which can lead to IgA-isotype switching [3].

To measure if sublingual boosting delivered in OGEL can improve local and systemic Th1 and Th17 responses, we re-stimulated splenocytes and cervical LN cells with CTH522 antigen and measured secretion of IFN-γ and IL-17A. As shown in **Figure 3A-D,** the secretion of IFN-γ by splenic T cells was higher than IL-17A, while the opposite was seen in cervical lymph nodes. Generally, mucosal boosting was beneficial to improve IFN-γ and IL-17A responses in both spleen and cervical lymph nodes after parenteral priming. Splenocytes from the group having received parenteral prime/loaded hydrogel sublingual boost secreted the highest amount of IFN-γ, although not statistically significant when compared to group that received only parenteral vaccine. However, in cervical lymph nodes, IFN-γ production was significantly higher in the group that had received parenteral prime/loaded hydrogel sublingual boost compared to parenteral vaccine alone ($p < 0.05$) (**Figure 3C)**.

Using a mucoadhesive hydrogel as carrier of CTH522 vaccine for sublingual boosting enhanced the secretion of IFN-γ and IL-17A in both spleen and cervical lymph nodes. Specifically, boosting with OGEL/CTH522 showed a 2-fold and 1.4-fold increase of IFN-γ and IL-17A secretion respectively in the spleen when compared to mucosal boosting with CTH522 alone. The same effect was observed in cervical lymph node samples, where animals boosted with OGEL/CTH522 presented a 3.2 and 4.3-fold enhancement in IFN-γ and IL-17A, respectively, compared to those receiving CTH522 alone, although these differences were not statistically significant. Overall, the systemic prime-sublingual boost strategy was more effective in inducing Th1/Th17 immune responses than parenteral priming alone

and boosting with antigen formulated in OGEL may further increase responses.

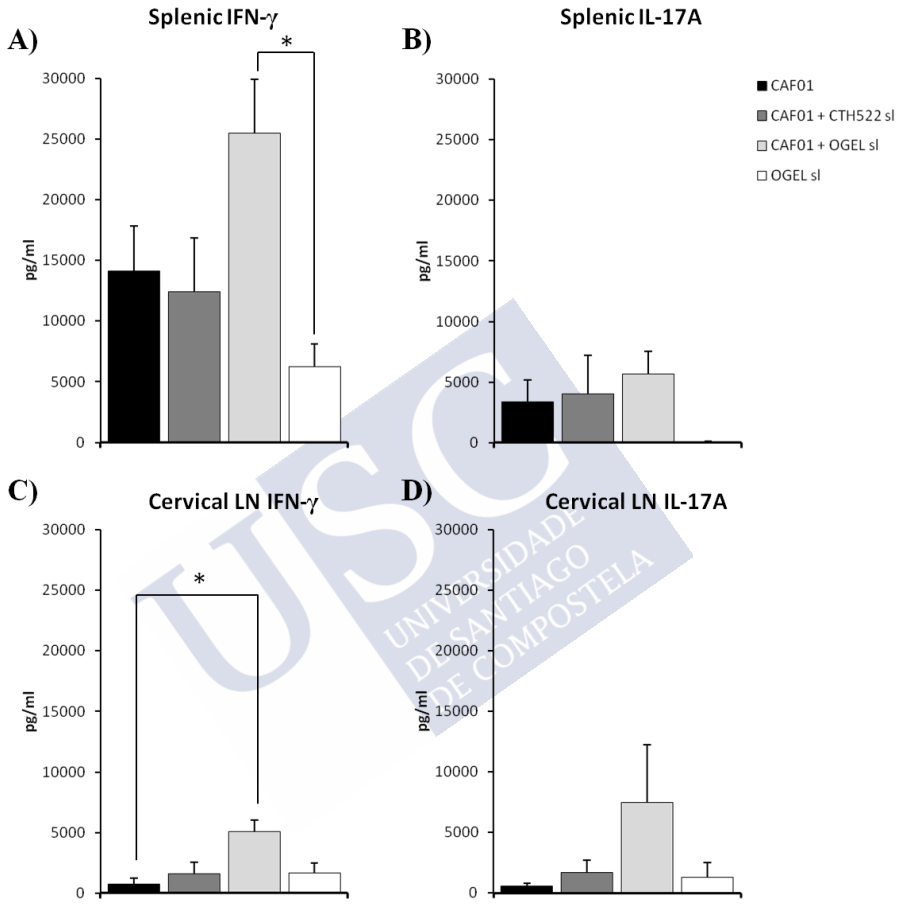

Figure 3. IFN-γ and IL17A cytokine production by splenocytes (A, B) and cervical lymph nodes cells (C, D) after being restimulated with CTH522. Results are expressed as mean ± SEM. * denotes statistically significant differences between depicted groups (p<0.05).

4.4. DISCUSSION

The use of mucosal tissues as vaccination route is grounded in the fact that most infections are initiated at the mucosal surfaces [40]. Novel vaccination strategies are mainly focused on subunit vaccines, including recombinant peptides and proteins, DNA, mRNA or

toxoids, owing to their higher safety profile and cheaper mass production. Nevertheless, these types of vaccines present the great disadvantage of being poorly immunogenic [5, 41]. This drawback can be even more pronounced when administered mucosally due to antigen dilution and/or entrapment in mucosal secretions and proteolytic degradation, hindering antigen uptake and delivery to the mucosa-associated lymphoid tissues [5]. In this sense, adjuvants as vaccine delivery platforms become crucial for achieving effective and long-lasting immunity.

Parenteral vaccines may be effective when the infection occurs in the urogenital tract because it is more permeable to transudation of serum antibodies than other mucosae. The antibody titers however must be high [23], and so parenteral vaccines frequently fail in inducing strong antibody responses at mucosal tissues.

The promotion of high IgA titers able to neutralize pathogens at the target mucosal surface(s) is extraordinarily challenging, even when a mucosal tissue is used as immunization site [42]. Several studies have hallmarked the synergistic effect of combined systemic and mucosal vaccination to generate strong local mucosal immunity and protective immunity either in mice and minipigs against chlamydia [3, 15, 16, 23] or in macaques against simian immunodeficiency virus [43]. Besides, the benefits of parenteral priming followed by mucosal boosting were also described for other mucosal pathogens such as *Mycobacterium tuberculosis* [44, 45]. In this work, mice were primed subcutaneously with the chlamydia subunit vaccine CTH522 incorporated in CAF01 followed by two mucosal boostings using the sublingual route to evaluate the potential synergic effect of both routes. The comparison between the two sublingual boosting strategies (antigen alone or embedded in a hydrogel) should allow to assess the utility of a new hydrogel platform to efficiently promote mucosal immune responses.

Sublingual vaccination can induce IgA responses with similar mucosal tropisms to nasal vaccination, but is generally considered less immunogenic [42]. In attempt to maximize CTH522 uptake by the sublingual mucosa and improve mucosal and systemic immune

responses, the antigen was loaded on the thermosensitive and mucoadhesive formulation OGEL.

The liquid texture of OGEL facilitates its application and extension on the sublingual mucosa, while its thermosensitive properties allow a fast sol-gel transition at body temperature, avoiding formulation leakage by swallowing. Furthermore, a highly mucoadhesive hydrogel should increase the contact time with sublingual epithelium and facilitate antigen uptake. These properties make OGEL a good candidate as a vaccine carrier for this route of administration [22, 46, 47]. OGEL is a ternary system whose components have interesting properties. PF127 has been reported to enhance drug permeation through different mucosae and could therefore potentially increase CTH522 permeation through sublingual tissue [22, 48]. HS1200 exhibited potential adjuvant properties by promoting proliferation of human macrophages [20]. Lastly, Gantrez® is a high bioadhesive anionic amphiphilic copolymer, previously used in oral vaccines as excipient of nanoparticles or microneedle patches [49-51].

Previous studies have used CAF01 as vaccine adjuvant against chlamydia [3, 23, 52, 53], reporting its capability for inducing immune responses with a Th1/Th17 profile together with high antibody titers. IFN-γ produced by Th1 cells plays a key role in the resolution of chlamydia infection, inhibiting Ct growth through different pathways [54-56]. Th17 cells have not been associated with a direct role against chlamydia, but stimulate neutrophil recruitment and are involved in the development of Th1 immunity [57] and production of mucosal IgA [3].

Our results point to a synergistic effect of parenteral and sublingual vaccination, as mice immunized by the two routes produced higher IgA titers and developed stronger cellular responses in splenocytes and cervical lymph nodes than when using a single route. Similar results were observed in mice simultaneously vaccinated intramuscularly and intranasally with *Chlamydia psittaci* antigens, adjuvanted with chitosan nanoparticles [58]. Our results are also in agreement with studies by Ralli-Jain et al. [16] and Carmichael et al. [15], using mice immunized with the recombinant major outer

membrane protein (rMOMP) of Ct and *Chlamydia muridarum*, respectively.

The results herein described that sublingual boosting after systemic priming could be a feasible strategy to induce systemic as well as mucosal immunity in the genital tract. In addition, our results suggest that the use of mucoadhesive vaccine delivery systems could be a strategy to maximize the boosting effect of sublingual immunization and therefore, improve mucosal immune responses in the genital tract. However, the success of this approach will depend on the development of highly mucoadhesive vaccine carriers capable of promoting a fast antigen permeation through sublingual tissue, thus ensuring an adequate stimulation of the immune system. Sublingual administration of CTH522 loaded OGEL after subcutaneous CAF01/CTH522 priming elicited IgA responses in serum and vaginal fluids, as well as IFN-γ and IL-17A secretion by spleen and cervical lymph node T cells.

Mouse oral anatomy differs from that of humans, particularly regarding the sublingual mucosa, which is highly keratinized in mice. High levels of keratinization strongly hinder the permeability of active substances across tissues [22, 59]. This limitation must be considered when these rodents are used as a model for testing the usefulness of drugs or vaccine systems by sublingual administration. Animal models with greater similarity to humans, such as primates, would be better suited to predict immune responses, but costs and ethical issues limit their use [60].

4.5. CONCLUSIONS

ANN together with genetic algorithms have demonstrated its potential to optimize a ternary hydrogel formulation through a reduced experimental design, giving rise to OGEL, a highly mucoadhesive and thermosensitive hydrogel suitable as a vaccine carrier for sublingual administration. OGEL has shown utility as a carrier of the chlamydia vaccine CTH522 in a mouse model. The co-administration of CAF01 and OGEL loaded with CTH522 subunit vaccine significantly enhanced IFN-γ production by cervical lymph nodes when compared with mice exclusively immunized parenterally.

REFERENCES

[1] R. Ramanathan, K. Woodrow, Engineering immunity in the mucosal niche against sexually transmitted infections, Wiley Interdiscip Rev Nanomed Nanobiotechnol, 8 (2016) 107-122.
[2] G. Häcker, Biology of Chlamydia, Springer International Publishing, 2018.
[3] J.E. Wern, M.R. Sorensen, A.W. Olsen, P. Andersen, F. Follmann, Simultaneous Subcutaneous and Intranasal Administration of a CAF01-Adjuvanted Chlamydia Vaccine Elicits Elevated IgA and Protective Th1/Th17 Responses in the Genital Tract, Front Immunol, 8 (2017) 569.
[4] M. Nizard, M.O. Diniz, H. Roussel, T. Tran, L.C. Ferreira, C. Badoual, E. Tartour, Mucosal vaccines: novel strategies and applications for the control of pathogens and tumors at mucosal sites, Hum Vaccin Immunother, 10 (2014) 2175-2187.
[5] A. Miquel-Clopes, E.G. Bentley, J.P. Stewart, S.R. Carding, Mucosal vaccines and technology, Clin Exp Immunol, 196 (2019) 205-214.
[6] M.N. Kweon, Sublingual mucosa: A new vaccination route for systemic and mucosal immunity, Cytokine, 54 (2011) 1-5.
[7] J. Holmgren, C. Czerkinsky, Mucosal immunity and vaccines, Nat Med, 11 (2005) S45-53.
[8] C. Hervouet, C. Luci, N. Cuburu, M. Cremel, S. Bekri, L. Vimeux, C. Maranon, C. Czerkinsky, A. Hosmalin, F. Anjuere, Sublingual immunization with an HIV subunit vaccine induces antibodies and cytotoxic T cells in the mouse female genital tract, Vaccine, 28 (2010) 5582-5590.
[9] H.X. Tan, A.K. Wheatley, R. Esterbauer, S. Jegaskanda, J.J. Glass, D. Masopust, R. De Rose, S.J. Kent, Induction of vaginal-resident HIV-specific CD8 T cells with mucosal prime-boost immunization, Mucosal Immunol, 11 (2018) 994-1007.
[10] A. Sato, A. Suwanto, M. Okabe, S. Sato, T. Nochi, T. Imai, N. Koyanagi, J. Kunisawa, Y. Kawaguchi, H. Kiyono, Vaginal memory T cells induced by intranasal vaccination are critical for protective T cell recruitment and prevention of genital HSV-2 disease, J Virol, 88 (2014) 13699-13708.

[11] Y. Fukuyama, K. Okada, M. Yamaguchi, H. Kiyono, K. Mori, Y. Yuki, Nasal Administration of Cholera Toxin as a Mucosal Adjuvant Damages the Olfactory System in Mice, PLoS One, 10 (2015) e0139368.
[12] D.I. Bernstein, M.F. Pasetti, R. Brady, A.D. Buskirk, R. Wahid, M. Dickey, M. Cohen, H. Baughman, J. El-Khorazaty, N. Maier, M.B. Sztein, S. Baqar, A.L. Bourgeois, A Phase 1 dose escalating study of double mutant heat-labile toxin LTR192G/L211A (dmLT) from Enterotoxigenic Escherichia coli (ETEC) by sublingual or oral immunization, Vaccine, 37 (2019) 602-611.
[13] C. Ramirez Sevilla, E. Gomez Lanza, J.L. Manzanera, J.A.R. Martin, M.A.B. Sanz, Active immunoprophyilaxis with uromune(R) decreases the recurrence of urinary tract infections at three and six months after treatment without relevant secondary effects, BMC Infect Dis, 19 (2019) 901.
[14] Z. Huo, S.L. Bissett, R. Giemza, S. Beddows, C. Oeser, D.J. Lewis, Systemic and mucosal immune responses to sublingual or intramuscular human papilloma virus antigens in healthy female volunteers, PLoS One, 7 (2012) e33736.
[15] J.R. Carmichael, S. Pal, D. Tifrea, L.M. de la Maza, Induction of protection against vaginal shedding and infertility by a recombinant Chlamydia vaccine, Vaccine, 29 (2011) 5276-5283.
[16] P. Ralli-Jain, D. Tifrea, C. Cheng, S. Pal, L.M. de la Maza, Enhancement of the protective efficacy of a Chlamydia trachomatis recombinant vaccine by combining systemic and mucosal routes for immunization, Vaccine, 28 (2010) 7659-7666.
[17] F. Anjuere, S. Bekri, F. Bihl, V.M. Braud, N. Cuburu, C. Czerkinsky, C. Hervouet, C. Luci, B cell and T cell immunity in the female genital tract: potential of distinct mucosal routes of vaccination and role of tissue-associated dendritic cells and natural killer cells, Clin Microbiol Infect, 18 Suppl 5 (2012) 117-122.
[18] C. Hervouet, C. Luci, S. Bekri, T. Juhel, F. Bihl, V.M. Braud, C. Czerkinsky, F. Anjuere, Antigen-bearing dendritic cells from the sublingual mucosa recirculate to distant systemic lymphoid organs to prime mucosal CD8 T cells, Mucosal Immunol, 7 (2014) 280-291.

[19] A.T. Jones, X. Shen, K.L. Walter, C.C. LaBranche, L.S. Wyatt, G.D. Tomaras, D.C. Montefiori, B. Moss, D.H. Barouch, J.D. Clements, P.A. Kozlowski, R. Varadarajan, R.R. Amara, HIV-1 vaccination by needle-free oral injection induces strong mucosal immunity and protects against SHIV challenge, Nat Commun, 10 (2019) 798.
[20] L. Garcia-del Rio, P. Diaz-Rodriguez, M. Landin, Design of novel orotransmucosal vaccine-delivery platforms using artificial intelligence, European Journal of Pharmaceutics and Biopharmaceutics, 159 (2021) 36-43.
[21] Y. Wu, Q. Li, G. Shim, Y.K. Oh, Melanin-loaded CpG DNA hydrogel for modulation of tumor immune microenvironment.
[22] J.A. White, J.S. Blum, N.A. Hosken, J.O. Marshak, L. Duncan, C. Zhu, E.B. Norton, J.D. Clements, D.M. Koelle, D. Chen, W.C. Weldon, M.S. Oberste, M. Lal, Serum and mucosal antibody responses to inactivated polio vaccine after sublingual immunization using a thermoresponsive gel delivery system, Hum Vaccin Immunother, 10 (2014) 3611-3621.
[23] E. Lorenzen, F. Follmann, S. Boje, K. Erneholm, A.W. Olsen, J.S. Agerholm, G. Jungersen, P. Andersen, Intramuscular Priming and Intranasal Boosting Induce Strong Genital Immunity Through Secretory IgA in Minipigs Infected with Chlamydia trachomatis, Front Immunol, 6 (2015) 628.
[24] S. Abraham, H.B. Juel, P. Bang, H.M. Cheeseman, R.B. Dohn, T. Cole, M.P. Kristiansen, K.S. Korsholm, D. Lewis, A.W. Olsen, L.R. McFarlane, S. Day, S. Knudsen, K. Moen, M. Ruhwald, I. Kromann, P. Andersen, R.J. Shattock, F. Follmann, Safety and immunogenicity of the chlamydia vaccine candidate CTH522 adjuvanted with CAF01 liposomes or aluminium hydroxide: a first-in-human, randomised, double-blind, placebo-controlled, phase 1 trial, The Lancet Infectious Diseases, 19 (2019) 1091-1100.
[25] J.C. Dejon-Agobe, U. Ateba-Ngoa, A. Lalremruata, A. Homoet, J. Engelhorn, O.P. Nouatin, J.R. Edoa, J.F. Fernandes, M. Esen, Y.D. Mouwenda, E.M. Betouke Ongwe, M. Massinga-Loembe, S.L. Hoffman, B.K.L. Sim, M. Theisen, P.G. Kremsner, A.A. Adegnika, B. Lell, B. Mordmuller, Controlled Human Malaria Infection of Healthy

Adults With Lifelong Malaria Exposure to Assess Safety, Immunogenicity, and Efficacy of the Asexual Blood Stage Malaria Vaccine Candidate GMZ2, Clin Infect Dis, 69 (2019) 1377-1384.
[26] V.R. Roman, K.J. Jensen, S.S. Jensen, C. Leo-Hansen, S. Jespersen, D. da Silva Te, C.M. Rodrigues, C.M. Janitzek, L. Vinner, T.L. Katzenstein, P. Andersen, I. Kromann, L.V. Andreasen, I. Karlsson, A. Fomsgaard, Therapeutic vaccination using cationic liposome-adjuvanted HIV type 1 peptides representing HLA-supertype-restricted subdominant T cell epitopes: safety, immunogenicity, and feasibility in Guinea-Bissau, AIDS Res Hum Retroviruses, 29 (2013) 1504-1512.
[27] J. Davidsen, I. Rosenkrands, D. Christensen, A. Vangala, D. Kirby, Y. Perrie, E.M. Agger, P. Andersen, Characterization of cationic liposomes based on dimethyldioctadecylammonium and synthetic cord factor from M. tuberculosis (trehalose 6,6'-dibehenate)-a novel adjuvant inducing both strong CMI and antibody responses, Biochim Biophys Acta, 1718 (2005) 22-31.
[28] D. Christensen, R. Mortensen, I. Rosenkrands, J. Dietrich, P. Andersen, Vaccine-induced Th17 cells are established as resident memory cells in the lung and promote local IgA responses, Mucosal Immunol, 10 (2017) 260-270.
[29] G.K. Pedersen, P. Andersen, D. Christensen, Immunocorrelates of CAF family adjuvants, Semin Immunol, 39 (2018) 4-13.
[30] F. Rose, K. Karlsen, P.R. Jensen, R.U. Jakobsen, G.K. Wood, K.D. Rand, H. Godiksen, P. Andersen, F. Follmann, C. Foged, Unusual Self-Assembly of the Recombinant Chlamydia trachomatis Major Outer Membrane Protein-Based Fusion Antigen CTH522 Into Protein Nanoparticles.
[31] L. Garcia-Del Rio, P. Diaz-Rodriguez, M. Landin, New tools to design smart thermosensitive hydrogels for protein rectal delivery in IBD, Mater Sci Eng C Mater Biol Appl, 106 (2020) 110252.
[32] L. Pindakova, V. Kasparkova, K. Kejlova, M. Dvorakova, D. Krsek, D. Jirova, L. Kasparova, Behaviour of silver nanoparticles in simulated saliva and gastrointestinal fluids, Int J Pharm, 527 (2017) 12-20.

[33] C.B. Roces, S. Khadke, D. Christensen, Y. Perrie, Scale-Independent Microfluidic Production of Cationic Liposomal Adjuvants and Development of Enhanced Lymphatic Targeting Strategies, Mol Pharm, 16 (2019) 4372-4386.
[34] A.W. Olsen, F. Follmann, K. Erneholm, I. Rosenkrands, P. Andersen, Protection Against Chlamydia trachomatis Infection and Upper Genital Tract Pathological Changes by Vaccine-Promoted Neutralizing Antibodies Directed to the VD4 of the Major Outer Membrane Protein, J Infect Dis, 212 (2015) 978-989.
[35] S. Murugappan, H.P. Patil, H.W. Frijlink, A. Huckriede, W.L. Hinrichs, Simplifying influenza vaccination during pandemics: sublingual priming and intramuscular boosting of immune responses with heterologous whole inactivated influenza vaccine, AAPS J, 16 (2014) 342-349.
[36] A. Borde, A. Ekman, J. Holmgren, A. Larsson, Effect of protein release rates from tablet formulations on the immune response after sublingual immunization, Eur J Pharm Sci, 47 (2012) 695-700.
[37] G.W. Canonica, P. Devillier, T. Casale, P. Demoly, C. Bos, E. Karagiannis, G. Passalacqua, U. Wahn, L. Mascarell, Clinical efficacy of sublingual immunotherapy tablets for allergic rhinitis is unlikely to be derived from in vitro allergen-release data, Expert Rev Clin Immunol, 15 (2019) 921-928.
[38] H.S. Hwang, S. Puth, W. Tan, V. Verma, K. Jeong, S.E. Lee, J.H. Rhee, More robust gut immune responses induced by combining intranasal and sublingual routes for prime-boost immunization, Hum Vaccin Immunother, 14 (2018) 2194-2202.
[39] A. Rossi, Z. Michelini, P. Leone, M. Borghi, M. Blasi, R. Bona, M. Spada, F. Grasso, A. Gugliotta, M.E. Klotman, A. Cara, D. Negri, Optimization of mucosal responses after intramuscular immunization with integrase defective lentiviral vector, PLoS One, 9 (2014) e107377.
[40] C. Czerkinsky, J. Holmgren, Mucosal delivery routes for optimal immunization: targeting immunity to the right tissues, Curr Top Microbiol Immunol, 354 (2012) 1-18.
[41] D. Christensen, Vaccine adjuvants: Why and how, Hum Vaccin Immunother, 12 (2016) 2709-2711.

[42] P.N. Boyaka, Inducing Mucosal IgA: A Challenge for Vaccine Adjuvants and Delivery Systems, J Immunol, 199 (2017) 9-16.
[43] A.D. Curtis, 2nd, K. Jensen, K.K.A. Van Rompay, R.R. Amara, P.A. Kozlowski, K. De Paris, A simultaneous oral and intramuscular prime/sublingual boost with a DNA/Modified Vaccinia Ankara viral vector-based vaccine induces simian immunodeficiency virus-specific systemic and mucosal immune responses in juvenile rhesus macaques, J Med Primatol, 47 (2018) 288-297.
[44] J.S. Woodworth, D. Christensen, J.P. Cassidy, E.M. Agger, R. Mortensen, P. Andersen, Mucosal boosting of H56:CAF01 immunization promotes lung-localized T cells and an accelerated pulmonary response to Mycobacterium tuberculosis infection without enhancing vaccine protection, Mucosal Immunol, 12 (2019) 816-826.
[45] A. Thakur, F.E. Pinto, H.S. Hansen, P. Andersen, D. Christensen, C. Janfelt, C. Foged, Intrapulmonary (i.pulmon.) Pull Immunization With the Tuberculosis Subunit Vaccine Candidate H56/CAF01 After Intramuscular (i.m.) Priming Elicits a Distinct Innate Myeloid Response and Activation of Antigen-Presenting Cells Than i.m. or i.pulmon. Prime Immunization Alone, Front Immunol, 11 (2020) 803.
[46] W. Domm, L. Brooks, H.L. Chung, C. Feng, W.J. Bowers, G. Watson, J.L. McGrath, S. Dewhurst, Robust antigen-specific humoral immune responses to sublingually delivered adenoviral vectors encoding HIV-1 Env: association with mucoadhesion and efficient penetration of the sublingual barrier, Vaccine, 29 (2011) 7080-7089.
[47] P. Moingeon, V. Lombardi, V. Baron-Bodo, L. Mascarell, Enhancing Allergen-Presentation Platforms for Sublingual Immunotherapy, J Allergy Clin Immunol Pract, 5 (2017) 23-31.
[48] D. Monti, S. Burgalassi, M.S. Rossato, B. Albertini, N. Passerini, L. Rodriguez, P. Chetoni, Poloxamer 407 microspheres for orotransmucosal drug delivery. Part II: In vitro/in vivo evaluation, Int J Pharm, 400 (2010) 32-36.
[49] A. Ripolin, J. Quinn, E. Larraneta, E.M. Vicente-Perez, J. Barry, R.F. Donnelly, Successful application of large microneedle patches by human volunteers, Int J Pharm, 521 (2017) 92-101.
[50] J. Ochoa, J.M. Irache, I. Tamayo, A. Walz, V.G. DelVecchio, C. Gamazo, Protective immunity of biodegradable nanoparticle-based

vaccine against an experimental challenge with Salmonella Enteritidis in mice, Vaccine, 25 (2007) 4410-4419.
[51] S. Gómez, C. Gamazo, B. San Roman, C. Vauthier, M. Ferrer, J.M. Irachel, Development of a novel vaccine delivery system based on Gantrez nanoparticles, J Nanosci Nanotechnol, 6 (2006) 3283-3289.
[52] J. Hansen, K.T. Jensen, F. Follmann, E.M. Agger, M. Theisen, P. Andersen, Liposome delivery of Chlamydia muridarum major outer membrane protein primes a Th1 response that protects against genital chlamydial infection in a mouse model, J Infect Dis, 198 (2008) 758-767.
[53] N. Nguyen, A.W. Olsen, E. Lorenzen, P. Andersen, M. Hvid, F. Follmann, J. Dietrich, Parenteral vaccination protects against transcervical infection with Chlamydia trachomatis and generate tissue-resident T cells post-challenge, NPJ Vaccines, 5 (2020) 7.
[54] R. Verma, R. Sahu, S. Dixit, S.A. Duncan, G.H. Giambartolomei, S.R. Singh, V.A. Dennis, The Chlamydia M278 Major Outer Membrane Peptide Encapsulated in the Poly(lactic acid)-Poly(ethylene glycol) Nanoparticulate Self-Adjuvanting Delivery System Protects Mice Against a Chlamydia muridarum Genital Tract Challenge by Stimulating Robust Systemic and Local Mucosal Immune Responses, Front Immunol, 9 (2018) 2369.
[55] L. Kari, W.M. Whitmire, D.D. Crane, N. Reveneau, J.H. Carlson, M.M. Goheen, E.M. Peterson, S. Pal, L.M. de la Maza, H.D. Caldwell, Chlamydia trachomatis native major outer membrane protein induces partial protection in nonhuman primates: implication for a trachoma transmission-blocking vaccine, J Immunol, 182 (2009) 8063-8070.
[56] D.C. Gondek, N.R. Roan, M.N. Starnbach, T cell responses in the absence of IFN-gamma exacerbate uterine infection with Chlamydia trachomatis, J Immunol, 183 (2009) 1313-1319.
[57] C.P. O'Meara, C.W. Armitage, M.C. Harvie, D.W. Andrew, P. Timms, N.Y. Lycke, K.W. Beagley, Immunity against a Chlamydia infection and disease may be determined by a balance of IL-17 signaling, Immunol Cell Biol, 92 (2014) 287-297.

[58] Y. Li, C. Wang, Z. Sun, J. Xiao, X. Yan, Y. Chen, J. Yu, Y. Wu, Simultaneous Intramuscular And Intranasal Administration Of Chitosan Nanoparticles-Adjuvanted Chlamydia Vaccine Elicits Elevated Protective Responses In The Lung, Int J Nanomedicine, 14 (2019) 8179-8193.
[59] J. Masek, D. Lubasova, R. Lukac, P. Turanek-Knotigova, P. Kulich, J. Plockova, E. Maskova, L. Prochazka, S. Koudelka, N. Sasithorn, J. Gombos, E. Bartheldyova, F. Hubatka, M. Raska, A.D. Miller, J. Turanek, Multi-layered nanofibrous mucoadhesive films for buccal and sublingual administration of drug-delivery and vaccination nanoparticles - important step towards effective mucosal vaccines, J Control Release, 249 (2017) 183-195.
[60] T. Kaser, J.A. Pasternak, M. Delgado-Ortega, G. Hamonic, K. Lai, J. Erickson, S. Walker, J.R. Dillon, V. Gerdts, F. Meurens, Chlamydia suis and Chlamydia trachomatis induce multifunctional CD4 T cells in pigs, Vaccine, 35 (2017) 91-100.

USC UNIVERSIDADE DE SANTIAGO DE COMPOSTELA

5. CHAPTER III: NEW TOOLS TO DESIGN SMART THERMOSENSITIVE HYDROGELS FOR PROTEIN RECTAL DELIVERY IN IBD

*The results from this chapter and its corresponding annex, have already been published as L. Garcia-Del Rio[1], P. Diaz-Rodriguez[2], M. Landin[1], New tools to design smart thermosensitive hydrogels for protein rectal delivery in IBD, Mater Sci Eng C Mater Biol Appl, 106 (2020) 110252.
ISSN: 0928-4931; E-ISSN: 1873-3441.

[1]R+D Pharma Group (GI-1645), Department of Pharmacology, Pharmacy and Pharmaceutical Technology, Facultad de Farmacia, Universidade de Santiago de Compostela-Campus Vida, 15782, Santiago de Compostela, Spain.
[2]Departament of Chemical Engineering and Pharmaceutical Technology, Facultad de Ciencias de la Salud, Universidad de La Laguna (ULL), Campus de Anchieta, 38200, La Laguna, Spain.

USC
UNIVERSIDADE
DE SANTIAGO
DE COMPOSTELA

ABSTRACT

Local treatment of Inflammatory Bowel Disease (IBD) has been pointed out to be a novel therapeutic approach with several advantages when compared to conventional therapies. However, the development of systems able to fulfil the requirements of this administration route is not an easy task. The present work suggests the utilization of Artificial Intelligence Techniques (AIT) as an instrument to understand polymer-polymer interactions towards obtaining thermosensitive hydrogels suitable for protein rectal administration in IBD. Enemas composed by Pluronic® F127 and F68 and Methocel® K4M were developed and characterized. Two experimental designs were carried out in order to determine the effect of each polymer on their texturometric and rheological behaviour. Using the results of the first experimental design we can justify the inclusion of each raw material PF127, PF68 and MK4M in the formulation and conclude that a compromise solution is necessary to obtain thermosensitive hydrogels of the required properties. The results of the second experimental design allowed concluding that PF127 ruled mainly syringeability and bioadhesion work. On the other hand, PF68 modulated principally gelation temperature, viscosity and protein release from hydrogel matrix. Finally, MK4M influenced bioadhesiveness and mostly determined viscosity. AIT also allowed delimiting the design space to produce easy administrable and highly bioadhesive enemas that undergo fast sol-gel transitions at body temperature.

USC
UNIVERSIDADE
DE SANTIAGO
DE COMPOSTELA

5.1. INTRODUCTION

Inflammatory Bowel Disease (IBD) is the general term enclosing a group of inflammatory disorders involving the gastrointestinal tract (GIT) [1]. They are systemic, complex, multifactorial and chronic pathologies characterized by periods of relapsing and remitting inflammation. They are usually accompanied with stomach and abdominal pain, diarrhoea, cramping, bloody stool together with a decrease in the mucus layer thickness and spreading conditioned by the inflammation grade [2-4].

While the aetiology of IBD has not been elucidated yet [5, 6], the main goal of the current treatments is focused on restoring the enteric mucosa homeostasis. Despite significant advances in IBD medical management, several problems remain to be solved as side effects or failure in controlling the inflammatory process [5, 7, 8]. New therapeutic strategies for IBD management are constantly being proposed, such as novel anti-inflammatory molecules, bacteriophages, cell therapy or its derivatives [6, 8-11]. Different attempts have been carried out to target ulcerated and eroded intestinal mucosa, for example nanoparticulated systems [3, 12, 13], hydrogels [4, 14-16] and tablets [7, 17]. As an example, local injections of anti-TNF-α agents, such as infliximab and adalimumab, have been administered in perianal fistulas and/or intestinal lesions of patients with Crohn's Disease, which has allowed, although not in all patients, to increase their therapeutic effect and minimise their adverse reactions [18, 19]. The design of colon-targeted dosage forms administered by oral or rectal route has been pointed out to be a good strategy for mucosa restoration. Enemas produce better therapeutic responses and earlier patient's recovery than oral treatments due to the local effect of the drug, which also improves IBD patients compliance [14, 16, 20].

The combination of polymers in a hydrogel system that simultaneously confer thermosensitivity, mucoadhesion and load capacity of active molecules ensuring biocompatibility, implies the difficulty associated with the design of multicomponent formulations. Therefore, it is essential to understand and control how the interaction between components occurs.

Artificial Intelligence Techniques (AIT) such as Artificial Neural Networks (ANN), fuzzy logic and genetic algorithms are techniques able to model the ingredients and operation conditions effect on the pharmaceutical systems characteristics [26]. Nano and microparticulated systems [27, 28] and hydrogels [29, 30] have been already successfully modelled and optimized using AIT, giving drug delivery platforms with desirable properties.

On this basis, the objective of this work is to demonstrate the utility of AIT to help in the establishment of the design space of ternary hydrogel formulations with appropriate characteristics for the treatment of IBD ulcers. Polymers will be combined to give the systems thermosensitivity and mucoadhesion capacity, which should facilitate their administration, extensibility on the mucosa and retention in the rectal tract. The colonic delivery of drugs from those systems will be simulated using a model protein.

5.2. MATERIALS AND METHODS

5.2.1. Materials

Pluronic® F127 (PF127), Pluronic® F68 (PF68), Bovine Serum Albumin (BSA) and saline buffer pH 7.4 were purchased from Sigma-Aldrich (MO, USA). Methocel® K4M (MK4M) was obtained from The Dow Chemical Company (Michigan, USA). Cell Strainers of 40 µm pore size were purchased from Corning Incorporated (Durham, USA). Pierce™ BCA Protein Assay Kit was bought from ThermoScientific (Rockford, USA).

5.2.2. Experimental designs

A reduced experimental design for 3 components (PF127, PF68 and MK4M) with a minimum pattern of 3, was generated using a Balance Density Method through DataForm® v.3.1 software (Intelligensys Ltd., UK). As a result, 9 compositions were designed, combining different proportions of three polymers (**Table 1**). In this first experimental design, the pre-established concentration range was wide in order to create the knowledge space.

Table 1. Composition of the formulations of the experimental design 1. Percentages (w/w) of Pluronic® F127 (PF127), Pluronic® F68 (PF68) and Methocel® K4M (MK4M) obtained by DataForm®software using the Balance Density Method. Data included as inputs to train the Artificial Neural Network for experimental design 1.

Sample	Composition (%)		
	PF127	PF68	MK4M
H1	10.4	9.5	0.5
H2	17.9	1.9	1
H3	14.7	5.2	0.5
H4	2.9	17	0.5
H5	19	1	0
H6	14.1	5.7	1
H7	11.4	8.5	0.5
H8	19.8	0	1
H9	4.8	15.2	0

Afterwards, a second experimental design with narrower concentration ranges of the three components (**Table 2**) was carried out in order to better model the effects of polymer composition on the formulation characteristics and establish the design space of enema formulations with adequate gelation temperature and rheological properties. As a result, 11 hydrogels were designed and prepared.

Table 2. Composition of the formulations of the experimental design 2. Percentages (w/w) of Pluronic® F127 (PF127), Pluronic® F68 (PF68) and Methocel® K4M (MK4M) obtained by DataForm® software using the Balance Density Method. Data included as inputs to train the Artificial Neural Network for experimental design 2.

Sample	Composition (%)		
	PF127	PF68	MK4M
H10	17	5	0.25
H11	15	0	0.5
H12	19	2.5	0
H13	15	2.5	0.25
H14	17	0	0.5
H15	19	5	0
H16	19	5	0.25
H17	17	2.5	0.5
H18	15	0	0
H19	17	2.5	0
H20	18.8	2.3	0.1

5.2.3. Hydrogel preparation

PF127 (%w/w) and PF68 (%w/w) were dissolved at the desired concentrations in saline buffer at 4 °C overnight. Then, MK4M (%w/w) was incorporated to these solutions, previously cooled in an ice bath, and dissolved under magnetic stirring until clear and homogeneous solutions were obtained. Hydrogels were stored at 4 °C until characterization.

5.2.4. Texturometric analysis

Syringeability and bioadhesion studies were performed using a TA XT Plus Texture Analyzer (Surrey, UK), as previously published by Blanco-Fuente et al. [31] and Campaña-Seoane et al. [32] with slight modifications. Syringeability was computed as the work (mJ) required for expelling the hydrogel loaded into a syringe through a needle at room temperature. For this purpose, each hydrogel was

carefully loaded into 1 mL syringes avoiding air bubbles formation. Syringes were then placed vertically on a support, leaving a distance between the syringe plunger and the texturometer punch. The punch descended at 2 mm/s and pressed the plunger of the syringe through a distance of 2 cm. All measurements were made by quadruplicate.

Bioadhesion at 37 °C was evaluated using goat tanned leather. Firstly, two goat tanned leather pieces were fixed to the punch and the lower support of the texturometer. Then, formulations were placed on the tanned leather of the lower support and the punch descended at 1 mm/s, applying a force of 0.5 N during 60 s over the samples. After that, the punch rose, and the force exerted was represented versus the distance. The area under the curve (mJ) corresponded to the bioadhesiveness work of the hydrogel. All measurements were repeated at least four times.

5.2.5. Rheological assessment

The gelation temperature (T_{gel}) and viscosity of the prepared hydrogels were evaluated using a rheometer AR1000-N (TA Instruments, UK). Storage (G') and loss (G") moduli were recorded employing a conical geometry of 6 cm Ø and 2.1 degrees, establishing a temperature ramp from 20 to 40 °C at 0.3 °C/min and angular frequency of 5 rad/s. The crossover of both moduli when subjected to variable temperatures allowed establishing the T_{gel} (ºC) of each hydrogel while complex viscosity values (Pa.s) were measured at 20 °C.

5.2.6. Protein loading and in vitro release studies

Protein release studies were performed on the formulations of the second experimental design using simulated colonic fluid (SCoF) described by Marques et al. [33]. BSA was chosen as model protein to assess the release rate of the developed hydrogels. Firstly, BSA (3%w/v) was added to each hydrogel. Then the protein was dissolved under magnetic stirring and hydrogels were storage overnight at 4 ºC. The release assay was carried out in an orbital shaker Tritamax 1000 (Heidolph Instruments, Germany) at 400 rpm and 37 ºC. The release media, 8 mL of SCoF, was placed in a 6-well plate, containing Corning® Cell Strainers of 40 µm of pore size and placed on the

orbital shaker at 37 ºC. Secondly, 1.5 mL of BSA loaded hydrogels were placed into the strainer chamber. At selected time points, 5, 10, 15, 60, 90 and 120 minutes, 1 mL of SCoF was removed and replaced with fresh media. Samples collected at each time point were frozen until protein quantification. Pierce™ BCA Protein Assay was performed for the measurement of released BSA according to the manufacturer's protocol. Absorbance was assessed using a FLUOstar OPTIMA plate reader (BMG Labtech, Germany) and the amount of released protein were obtained by using validated calibration curves, as well as, adequate controls.

5.2.7. Data modelization using Artificial Neural Networks

FormRules® v4.03 (Intelligensys Ltd., UK) was used for modelling experimental results of formulations for both experimental designs. FormRules® v4.03 is a hybrid AIT that combines ANN and fuzzy logic technologies, being able to predict the influence of each formulation ingredient on the evaluated parameters and express the models using simple "IF-THEN" rules. PF127, PF68 and MK4M concentration in the formulations were established as inputs while the systems properties (syringeability, bioadhesion at 37 ºC, T_{gel} and complex viscosity) were introduced as outputs. "IF-THEN" rules were used to understand how outputs were affected by inputs [28]. **Figure 1** shows a general overview of the whole process, since the experimental design obtaining to ANN analysis.

The default training parameters of the software were used for modelling. The software contains various statistical fitness criteria. Among them, Structural Risk Minimisation (SRM) was used to model all outputs (C1 range = 0.82-0.62 and C2 = 4.8). The predictability and accuracy of models generated were assessed. Coefficient of determination (R^2) was used as indicative of predictability and it was calculated as follows [28]:

$$R^2 = \left[1 - \frac{\sum_{i=1}^{n}(y_i - y_i^*)^2}{\sum_{i=1}^{n}(y_i - y_i^{**})^2}\right] \times 100$$

Where, y_i represents the experimental value of the output in the data set, y_i^* is the predicted value of the output computed by the model

and finally, y_i^{**} is the mean value of the parameter that is being evaluated. R^2 higher than 70% are indicative of good model predictabilities [30], so high correlation between experimental and predicted outputs.

The accuracy of the models was established by comparison of experimental and calculated results through an ANOVA; a calculated f value higher than f critical values for the corresponding degrees of freedom, indicates that there are not statistical differences between experimental and predicted outputs [34].

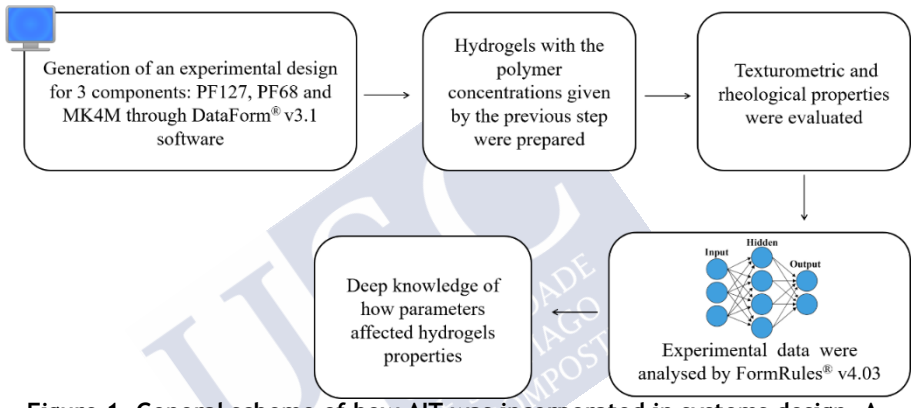

Figure 1. General scheme of how AIT was incorporated in systems design. A reduce experimental design was obtained through DataForm® v3.01 software. Thus, hydrogels of different composition were made in cold saline buffer and their texturometric and rheological properties were tested. Generated experimental database were analysed employing FormRules® v4.03 to determine the effect of each polymer on their texturometric and rheological behaviour generating the knowledge or design space. This process allowed to know deeply how parameters affected hydrogel properties.

5.3. RESULTS

5.3.1. Knowledge space analysis

The aim of the preliminary study performed in experimental design 1 was to establish the knowledge space of the formulations, elucidating the suitability of the selected polymers for the required application and analyzing their influence on syringeability, bioadhesion, gelation temperature (T_{gel}) and complex viscosity. Experimental results are shown in **Table 3**. These parameters are

critical for obtaining hydrogels of easy administration and high bioadhesion. **Table 4** shows the characteristics of the models generated by FormRules® v4.03 for each property. All models present $R^2 \geq 73\%$ values, indicating their good predictability. However, only syringeability, bioadhesion and viscosity models showed computed f values higher than critical f values, being statistically significant. There was a lack of data in the T_{gel} results as a significant number of formulations did not gel within the limits of the assay, reducing the number of degrees of freedom of the model.

In general terms, the most significant information gained from this first experimental design could be summarized as follows:

1) Syringeability is mainly determined by PF68 concentration (**Table 4**). The addition of PF68 reduces the work required for the administration of the hydrogel. Consequently, enemas having percentages above 8.5% of PF68 would present lower syringeability work values than 73.10 mJ (**Annex II, Table A2.1**).

2) Bioadhesion is mainly determined by the concentration of PF68 in the polymeric mixture. However, the concentration of MK4M also influences on this property (**Table 4**). According to the "IF-THEN" rules (**Annex II, Table A2.1**), the highest bioadhesion values could be obtained using medium concentrations of PF68 (1.9% - 10.5%) and MK4M (0.25% - 0.75%).

3) Viscosity at 20 °C is modulated by PF127 concentration (**Table 4**). Thermosensitive hydrogels with low viscosity values would be achieved using proportions of PF127 between 4.95% and 14.85%.

4) Despite T_{gel} was not accurately modelled, **Table 4** shows is modulated by the percentage of PF127. Percentages around 15% of PF127 and below of 8.5% of PF68 would be required in order to obtain enemas able to gel under 37 °C if medium proportions of MK4M are used. Thus, for obtaining enemas of adequate T_{gel} it would be necessary to achieve a compromise between the amounts of both Pluronic® in the polymeric blends.

Altogether, we could conclude that combinations of PF127, PF68 and MK4M can be useful to design thermosensitive hydrogels for rectal administration modulating bioadhesiveness, syringeability, viscosity and sol-gel transition of the formulations.

Table 3. Means and standard deviations values in milliJoules (mJ) for syringeability and bioadhesion work, as well as T_{gel} (°C) and viscosity (Pa.s) from hydrogels obtained in the experimental design 1. Data used as outputs to train the artificial neural network for the experimental design 1.

Sample	Syringeability (mJ)	Bioadhesion work (mJ)	Complex viscosity at 20 °C (Pa.s)	T_{gel} (°C)
H1	62.92 ± 0.97	0.488 ± 0.19	0.06 ± 0.00	38.05 ± 0.53
H2	184.3 ± 5.81	0.228 ± 0.14	Gelled	<20
H3	97.45 ± 3.15	0.610 ± 0.28	0.10 ± 0.02	29.52 ± 0.85
H4	63.12 ± 3.64	0.198 ± 0.12	0.08 ± 0.00	>40
H5	163.1 ± 7.80	0.327 ± 0.06	0.67 ± 0.54	20.63 ± 0.40
H6	121.9 ± 10.0	0.401 ± 0.13	0.28 ± 0.07	28.78 ± 0.81
H7	73.10 ± 3.92	0.540 ± 0.08	0.07 ± 0.03	35.23 ± 2.37
H8	251.5 ± 28.1	0.126 ± 0.04	Gelled	<20
H9	44.50 ± 1.34	0.103 ± 0.04	0.02 ± 0.00	>40

Table 4. Inputs selected by FormRules® to explain the variability of the outputs for experimental design 1 and parameters to assess the quality of the generated models. The submodels with highest effect on the output are highlighted.

Outputs	Submodel	Inputs from FormRules®	R^2	Computed f value	Degrees of freedom	f critical for p<0.1
Syringeability	**1**	**PF68**	73.92	8.50	2 and 6	3.46
Bioadhesion work	**1** 2	**PF68** MK4M	98.43	37.62	5 and 3	5.31
Viscosity	**1**	**PF127**	85.87	6.07	3 and 3	5.39
T_{gel}	**1**	**PF127**	75.63	0	4 and 0	-

5.3.2. Design space analysis

On this basis, to properly define the design space for suitable formulations, a second experimental design (**Table 2**) was carried out. The limits of the variables were established considering: a) the minimum percentage of PF127 necessary for getting hydrogels with sol-gel transition temperatures lower than the body temperature and b) the concentration range of PF68 and MK4M for obtaining hydrogels with good bioadhesiveness.

Results for the experimental design 2 are represented in **Table 5**. FormRules® v4.03 allowed to determine the effect of each component on the evaluated parameters for the new database and express the results as "IF…THEN" rules (**Annex II, Tables A2.2**). **Table 6** shows the main ingredients that ruled each property and the parameters that indicate the quality of the models. All models present good predictability ($R^2 \geq 71\%$).

Table 5. Results of texturometric and rheological assays from hydrogels obtained in the experimental design 2. Data used as outputs to train the artificial neural network for the experimental design 2.

Sample	Syringeability (mJ)	Bioadhesion work (mJ)	Complex Viscosity at 20 °C (Pa.s)	T_{gel} (°C)
H10	187.5 ± 20.9	0.367 ± 0.05	0.10 ± 0.02	27.49 ± 1.18
H11	105.1 ± 15.7	0.287 ± 0.05	0.73 ± 0.92	22.41 ± 2.40
H12	237.2 ± 24.8	0.408 ± 0.15	0.18 ± 0.05	22.53 ± 1.53
H13	103.7 ± 9.01	0.296 ± 0.05	0.05 ± 0.01	27.99 ± 0.58
H14	166.6 ± 18.3	0.406 ± 0.06	0.51 ± 0.57	21.35 ± 1.20
H15	262.8 ± 5.63	0.469 ± 0.08	0.15 ± 0.01	24.89 ± 0.63
H16	NOT SYRINGEABLE	0.425 ± 0.06	0.58 ± 0.47	22.25 ± 2.47
H17	208.6 ± 9.96	0.362 ± 0.12	0.17 ± 0.06	23.53 ± 1.31
H18	86.50 ± 5.97	0.254 ± 0.05	0.03 ± 0.00	23.66 ± 0.39
H19	156.8 ± 6.41	0.328 ± 0.08	0.08 ± 0.00	25.47 ± 0.46
H20	260.9 ± 9.38	0.493 ± 0.11	0.18 ± 0.03	22.71 ± 0.35

Table 6. Significant inputs from FormRules® models for the diverse outputs performed and parameters to evaluate the quality of submodels obtained for experimental design 2. The most important submodels are highlighted.

Output	Submodel	Inputs from FormRules®	R^2	Computed f value	Degrees of freedom	f critical for p<0.1
Syringeability	**1**	**PF127**	93.80	52.93	2 and 7	4.74
Bioadhesion work	**1** 2	**PF127** MK4M	86.59	15.06	3 and 7	4.34
Viscosity	**1**	**PF68xMK4M**	71.04	3.68	4 and 6	4.53
T_{gel}	**1** 2	**PF68** PF127	72.67	6.20	3 and 6	4.76

5.3.2.1. PF127 determines syringeability

Within the limits of experimental design 2, syringeability is mainly conditioned by the concentration of PF127 (**Table 6**). **Figure 2A** represents the effect of PF127 and MK4M on this property. Thus, low syringeability values would be obtained employing PF127 percentages below 18% (blue area). Thereby, enemas H18 (15/0/0), H13 (15/2.5/0.25) and H11 (15/0/0.5) with mean syringeability values of 86.50 ± 5.97, 103.7 ± 9.01 and 105.1 ± 15.7 mJ respectively, were the most syringeable formulations. Moreover, it is interesting to hallmark that for sample H16, having a 19% of PF127 and a 0.25% of MK4M, syringeability was impossible to be measured owing to the inability of the hydrogel to pass through the needle.

5.3.2.2. PF127 and MK4M rule bioadhesiveness

Bioadhesion work variations are explained by two submodels, including PF127 as the main variable together with MK4M (**Table 6**). Both polymers have positive effects on bioadhesion work values (blue area of **Figure 2B**). In accordance to the model, samples H20 (0.493 ± 0.11 mJ), H15 (0.469 ± 0.08 mJ) and H16 (0.425 ± 0.06 mJ) were the highest bioadhesive hydrogels. Their composition were 18.80/2.30/0.1, 19/5/0 and 19/5/0.25, respectively.

5.3.2.3. PF127 and MK4M determine viscosity

The experimental values for viscosity are indicated on **Table 5**. As shown in **Table 6**, FormRules® v4.03 was able to define the interactive effect of PF127 and MK4M on viscosity, even though, the model obtained was not statistically significant (computed f value < critical f value). The analysis of the "IF…THEN" rules indicates that the highest viscous hydrogels are those including high proportion of MK4M and low proportion of PF127. According to these rules, experimental results show that the highest viscous hydrogel was H11 which has the following proportions of PF127/PF68/MK4M: 15/0/0.5. On the contrary, H18 (15/0/0), H13 (15/2.50/0.25) and H19 (17/2.50/0), formulations with low proportions of MK4M were the most fluid hydrogels having mean viscosity values of 0.03 ± 0.00, 0.05 ± 0.01 and 0.08 ± 0.00 Pa.s, respectively.

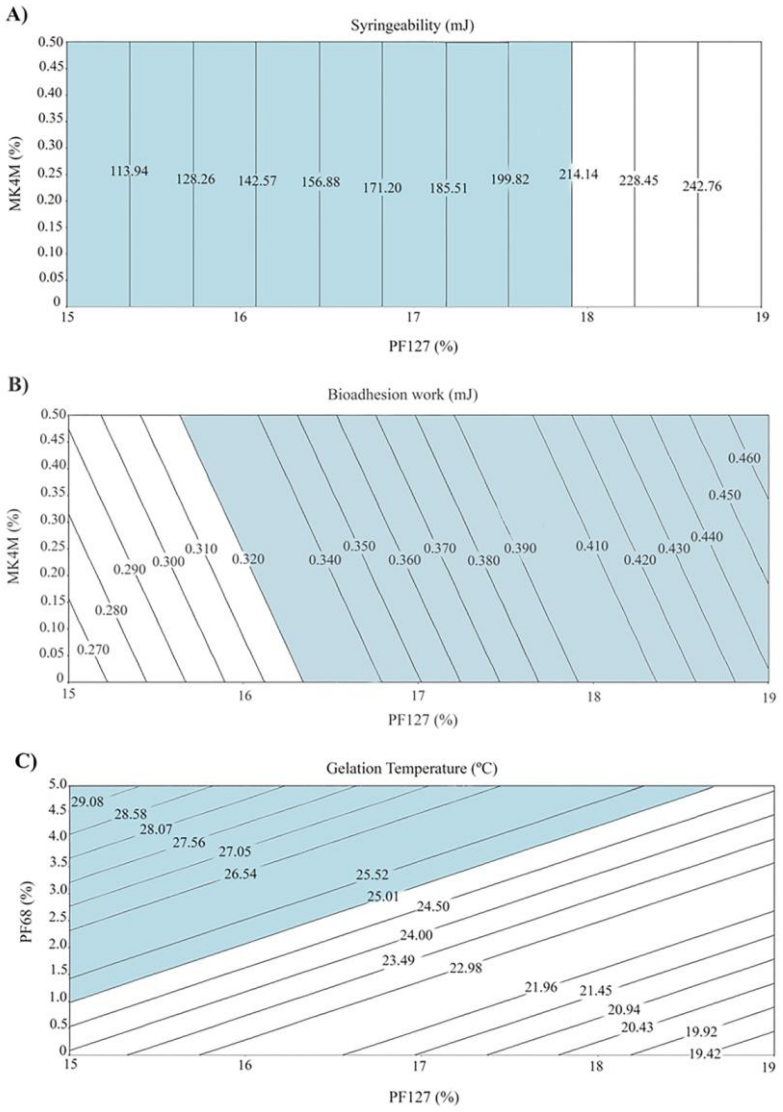

Figure 2. 2D plots generated by FormRules® showing the relation between inputs and outputs for experimental design 2. A) Low syringeability values would be obtained employing proportions of PF127 below 17.25% (blue area). B) The hydrogels made with high percentages of PF127 (>17.75%) and MK4M (>0.25%), would present the highest values of bioadhesion work (blue area). C) Hydrogels made with high or low concentrations of PF68 (>2.25%) and PF127 (<17%) respectively, would exhibit low T_{gel} values (blue area).

5.3.2.4. PF68 rules mainly the T_{gel}

Experimental data results are displayed in **Table 5**. T_{gel} was mainly modulated by PF68 (**Table 6**). However, PF127 also had an influence on this parameter. As it is shown in **Figure 2C** hydrogels with low T_{gel} would be accomplished employing low proportions of PF68 (<1%) or high amounts of PF127 (>16%), whereas, enemas with high sol-gel transition values (blue area) could be reached using percentages of PF68 higher than 1% and low quantities of PF127 (<18%). **Figure 3** shows the thermosensitivity properties of hydrogels. In order to show it, equal volumes of the same hydrogel were heated up 37 °C and compared with the same one stored at 4 °C.

Figure 3. Example of a thermosensitivity hydrogel, presenting sol-gel transition when was heated up 37 ˚C. It was compared with the same hydrogel stored at 4˚C.

5.3.2.5. *In vitro* protein release studies

Protein release assays were also performed for formulations of experimental design 2. As BSA (3%w/v) was completely dissolved in the hydrogels matrix, the loading efficiency of hydrogels was 100%. **Figure 4** shows several examples of the formulations release profiles. All of them show immediate release profile in SCoF (>80% protein released at 10 minutes). In the case of H11, the release profile is higher than 100% and then slowed down due to the own variability of the technique.

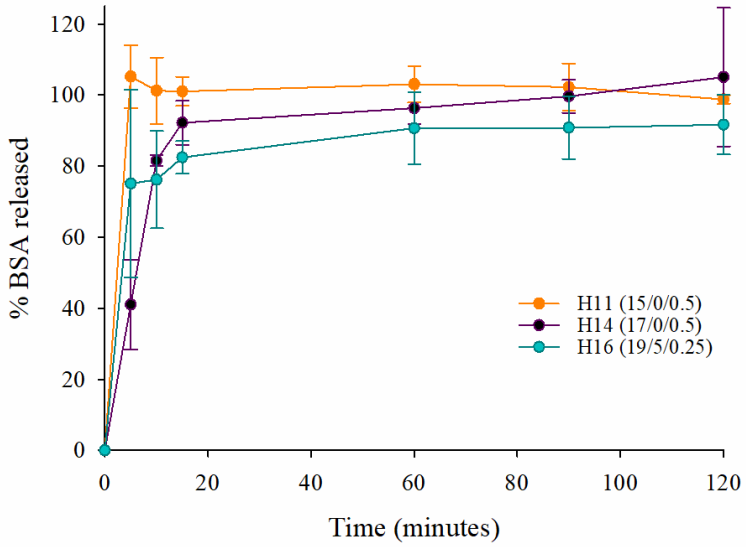

Figure 4. Release profile of formulations H11, H14 and H16 in medium SCoF that were carried out in an orbital shaker at 400 rpm and 37 °C.

5.4. DISCUSSION

The main goal of the current work is to achieve suitable enemas for potential colonic delivery of immunomodulatory proteins, useful for mucosa restoration in the treatment of IBD patients. To this end, we propose the use of liquid systems for rectal administration, capable of gelling at body temperature with good mucoadhesive capacity that facilitates their retention on the mucosa. The administration of therapeutic agents in such systems should allow local treatment of the mucosa, with reduced doses and diminished side effects. The selected polymers for this study are GRAS substances proved and recognized by the FDA for topical use [35-37]. Pluronic®, also known as poloxamers, are amphiphilic, thermosensitive and bioadhesive triblock copolymers. They share the general chemical structure shown in **Figure 5A**. PF127 and PF68 are widely used in the pharmaceutical field owing to their low toxicity, high solubilisation capacity and release modulation [38-40]. PF127 allows an easy elaboration of *in situ* gelation hydrogels without using organic solvents. This property

makes PF127 a versatile polymer adequate for preparation of oral, inhaled, intravenous, topical and ophthalmic formulations. PF68, among other characteristics, is usually used to modulate the gelation temperature of PF127 [38, 41]. Hydroxypropylcellulose, which chemical formula is represented in **Figure 5B**, is a polysaccharide able to generate robust hydrogels capable to resist gastrointestinal peristaltic movements and control drug release [36, 39]. MK4M is a variety with high grade viscosity, which can be used as viscosity enhancer also providing good mucoadhesive strength [42, 43].

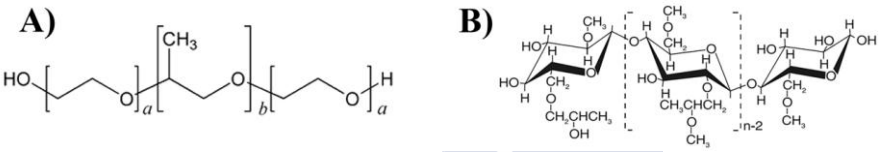

Figure 5. Chemical formulas of selected polymers obtained from manufacturer's datasheet. A) General structure of Pluronic® polymers which differ in their chain lengths, wherein a=101 and *b*=56 for PF127 and a=80 and *b*=27 for PF68 B) General chemical formula of hydroxypropyl methylcellulose.

AIT succeeded in generating models useful for understanding the experimental data obtained during the development of thermosensitive enemas. Firstly, neurofuzzy logic software allowed to establish a knowledge space and justify the use of all the selected formulation ingredients [26]. As a result of the first experimental design analysis, it was also possible to establish the concentration range for each material. In order to achieve high bioadhesive hydrogels, mid proportions of PF68 and MK4M must be used. Moreover, the minimum percentage of PF127 necessary to obtain systems that gel at body temperature is 15%. Additionally, percentages of PF68 in the formulation upper than 8.5% could also compromise gelation of hydrogels at body temperature.

The analysis of the second experimental design by FormRules® allowed a deeply awareness of the composition effect on the hydrogel characteristics. The incorporation of PF127 at concentrations equal or above 15% to guarantee the gelation turned this polymer into the main factor that governs the ternary systems properties. The textural and rheological properties are modulated by the percentage of PF127 in the formulation (**Table 6**), and are determined by the micelle

formation and/or its disruption due to the presence of PF68 or MK4M in the hydrogel.

The micellization process of Pluronic®, and therefore its gelation, depends mainly on the length of the hydrophobic chain (PPO). PF68 exhibits higher T_{gel} than PF127 due to its shorter PPO chain [44]. Their combination in binary systems allows tailoring the gelation temperature [41, 45, 46]. The T_{gel} model (**Table 6**), points out the interaction between both Pluronic®, indicating that PF68 interfere on the micellization process of PF127. Gelation phenomenon is driven first by the dehydration of PPO block, and after by the rearrangement of formed micelles depending on the interaction between hydroxyl groups [79]. The presence of PF68 disturbs the micelle entanglement and hydrogen bonds formation of PF127, leading to an increase in the T_{gel}. [46].

Appropriate syringeability (<200 mJ) at room temperature is the second requirement for this type of dosage forms. Important variations in syringeability can be observed within the limits of the experimental design 2 (**Table 5**), mainly determined by the percentage of PF127 in the formulation (**Table 6**). Syringeability is closely related to T_{gel} and viscosity, formulations that gel at very low temperatures or have high viscosity are unable to be administered in the conditions of the study (*e.g*. H16).

The binding of the formulation to the biological substrate is the third aspect to be considered. Poloxamers and MK4M are materials that modulate bioadhesion. It has been described that PF68 exhibits more mucoadhesion capacity than PF127 due to its higher PEO/PPO ratio (3.47 *vs* 2.93) [38]. The bioadhesive character of the PEO component relies on its capacity for binding to mucin oligosaccharide chains, showing good applicability for the development of oral or intranasal formulations [47-49]. The addition of MK4M also provides bioadhesiveness since, firstly, is capable of establishing electrostatic interactions with mucus glycoproteins [48], and secondly, improves the mechanical properties of the designed systems [42, 43] which has been related to mucoadhesion [39, 50, 51]. Some authors have described the use of poloxamers together with cellulose derivatives gives a synergistic effect on the bioadhesion of the formulations [39,

51, 52]. Although our models show both types of polymers have a positive outcome on bioadhesion, we did not observe a synergistic effect.

However, our model shows an interactive effect between PF127 and MK4M on viscosity. High proportions of MK4M act as viscosity enhancer when PF127 is up to 17% [45, 53]. Above this ratio, the effect of MK4M is damped. This could be explained by the increase of PF127 in polymeric blends that leads to more rigid and entangled hydrogel networks [45, 54, 55].

In order to evaluate how the composition affects therapeutic agent release from the ternary systems, a model protein, BSA, was incorporated into the hydrogel networks and its release evaluated. All formulations have shown immediate release profiles. Neither PF127 nor MK4M, which are excipients used for controlled release, promoted the long-term retention of the protein during the release studies, reaching over 80% after 10 min. The incorporation of PF68 is determinant to explain this phenomenon. Bouchemal et al. [52] have recently pointed out that the combination of PF68 and PF127 do not promote the formation of mixed micelles, which leads to segregation of both polymers. They have demonstrated that when comparing hydrogels composed by percentages of 22.5/2.5/1 and 20/0/1 of PF127/P188/MK4M respectively, drug release was faster for the hydrogel containing PF68, despite being more viscous. Our results agree with those findings, the immediate release effect seeing in our hydrogels could be due to a more disorganized hydrogel network promoted by the addition of PF68.

In the case of the bioadhesive thermosensitive rectal systems under study, the immediate disposition of the loaded protein is not an inconvenience, but rather a benefit, a rapid supply of the therapeutic molecules in the damaged colonic tissue favours the onset of action of the drug, as well as its local absorption [52]. Furthermore, the incorporation of peptides or proteins on the hydrogel network should increase their stability in the colon lumen when compared to the free forms previously studied for IBD management [18, 19].

5.5. CONCLUSIONS

AIT succeeded in modelling most of the hydrogels properties as a function of its composition using a reduced database from balance density experimental designs. Enemas composed by PF127, PF68 and MK4M were prepared, and the effect of composition in the final formulations properties was investigated. Two experimental designs were performed and analyzed using ANN in order to acquire a deep knowledge of how composition determines the texturometric and rheological characteristics of the different hydrogels evaluated. ANN enabled the obtaining of a design space in order to achieve smart thermosensitive enemas suitable for protein delivery (Blue areas in **Figure 1**). This design space should allow the attainment of optimized hydrogels of easy administration which present a fast transition from liquid to solid state once at body temperature. Thereby, as was previously reported in literature, the possible leakage and dilution of the drug delivery system into the colon lumen would be minimized. These smart formulations also would exhibit good bioadhesiveness to living tissues and a rapid drug release, in order to promote an immediate effect over the intestinal damaged mucosa.

REFERENCES

[1] Q. Zhang, H. Tao, Y. Lin, Y. Hu, H. An, D. Zhang, S. Feng, H. Hu, R. Wang, X. Li, J. Zhang, A superoxide dismutase/catalase mimetic nanomedicine for targeted therapy of inflammatory bowel disease, Biomaterials, 105 (2016) 206-221.

[2] R. Awasthi, M. Kumar, Development of Metronidazole-Loaded Colon-Targeted Microparticulate Drug Delivery System, Polymers in Medicine, 45 (2015) 57-65.

[3] C. Corbo, W.E. Cromer, R. Molinaro, N.E. Toledano Furman, K.A. Hartman, E. De Rosa, C. Boada, X. Wang, D.C. Zawieja, M. Agostini, F. Salvatore, B.P. Abraham, E. Tasciotti, Engineered biomimetic nanovesicles show intrinsic anti-inflammatory properties for the treatment of inflammatory bowel diseases, Nanoscale, 9 (2017) 14581-14591.

[4] J. Zhou, M. O'Keeffe, G. Liao, F. Zhao, C. Terhorst, B. Xu, Design and Synthesis of Nanofibers of Self-assembled de novo Glycoconjugates towards Mucosal Lining Restoration and Anti-Inflammatory Drug Delivery, Tetrahedron, 72 (2016) 6078-6083.

[5] G. Rogler, L. Biedermann, M. Scharl, New insights into the pathophysiology of inflammatory bowel disease: microbiota, epigenetics and common signalling pathways, Swiss Med Wkly, 148 (2018) w14599.

[6] M. Galtier, L. De Sordi, A. Sivignon, A. de Vallee, D. Maura, C. Neut, O. Rahmouni, K. Wannerberger, A. Darfeuille-Michaud, P. Desreumaux, N. Barnich, L. Debarbieux, Bacteriophages Targeting Adherent Invasive Escherichia coli Strains as a Promising New Treatment for Crohn's Disease, J Crohns Colitis, 11 (2017) 840-847.

[7] A.M. Newton, P. Lakshmanan, Effect of HPMC - E15 LV premium polymer on release profile and compression characteristics of chitosan/ pectin colon targeted mesalamine matrix tablets and in vitro study on effect of pH impact on the drug release profile, Recent Pat Drug Deliv Formul, 8 (2014) 46-62.

[8] I. Catalan-Serra, O. Brenna, Immunotherapy in inflammatory bowel disease: Novel and emerging treatments, Hum Vaccin Immunother, (2018) 1-15.

[9] P. Martinez-Montiel Mdel, G.J. Gomez-Gomez, A.I. Flores, Therapy with stem cells in inflammatory bowel disease, World J Gastroenterol, 20 (2014) 1211-1227.
[10] S. Pouya, M. Heidari, K. Baghaei, H. Asadzadeh Aghdaei, A. Moradi, S. Namaki, M.R. Zali, S.M. Hashemi, Study the effects of mesenchymal stem cell conditioned medium injection in mouse model of acute colitis, Int Immunopharmacol, 54 (2018) 86-94.
[11] B. Verstockt, M. Ferrante, S. Vermeire, G. Van Assche, New treatment options for inflammatory bowel diseases, J Gastroenterol, 53 (2018) 585-590.
[12] M. Naeem, J. Bae, M.A. Oshi, M.S. Kim, H.R. Moon, B.L. Lee, E. Im, Y. Jung, J.W. Yoo, Colon-targeted delivery of cyclosporine A using dual-functional Eudragit((R)) FS30D/PLGA nanoparticles ameliorates murine experimental colitis, Int J Nanomedicine, 13 (2018) 1225-1240.
[13] B. Xiao, Q. Chen, Z. Zhang, L. Wang, Y. Kang, T. Denning, D. Merlin, TNFalpha gene silencing mediated by orally targeted nanoparticles combined with interleukin-22 for synergistic combination therapy of ulcerative colitis, J Control Release, 287 (2018) 235-246.
[14] S.K. Ramadass, S. Perumal, S.L. Jabaris, B. Madhan, Preparation and evaluation of mesalamine collagen in situ rectal gel: a novel therapeutic approach for treating ulcerative colitis, Eur J Pharm Sci, 48 (2013) 104-110.
[15] Y. Yuan, Y. Cui, L. Zhang, H.P. Zhu, Y.S. Guo, B. Zhong, X. Hu, L. Zhang, X.H. Wang, L. Chen, Thermosensitive and mucoadhesive in situ gel based on poloxamer as new carrier for rectal administration of nimesulide, Int J Pharm, 430 (2012) 114-119.
[16] Y.C. You, L.Y. Dong, K. Dong, W. Xu, Y. Yan, L. Zhang, K. Wang, F.J. Xing, In vitro and in vivo application of pH-sensitive colon-targeting polysaccharide hydrogel used for ulcerative colitis therapy, Carbohydr Polym, 130 (2015) 243-253.
[17] A.K. De, P. Bhattacharya, S. Datta, A. Mukherjee, Evaluation of in vivo efficacy and toxicity of prednisolone-loaded hydrogel-based drug delivery device, Int J Pharm Investig, 3 (2013) 225-233.

[18] L. Biancone, M. Cretella, C. Tosti, G. Palmieri, C. Petruzziello, A. Geremia, E. Calabrese, F. Pallone, Local injection of infliximab in the postoperative recurrence of Crohn's disease, Gastrointest Endosc, 63 (2006) 486-492.
[19] F. Tonelli, F. Giudici, C.R. Asteria, Effectiveness and safety of local adalimumab injection in patients with fistulizing perianal Crohn's disease: a pilot study, Dis Colon Rectum, 55 (2012) 870-875.
[20] A.C. Santos Akkari, E.V. Ramos Campos, A.F. Keppler, L.F. Fraceto, E. de Paula, G.R. Tofoli, D.R. de Araujo, Budesonide-hydroxypropyl-beta-cyclodextrin inclusion complex in binary poloxamer 407/403 system for ulcerative colitis treatment: A physico-chemical study from micelles to hydrogels, Colloids Surf B Biointerfaces, 138 (2016) 138-147.
[21] J. Chen, R. Zhou, L. Li, B. Li, X. Zhang, J. Su, Mechanical, rheological and release behaviors of a poloxamer 407/ poloxamer 188/carbopol 940 thermosensitive composite hydrogel, Molecules, 18 (2013) 12415-12425.
[22] H. Laroui, E. Viennois, B. Xiao, B.S. Canup, D. Geem, T.L. Denning, D. Merlin, Fab'-bearing siRNA TNFalpha-loaded nanoparticles targeted to colonic macrophages offer an effective therapy for experimental colitis, J Control Release, 186 (2014) 41-53.
[23] R. Waters, S. Pacelli, R. Maloney, I. Medhi, R.P. Ahmed, A. Paul, Stem cell secretome-rich nanoclay hydrogel: a dual action therapy for cardiovascular regeneration, Nanoscale, 8 (2016) 7371-7376.
[24] K.O. Allbright, J.M. Bliley, E. Havis, D.Y. Kim, G.A. Dibernardo, D. Grybowski, M. Waldner, I.B. James, W.N. Sivak, J.P. Rubin, K.G. Marra, Delivery of adipose-derived stem cells in poloxamer hydrogel improves peripheral nerve regeneration, Muscle Nerve, 58 (2018) 251-260.
[25] J. Xu, M. Tam, S. Samaei, S. Lerouge, J. Barralet, M.M. Stevenson, M. Cerruti, Mucoadhesive chitosan hydrogels as rectal drug delivery vessels to treat ulcerative colitis, Acta Biomater, 48 (2017) 247-257.
[26] M. Landín, Introducción al uso de sistemas de inteligencia artificial para modelizar, comprender y optimizar formulaciones

farmacéuticas, in: Biomateriais aplicados ao desenvolvimento de sistemas terapêuticos avançados, 2015, pp. 521-554.
[27] M.O. Jara, J. Catalan-Figueroa, M. Landin, J.O. Morales, Finding key nanoprecipitation variables for achieving uniform polymeric nanoparticles using neurofuzzy logic technology, Drug Deliv Transl Res, (2017).
[28] R. Rodriguez-Dorado, M. Landin, A. Altai, P. Russo, R.P. Aquino, P. Del Gaudio, A novel method for the production of core-shell microparticles by inverse gelation optimized with artificial intelligent tools, Int J Pharm, 538 (2018) 97-104.
[29] R. Lopez-Cebral, V. Romero-Caamano, B. Seijo, C. Alvarez-Lorenzo, M. Martin-Pastor, A. Concheiro, M. Landin, A. Sanchez, Spermidine cross-linked hydrogels as a controlled release biomimetic approach for cloxacillin, Mol Pharm, 11 (2014) 2358-2371.
[30] P. Diaz-Rodriguez, M. Landin, Smart design of intratumoral thermosensitive beta-lapachone hydrogels by Artificial Neural Networks, Int J Pharm, 433 (2012) 112-118.
[31] H. Blanco-Fuente, S. Anguiano-Igea, F.J. Otero-Espinar, J. Blanco-Méndez, In-vitro bioadhesion of carbopol hydrogels, International Journal of Pharmaceutics, 142 (1996) 169-174.
[32] M. Campana-Seoane, A. Peleteiro, R. Laguna, F.J. Otero-Espinar, Bioadhesive emulsions for control release of progesterone resistant to vaginal fluids clearance, Int J Pharm, 477 (2014) 495-505.
[33] M.R.C. Marques, R. Loebenberg, M. Almukainzi, Simulated biological fluids with possible application in dissolution testing, Dissolution Technologies, 18 (2011) 15-28.
[34] H. Rouco, P. Diaz-Rodriguez, S. Rama-Molinos, C. Remunan-Lopez, M. Landin, Delimiting the knowledge space and the design space of nanostructured lipid carriers through Artificial Intelligence tools, Int J Pharm, 553 (2018) 522-530.
[35] A. Pitto-Barry, N.P.E. Barry, Pluronic® block-copolymers in medicine: from chemical and biological versatility to rationalisation and clinical advances, Polymer Chemistry, 5 (2014) 3291-3297.
[36] B. Wu, N. Shun, X. Wei, W. Wu, Characterization of 5-fluorouracil release from hydroxypropylmethylcellulose compression-coated tablets, Pharm Dev Technol, 12 (2007) 203-210.

[37] M. Ghimire, L.A. Hodges, J. Band, B. O'Mahony, F.J. McInnes, A.B. Mullen, H.N. Stevens, In-vitro and in-vivo erosion profiles of hydroxypropylmethylcellulose (HPMC) matrix tablets, J Control Release, 147 (2010) 70-75.
[38] X. Chen, F. Zhi, X. Jia, X. Zhang, R. Ambardekar, Z. Meng, A.R. Paradkar, Y. Hu, Y. Yang, Enhanced brain targeting of curcumin by intranasal administration of a thermosensitive poloxamer hydrogel, J Pharm Pharmacol, 65 (2013) 807-816.
[39] G. Dumortier, J.L. Grossiord, F. Agnely, J.C. Chaumeil, A review of poloxamer 407 pharmaceutical and pharmacological characteristics, Pharm Res, 23 (2006) 2709-2728.
[40] A. Fakhari, M. Corcoran, A. Schwarz, Thermogelling properties of purified poloxamer 407, Heliyon, 3 (2017) e00390.
[41] X. Xu, Y. Shen, W. Wang, C. Sun, C. Li, Y. Xiong, J. Tu, Preparation and in vitro characterization of thermosensitive and mucoadhesive hydrogels for nasal delivery of phenylephrine hydrochloride, Eur J Pharm Biopharm, 88 (2014) 998-1004.
[42] B.K. Nanjwade, R.V. Deshmukh, K.R. Gaikwad, K.A. Parikh, F.V. Manvi, Formulation and evaluation of micro hydrogel of Moxifloxacin hydrochloride, Eur J Drug Metab Pharmacokinet, 37 (2012) 117-123.
[43] K. Kumar, N. Dhawan, H. Sharma, S. Vaidya, B. Vaidya, Bioadhesive polymers: novel tool for drug delivery, Artif Cells Nanomed Biotechnol, 42 (2014) 274-283.
[44] E. Giuliano, D. Paolino, M. Fresta, D. Cosco, Mucosal Applications of Poloxamer 407-Based Hydrogels: An Overview, Pharmaceutics, 10 (2018).
[45] M. Mansour, S. Mansour, N.D. Mortada, S.S. Abd Elhady, Ocular poloxamer-based ciprofloxacin hydrochloride in situ forming gels, Drug Dev Ind Pharm, 34 (2008) 744-752.
[46] N. Zeng, G. Dumortier, M. Maury, N. Mignet, V. Boudy, Influence of additives on a thermosensitive hydrogel for buccal delivery of salbutamol: relation between micellization, gelation, mechanic and release properties, Int J Pharm, 467 (2014) 70-83.

[47] Y. Li, P.I. Lee, A new bioerodible system for sustained local drug delivery based on hydrolytically activated in situ macromolecular association, Int J Pharm, 383 (2010) 45-52.
[48] N. Salamat-Miller, M. Chittchang, T.P. Johnston, The use of mucoadhesive polymers in buccal drug delivery, Adv Drug Deliv Rev, 57 (2005) 1666-1691.
[49] J.S. Park, Y.K. Oh, H. Yoon, J.M. Kim, C.K. Kim, In situ gelling and mucoadhesive polymer vehicles for controlled intranasal delivery of plasmid DNA, J Biomed Mater Res, 59 (2002) 144-151.
[50] M.A. Marzouk, D.A. Osman, A.I. Abd El-Fattah, Formulation and in vitro evaluation of a thermoreversible mucoadhesive nasal gel of itopride hydrochloride, Drug Dev Ind Pharm, 44 (2018) 1857-1867.
[51] M. Rao, D.K. Agrawal, C. Shirsath, Thermoreversible mucoadhesive in situ nasal gel for treatment of Parkinson's disease, Drug Dev Ind Pharm, 43 (2017) 142-150.
[52] K. Bouchemal, A. Aka-Any-Grah, N. Dereuddre-Bosquet, L. Martin, V. Lievin-Le-Moal, R. Le Grand, V. Nicolas, D. Gibellini, D. Lembo, C. Pous, A. Koffi, G. Ponchel, Thermosensitive and mucoadhesive pluronic-hydroxypropylmethylcellulose hydrogel containing the mini-CD4 M48U1 is a promising efficient barrier against HIV diffusion through macaque cervicovaginal mucus, Antimicrob Agents Chemother, 59 (2015) 2215-2222.
[53] K. Zhang, X. Shi, X. Lin, C. Yao, L. Shen, Y. Feng, Poloxamer-based in situ hydrogels for controlled delivery of hydrophilic macromolecules after intramuscular injection in rats, Drug Deliv, 22 (2015) 375-382.
[54] M.A.F. Z, A. Vangala, M. Longman, K.A. Khaled, A.K. Hussein, O.H. El-Garhy, R.G. Alany, Poloxamer-based thermoresponsive ketorolac tromethamine in situ gel preparations: Design, characterisation, toxicity and transcorneal permeation studies, Eur J Pharm Biopharm, 114 (2017) 119-134.
[55] N. Morsi, D. Ghorab, H. Refai, H. Teba, Ketoroloac tromethamine loaded nanodispersion incorporated into thermosensitive in situ gel for prolonged ocular delivery, Int J Pharm, 506 (2016) 57-67.

USC
UNIVERSIDADE
DE SANTIAGO
DE COMPOSTELA

6. CHAPTER IV: TAILORED HYDROGELS AS DELIVERY PLATFORMS FOR CONDITIONED MEDIUM FROM MESENCHYMAL STEM CELLS IN A MOUSE MODEL OF ACUTE COLITIS

USC UNIVERSIDADE DE SANTIAGO DE COMPOSTELA

USC
UNIVERSIDADE
DE SANTIAGO
DE COMPOSTELA

ABSTRACT

Inflammatory bowel disease (IBD), including Crohn's disease (CD) and ulcerative colitis (UC), is increasingly prevalent and current therapies are not completely effective. Mesenchymal stem cells are emerging as a promising therapeutic option. Here, we evaluate the effect of local hydrogel application loaded with conditioned medium (CM) from human uterine cervical stem cells (hUCESC-CM) in an experimental mouse model of acute colitis. Colitis induction was carried out in C57BL/6 mice by dissolving dextran sulfate sodium (DSS) in drinking water for 9 days. Ulcers were treated by rectal administration of either mesalazine (as positive control) or a mucoadhesive and thermosensitive hydrogel loaded with hUCESC-CM (H-hUCESC-CM). Body weight changes, colon length, and histopathological analysis were evaluated. In addition, pro-inflammatory TNF-α, IL-6, and IFN-γ mRNA levels were measured by qPCR. Treatment with H-hUCESC-CM inhibited body weight loss and colon shortening and induced a significant decrease in colon mucosa degeneration as well as TNF-α, IFN-γ and IL-6 mRNA levels. Our data indicate that H-hUCESC-CM effectively alleviated DSS-induced colitis in mice, suggesting that H-hUCESC-CM may represent an attractive cell-free therapy for local treatment of IBD.

USC
UNIVERSIDADE
DE SANTIAGO
DE COMPOSTELA

6.1. INTRODUCTION

Inflammatory bowel disease (IBD) represents a group of pathogenic, chronic, and degenerative disorders defined by recurrent inflammation of the gastrointestinal tract. The two major forms are ulcerative colitis (UC) and Crohn's disease (CD). It is estimated that as many as 1.4 million Americans and 2.4 million Europeans are suffering from this disease [1]. In addition, the incidence and prevalence of IBD have increased dramatically over the last few decades, growing as a public health concern since they can lead to life-threatening problems [2,3]. IBD is multifactorial and its aetiology is not precisely known. IBD involves an abnormal systemic and mucosal immune response against intraluminal antigens, favoured by microbial factors and alterations of the mucosal barrier, in genetically predisposed individuals [4,5].

The current treatment for IBD begins with 5-aminosalicylic acids (5-ASA) and antibiotics, followed by corticosteroids, immunomodulators and biologic agents. When all else fails, patients undergo surgery [6]. However, current therapies are often not completely effective and may have side effects related to the gastrointestinal tract and liver. Therefore, there is great interest in the development of more effective drugs for IBD treatment [7].

Mesenchymal stem cells (MSCs) are fibroblast-like and multipotent progenitors that can be isolated from the connective tissue of most organs [8]. MSCs express defined surface markers, including CD90, CD73, and CD105, and present immunoregulatory and regenerative properties. MSCs are considered a promising medical alternative for the treatment of various inflammatory and autoimmune diseases. They have shown to target injured tissue, secrete paracrine anti-inflammatory factors, and induce inhibition of T-cell proliferation, B-cell function, and dendritic cell maturation, via secretion of soluble factors [9]. Therefore, stem cell therapies have emerged as novel therapeutic tools for IBD patients who respond poorly to conventional anti-inflammatory treatments [10]. Several studies have demonstrated that MSCs from different origin ameliorate certain parameters such as body weight, bleeding, stool consistence, mortality rate, colon length, inflammation-associated histological changes, and inflammatory cytokine expression in experimental colitis

[11]. Furthermore, products derived from MSCs such as conditioned medium (CM), MSCs extracts and exosomes have also been tested [12,13,14]. Clinical trials suggest that local application of MSCs is a safe and beneficial therapeutic approach for the healing of perianal fistulas in CD patients [15,16]. Therefore, MSCs may represent a promising therapy for IBD. Nevertheless, many questions concerning the optimal origin and source of MSCs, dosage and routes of administration remain unresolved.

A new population of MSCs has been isolated and characterized, called human uterine cervical stem cells (hUCESCs), which are obtained from the transition zone of the uterine cervix of healthy women through Pap cervical smears. hUCESCs present a high rate of proliferation in culture, with a doubling index of 1.76 in 24 hours. It has also been found that conditioned medium from hUCESCs (hUCESC-CM) displayed a potent antitumor effect against breast and cervical cancer cells, and also against stromal cells by inhibiting proliferation and invasion of cancer-associated fibroblasts (CAFs) and, inhibiting and reverting monocyte to macrophage differentiation [17]. Recent studies also demonstrated the beneficial effects of hUCESC-CM on corneal wound healing and ocular inflammation in rat and rabbit models as well as its anti-microbial properties [18-21].

In the present study involving a DSS-induced colitis mice model, it is evaluated whether an optimized mucoadhesive hydrogel applied locally as a hUCESC-CM delivery platform could morphologically repair the damaged tissue in the colonic area by increasing hUCESC-CM residence time and controlling its release.

6.2. MATERIALS AND METHODS

6.2.1. Materials

Pluronic® F127 (PF127) and F68 (PF68), Foetal Bovine Serum (FBS), Dulbecco's Modified Eagle Medium: Nutrient Mixture F-12 (DMEM-F12) and phosphate buffered saline (PBS) were acquired from Sigma-Aldrich (San Luis, USA). Methocel® K4M (MK4M) was purchased from Dow (Des Moines, USA). Round tip 24Gx1.5" and 26-gauge needles were obtained from PetSurgical (Phoenix, USA). Dextran sulfate sodium (DSS) was acquired from MP Biomedicals

(Illkirch, France). Mesalazine (Claversal foam, 1g) was provided by FAES FARMA (Madrid, Spain).

6.2.2. Hydrogel development and preparation

A mucoadhesive and thermosensitive hydrogel suitable for rectal administration was developed and optimized using INForm® v.5.01 software (Intelligensys, Ltd. UK) that combines Artificial Neural Networks (ANN) and genetic algorithms (GA). PF127, PF68 and MK4M were selected as formulation components based on their thermosensitive and bioadhesive properties [22]. A Balance Density Experimental Design (DataForm® v3.1, Intelligensys, Ltd, UK) was established to analyze the influence of each ingredient on several parameters (syringeability, bioadhesion and gelation temperature (T_{gel}). After ANN modelization, the composition of a hydrogel with adequate syringeability (< 86 mJ), bioadhesion higher than 0.254 mJ, and T_{gel} in the range of 25-27 °C was obtained. The composition selected as optimal hydrogel formulation by the ANN model and GA includes 16.34% of PF127, 2.55% of PF68 and 0.26% of MK4M.

The optimized hydrogel was prepared by dissolving accurate amounts of PF127 and PF68 in cold dissolution media at 4 °C overnight. Then, MK4M (%w/w) was added to this solution after prior cooling in an ice bath and dissolved under magnetic stirring until a homogeneous and clear solution was obtained. Hydrogel sterilization was carried out by autoclaving (Trade Raypa® steam sterilizer AES-12, Barcelona, Spain). Sterile hydrogels were stored at 4 °C until use. Three dissolution media were selected to perform the current study: double distilled water (ddH_2O), cell culture media (DMEM-F12), and phosphate buffered saline (PBS).

Hydrogels prepared with PBS (H-PBS) were used to validate the ANN model. Hydrogels prepared in cell culture media (H-DMEM-F12) were used as controls. Lyophilized hUCESC-CM was resuspended in the optimized hydrogel prepared with ddH_2O to obtain the hUCESC-CM loaded hydrogel (H-hUCESC-CM).

6.2.3. Hydrogel Characterization

6.2.3.1. Texturometric analysis

Syringeability and bioadhesion were evaluated using a TA XT Plus Texture Analyzer (Surrey, UK), following a protocol previously reported [22]. Syringeability at room temperature was measured by computing the work (mJ) required to expel the hydrogel loaded into a 1 ml syringe through a needle of 24Gx1.5". Briefly, syringes were loaded with the optimized hydrogel avoiding air bubble formation. Afterwards, syringes were placed vertically on a support and the punch of the texturometer descended at 2 mm/s, pressing the piston of the syringe a distance of 2 cm. All measurements were carried out six times.

Bioadhesion at 37°C was analyzed by placing 75 µl of each formulation on goat tanned leather, previously fixed in the lower support of the texturometer. Then, the texturometer punch also covered with leather descended at 1 mm/s and exerted a force of 0.5 N during 60 s over the sample. The area under the curve of the force-distance plot generated represented the bioadhesiveness (mJ) of the hydrogel. All measurements were carried out six times.

6.2.3.2. Rheological analysis

A rheometer AR1000-N (TA Instruments, UK) was used to determine the gelation temperature (T_{gel}) and the hydrogel stability at 37 °C. The T_{gel} was calculated as the crossover of the storage (G') and loss (G") moduli of the formulation, using a conical geometry of 6 cm Ø and 2.1° at a fixed angular frequency of 5 rad/s and establishing a temperature ramp from 20 to 40°C at 0.3°C/min. To evaluate the stability of the hydrogel at body temperature, the G' and G" values were recorded at 37 °C at variable angular frequencies from 0.5 to 50 rad/s.

6.2.3.3. Stability assessments

The effect of storage on the texturometric and rheological parameters of the optimized hydrogel was re-evaluated at 2 weeks and one month at 4 °C.

6.2.4. Cell Cultures and hUCESC-CM preparation

Culture of hUCESC was carried out as previously described [17]. Briefly, cells were cultured in 90 mm Petri dishes at 70% confluence in 5 ml of DMEM-F12 culture medium supplemented with FBS (10%) at 37 °C for 48 h in air-CO_2 (95:5) atmosphere. Cells were washed three times in PBS and cultured again in 5 ml of DMEM-F12 without FBS. After 48h, the medium was centrifuged for 5 min at 300 g to remove cellular debris, supernatant was collected, and used either immediately or lyophilized (SP Scientific, 25L Genesis 5 Q EL-85, Gardiner, USA) and stored at -80 °C until used.

6.2.5. Hydrogel loading with hUCESC-CM

Lyophilized hUCESC-CM (from 5 ml culture) and lyophilized DMEM-F12 medium (as control) were resuspended in 5 ml of the optimized hydrogel prepared in ddH_2O at room temperature to obtain the hUCESC-CM-loaded hydrogel (H-hUCESC-CM) and the control hydrogel (H-DMEM-F12).

6.2.6. *In vivo* assay

6.2.6.1. Ethics statement

This study adhered to national regulations and was approved by the regional Ethics and Investigation Committee (Comité Ético de Investigación Clínica Regional del Principado de Asturias). Cervical smears were obtained from patients who underwent a routine gynecological check-up at Fundación Hospital de Jove, Asturias, Spain. All patients provided informed written consent. All animal studies were approved by the Universidade de Santiago de Compostela Ethics Committee for Animal Experiments.

6.2.6.2. Mice

Eight-week-old male C57BL/6 mice were purchased from the Central Animal Facility, Universidade de Santiago de Compostela (Santiago de Compostela, Spain). Mice were housed 3 weeks before the experiment for adaptation and to acquire local bacterial flora before the experiment. Access to adequate water and food for mice was provided, and all the tests were carried out according to the

approval of the Universidade de Santiago de Compostela Ethics Committee for Animal Experiments.

6.2.6.3. Colitis induction and experimental groups

In vivo experiments were performed for 16 days according to Wirz et al. [23] (**Figure 1**). Acute colitis was induced in C57BL/6 mice by administration of 3.5% dextran sulphate sodium (DSS) in drinking water for 9 days. Treatments were performed between days 10 and 15 by rectal administration of 75 µl twice a day. Before rectal administration, mice were anesthetized by inhalation of isoflurane (2.5% for induction and 1-2% for maintenance) using a calibrated vaporizer. Rectal administration was given with a 26-gauge probe needle with rounded tip inserted about 2 cm. Formulation was injected slowly, using the gel itself as a lubricating agent to impregnate the cannula so as not to cause damage in the intestinal wall and keeping the mouse immobile for a couple of minutes to ensure the immediate retention of the treatment.

Animals were divided into 5 groups of 6 mice per group, as follows: a) Healthy control group (H); b) No-treatment group (NT): mice without treatment after DSS administration; c) H-DMEM-F12 control group: mice treated with H-DMEM-F12 after DSS administration; d) H-hUCESC-CM group: mice treated with H-hUCESC-CM after DSS administration; and e) mesalazine group (MZ): mice treated with mesalazine foam after DSS administration.

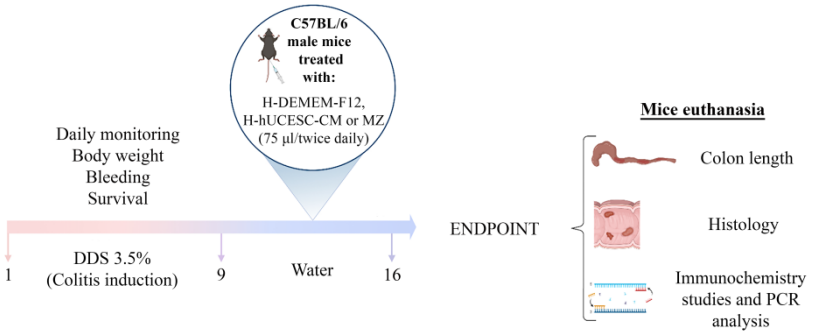

Figure 1. Study design for DSS-induced colitis. Acute colitis was induced in C57BL/6 mice by administering 3.5% dextran sulphate sodium (DSS) in drinking water for 9 days. Between 10 and 15 days, 75 µl of each treatment was rectally administered twice daily using a 26-gauge probe needle. On day 16 animals

were sacrificed. NT: non-treated, H-DMEM-F-12: DMEM-F12-loaded hydrogel; H-hUCESC-CM: H-hUCESC-CM-loaded hydrogel; MZ: mesalazine.

6.2.6.4. Clinical symptoms evaluation and colon macroscopic examination

Clinical signs of colitis, including survival, body weight, stool consistency and bleeding severity were recorded. At the endpoint of the experiment, the intestine was removed, and the colon was separated from the small intestine. Colon length, including cecum, was measured.

6.2.6.5. Histological evaluation

Tissue sampling for histological analysis were performed by cutting three colonic fragments (0.5 cm each) with respect to cecum: proximal colon, mid colon, and distal colon. A piece (0.2-0.4 mm) from each fragment was fixed in 10% formalin and embedded in paraffin, and 5 μm thick paraffin tissue sections were cut, deparaffinized, rehydrated and stained with hematoxylin and eosin (H&E) to be graded for intestinal epithelial changes by a blinded expert pathologist (LOG). Based on a previously published score [23], the following parameters were evaluated: degree of inflammation and cell infiltration (0, none; 1, slight; 2, moderate; 3, severe), microscopic ulcerations (0, none; 1, focal; 2, extensive), crypt architecture (0, normal; 3, severe crypt distortion with loss of entire crypts), epithelial atrophy (0, none; 1, slight; 2, moderate; 3, severe), and epithelial dysplasia (0, none; 1, low grade; 2, high). Histological damage score is the sum of each individual score. It should be noted that unlike human UC, crypt abscesses are not characteristic of this model and are rarely seen.

6.2.6.6. RNA Extraction and Quantitative Real Time PCR

Tumor necrosis factor-alpha (TNF-α), Interleukin 6 (IL-6), interferon-gamma (IFN-γ), and 18S (as control) mRNA expression levels were evaluated by real-time PCR. RNA extraction was performed using tissue from the most proximal zone. cDNA synthesis was carried out from 1.5 μ*g* of RNA. Samples were denatured at 94 °C for 10 s, annealed at 58 °C for 10 s and extended at 72 °C for 10 s for a total 35 cycles. PCR products formed in each cycle were evaluated

based on SYBR Green fluorescence with 18S as endogenous control. Primers sequences are shown in **Table 1**.

Table 1. Primer sequences designed to evaluate TNF-α, IFN-γ, IL-6 and 18S (as control) mRNA by RT-PCR.

Gene	Forward	Reverse
TNF-α	aggctgccccgactacgt	gactttctcctggtatgagatagcaaa
IFN-γ	cagcaacagcaaggcgaaa	ctggacctgtgggttgttgac
IL-6	acaagtcggaggcttaattacacat	ttgccattgcacaactctttt
18S	cccctcgatgactttagctgagtgt	cgccggtccaagaatttcacctct

6.2.7. Statistical analysis

In all experiments, mean ± standard error of the mean (SEM) was calculated. Experiments were performed at least in triplicate. One-way ANOVA followed by Tukey's and LSD post-hoc tests were used for multiple comparison. PASW 18.0 and GraphPad Prism software were used for all calculations. Level of significance was $p<0.05$.

6.3. RESULTS

6.3.1. Hydrogel preparation and characterization

Modelling of the experimental design results by ANN and the GA allowed us to determine the composition of an optimized hydrogel using PBS as dissolution medium. The liquid texture of this hydrogel at room temperature facilitates its application and extension on the rectal mucosa. In addition, its thermosensitive and bioadhesive properties favour gelation at body temperature and retention on the ulcerated epithelium. Thus, the model predicted an optimized formulation composed of 16.34% of PF127, 2.55% of PF68 and 0.26% of MK4M in PBS. Both, predicted and experimental data agree and are shown in **Table 2**. Despite the increase in values for syringeability, rectal administration is still possible using the 26-gauge probe needle.

Table 2. Texturometric and rheological values predicted by the ANN model and experimental values obtained after hydrogel characterization. Data are presented as mean ± SEM.

Parameter	Predicted by ANN	H-PBS
Syringeability (mJ)	141.92	170 ± 0.95
Bioadhesion work (mJ)	0.33	0.31 ± 0.02
T_{gel} (°C)	27.2	26.9 ± 0.20

As a step forward in pursuing the H-hUCESC-CM, we prepared the optimized hydrogel formulation using the hUCESC culture media (DMEM-F12) to ensure adequate performance. **Figure 2** shows the rheological properties of H-PBS and H-DMEM-F12. Temperature (**Figure 2A**) and angular frequency (**Figure 2B**) profiles for both hydrogels are superimposed indicating their similitude. There are no statistically significant differences between H-DMEM-F12 and H-PBS characteristics.

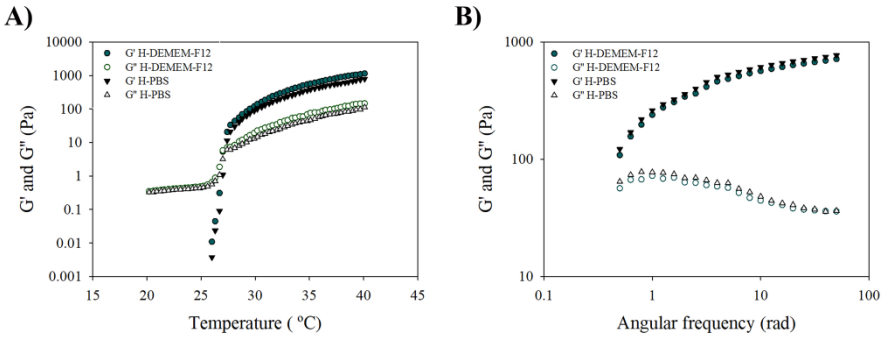

Figure 2. Variation of the storage (G') and loss (G") moduli as a function of temperature (A) and angular frequency (B) for H-DMEM-F12 and H-PBS. The crossover between both moduli is represented by T_{gel}.

Table 3 shows the evolution of H-DMEM-F12 parameters during storage. No statistically significant differences were observed for syringeability work and T_{gel} over time. However, bioadhesion was significantly increased at 2 and 4 weeks of storage (p<0.01).

Table 3. Properties of the H-DEMEM-F12 after variable storage time at 4°C. Data are presented as mean ± SEM.

Parameter	Day 0	2 Weeks	4 Weeks
Syringeability (mJ)	176.17 ± 1.30	182.15 ± 1.64	175.79 ± 1.19
Bioadhesion work (mJ)	0.270 ± 0.01	0.327 ± 0.03	0.520 ± 0.03
Tgel (°C)	26.89 ± 0.07	26.77 ± 0.18	26.17 ± 0.20

6.3.2. Inducement of DSS-associated colitis in C57BL/6 mice

In DSS induced colitis model, mice showed sequentially initial, mild, and severe clinical signs of disease (weight loss, diarrhoea occurrence and blood in stools) after 3-day treatment with DSS. Macroscopic and microscopic lesions induced by DSS were confirmed in all mice. None of the mice died during the study and no side effects due to the H-hUCESC-CM administration were detected.

6.3.3. Effect of H-hUCESC-CM on body weight and colon length

Weight measurements were performed daily. It is known that body weight loss is a key indicator of colitis development in DSS-treated mice [24]. As expected, DSS-treated mice lost weight rapidly, being the lowest on day 9, and then gradually recovering in all mouse groups (**Figure 3**). The highest average weight recovery was in the H-hUCESC-CM group, which was significantly higher at 15 days than the MZ-treated group.

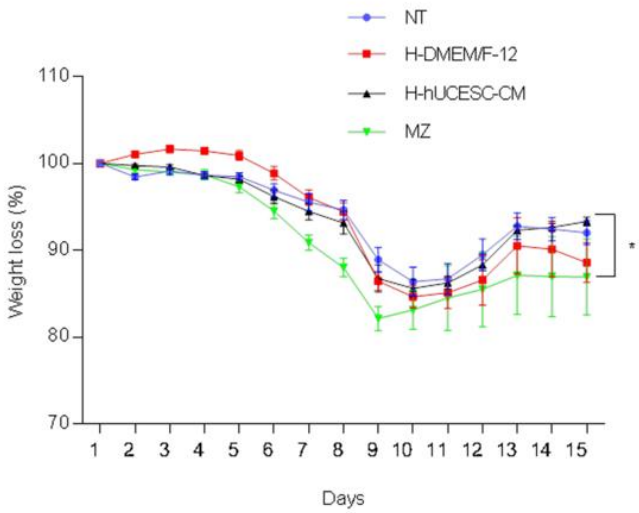

Figure 3. H-hUCESC-CM ameliorates DSS-induced colitis. Daily body weight measurement as percentage of starting weight. * indicates a significant (p<0.05) difference in body weight at day 15 between H-hUCESC-CM and MZ mice.

Administration of DSS causes a significant (p<0.001) decrease in colon length in all groups of mice as compared to control H mice. Interestingly, only H-hUCESC-CM treatment significantly (p<0.05) increased colon length with respect to NT-group (**Figure 4A-B**).

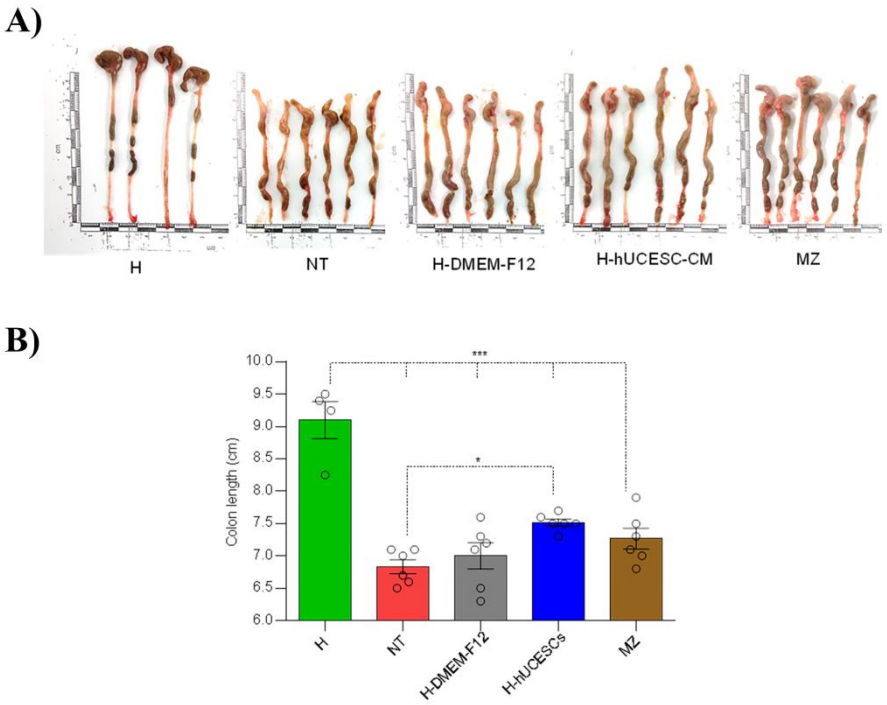

Figure 4. H-hUCESC-CM ameliorates DSS-induced colitis. A) Colon length images at day 16. B) Colon length values at day 16. DSS-induced colon shortening, but treatment H-hUCESC-CM significantly reduced these changes with respect to NT mice. Data are expressed as mean ± SEM. *=*p*<0.05; *=*p*<0.001.**

6.3.4. H-hUCESC-CM hydrogel reduced the extension and severity of intestinal lesions

Colon evaluation by H&E showed that DSS treatment in NT mice induced a high degradation of mucosal architecture, inflammatory cell infiltration, ulceration, edema, destruction of epithelial cells, and diffused depletion of goblet cells as well as intense collapse of crypts. **Figure 5** shows representative examples of histopathology analysis performed after H&E staining. These changes were significantly reduced in the H-hUCESC-CM treated mice, which presented only limited colonic mucosal congestion and edema, scattered erosions, healing ulcers, and less inflammatory cell infiltration. Mice from the H group showed normal mucosal architecture and regular goblet cells (**Figure 5**). Histological score values in three colon locations with

respect to cecum (proximal, mid, and distal) (**Figure 6A**) indicate that H-hUCESC-CM administration reduces histological score in all locations with respect to NT mice**,** however differences were only statistically significant for distal location (**Figure 6B-D**). As expected, the highest histological score in this location was for the NT group, which was significant (p<0.05) with respect to the H mice. Mice treated with H-hUCESC-CM also showed significantly (p<0.05) reduced scores with respect to NT mice. Though not significant, reduced score were observed in H-hUCESC-CM-treated mice with respect to NT group in all the other colon location.

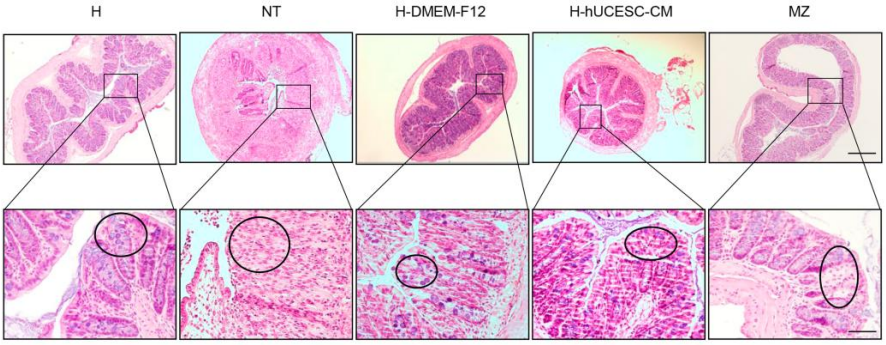

Figure 5. Histological evaluation of colon. Representative mice colon sections stained with H&E. Microphotographs shown areas of normal epithelium (H), ulceration and severe inflammatory reaction (NT), glandular distortion (H-DMEM-F12), mild inflammation (H-hUCESC-CM), and atrophy (MZ).

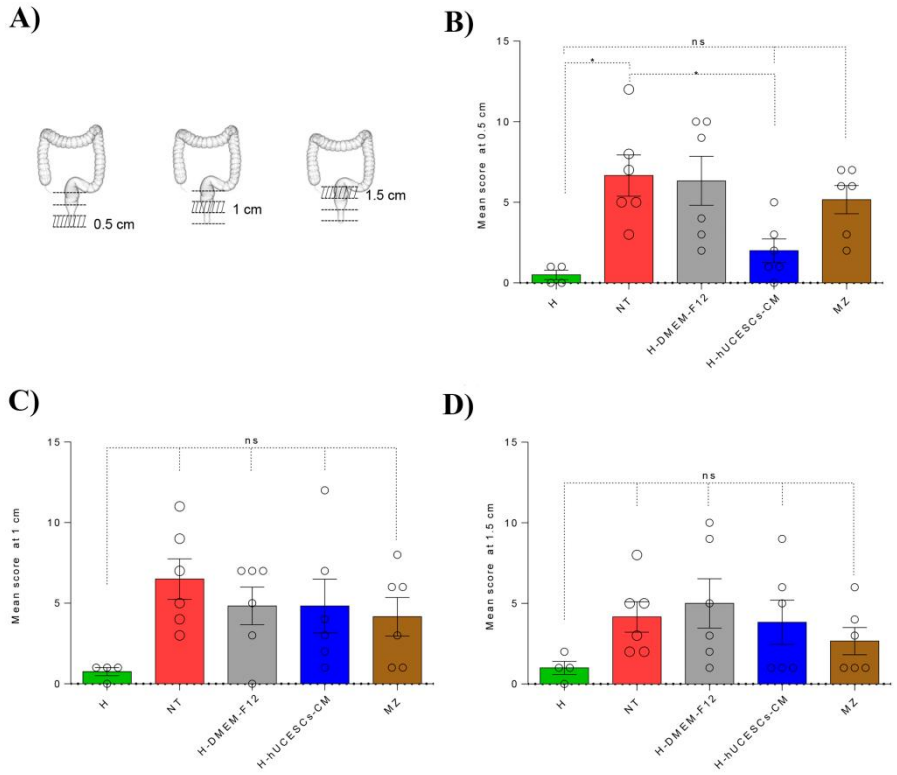

Figure 6. Histological evaluation of colon (continuation). A) Representative picture of histological analysis. Analyses were done in three colonic fragments: distal, mid, and proximal (with respect to cecum). B) Colon epithelial score in the distal fragment (based on inflammation and cell infiltration, microscopic ulcerations, crypt architecture, epithelial atrophy, and epithelial dysplasia, see Methods). C) Colon epithelial score in the middle fragment. D) Colon epithelial score in the proximal fragment. Data are expressed as mean ± SEM. H: healthy mice, NT: non treated mice, H-DMEM-F-12: DMEM-F12-loaded hydrogel treated mice; H-hUCESC-CM: H-hUCESC-CM-loaded hydrogel treated mice; MZ: mesalazine-treated mice. *=p<0.05; ns=not significant. Scale bar: 500 mm for low (upper) and 100 mm for high (below) magnification.

Statistical differences within groups were also found with respect to specific histopathological parameters, such as inflammation, atrophy, and epithelial dysplasia. Specific scores for these parameters in distal colon were significantly lower with respect to NT mice (p<0.01, p<0.05, and p<0.05, respectively) after treatment with H-hUCESC-CM (**Figure 7**). An example of inflammation, atrophy, and

dysplasia in NT, H-DMEM-F12, H-hUCESC-CM and MZ mouse groups after H&E staining is shown in **Figure 8**.

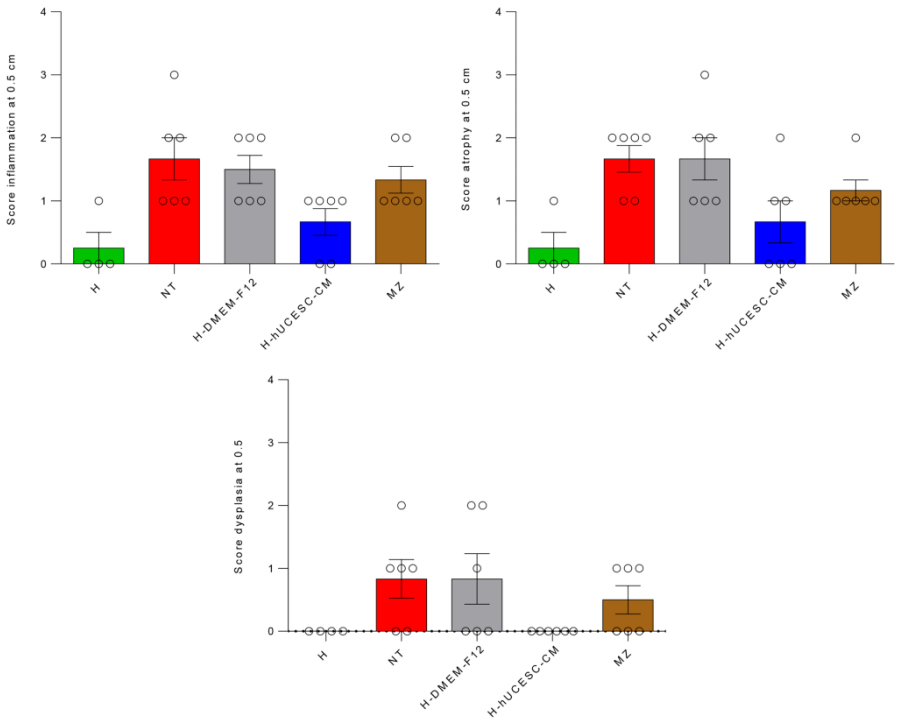

Figure 7. Representative histological score in the distal colon fragment. Score values of inflammation, atrophy, and epithelial dysplasia in healthy (H), and treated and non-treated DSS-induced mice.

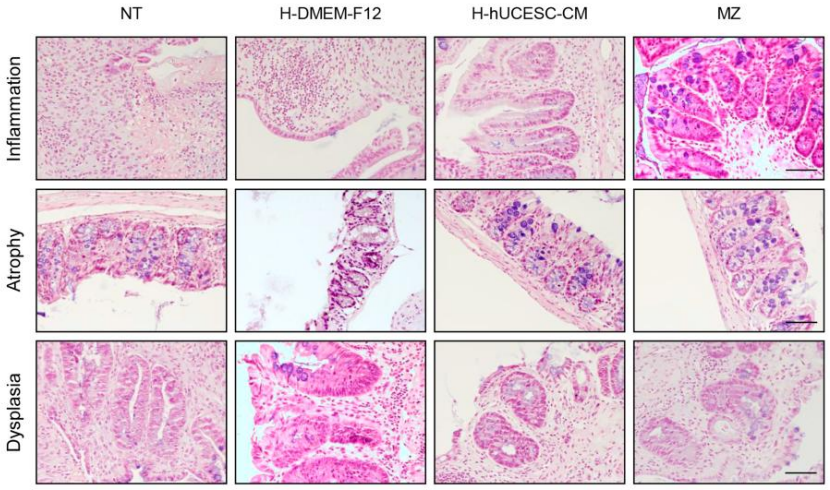

Figure 8. Representative histological score in the distal colon fragment (continuation). Microphotography of representative examples of inflammation, atrophy, and dysplasia in DSS-induced mice non-treated (NT) and treated with H-DMEM-F12, H-hUCESC-CM, and mesalazine (MZ). *=p<0.05; ns=not significant. Scale bar: 100 mm.

6.3.5. H-hUCESC-CM pro-inflammatory cytokines in colon

TNF-α, IL-6, and IFN-γ mRNA expression levels in the different mouse groups are shown in **Figure 9**. TNF-α, IFN-γ and IL-6 mRNA expression levels were significantly higher in the NT mice with respect to H mice (p<0.0001, p<0.01, and p<0.0001, respectively). All the cytokines evaluated significantly decreased after treatment with H-hUCESC-CM as compared with NT mice (p<0.0001). Importantly, TNF-α, IFN-γ and IL-6 mRNA expression levels of H mice were similar (not significant) to both H-hUCESC-CM and MZ treated mice.

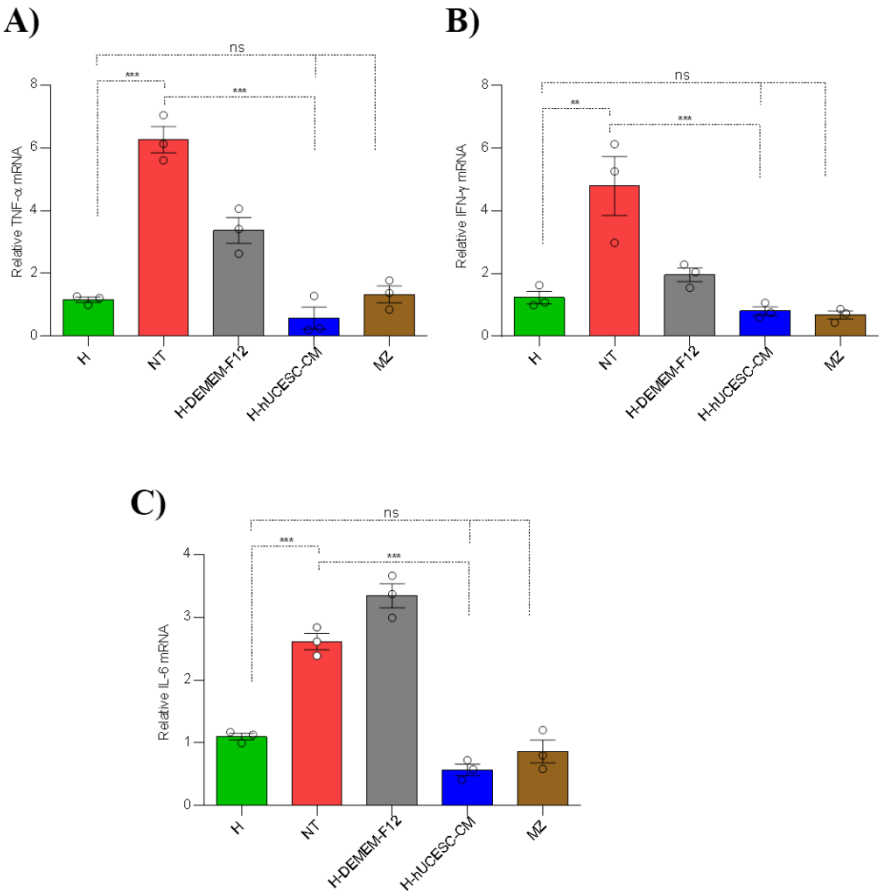

Figure 9. Real-time PCR of pro-inflammatory cytokines in colon samples. A) Tumour necrosis factor-alpha (TNF-α), B) Interferon-gamma (IFN-γ) and C) Interleukin-6 (IL-6) mRNA expression levels in colon of mice. Data are expressed as mean ± SEM. ns= not significant. **=*p*<0.01; *=*p*<0.001.**

6.4. DISCUSSION

In the present study we demonstrate that local administration of H-hUCESC-CM has therapeutic effects in an acute DSS-induced colitis mouse model. These beneficial effects comprise body weight recovery, improved colon length and histological colitis score, and decreased pro-inflammatory cytokine expression.

Mucosal membranes are excellent sites for drug delivery owing to their high permeability, lower risk of overdose and local treatment. However, the major drawback of drug delivery via mucosal membranes is the limited retention time at the mucosal tissue surface [25,26]. To address this limitation an adequate ternary formulation for rectal administration was developed to evaluate the potential usefulness of hUCESC-CM for IBD treatment. This system is composed of two Pluronic® and a hydroxypropylcellulose (MK4M). Pluronic® are amphiphilic, thermosensitive and bioadhesive triblock copolymers widely used in the pharmaceutical field to produce *in situ* gelation hydrogels [27]. Often, PF127 and PF68 are used in combination to obtain hydrogels with specific gelation temperatures [28]. Hydroxypropylcellulose is a cellulose derivative with high viscosity grade that generates robust and mucoadhesive networks capable of controlling the release of drugs. Thus, the combination of these compounds should increase the binding of the hydrogel to the colonic and rectal mucosae [29].

The use of ANN made it possible to obtain an optimized bioadhesive hydrogel that was stable and suitable for rectal administration of hUCESC-CM. Its mucoadhesive and thermosensitive character together with its suitable syringeability ensures adequate administration and extensibility in liquid form on the colonic tissue. The low T_{gel} (27 °C) of H-DMEM-F12 enables a faster transition from liquid to solid state by the Pluronic® polymeric chains rearrangement, reducing leakage and dilution of the systems in biological fluids [27]. Moreover, the incorporation of MK4M improves hydrogel bioadhesion for a longer and closer interaction between hUCESC-CM and colonic and rectal mucosae [27,30]. Thus, the residence time of the drug delivery system in the colon increases, enhancing drug absorption, as well as efficacy and bioavailability.

With respect to NT mice, we found that H-hUCESC-CM treatment significantly improved several histopathological parameters, such as colon length and histological score. Specifically, the lower grade of atrophy, inflammation and dysplasia suggests that H-hUCESC-CM acts upon several targets. It is known that molecular and cellular mechanisms responsible for MSC-mediated attenuation of

murine colitis involved suppression of colon inflammation, promotion of angiogenesis and regeneration of damaged epithelium, leading to an enhanced healing process in the injured colon [31-33]. It is worth noting that, compared to the standard formulation (MZ), treatment with H-hUCESC-CM improved histological score only at distal colon, which is interesting because histopathological damage by DSS is predominantly found in distal colonic location [34].

It has been previously demonstrated in a dry eye rat model that hUCESC-CM treatment significantly improves epithelial regeneration and decreases pro-inflammatory cytokines [18]. hUCESC-CM contains high levels of proteins such as tissue inhibitors of metalloproteinases -1 and -2, fibroblast growth factor -6 and -7, urokinase receptor, and hepatocyte growth factor, that could mediate regenerative effects [17-20]. In the present study, it was also found that mice treated with H-hUCESC-CM showed a significant decrease in TNF-α, IL-6 and INF-γ mRNA expression. TNF-α is considered the most potent pro-inflammatory cytokine in the pathogenesis of IBD. In fact, anti-TNF-α agents, such as infliximab, are highly effective in the treatment of moderate to severe intestinal disease [35]. Experimental data show that hydrogel alone also conferred a partial benefit on some pro-inflammatory cytokines such as TNF-α and IFN-γ. Multiple biological effects are attributed to PF68 and to PF127, such as membrane resealing agent, antithrombotic, skin wound cleaner, and emulsifying agent in artificial blood [36,37]. Hence, partial benefit observed in colon of mice treated with H-DMEM-F12 could be explained by partial anti-inflammatory and resealing properties of the polymers included in the formulation.

Earlier studies attributed the effects of MSC therapies to their capacity for local engrafting and differentiating into multiple tissue types, however, more recent studies show that implanted cells do not survive for long [38,39]. This suggests that the beneficial effects of MSC therapy could be derived from secreted bioactive factors regulating key biologic processes [40]. Therefore, secretome derivatives such as CM or exosomes, may be preferable to cell administration in terms of manufacture, storage and handling. The use of MSC-CM mitigates certain safety considerations related to the

transplantation of living cells such as immune compatibility, emboli formation, tumorigenicity, and transmission of infections [41]. One limitation of this study is that only a single concentration of H-hUCESC-CM was evaluated. It is known that the effectiveness of this type of therapy may vary depending on the dose and frequency of administration. Further research is necessary to elucidate these aspects as well as underlying mechanisms and components of hUCESC-CM.

6.5. CONCLUSIONS

This study demonstrates that local administration of hUCESC-CM in bioadhesive thermosensitive hydrogels improves residence time in target sites and increases interaction with rectal and colonic mucosae, inducing therapeutic anti-inflammatory and regenerative activity in experimental colitis. Thus, these data suggest that H-hUCESC-CM may represent an attractive tool for cell-free therapy in IBD local treatment.

USC UNIVERSIDADE DE SANTIAGO DE COMPOSTELA

REFERENCES

[1] J. Cosnes, C. Gower-Rousseau, P. Seksik, A. Cortot, Epidemiology and natural history of inflammatory bowel diseases, Gastroenterology, 140 (2011) 1785-1794.

[2] J. Burisch, N. Pedersen, S. Cukovic-Cavka, M. Brinar, I. Kaimakliotis, D. Duricova, O. Shonova, I. Vind, S. Avnstrom, N. Thorsgaard, V. Andersen, S. Krabbe, J.F. Dahlerup, R. Salupere, K.R. Nielsen, J. Olsen, P. Manninen, P. Collin, E.V. Tsianos, K.H. Katsanos, K. Ladefoged, L. Lakatos, E. Bjornsson, G. Ragnarsson, Y. Bailey, S. Odes, D. Schwartz, M. Martinato, G. Lupinacci, M. Milla, A. De Padova, R. D'Inca, M. Beltrami, L. Kupcinskas, G. Kiudelis, S. Turcan, O. Tighineanu, I. Mihu, F. Magro, L.F. Barros, A. Goldis, D. Lazar, E. Belousova, I. Nikulina, V. Hernandez, D. Martinez-Ares, S. Almer, Y. Zhulina, J. Halfvarson, N. Arebi, S. Sebastian, P.L. Lakatos, E. Langholz, P. Munkholm, g. EpiCom, East-West gradient in the incidence of inflammatory bowel disease in Europe: the ECCO-EpiCom inception cohort, Gut, 63 (2014) 588-597.

[3] G.J. Gomez-Gomez, A. Masedo, C. Yela, P. Martinez-Montiel Mdel, B. Casis, Current stage in inflammatory bowel disease: What is next?, World J Gastroenterol, 21 (2015) 11282-11303.

[4] B. Chassaing, A. Darfeuille-Michaud, The commensal microbiota and enteropathogens in the pathogenesis of inflammatory bowel diseases, Gastroenterology, 140 (2011) 1720-1728.

[5] T.T. MacDonald, I. Monteleone, M.C. Fantini, G. Monteleone, Regulation of homeostasis and inflammation in the intestine, Gastroenterology, 140 (2011) 1768-1775.

[6] A. Thomas, N. Lodhia, Advanced therapy for inflammatory bowel disease: a guide for the primary care physician, J Am Board Fam Med, 27 (2014) 411-420.

[7] S. Mozaffari, S. Nikfar, A.H. Abdolghaffari, M. Abdollahi, New biologic therapeutics for ulcerative colitis and Crohn's disease, Expert Opin Biol Ther, 14 (2014) 583-600.

[8] H.E. Young, M.L. Mancini, R.P. Wright, J.C. Smith, A.C. Black, Jr., C.R. Reagan, P.A. Lucas, Mesenchymal stem cells reside within the connective tissues of many organs, Dev Dyn, 202 (1995) 137-144.

[9] S. Meirelles Lda, A.M. Fontes, D.T. Covas, A.I. Caplan, Mechanisms involved in the therapeutic properties of mesenchymal stem cells, Cytokine Growth Factor Rev, 20 (2009) 419-427.
[10] S.K. Hosseini-Asl, D. Mehrabani, F.K. Karimi-Busheri, Therapeutic effect of mesenchymal stem cells in ulcerative colitis: a review on achievements and challenges. J Clin Med, 9 (2020) 3922.
[11] X. Shi, Q. Chen, F. Wang, Mesenchymal stem cells for the treatment of ulcerative colitis: a systematic review and meta-analysis of experimental and clinical studies, Stem Cell Res Ther, 10 (2019) 266.
[12] E. Legaki, M.G. Roubelakis, G.E. Theodoropoulos, A. Lazaris, A. Kollia, G. Karamanolis, E. Marinos, M. Gazouli, Therapeutic Potential of Secreted Molecules Derived from Human Amniotic Fluid Mesenchymal Stem/Stroma Cells in a Mice Model of Colitis, Stem Cell Rev, 12 (2016) 604-612
[13] J.Y. Song, H.J. Kang, J.S. Hong, C.J. Kim, J.Y. Shim, C.W. Lee, J. Choi, Umbilical cord-derived mesenchymal stem cell extracts reduce colitis in mice by re-polarizing intestinal macrophages, Sci Rep, 7 (2017) 9412.
[14] Y. Wu, W. Qiu, X. Xu, J. Kang, J. Wang, Y. Wen, X. Tang, Y. Yan, H. Qian, X. Zhang, W. Xu, F. Mao, Exosomes derived from human umbilical cord mesenchymal stem cells alleviate inflammatory bowel disease in mice through ubiquitination, Am J Transl Res, 10 (2018) 2026-2036
[15] J. Panes, D. Garcia-Olmo, G. Van Assche, J.F. Colombel, W. Reinisch, D.C. Baumgart, A. Dignass, M. Nachury, M. Ferrante, L. Kazemi-Shirazi, J.C. Grimaud, F. de la Portilla, E. Goldin, M.P. Richard, A. Leselbaum, S. Danese, A.C.S.G. Collaborators, Expanded allogeneic adipose-derived mesenchymal stem cells (Cx601) for complex perianal fistulas in Crohn's disease: a phase 3 randomised, double-blind controlled trial, Lancet, 388 (2016) 1281-1290.
[16] J. Panes, D. Garcia-Olmo, G. Van Assche, J.F. Colombel, W. Reinisch, D.C. Baumgart, A. Dignass, M. Nachury, M. Ferrante, L. Kazemi-Shirazi, J.C. Grimaud, F. de la Portilla, E. Goldin, M.P. Richard, M.C. Diez, I. Tagarro, A. Leselbaum, S. Danese, A.C.S.G. Collaborators, Long-term Efficacy and Safety of Stem Cell Therapy

(Cx601) for Complex Perianal Fistulas in Patients With Crohn's Disease, Gastroenterology, 154 (2018) 1334-1342 e1334.
[17] N. Eiro, J. Sendon-Lago, S. Seoane, M.A. Bermudez, M.L. Lamelas, T. Garcia-Caballero, J. Schneider, R. Perez-Fernandez, F.J. Vizoso, Potential therapeutic effect of the secretome from human uterine cervical stem cells against both cancer and stromal cells compared with adipose tissue stem cells, Oncotarget, 5 (2014) 10692-10708.
[18] M.A. Bermudez, J. Sendon-Lago, N. Eiro, M. Trevino, F. Gonzalez, E. Yebra-Pimentel, M.J. Giraldez, M. Macia, M.L. Lamelas, J. Saa, F. Vizoso, R. Perez-Fernandez, Corneal epithelial wound healing and bactericidal effect of conditioned medium from human uterine cervical stem cells, Invest Ophthalmol Vis Sci, 56 (2015) 983-992.
[19] M.A. Bermudez, J. Sendon-Lago, S. Seoane, N. Eiro, F. Gonzalez, J. Saa, F. Vizoso, R. Perez-Fernandez, Anti-inflammatory effect of conditioned medium from human uterine cervical stem cells in uveitis, Exp Eye Res, 149 (2016) 84-92.
[20] J. Sendon-Lago, S. Seoane, A. Martinez-Ordonez, N. Eiro, J. Saa, F.J. Vizoso, F. Gonzalez, R. Perez-Fernandez, M.A. Bermudez, Corneal regeneration by conditioned medium of human uterine cervical stem cells is mediated by TIMP-1 and TIMP-2, Exp Eye Res, 180 (2019) 110-121.
[21] J. Schneider, E. Mateo, C. Marcos-Arias, N. Eiro, F. Vizoso, R. Perez-Fernandez, E. Eraso, G. Quindos, Antifungal Activity of the Human Uterine Cervical Stem Cells Conditioned Medium (hUCESC-CM) Against Candida albicans and Other Medically Relevant Species of Candida, Front Microbiol, 9 (2018) 2818.
[22] L. Garcia-Del Rio, P. Diaz-Rodriguez, M. Landin, New tools to design smart thermosensitive hydrogels for protein rectal delivery in IBD, Mater Sci Eng C Mater Biol Appl, 106 (2020) 110252.
[23] S. Wirtz, V. Popp, M. Kindermann, K. Gerlach, B. Weigmann, S. Fichtner-Feigl, M.F. Neurath, Chemically induced mouse models of acute and chronic intestinal inflammation, Nat Protoc, 12 (2017) 1295-1309.

[24] H.S. Cooper, S.N. Murthy, R.S. Shah, D.J. Sedergran, Clinicopathologic study of dextran sulfate sodium experimental murine colitis, Lab Invest, 69 (1993) 238-249.
[25] H. Laroui, S.A. Ingersoll, H.C. Liu, M.T. Baker, S. Ayyadurai, M.A. Charania, F. Laroui, Y. Yan, S.V. Sitaraman, D. Merlin, Dextran sodium sulfate (DSS) induces colitis in mice by forming nano-lipocomplexes with medium-chain-length fatty acids in the colon, PLoS One, 7 (2012) e32084.
[26] A.A. Koffi, F. Agnely, G. Ponchel, J.L. Grossiord, Modulation of the rheological and mucoadhesive properties of thermosensitive poloxamer-based hydrogels intended for the rectal administration of quinine, Eur J Pharm Sci, 27 (2006) 328-335.
[27] Y. Yuan, Y. Cui, L. Zhang, H.P. Zhu, Y.S. Guo, B. Zhong, X. Hu, L. Zhang, X.H. Wang, L. Chen, Thermosensitive and mucoadhesive in situ gel based on poloxamer as new carrier for rectal administration of nimesulide, Int J Pharm, 430 (2012) 114-119.
[28] F.U. Din, O. Mustapha, D.W. Kim, R. Rashid, J.H. Park, J.Y. Choi, S.K. Ku, C.S. Yong, J.O. Kim, H.G. Choi, Novel dual-reverse thermosensitive solid lipid nanoparticle-loaded hydrogel for rectal administration of flurbiprofen with improved bioavailability and reduced initial burst effect, Eur J Pharm Biopharm, 94 (2015) 64-72.
[29] A.C. Santos Akkari, E.V. Ramos Campos, A.F. Keppler, L.F. Fraceto, E. de Paula, G.R. Tofoli, D.R. de Araujo, Budesonide-hydroxypropyl-beta-cyclodextrin inclusion complex in binary poloxamer 407/403 system for ulcerative colitis treatment: A physico-chemical study from micelles to hydrogels, Colloids Surf B Biointerfaces, 138 (2016) 138-147.
[30] N. Salamat-Miller, M. Chittchang, T.P. Johnston, The use of mucoadhesive polymers in buccal drug delivery, Adv Drug Deliv Rev, 57 (11) 1666-1691.
[31] J. Yang, Z. Chen, D. Pan, H. Li, J. Shen, Umbilical Cord-Derived Mesenchymal Stem Cell-Derived Exosomes Combined Pluronic F127 Hydrogel Promote Chronic Diabetic Wound Healing and Complete Skin Regeneration, Int J Nanomedicine, 15 (2020) 5911-5926.

[32] P. Ahangar, S. J. Mills, A.J. Cowin, Mesenchymal Stem Cell Secretome as an Emerging Cell-Free Alternative for Improving Wound Repair, Int J Mol Sci, 21 (2020) 7038.
[33] Q.Q. Chen, L. Yan, C.Z. Wang, W.H. Wang, H. Shi, B.B. Su, Q.H. Zeng, H.T. Du, J. Wan, Mesenchymal stem cells alleviate TNBS-induced colitis by modulating inflammatory and autoimmune responses, World J Gastroenterol, 19 (2013) 4702-4717.
[34] L.A. Dieleman, M.J. Palmen, H, Akol, E. Bloemena, A.S. Peña, S.G. Meuwissen, E.P. Van Rees, Chronic experimental colitis induced by dextran sulphate sodium (DSS) is characterized by Th1 and Th2 cytokines, Clin Exp Immunol 114 (1998) 385-391.
[35] S. Danese, C. Fiocchi, Ulcerative colitis, N Engl J Med, 365 (2011) 1713-1725.
[36] G.M. Soliman, G. Fetih, A.M. Abbas, Thermosensitive bioadhesive gels for the vaginal delivery of sildenafil citrate: in vitro characterization and clinical evaluation in women using clomiphene citrate for induction of ovulation, Drug Dev Ind Pharm, 43 (2017) 399-408.
[37] Y. Liu, W-L. Lu, J-C. Wang, X. Zhang, H. Zhang, X-Q. Wang, T-Y. Zhou, Q. Zhang, Controlled delivery of recombinant hirudin based on thermo-sensitive Pluronic F127 hydrogel for subcutaneous administration: In vitro and in vivo characterization, J Control Release, 117 (2007) 387-95.
[38] G. Maguire, Stem cell therapy without the cells, Commun Integr Biol, 6 (2013) e26631.
[39] C.F. de Aguiar, A. Castoldi, V. Andrade-Oliveira, A. Ignacio, F.F. da Cunha, R.J.F. Felizardo, E.J. Bassi, N.O.S. Camara, D.C. de Almeida, Mesenchymal stromal cells modulate gut inflammation in experimental colitis, Inflammopharmacology, 26 (2018) 251-260.
[40] F.J. Vizoso, N. Eiro, L. Costa, P. Esparza, M. Landin, P. Diaz-Rodriguez, J. Schneider, R. Perez-Fernandez, Mesenchymal stem cells in homeostasis and systemic diseases: hypothesis, evidences, and therapeutic opportunities, Int J Mol Sci, 20 (2019) 3738.
[41] F.J. Vizoso, N. Eiro, S. Cid, J. Schneider, R. Perez-Fernandez, Mesenchymal stem cell secretome: toward cell-free therapeutic

strategies in regenerative medicine, Int J Mol Sci, 18 (2017) 1852-1870.

USC UNIVERSIDADE DE SANTIAGO DE COMPOSTELA

7. CONCLUSIONS

USC
UNIVERSIDADE
DE SANTIAGO
DE COMPOSTELA

This work is focused on exploring the potential of ternary combinations of selected polymers to produce highly bioadhesive and thermosensitive hydrogels with advanced performance for sublingual and rectal delivery. This task was assisted by Artificial Intelligence Techniques (AIT), including neurofuzzy logic, Artificial Neural Networks (ANN) and Genetic Algorithms (GA). The results have allowed us to draw the following conclusions:

1. Artificial intelligence tools enable to easily study the knowledge space and establish the design space of rectal and sublingual ternary formulations, even using extremely reduced experimental designs (balanced density experimental designs). The experimental data modelling with hybrid technologies indeed resulted in formulations with advanced performance. Neurofuzzy logic, allows establishing how the components of the formulations and their interactions affect the texturometric, rheological and release behaviour of ternary hydrogels, thus acquiring in-depth knowledge about their role on systems performance. On the other hand, the combination of ANN and GA allows the optimization of several variables simultaneously, finding the best possible formulation within the design space.

   Thus, AI approaches arise as powerful tools for delimiting the design space of ternary hydrogels and the subsequent development of optimized delivery systems of desired characteristics that meet the demands for mucosal administration.

2. An adequate combination of PF127, HS1200 and Gantrez (AN119 or S97) is useful for obtaining thermosensitive and mucoadhesive hydrogels of suitable characteristics for the mucosal administration of therapeutic molecules (high gel strength, bioadhesion and cohesion, and fast drug release). Moreover, HS1200 showed immunostimulatory capacity, rising as a potential polymer with suitable characteristics for the development of vaccines.

   The achieved optimal hydrogel for vaccine delivery was able to spread over the sublingual mucosa, prevent antigen leakage by

swallowing or dilution on salivary fluid, and induce its rapid release to guarantee complete absorption through the oral mucosa tissue.

Both, the optimal formulation and CAF01 liposomes including the Chlamydia CTH522 subunit vaccine, were tested in mice to assess the systems immunogenicity, showing an immunization strategy-dependent efficacy. The results demonstrated the combined parenteral-sublingual booster immunization was able to significantly enhance the IFN-γ production by cervical lymph nodes and elicited a local IgA immune response in the genital tract compared to parenteral immunization alone.

3. Adequate combinations of PF127, PF68 and MK4M are useful to prepare enemas that undergo fast transition from liquid to solid state once at body temperature, minimizing the leakage and dilution of the therapeutic molecules. These smart formulations exhibit good bioadhesiveness and a rapid drug release, designed to promote an immediate effect over the damaged intestinal mucosa. An optimal hydrogel was developed based on the desired formulation characteristics showing appropriate syringeability, bioadhesion and gelation temperature.

   The incorporation of conditioned medium from human uterine cervical stem cells (hUCESC-CM) to the mucoadhesive and thermosensitive optimized hydrogel, facilitates its rectal administration in a murine model of ulcerative colitis and, ensures its adequate extensibility and retention on both colonic and rectal mucosae. The optimal hydrogel loaded with hUCESC-CM significantly reduces colon shortening as well as the extension and severity of intestinal lesions by diminishing the grade of atrophy, inflammation, and dysplasia, compared to control group (untreated). Remarkably, the histological score in the distal colon was also improved with respect to the standard formulation for local IBD treatment (mesalazine treatment).

   Moreover, the administration of the optimized unloaded hydrogel reduces the expression of pro-inflammatory cytokines such as

TNF-α and IFN-γ, indicating its potential anti-inflammatory effect due to its particular composition. The loading of the hydrogel with hUCESC-CM further increases the exerted pro-inflammatory response demonstrating the anti-inflammatory effect of the formulation on the mucosa and therefore, its utility in the local treatment of IBD.

In general, we demonstrate the development of complex multicomponent systems is greatly facilitated by Artificial Intelligence approaches, since their use allows a significant reduction of experiments saving costs and time. In addition, the deep knowledge of the pharmaceutical systems that derives from their use allows the establishment of the adequate design space for each formulation following the Quality by Design criteria and therefore, facilitates the transference of the best formulations to clinic.

USC UNIVERSIDADE DE SANTIAGO DE COMPOSTELA

USC
UNIVERSIDADE
DE SANTIAGO
DE COMPOSTELA

ANNEX I

USC
UNIVERSIDADE
DE SANTIAGO
DE COMPOSTELA

Table A1.1. Set of "IF-THEN" rules for gelation temperature for the experimental design obtained through AIT. Degree of membership in parentheses. Blue colour indicates the combination of inputs that led to the highest value of the output, while red colour shows the combination of inputs giving the lowest value.

Rules for T_{gel}		
Submodel 1		
IF PF127 is LOW AND Gantrez is LOW_1(4)	THEN Tgel is	LOW (0.65)
IF PF127 is LOW AND Gantrez is MID_2(4)	THEN Tgel is	LOW (0.82)
IF PF127 is LOW AND Gantrez is MID_3(4)	THEN Tgel is	HIGH (0.82)
IF PF127 is LOW AND Gantrez is HIGH_4(4)	THEN Tgel is	HIGH (1.00)
IF PF127 is MID AND Gantrez is LOW_1(4)	THEN Tgel is	HIGH (0.97)
IF PF127 is MID AND Gantrez is MID_2(4	THEN Tgel is	LOW (1.00)
IF PF127 is MID AND Gantrez is MID_3(4)	THEN Tgel is	LOW (1.00)
IF PF127 is MID AND Gantrez is HIGH_4(4)	THEN Tgel is	LOW (0.72)
IF PF127 is HIGH AND Gantrez is LOW_1(4	THEN Tgel is	LOW (1.00)
IF PF127 is HIGH AND Gantrez is MID_2(4)	THEN Tgel is	LOW (1.00)
IF PF127 is HIGH AND Gantrez is MID_3(4)	THEN Tgel is	LOW (1.00)
IF PF127 is HIGH AND Gantrez is HIGH_4(4)	THEN Tgel is	LOW (1.00)
Submodel 2		
IF HS1200 is LOW	THEN Tgel is	LOW (0.56)
IF HS1200 is HIGH	THEN Tgel is	LOW (0.51)

Table A1.2. Set of "IF-THEN" rules for mucoadhesion at 37 ºC for the experimental design obtained through AIT. Degree of membership in parentheses. Blue colour indicates the combination of inputs that led to the highest value of the output, while red colour shows the combination of inputs giving the lowest value.

Rules for Mucoadhesion		
Submodel 1		
IF PF127 is LOW_1(4) AND Gantrez is LOW	THEN Mucoadhesion is	LOW(1.00)
IF PF127 is LOW_1(4) AND Gantrez is HIGH	THEN Mucoadhesion is	LOW (0.93)
IF PF127 is MID_2(4) AND Gantrez is LOW	THEN Mucoadhesion is	HIGH (0.70)
IF PF127 is MID_2(4) AND Gantrez is HIGH	THEN Mucoadhesion is	LOW (0.87)
IF PF127 is MID_3(4) AND Gantrez is LOW	THEN Mucoadhesion is	HIGH (1.00)
IF PF127 is MID_3(4) AND Gantrez is HIGH	THEN Mucoadhesion is	HIGH (1.00)
IF PF127 is HIGH_4(4) AND Gantrez is LOW	THEN Mucoadhesion is	HIGH (0.70)
IF PF127 is HIGH_4(4) AND Gantrez is HIGH	THEN Mucoadhesion is	HIGH (0.82)

Table A1.3. Set of "IF-THEN" rules for gel strength at 37 ºC for the experimental design obtained through AIT. Degree of membership in parentheses. Blue colour indicates the combination of inputs that led to the highest value of the output, while red colour shows the combination of inputs giving the lowest value.

Rules for Gel strength		
Submodel 1		
IF PF127 is LOW AND Gantrez is LOW_1(4)	THEN Gel strength is	HIGH (1.00)
IF PF127 is LOW AND Gantrez is MID_2(4)	THEN Gel strength is	HIGH (0.86)
IF PF127 is LOW AND Gantrez is MID_3(4)	THEN Gel strength is	LOW (1.00)
IF PF127 is LOW AND Gantrez is HIGH_4(4)	THEN Gel strength is	LOW (1.00)
IF PF127 is MID AND Gantrez is LOW_1(4)	THEN Gel strength is	LOW (1.00)
IF PF127 is MID AND Gantrez is MID_2(4	THEN Gel strength is	LOW (1.00)
IF PF127 is MID AND Gantrez is MID_3(4)	THEN Gel strength is	LOW (1.00
IF PF127 is MID AND Gantrez is HIGH_4(4)	THEN Gel strength is	LOW (1.00
IF PF127 is HIGH AND Gantrez is LOW_1(4)	THEN Gel strength is	HIGH (1.00)
IF PF127 is HIGH AND Gantrez is MID_2(4)	THEN Gel strength is	HIGH (1.00)
IF PF127 is HIGH AND Gantrez is MID_3(4)	THEN Gel strength is	LOW (1.00
IF PF127 is HIGH AND Gantrez is HIGH_4(4)	THEN Gel strength is	HIGH (1.00)
Submodel 2		
IF HS1200 is LOW	THEN Gel strength is	HIGH (0.58)
IF HS1200 is HIGH	THEN Gel strength is	LOW (0.78)
Submodel 3		
IF Gantrez type is S97	THEN Gel strength is	HIGH (0.50)
IF Gantrez type is AN119	THEN gel strength is	LOW (0.70)

Table A1.4. Set of "IF-THEN" rules for cohesion at 37 ºC for the experimental design obtained through AIT. Degree of membership in parentheses. Blue colour indicates the combination of inputs that led to the highest value of the output, while red colour shows the combination of inputs giving the lowest value

Rules for Cohesion		
Submodel 1		
IF PF127 is LOW	THEN Cohesion is	HIGH (1.00)
IF PF127 is HIGH	THEN Cohesion is	LOW (0.95)

Table A1.5. Set of "IF-THEN" rules for adhesion work at 37 ºC for the experimental design obtained through AIT. Degree of membership in parentheses. Blue colour indicates the combination of inputs that led to the highest value of the output, while red colour shows the combination of inputs giving the lowest value.

Rules for Adhesion work		
Submodel 1		
IF PF127 is LOW AND Gantrez is LOW	THEN Adhesion work is	LOW (0.85)
IF PF127 is LOW AND Gantrez is MID	THEN Adhesion work is	LOW (0.77)
IF PF127 is LOW AND Gantrez is HIGH	THEN Adhesion work is	LOW (1.00)
IF PF127 is MID AND Gantrez is LOW	THEN Adhesion work is	LOW (1.00)
IF PF127 is MID AND Gantrez is MID	THEN Adhesion work is	HIGH (0.65)
IF PF127 is MID AND Gantrez is HIGH	THEN Adhesion work is	LOW (1.00)
IF PF127 is HIGH AND Gantrez is LOW	THEN Adhesion work is	HIGH (1.00)
IF PF127 is HIGH AND Gantrez is MID	THEN Adhesion work is	HIGH (1.00)
IF PF127 is HIGH AND Gantrez is HIGH	THEN Adhesion work is	HIGH (1.00)
Submodel 2		
IF Gantrez type S97	THEN Adhesion work is	LOW (0.57)
IF Gantrez type AN119	THEN Adhesion work is	LOW (0.84)
Submodel 3		
IF HS1200 is LOW	THEN Adhesion work is	LOW (0.59)
IF HS1200 is HIGH	THEN Adhesion work is	LOW (0.82)

Table A1.6. Set of "IF-THEN" rules for GMFreleased at 5 minutes at 37 ºC for the experimental design obtained through AIT. Degree of membership in parentheses. Blue colour indicates the combination of inputs that led to the highest value of the output, while red colour shows the combination of inputs giving the lowest value

Rules for GMF released at 5 minutes		
Submodel 1		
IF PF127 is LOW	THEN GMF released at 5 min is	HIGH (0.83)
IF PF127 is MID	THEN GMF released at 5 min is	HIGH (1.00)
IF PF127 is HIGH	THEN GMF released at 5 min is	LOW (1.00)
Submodel 2		
IF Gantrez is LOW	THEN GMF released at 5 min is	HIGH (0.95)
IF Gantrez is MID	THEN GMF released at 5 min is	LOW (0.75)
IF Gantrez is HIGH	THEN GMF released at 5 min is	LOW (0.50)

Table A1.7. Set of "IF-THEN" rules for total GMF release time at 37 ºC for the experimental design obtained through AIT. Degree of membership in parentheses. Blue colour indicates the combination of inputs that led to the highest value of the output, while red colour shows the combination of inputs giving the lowest value

Rules for Total GMF release time		
Submodel 1		
IF PF127 is LOW AND Gantrez type is S97	THEN Total release time is	LOW (1.00)
IF PF127 is LOW AND Gantrez type is AN119	THEN Total release time is	HIGH (0.58)
IF PF127 is MID AND Gantrez type S97	THEN Total release time is	LOW (1.00)
IF PF127 is MID AND Gantrez type is AN119	THEN Total release time is	LOW (1.00)
IF PF127 is HIGH AND Gantrez type is S97	THEN Total release time is	HIGH (1.00)
IF PF127 is HIGH AND Gantrez type is AN119	THEN Total release time is	HIGH (0.74)
Submodel 2		
IF Gantrez is LOW	THEN Total release time is	LOW (1.00)
IF Gantrez is MID	THEN Total release time is	LOW (0.61)
IF Gantrez is HIGH	THEN Total release time is	HIGH (0.59)
Submodel 3		
IF HS1200 is LOW	THEN Total release time is	LOW (0.64)
IF HS1200 is MID	THEN Total release time is	LOW (1.00)
IF HS1200 is HIGH	THEN Total release time is	HIGH (0.54)

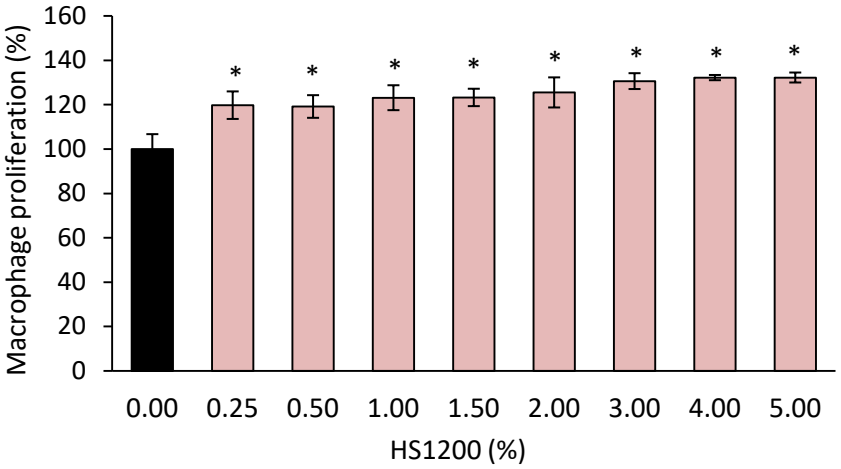

Figure A1. Effect of HS1200 treatments on cell proliferation of THP-1 derived macrophages after incubation for 24 h. Assays were performed in triplicate and results are expressed as mean ± SD. * denotes statistically significant differences ($p < 0.05$) compared to control, human macrophages without treatment.

USC
UNIVERSIDADE
DE SANTIAGO
DE COMPOSTELA

ANNEX II

USC
UNIVERSIDADE
DE SANTIAGO
DE COMPOSTELA

Table A2.1. Set of "IF-THEN" rules for syringeability work, bioadhesion work at 37 ºC, viscosity at 20 ºC and Tgel of experimental design 1. Degree of membership in parentheses. Blue colour indicates the combination of inputs that led to the highest value of the output, while red colour shows the combination of inputs giving the lowest value.

Rules for Syringeability work		
Submodel 1		
IF PF188 is LOW	THEN Syringeability is	HIGH (0.69)
IF PF188 is HIGH	THEN Syringeability is	LOW (1.00)
Rules for Bioadhesion work at 37 ºC		
Submodel 1		
IF PF188 is LOW	THEN Bioadhesion at 37 ºC is	LOW (0.80)
IF PF188 is MID	THEN Bioadhesion at 37 ºC is	HIGH (1.00)
IF PF188 is HIGH	THEN Bioadhesion at 37 ºC is	LOW (1.00)
Submodel 2		
IF HPMC K4M is LOW	THEN Bioadhesion at 37 ºC is	LOW (0.67)
IF HPMC K4M is MID	THEN Bioadhesion at 37 ºC is	HIGH (0.88)
IF HPMC K4M is HIGH	THEN Bioadhesion at 37 ºC is	LOW (1.00)
Rules for Viscosity		
Submodel 1		
IF PF127 is LOW	THEN Viscosity at 20 ºC is	LOW (0.94)
IF PF127 is MID	THEN Viscosity at 20 ºC is	LOW (1.00)
IF PF127 is HIGH	THEN Viscosity at 20 ºC is	HIGH (0.90)
Rules for T_{gel}		
Submodel 1		
IF PF127 is LOW	THEN Tgel is	LOW (0.85)
IF PF127 is MID	THEN Tgel is	HIGH (1.00)
IF PF127 is HIGH	THEN Tgel is	LOW (1.00)

Table A2.2. Set of "IF-THEN" rules for syringeability work, bioadhesion work at 37 ºC, viscosity at 20 ºC and Tgel of experimental design 2. Degree of membership in parentheses. Blue colour indicates the combination of inputs that led to the highest value of the output, while red colour shows the combination of inputs giving the lowest value.

Rules for Syringeability work		
Submodel 1		
IF PF127 is LOW	THEN Syringeability is	LOW (0.93)
IF PF127 is HIGH	THEN Syringeability is	HIGH (0.97)
Rules for Bioadhesion work at 37 ºC		
Submodel 1		
IF PF127 is LOW	THEN Bioadhesion at 37 ºC is	LOW (0.89)
IF PF127 is HIGH	THEN Bioadhesion at 37 ºC is	HIGH (0.82)
Rules for Viscosity		
Submodel 1		
IF HPMC K4M is LOW AND PF127 is LOW	THEN Viscosity at 20 ºC is	LOW (1.00)
IF HPMC K4M is LOW AND PF127 is MID	THEN Viscosity at 20 ºC is	LOW (0.93)
IF HPMC K4M is LOW AND PF127 is HIGH	THEN Viscosity at 20 ºC is	LOW (0.99)
IF HPMC K4M is HIGH AND PF127 is LOW	THEN Viscosity at 20 ºC is	HIGH (1.00)
IF HPMC K4M is HIGH AND PF127 is MID	THEN Viscosity at 20 ºC is	LOW (1.00)
IF HPMC K4M is HIGH AND PF127 is HIGH	THEN Viscosity at 20 ºC is	LOW (1.00)
Submodel 2		
IF PF188 is LOW	THEN Viscosity at 20 ºC is	HIGH (0.52)
IF PF188 is MID	THEN Viscosity at 20 ºC is	LOW (1.00)
IF PF188 is HIGH	THEN Viscosity at 20 ºC is	LOW (0.97)
Rules for T_{gel}		
Submodel 1		
IF PF188 is LOW	THEN Tgel is	LOW (1.00)
IF PF188 is HIGH	THEN Tgel is	HIGH (1.00)
Submodel 2		
IF PF127 is LOW	THEN Tgel is	HIGH (1.00)
IF PF127 is HIGH	THEN Tgel is	LOW (1.00)
IF PF188 is LOW	THEN Tgel is	LOW (1.00)

STATEMENTS: CONFLICTS OF INTERESTS, IMAGE USE, CELL CULTURE, *IN VIVO* ASSAYS AND PUBLISHED CONTENT

USC UNIVERSIDADE DE SANTIAGO DE COMPOSTELA

USC
UNIVERSIDADE
DE SANTIAGO
DE COMPOSTELA

CONFLICT OF INTERESTS

The author declares no conflict of interest related with the materials or topics discussed in this work.

IMAGE USE

All the images presented in this manuscript were created by the author of the thesis. In the case of images reused from publications derived from the research developed by the candidate, included outside the published sections, proper citation to the original source can be found at the bottom of the figures.

CELL CULTURE

The cell line employed in this work was obtained from commercially available resources (American Type Culture Collection, ATCC®): THP-1 (ATCC, TIB-202™) human monocytic cell line. Cells were only used for the research purposes previously specified in this manuscript and were cultured under the conditions recommended by suppliers. Both, the isolation and growth of mesenchymal stem cells from the human uterine cervix (human uterine cervical stromal cells, hUCESCs) were obtained following ethical procedures and conducted in accordance with the regulations set by the Regional Government of the Principality of Asturias.

IN VIVO ASSAYS

The animal research studies carried out in Chapter II were conducted in accordance with the regulations set by the National Committee for the Protection of Animals used for Scientific Purposes and in accordance with the European Community Directive 86/609. The animal research studies carried out in Chapter III were conducted in accordance with the regulations set by the Regional Government of Galicia.

PUBLISHED CONTENT

Part of this thesis manuscript is a reproduction of publications derived from the research developed by the PhD candidate during her predoctoral period. Published sections along with quality criteria of the publications will be specified on the following page:

List of articles:	1. Chapter I was published as research article. 2. Chapter III was published as research article
Title:	1. "Design of novel orotransmucosal vaccine-delivery platforms using artificial intelligence". 2. "New tools to design smart thermosensitive hydrogels for protein rectal delivery in IBD".
Year:	1.2021. 2.2020.
Journal:	1. European Journal of Pharmaceutics and Biopharmaceutics. 2. Materials Science & Engineering C.
Volume, pages/ article number:	1. Volume 159; pages 36-43. 2. Volume 106; article number 110252.
PhD candidate contribution:	1. The contribution of the PhD candidate to this publication consisted in work planning and data acquisition, except in the case of proliferation assays in human macrophages. These data were obtained by a contributing author. Besides, the candidate was also responsible for data analysis and writing of the original draft. 2.The contribution of the PhD candidate to this publication consisted in work planning; data acquisition; analysis and writing of the original draft.
Quality indexes:	1. The journal in which Chapter I was published presented an Impact Factor of 4.604 in 2019, belonging to quartile 1 in "Pharmacology and Pharmacy" (rank 40/271) and "Pharmacology & Toxicology" (rank 26/281) categories. 2. The journal in which Chapter III was published displayed an Impact Factor of 5.880 in 2019, belonging to quartile 1 in "Materials Science, Biomaterials" (rank 8/38) and "Materials Science" (rank 36/390) categories.

Ethical considerations:
Chapters I and III have been published as journal articles, edited by Elsevier. In both cases appropriate permission has been requested, and written authorization has been obtained.

USC UNIVERSIDADE DE SANTIAGO DE COMPOSTELA

USC
UNIVERSIDADE
DE SANTIAGO
DE COMPOSTELA

CHECKLISTS AND PERMISSIONS

USC
UNIVERSIDADE
DE SANTIAGO
DE COMPOSTELA

Checklist for **statistical analysis**.

	Yes/No
Type and applicability of test used	
Comparisons of interest are clearly defined	Yes
Name of tests applied are clearly stated.	Yes
All statistical methods identified unambiguously.	Yes
Justification for use of test is given.	Yes
Data meet all assumptions of tests applied (non-normal data sets, small sample sizes)	Yes
Adjustments made for multiple testing is explained.	N/A
Details about the test	
n is reported at the start of the study and for each analysis thereafter.	Yes
Sample size calculation (or justification) is given.	Yes
Alpha level is given for all statistical tests.	Yes
Tests are clearly identified as one or two-tailed.	Yes
Randomization procedures or other ways to eliminate bias in sampling are described.	N/A
Summary of descriptive statistics	
n for each data set is clearly stated	Yes
A clearly labelled measure of centre (e.g. mean or median) is given	Yes
A clearly labelled measure of variability (e.g. standard deviation, range, percentiles) is given.	Yes
All numbers following a ± sign are identified as standard errors (s.e.m.) or standard deviations (s.d.).	Yes
Extras	
Any unusual or complex statistical methods are clearly defined and explained.	Yes
Any data exclusions are stated and explained.	N/A
Any discrepancies in the value of n between analyses are clearly explained and justified.	Yes
Data transformations (logarithmic, ….) are explained	Yes
Graphs	
Any distorted effect sizes (e.g. by truncation of y axis) are clearly labelled and justified.	Yes
Error bars in graphs, or confidence intervals, are included, or their absence is explained.	Yes

PhD Student signature

Checklist for Thesis that include experimental animals. **EXPERIMENTAL ANIMALS ARRIVE.**

Yes/No/NA		page
	Title	
Yes	Provide as accurate and concise a description of the content of the article as possible.	97; 157
	Abstract	
Yes	Provide an accurate summary of the background, research objectives, including details of the species or strain of animal used, key methods, principal findings and conclusions of the study.	99; 159
	Background	
Yes	Provide an accurate summary of the background, research objectives, including details of the species or strain of animal used, key methods, principal findings and conclusions of the study.	101; 161
Yes	Explain how and why the animal species and model being used can address the scientific objectives and, where appropriate, the study's relevance to human biology.	102; 162
	Objectives	
Yes	Clearly describe the primary and any secondary objectives of the study, or specific hypotheses being tested.	102; 162
	Methods	
	Ethical statement	
Yes	Indicate the nature of the ethical review permissions, relevant licenses, and national or institutional guidelines for the care and use of animals, that cover the research.	108;165
	Study design	
Yes	Number of experimental and control groups	108; 165
Yes	Steps taken to minimize the effects of subjective bias when allocating animals to treatment (e.g. randomization procedure) and when assessing results (e.g. if done, describe who was blinded and when).	167
Yes	The experimental unit (e.g. a single animal, group or cage of animals). A time-line diagram or flow chart can be useful to illustrate how complex study designs were carried out.	109; 166
	Experimental procedures	
Yes	How (e.g. drug formulation and dose, site and route of administration, anesthesia and analgesia used [including monitoring], surgical procedure, method of euthanasia). Provide details of any specialist equipment used, including supplier(s).	108; 166
N/A	When (e.g. time of day).	
N/A	Where (e.g. home cage, laboratory, water maze).	
Yes	Why (e.g. rationale for choice of specific anesthetic, route of administration, drug dose used).	108; 166
	Experimental animals	
Yes	Provide details of the animals used, including species, strain, sex, developmental stage (e.g. mean or median age plus age range) and weight (e.g. mean or median weight plus weight range).	108;166
Yes	Provide further relevant information such as the source of animals, international strain nomenclature, genetic modification status (e.g. knock-out or transgenic), genotype, health/immune status, drug or test naïve, previous procedures, etc.	108; 166

	Housing and husbandry	
N/A	Housing (type of facility e.g. specific pathogen free [SPF]; type of cage or housing; bedding material; number of cage companions; tank shape and material etc. for fish).	
Yes	Husbandry conditions (e.g. breeding program, light/dark cycle, temperature, quality of water etc for fish, type of food, access to food and water, environmental enrichment).	165
Yes	Welfare-related assessments and interventions that were carried out prior to, during, or after the experiment.	170
	Sample size	
Yes	Specify the total number of animals used in each experiment, and the number of animals in each experimental group.	108; 166
N/A	Explain how the number of animals was arrived at. Provide details of any sample size calculation used.	
N/A	Indicate the number of independent replications of each experiment, if relevant.	
	Allocating animals to experimental groups	
N/A	Indicate the number of independent replications of each experiment, if relevant.	
N/A	Describe the order in which the animals in the different experimental groups were treated and assessed.	
	Experimental outcomes	
Yes	Clearly define the primary and secondary experimental outcomes assessed (e.g. cell death, molecular markers, behavioral changes).	
	Statistical methods	
Yes	Provide details of the statistical methods used for each analysis.	111; 168
Yes	Specify the unit of analysis for each dataset (e.g. single animal, group of animals, single neuron).	112; 169
N/A	Describe any methods used to assess whether the data met the assumptions of the statistical approach.	
	Results and discussion	
	Basal data	
Yes	For each experimental group, report relevant characteristics and health status of animals (e.g. weight, microbiological status, and drug or test naïve) prior to treatment or testing (this information can often be tabulated).	171-177
	Numbers analyzed	
Yes	Report the number of animals in each group included in each analysis. Report absolute numbers (e.g. 10/20, not 50%).	108; 166
N/A	If any animals or data were not included in the analysis, explain why.	
	Outcomes and estimation	
Yes	Report the results for each analysis carried out, with a measure of precision (e.g. standard error or confidence interval).	113; 115; 171-177
	Adverse events	
N/A	Give details of all important adverse events in each experimental group.	
N/A	Describe any modifications to the experimental protocols made to reduce adverse events.	
	Interpretation/scientific implications	
Yes	Interpret the results, taking into account the study objectives and	115; 177

	hypotheses, current theory and other relevant studies in the literature.	
Yes	Comment on the study limitations including any potential sources of bias, any limitations of the animal model, and the imprecision associated with the results.	118; 180
N/A	Describe any implications of your experimental methods or findings for the replacement, refinement or reduction (the 3Rs) of the use of animals in research.	
	Generalizability/translation	
N/A	Comment on whether, and how, the findings of this study are likely to translate to other species or systems, including any relevance to human biology.	
	Funding	
No	List all funding sources (including grant number) and the role of the funder(s) in the study.	

Based on The ARRIVE guidelines: Animal Research: Reporting of *In Vivo* Experiments.

PhD Student signature

Checklist for recommendations of **Thesis EDI saúde. GENERAL**

Yes-No-N/A		Page
For all Thesis		
Yes	Declaration of potential conflicts of interests	207
Yes	Declaration on the origin and copyright status of non original figures, with permission if necessary. Include them in the text of each figure	207
Yes	Checklist of statistics adequacy if no other checklists apply.	213
For Thesis involving human experimentation, human samples, or personal data.		
Yes	Declaration on approval by the research ethics committee.	219
Yes	Code number of the study.	219; 220
No	Copy of ethics report	
N/A	Declaration that data are based on anonymous information, and no approval of the ethics committee is needed.	
N/A	If it is an observational study, STROBE checklist.	
For Thesis that include a clinical assay		
N/A	Declaration of its authorization by the Agencia Española de Medicamentos y productos sanitarios.	
N/A	Copy of the authorization	
N/A	CONSORT Checklist	
For Thesis that use embryonic or induced human stem cells		
Yes	Declaration on its authorization	219
Yes	Reference of the authorization	219
Yes	Copy of the authorization	219
For Thesis that include animal experimentation		
Yes	Declaration of its authorization	218; 220
Yes	Code number of the authorization of the animal experimentation Project.	218; 220
Yes	Register number of the centro de usuario autorizado if experiments were made in Spain	220
N/A	Copy of the capacitation certificate if the experiments were made by the Thesis autor.	
Yes	Person, company or service that performed the experiments if applicable.	218; 220
Yes	ARRIVE Checklist	214

PhD Student signature

STATENS SERUM INSTITUT

Dennis Christensen Head of the vaccine adjuvant research, Department of Infectious Disease Immunology, Center for Vaccine Research, Statens Serum Institut (SSI)

Declare that:

The animal research studies carried out by Lorena Garcia del Rio during her internship at SSI, performing the research project entitled "Hydrogels as vaccine carriers: evaluation of their vaccine immunogenicity" within the frame of the COST Action CA16231 "European Network of Vaccine Adjuvants" (ENOVA), were conducted in accordance with the regulations set by the National Committee for the Protection of Animals used for Scientific Purposes and in accordance with the European Community Directive 86/609.

In addition, animals were handled by authorized staff and the authorization number of this animal experimental assay is 2017-15-0201-01363.

sgd:

Dennis Christensen

Head of the Vaccine Adjuvant Research
Center for Vaccine Research
Statens Serum Institut, Copenhagen, DK
E-mail: den@ssi.dk
Office: +45 3268 3804

SERVICIO DE SALUD
DEL PRINCIPADO DE ASTURIAS

HOSPITAL UNIVERSITARIO CENTRAL DE ASTURIAS
Comité Ético de Investigación Clínica
Regional del Principado de Asturias
C/ Celestino Villamil s/n
33006.-Oviedo
Tfno: 985.10.79.27/985.10.80.28
Fax: 985.10.87.11
e-mail: ceicr_asturias@hca.es
Área Sanitaria

Oviedo, 6 de Agosto de 2013

El Comité Ético de Investigación Clínica Regional del Principado de Asturias, ha revisado el Proyecto de Investigación nº 100/13, titulado: "ESTUDIO PRECLÍNICO DE LA POTENCIALIDAD TERAPÉUTICA DE LAS CÉLULAS MADRE MESENQUIMALES DE CERVIX UTERINO". Investigador Principal Dr. Francisco J. Vizoso de la Unidad de Investigación del Hospital de Jove

El Comité ha tomado el acuerdo de considerar que el citado proyecto reúne las condiciones éticas necesarias para poder realizarse y en consecuencia emite su autorización.

Le recuerdo que deberá guardarse la máxima confidencialidad de los datos utilizados en este proyecto.

Fdo: Eduardo Arnáez Moral
Secretario del Comité Ético de Investigación
Clínica Regional del Principado de Asturias

SERVICIO DE SALUD
DEL PRINCIPADO DE ASTURIAS
HOSPITAL UNIVERSITARIO CENTRAL DE ASTURIAS
COMITE ETICO DE INVESTIGACIÓ
CLINICA REGIONAL DEL PRINCIPADO D

XUNTA DE GALICIA
CONSELLERÍA DO MEDIO RURAL

Departamento Territorial
Edificio Administrativo de Servizos Múltiples
Vicente Ferrer, 2
15071 – A Coruña

REXISTRO XERAL DA XUNTA DE GALICIA
REXISTRO DO EDIFICIO ADMINISTRATIVO DE A CORUÑA
A CORUÑA
Data 25/12/2017 14:19:21
SAÍDA 152791 / RX 1850544

José Manuel Cifuentes
Departamento de Anatomía
Facultade de Veterinaria
Campus Universitario
27002 Lugo

RESOLUCIÓN DE AUTORIZACIÓN DE PROXECTOS DE EXPERIMENTACIÓN ANIMAL

Expediente núm.: 15010/17/006 **Data de inicio:** 22.12.2017
Persoa interesada: Román Pérez Fernández **Forma de inicio:** solicitude do interesado
Procedemento: resolución de autorización

ANTECEDENTES

A persoa interesada, como representante do centro CIMUS (Universidade de Santiago de Compostela), presentou con data 19.12.2017 e rexistro de entrada 129035/3096751, unha solicitude para a realización do proxecto de experimentación animal, cuxos datos se detallan a continuación:

Denominación do proxecto: Tratamentos de enfermidades intestinais inflamatorias con medio condicionado procedente de células madre uterinas
Nome do centro usuario: Animalario do CIMUS
Persoa responsable do proxecto: Román Pérez Fernández
Establecemento onde se realizarán os procedementos do proxecto (ou lugar xeográfico no caso de traballos de campo): Animalario do CIMUS
Clasificación do proxecto : Tipo I ☐ Tipo II ☒ Tipo III ☐

CONSIDERACIÓNS LEGAIS E TÉCNICAS

1. O Real decreto 53/2013, de 1 de febreiro (BOE 34, do 8 de febreiro), polo que se establecen as normas básicas aplicables para a protección dos animais utilizados en experimentación e outros fins científicos, incluíndo a docencia, establece no seu artigo 33 as condicións de autorizacións dos proxectos con animais de experimentación.

2. O artigo 88 da Lei 39/2015, de 1 de outubro, do procedemento administrativo común das administracións públicas (BOE 236, do 2 de outubro de 2015) establece que a resolución que poña fin o procedemento decidirá todas as cuestións expostas polos interesados e aquelas outras derivadas deste.

XUNTA DE GALICIA
CONSELLERÍA DO MEDIO RURAL

Departamento Territorial
Edificio Administrativo de Servizos Múltiples
Vicente Ferrer, 2
15071 – A Coruña

3. O Servizo de Gandaría da Coruña revisou a documentación achegada na solicitude e o resultado favorable da avaliación do proxecto, realizada polo órgano habilitado da Sección de Experimentación Animal do Comité de Bioética da Universidade de Santiago de Compostela.

Esta xefatura territorial é competente para ditar unha resolución, de conformidade co artigo 11 do Decreto 245/2009 de 30 de abril, polo que se regulan as delegacións territoriais da Xunta de Galicia (DOG 84, do 1 de maio de 2009) e o Decreto 166/2015, de 13 de novembro, polo que se aproba a estrutura orgánica da Consellería do Medio Rural (DOG 220, do 18 de novembro de 2015).

De acordo con todo o indicado, RESOLVO:

1 Autorizar o proxecto solicitado.
2 O mencionado proxecto non precisa someterse a unha avaliación retrospectiva.
3 A autorización deste proxecto terá unha duración dun ano, transcorrido o cal, deberá ser renovada esta autorización.

A citada autorización é unicamente válida nas condicións que figuran no expediente. Ante calquera cambio significativo no proxecto que poida ter efectos negativos sobre o benestar dos animais, deberá solicitar a confirmación da autorización ao Servizo Provincial de Gandaría.

Esta autorización poderá ser suspendida, no caso de que o proxecto non se leve a cabo de acordo coas condicións de autorización e retirala, previo expediente tramitado ao que se lle dará audiencia.

Contra a presente resolución, que non lle pon fin á vía administrativa, poderá interpoñer un recurso de alzada ante a conselleira de Medio Rural. O prazo comezará a contar dende o día seguinte ao da recepción desta resolución. Todo isto, segundo o disposto nos artigos 121 e 122 da citada Lei 39/2015.

Mediante este escrito notifícaselle ao CIMUS da USC esta resolución segundo o esixido no artigo 40.1 da antedita Lei 39/2015.

A Coruña, 28 de decembro de 2017
O xefe territorial

Manuel Rodríguez Vázquez

Asinado por: RODRIGUEZ VAZQUEZ, MANUEL
Cargo: JEFE TERRITORIAL
Data e hora: 29/12/2017 11:19:01

CVE: dUeeVO2V
Verificación: https://sede.xunta.gal/cve

CCC RightsLink®

Home | Help | Email Support | Sign in | Create Account

Design of novel orotransmucosal vaccine-delivery platforms using artificial intelligence

Author: Lorena Garcia-del Rio,Patricia Diaz-Rodriguez,Mariana Landin

Publication: European Journal of Pharmaceutics and Biopharmaceutics

Publisher: Elsevier

Date: February 2021

© 2020 Elsevier B.V. All rights reserved.

Journal Author Rights

Please note that, as the author of this Elsevier article, you retain the right to include it in a thesis or dissertation, provided it is not published commercially. Permission is not required, but please ensure that you reference the journal as the original source. For more information on this and on your other retained rights, please visit: https://www.elsevier.com/about/our-business/policies/copyright#Author-rights

BACK CLOSE WINDOW

© 2021 Copyright - All Rights Reserved | Copyright Clearance Center, Inc. | Privacy statement | Terms and Conditions
Comments? We would like to hear from you. E-mail us at customercare@copyright.com

USC UNIVERSIDADE DE SANTIAGO DE COMPOSTELA

Copyright Clearance Center
RightsLink®
Home
Help
Email Support
Sign in
Create Account
MATERIALS SCIENCE & ENGINEERING
New tools to design smart thermosensitive hydrogels for protein rectal delivery in IBD
Author: Lorena Garcia-del Rio,Patricia Diaz-Rodriguez,Mariana Landin
Publication: Materials Science and Engineering: C
Publisher: Elsevier
Date: January 2020
© 2019 Elsevier B.V. All rights reserved.
Please note that, as the author of this Elsevier article, you retain the right to include it in a thesis or dissertation, provided it is not published commercially. Permission is not required, but please ensure that you reference the journal as the original source. For more information on this and on your other retained rights, please visit: https://www.elsevier.com/about/our-business/policies/copyright#Author-rights
BACK
CLOSE WINDOW
© 2020 Copyright - All Rights Reserved | Copyright Clearance Center, Inc. | Privacy statement | Terms and Conditions
Comments? We would like to hear from you. E-mail us at customercare@copyright.com